Solar desiccant evaporative cooling with multivalent use of solar thermal heat

Tobias Bader

A thesis submitted in partial fulfilment
of the requirements of De Montfort University
for the degree of Doctor of Philosophy (PhD)

October 2014

Institute of Energy and Sustainable Development
De Montfort University Leicester

Foreword

"*The Stone Age came to an end not for a lack of stones and the oil Age will end not for a lack of oil; we transitioned to better solutions*." Sheik Yamani, Saudi Arabias former oil minister quoted by Greider (2000) as cited by Lombørg (2001).

When I began this research, I had professional experience in innovation management and technology benchmarking. Solar technology was a new field for me, however I have made the decision to play a part in sustainable energy engineering and contribute to a sustainable change with my future work. In the initial project phase I selected measurement sensors to be integrated into an already operating system. During the start of my work it was essential to accept that I did of course not have the same precognition in the different aspects of my research. A well-structured procedure and in-depth research of specialist literature helped me to acquire found knowledge. The innovative system to be investigated in-situ proved as complex undertaking, not only because of its technically sophisticated multivalent system design. In fact, the human factor played a significant role during the monitoring. On the one hand, the system operator unawarely tended to interfere with the system operation and thus challenged the evaluation of measurement results. On the other hand, the various protagonists being included in the compilation of data gave different answers to the same question. Continual asking and the involvement of additional advisors, from academic to blue collar employees, led me to a point, where I had to realise that I can only free myself from my lack of knowledge together with the team, following in an intuitive way. From time to time I realised, that I experienced the principle of Socrates "I know that I do not know" as he complies with Platons dialectics of asking questions (Weinelt 2013). According to Platon after having accepted that one does not know and having freed oneself from the nescience the way is free to intuition. This helped me to familiarise deeply with my research and successfully master this thesis.

Ingolstadt, in June 2014 *Tobias Bader*

Declaration

I declare that the content of this submission is my own work. The contents of the work have not been submitted for any other academic or professional award. I acknowledge that this thesis is submitted according to the conditions laid down in the regulations.

Furthermore, I declare that the work was carried out as part of the course for which I was registered at De Montfort University, United Kingdom from January 2010 until December 2014. I draw attention to any relevant considerations of rights of third parties.

Abstract

Solar DEC (Desiccant and Evaporative Cooling) air-conditioning is a renewable technological approach to the future air-conditioning of buildings driven with solar-thermal heat. The principal acceptance of solar air-conditioning has led to system prototypes mainly across Europe, however the diffusion of this innovative technology is proceeding slowly due to little field testing experience. In climates with coexisting heating demand particularly, a multivalent system approach that utilizes solar-heat not only for air-conditioning but also for hot water preparation and heating has potential as a feasible concept. However, previous research focused on systems using solar heat exclusively for the DEC-process.

This research contributes to the advancement of the solar DEC-technology with multivalent use of solar thermal heat. The investigation consists of an initial detailed in-situ monitoring analysis of a system prototype operated in an industrial environment, followed by the development of optimised system concepts and a climate-specific analysis of the solar DEC-technology. The monitoring provided in-depth knowledge about the system operation, revealing the reasons for the insufficient refrigeration capacity achieved in practice. A detailed simulation model for an entire multivalent solar DEC-system including the heat sinks, DEC-system, heating and hot-water preparation was developed and a DEC-control strategy has been formulated. A new optimised control strategy for multivalent systems with simultaneous sink supply concept was devised. A sensitivity analysis was carried out to investigate the key design parameters for the dimensioning of multivalent solar DEC-systems. The research concluded that the auxiliary primary energy consumption of the optimised system was lower by one third compared to the initial system. Finally, a methodological zoning approach was developed, to systematically produce design-specific outline data for the application of the solar DEC-technology at climatically different sites.

.

Acknowledgements

I would like to take this opportunity to express my hearty gratitude to my first supervisor Prof. Vic Hanby for his excellent support and guidance. I am grateful for his proof reading of this thesis and the revision throughout this research. I would also like to thank my second supervisor Dr. Simon Rees. Thanks also to Prof. Wilfried Zörner for initiating this research work.

I would like to extend my sincere thanks to my industrial project partners, in particular Mr. Josef Pastaschek, Mr. Walter Schneider, Mr. Georg Höckmeier, Dr. Uli Jakob and Mr. Wolfgang Friedl. They were always willing to give support when needed. Furthermore, I would like to thank Dr. Dirk Pietruschka and Dr. Jürgen Schumacher for their valuable support and advises regarding the application of the simulation software INSEL.

This work could not have been completed without the support and assistance of many colleagues. I am very thankful to all colleagues and students who accompanied me during my research, particularly to Dr. Sebastian Brandmayr, Christoph Reiter, Emilien Devaux, Eduard Horst, Dr. Yi Zhang, Dr. Square Fong, Michael Finkenzeller, Sarah Frawley, Dr. Christoph Trinkl and Bassem Gadelrab.

Moreover, I would like to express my appreciation to Prof. Christian Facchi, Prof. Walter Schober and Prof. Tobias Schrag, especially in the final phase of this research.

Last but not the least, I would like to express my heartfelt thanks to my beloved wife Boitumelo, my parents, my family, both in Germany and Africa and my friends. Their patience, motivation and support helped me maintain my spirit throughout the research. A special thank you to my dad. I cannot thank him enough for his invaluable aid and encouragement, particularly during difficult times.

Table of Contents

List of Figures

List of Tables

Abbreviations

AHU	Air handling unit
ASHRAE	American Society of Heating, Refrigerating and Air-Conditioning Engineers
$AlMg_3$	Aluminium alloy matrix material of heat recovery wheel
BBD	Box-Behnken Design
BP	Block Parameter Real
CARNOT	Conventional and Renewable Energy Systems Optimisation Toolbox
cf.	compare (Latin: confer)
CCD	Central Composite Design
CO_2	Carbon dioxide
COP	Coefficient of Performance electrical
DEC	Desiccant and Evaporative Cooling
DIN	Deutsches Institut für Normung
DoE	Design of Experiments
DW	Desiccant Wheel
°E	Longitude (degree East)
e.g.	exempli gratia
EN	European Norm
EU	European Union
EU-17 /25 /27	Member States of the European Union according to a particular enlargement
et al.	et alii
etc.	et cetera
FD	Full Factorial Design

FFD	Fractional Factorial Design
FORTRAN	Formula Translation programming language
FNP	Fraction of Non-Purchased Energy
GmbH	Gesellschaft mit beschränkter Haftung (German for company with limited liability)
HRW	Heat Recovery Wheel
HVAC	Heating Ventilation and Air-Conditioning
HW	Hot Water preparation
HWS	Hot Water Storage
HX	Heat Exchanger
IEA	International Energy Agency
ILK	Institut für Luft und Kältetechnik Dresden
ILK-h,x-Dia	Mollier diagram calculation software ILK
IN	Input
INSEL	Integrated Simulation Environment Language
IRADIA	Room Model Block IRADIA
ITW	Institut für Thermodynamik und Wärmetechnik Stuttgart
LiCl	Lithium Chloride
min	Minute
MW	Messwert (Measured Value)
Mtoe	Megatonnes of oil equivalent
°N	Latitude (degree North)
n. d.	No date
OFAT	One Factor at A Time
OUT	Output

p. pers.	per person
PER	Primary Energy Ratio
PMV	Predicted Mean Vote
PPD	Predicted Percentage Dissatisfied
Pt	Platin
PC	Personal Computer
RADI	Room model block RADI
RAH	Regeneration Air Heater
RHUM	Return Air Humidifier
SAH	Supply Air Heater
SBS	Solar Buffer Storage
SHC	Solar Heating and Cooling Programme IEA
SHUM	Supply Air Humidifier
SP	Block Parameter String
SPC	Solar Performance Coefficient
SR	Surface Radiator
Tab.	Table
Task 38	IEA Task Group “Solar Air-Conditioning and Refrigeration”
TRNSYS	Transient System Simulation Program
TRY	Test Reference Year
VDI	Verein Deutscher Ingenieure
WALL	Room model Wall Block
WALLX	Room model external Wall Block

Symbols

A	Area	[m²]
a	Heat transfer coefficient	[W m^{-2} K^{-1}]
b	Absorbance coefficient window	[-]
c	Heat capacity	[J kg^{-1} K^{-1}]
clo	Clothing factor	[m^2 K W^{-1}]
d	Diameter	[m]
D	Thickness	[m]
dT	Temperature Gradient	[K]
dt	Time step	[s]
E	Energy	[kWh]
EH	General hardness English degrees	[°e]
f	Consumption rate	[-]
f_{sol}	Solar Fraction	[-]
G	Solar irradiation	[W m^{-2}]
GH	General water hardness (German degree)	[°dH]
h	Enthalpy	[kJ kg^{-1}]
lat	Latitude (degree north)	[°]
$long$	Longitude (degree east)	[°E]
M	Metabolic Heat Production	[met]
m	Mass	[kg]
$\dot{m}$	Mass flow	[kg s^{-1}]
moy	Month of the year	[-]
n	Number	[-]
Q	Thermal energy /Heat	[J]
$\dot{Q}$	Heat Flux	[W]

p	Nominal pressure	[Pa]
P	Power	[W]
r	Enthalpy of vaporization	[kJ kg^{-1}]
R	Gas constant	[kJ kg^{-1} K^{-1}]
R^2	Statistical coefficient of determination	[-]
T	Temperature	[°C]
t	Time	[s]
U	Heat Loss Coefficient	[W m^{-2} K^{-1}]
$U_{eff,1}$	Linear heat loss Coefficient	[W m^{-2} K^{-1}]
$U_{eff,2}$	Quadratic temperature dep. heat loss coefficient	[W m^{-2} K^{-2}]
v	Speed	[m s^{-1}]
V	Volume	[m³]
$\dot{V}$	Volume flow	[m³ h^{-1}]
x	Absolute humidity	[g kg^{-1}]
z	Layer height	[m]

Subscripts

AHU	Air handling unit
air	Air
amb	Ambient air
aux	Auxiliary
$bottom$	Bottom node
$cool$	Cooling capacity related (supply to return)
col	Collector
$cold$	Refrigeration capacity related (ambient to supply
$cons$	Consumption
cw	Cold water
D	Dehumidifying demand
DEC	Desiccant and Evaporative Cooling System
$dehum$	Dehumidification
$downstream$	Downstream
dry	Dry
DW	Desiccant wheel
E	Referring to boiling state
e	Enforced convection
el	Electrical
eff	Effective
f	Referring to inter-layer heat exchange by convection and conduction
$FANS$	Fans
fl	Flow
$floor$	Floor
gst	Guest

$heat$	Heat
hum	humidification
HUM	Humidifier
HRD	Heating rod
HRW	Heat Recovery Wheel
HW	Hot water
HWS	Hot water storage
HX	Heat exchanger
$hyst$	Hysteresis
i	Node index
$ideal$	Ideal
in	Input
l	Lower
$load$	Load
$loss$	Loss
max	Maximum
min	Minimum
m	Average mean
n	Number
nom	Nominal
out	Output
p	Constant pressure air related
$pers$	Person
p,V	Referring to water vapour
p,G	Referring to dry air
pv	Constant water vapour related
RAH	Regeneration Air Heater

$real$	Real
reg	Regeneration
ret	Return air
$RHUM$	Return air humidifier
$room$	Room
S	Storage
s	Saturated
sat	Saturation
SAH	Supply air heater
SBS	Solar buffer storage
set	Set value
$SHUM$	Supply air humidifier
sol_heat	Solar heat management
sol	Solar
sky	Sky
$spec$	Specific
SPU	Solar circulation pump
sup	Supply air
th	Thermal
top	Top node
tot	Total
u	Upper
$upstream$	Upstream
use	Useful
V	Vapour
w	Water
$wall$	Wall

WG	Water glycol collector fluid
$wind$	Wind
$0°C$	State related to vaporization at 0 °C
100%	Referring to state with 100% relative humidity

Greek Symbols

α	Inclination angle	[°]
Γ	Gaussian error	[-]
δ	Boolean switch parameter (0,1)	[-]
Δ	Difference	[-]
∂	Partial differential	[-]
ε	Efficiency factor	[-]
ζ	Hotel occupancy	[-]
η	Efficiency	[-]
η_{col}	Collector efficiency	[-]
η_0	Zero loss efficiency	[-]
ϑ	Temperature	[°C]
$\varkappa$	distance of the CCD star points to centre	[-]
θ	Mode of operation	[-]
λ	Thermal heat conductivity	[W m^{-1} K^{-1}]
π	Pi	[-]
ρ	Density	[kg m^{-3}]
υ	Daily hot water consumption	[l]
φ	Relative humidity	[% r.h.]
Φ	Heat recovery ratio	[-]
Ψ	Humidity recovery ratio	[-]
ω	Rotational speed	[h^{-1}]

1 Introduction

1.1 Research Background

Every citizen of Western industrialised societies consumes an average amount of energy that approximates to a capacity of 53 to 105 energy work slaves (Dürr 2010). This translated citation of the German physicist Hans-Peter Emil Dürr illustrates the dilemma of human mankind in the engineered world of the 21st century in a figurative excessive way: tremendous energy consumption in some parts of the world and its negative global impact.

Most of the worldwide energy supply is based on non-renewable energy sources. This massive consumption of fossil primary energy affects the depletion of natural resources and its availability in the future. Furthermore, the use of non-renewable resources contributes to the anthropogenic greenhouse effect and global warming through CO_2-emissions. (Intergovernmental Panel on Climate Change 2007).

Hence, there is an international consensus, that by 2050 the developed economies such as wide parts of the European Union need to achieve 80-95% reduction in greenhouse gas emissions compared to 1990 levels (Energy Research Knowledge Centre 2013) to mitigate the risks of a changing global climate. This urges the transformation towards a more sustainable society and hence drives ahead the research and development of new, sustainable technologies, especially in the energy sector.

In Europe, buildings consume around 40% of the primary energy consumption due to its services (Henning et al. 2013). This is in line with publications of the European Commission (2004) quantifying the final energy consumption in the building sector with 435 Mtoe or 40.3% of the total EU-25 final energy end-use consumer.

Beyond residential and commercial energy consumption for heating, hot water, lighting and other operated equipment, the installed stock of air conditioning applications in the EU-27 states is expected to increase from around 180 GW in

2010 to around 240 GW in 2020 and 270 GW in 2025 (European Commission 2012). Taken as a whole, HVAC (Heating Ventilation and Air-Conditioning) systems represent the most energy consuming appliances, contributing up to 20% to the final energy consumption in developed countries (Pérez-Lombard et al. 2011 as cited by Wrobel et al. 2013). Sophisticated living and working standards and reduced prices for air-conditioning units have caused a significant increase in the demand for air-conditioning in buildings, even where there was hardly any before.

Increased thermal loads, living standards and occupant comfort demands as well as architectural trends, such as a higher fraction of transparent areas in the building envelope contribute to an indoor climate with reduced thermal comfort. The higher loads affect the interior of buildings (e. g. office buildings, production plants, concert halls etc.) and hence contribute to significantly rising energy consumption for air-conditioning in heating dominated climates (Henning 2004a). The European cooling potential for the overall building stock is forecasted as 1370 TWh by the year 2020, of which 560 TWh are forecasted for the commercial environment (ECOHEATCOOL 2006 as cited by Henning et al. 2013).

This drives ahead the development of new, sustainable air-conditioning technologies, to create comfortable and convenient temperature and humidity conditions with a minimum consumption of primary energy sources. In order to supply quality air for a healthy room air environment, a full air-conditioning system provides functions to heat, cool, humidify, dehumidify, clean and convey air. This enhances the comfort for human beings occupying a room (Keller 2009).

For some years, the interest in research in sustainable air-conditioning processes has been growing. Nowadays, the commonly used technology for air-conditioning is electrically driven compression type refrigerating. However, this technology comes along with disadvantages of high energy consumption, CO_2-emissions and a climate damaging refrigerant.

Due to decreasing energy resources and an increasing awareness for the environment the ecologic and economic dimension is gaining more importance within purchasing and operating air-conditioning systems. In view of the above

and considering the importance of decoupling the electrical power load on the electric grid to avoid breakdowns in times of peak load, the use of solar-thermal energy for the air-conditioning of buildings carries a huge undeveloped potential. Especially regarding the fact that cooling loads and availability of solar radiation are approximately in phase. This shows the urgent need as well as the market opportunities for new technologies using alternative energy sources such as solar energy. However, despite its high potential, solar cooling is a technology where relatively little experience in field research exits.

From a primary energetic point of view, conventionally produced electrical power is in principle not very efficient for cooling, if not from renewable sources. In this regard, the use of solar thermal heat represents an alternative option to drive air-conditioning processes to decouple the cooling load from the electrical grid, especially during peak load times.

Solar air-conditioning is a process that uses low temperature heat sources instead of electricity for the air-conditioning of buildings. The International Energy Agency Solar Heating and Cooling Technology Roadmap (IEA 2012) forecasts that solar cooling could account for around 17% of world air-conditioning by 2050 (White and Goldsworthy 2013).

There are mainly three cooling processes operating with the thermal power of a solar collector: absorption cooling, adsorption cooling and desiccant and evaporative cooling (DEC). While adsorption and absorption cooling are closed-cycle sorption technologies providing cold water, the open-cycle DEC-process uses the cooling effect of evaporating water to regulate the air temperature through controlled dehumidification and humidification of the supply air. Therefore, it conditions the air directly and only uses water and air as working fluids. The direct conditioning of the air is a major advantage of DEC-systems as it becomes possible not only to adjust the air temperature, but also the humidity level of an air-conditioned space. Utilising absorbed solar thermal heat to drive the air-conditioning process the system approach is mostly independent of electricity.

Beyond cooling, solar heat can of course additionally be utilised for hot water consumption and heating. Hence a major aspect of this research focuses on the investigation and analysis of the solar DEC-technology with multivalent use of solar thermal heat.

1.2 Appraisal of Solar Desiccant and Evaporative Cooling Technology

DEC air-conditioning is in principle a process that uses low temperature heat sources instead of electricity for air-conditioning of buildings. By means of a series of air treatment functions, the technologies provide thermal comfort to a living space.

Thermal comfort is a measure used to evaluate the achieved comfort conditions in an analysed room and it is considered when improving the indoor climate of theatres, hotels and especially at work places in office buildings. In the context of thermal comfort, one has to comply with government regulations founded on complex standardisation framework, which is discussed in detail in section 5.2.2. According to that, air temperature and air humidity are to be conditioned with a DEC-system.

Therefore, as illustrated in Figure 1.1 and 1.2 for the standard DEC-cycle (Pennington cycle), the ambient air (position 1) is aspirated with a fan and dehumidified with a desiccant wheel by means of sorptive dehumidification. The process is almost adiabatic and heats the air with adsorption heat (2). This creates the potential for the consequent sensible heat recovery. The regenerative heat recovery wheel exchanges sensible heat from the supply air duct to the return air duct and therefore cools the supply air (3). Humidifiers cool the supply air to its desired state concerning temperature and humidity (4). The fan releases a small amount of heat into the supply air before the supply air enters the building (5). Room temperature and humidity are increased by internal sensible and latent loads (5 to 6).

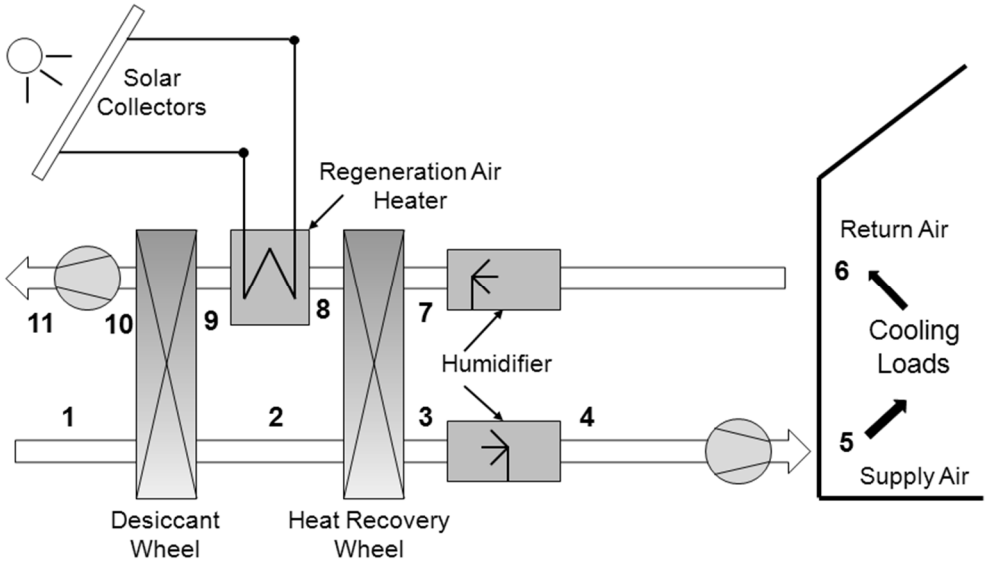

Figure 1.1: Scheme of a typical solar DEC-system (Pennington cycle)

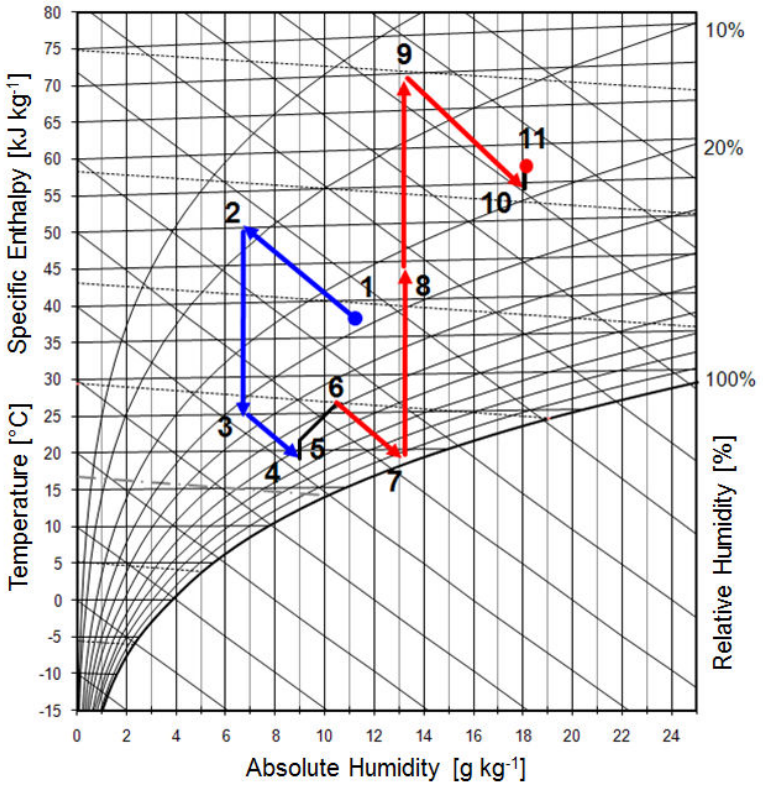

Figure 1.2: Change of air states during ideal DEC-process in the Mollier-Diagram (cf. Mollier 1923)

In the return air duct the air is humidified as close as possible to its saturation point (7) in order to reduce the temperature. As a result, this creates a reasonable

condition for the following heat recovery (8) in counter-flow with the supply air. After pre-heating the air by means of heat recovery, the return air is heated with regeneration heat by means of solar-thermal heat (9). The hot air is adjusted to a certain level to guarantee the adsorbed water in the pores of the desiccant wheel to be desorbed (10). As a result, the desiccant wheel is regenerated. The return air fan blows the exhaust air to the environment (11). Thus a DEC-plant conditions the room climate directly and leads to thermal comfort as it treats both air temperature and humidity level (cf. Bader et al. 2010a).

An assessment of the Oak Ridge National Laboratory (1992) in the United States dates the development of the DEC-technology based on a desiccant to the year 1910, before the advent of vapour compression cooling. The solid desiccant cycle, as it is essential to this research was introduced in 1960, by Munters Cargocaire Corporation based on the patents of Pennington (1955). The basic cycle is still state-of-the-art to systems nowadays. Beyond the standard Pennington cycle various DEC-cycles exist as alternative system options with modified functionality, as summarized in Table 1.1.

Table 1.1: DEC-system cycles

Main Cycles	**Extended Alternatives**	**Options**
Pennington Cycle	Recirculation cycle	Supply air heater
Bypass design	Dunkle Cycle	Integrated adiabatic cooling
Fresh air return air stream	Van-Zyl-Cycle 1	Solar regeneration heat
Circulating air	Van-Zyl-Cycle 2	Supply air chiller backup
		Double supply air chiller backup
		Cold-heat-coupling

An extensive literature review has highlighted that solar DEC-air-conditioning has been tested in a number of demonstration plants as documented by Erpenbeck 1999, Schürger 2007, Fong et al. 2010, Henning 2004b, Franzke and Heinrich 1997, La et al. 2010.

On the one hand, it was further found that technical reviews on the solar DEC-technology and relevant research work has been given by several scientists in a

number of publications (Balaras et al. 2007, Best and Ortega 1999, Fong et al. 2010, Henning 2005, Henning 2007, Klein and Reindl 2005, Kim and Ferreira 2008, Hwang et al. 2008, Pesaran et al. 1992; Pesaran and Neymark, 1995; Papadopoulos et al. 2003; Halliday et al. 2002; Wang et al. 2009). Hence this thesis does not attempt to give an extensive technology overview on the historical research and development of solar DEC-systems, but rather affiliates the given research tasks with the state-of-the-art in system monitoring and system simulation in the relevant sections 2.1 and 3.1.

On the other hand it became apparent that solar-driven DEC-systems are still a technology with relatively little field-tested experience. In particular, the analysis of multivalent system approaches to improve the integration of a solar-DEC-system in a multipurpose environment utilising solar heat for cooling, hot water supply and heating presented a research potential to the state-of-the-art.

The solar-driven DEC-system under investigation is in operation in a multifunctional office building in Ingolstadt (Germany) since 2006. The building has been accompanied with scientific investigations on the solar-thermal DEC-plant since the beginning of its operation (cf. Haller 2007). The results of previous research work on the DEC-plant operating with solar-thermal heat have shown that currently the system technology is not mature on a system level and still bears potential for efficiency improvement at component level. The current design principles for planning such plants are by far not sufficient. However, this is the requirement for a further spread of the technology. Previous analyses also showed that regarding an efficient operation, the high potential of the technology cannot yet be realised. Hence, an appreciable distribution of the technology urgently requires the development of scientifically and operationally proven, optimised and fail-safe plant concepts and control strategies (Henning 2004b).

Furthermore, Henning (2011) emphasises the importance to comprehend that using solar thermal energy to provide heating and cooling functions should not only go hand in hand with energy efficiency measures, but in fact with a holistic overall design of the building and the solar-assisted heating, ventilation and air-

conditioning system (HVAC). Only this fully integrated approach creates the chance to achieve the necessary cost-effectiveness for the overall system.

Currently, for system integrated, multivalent solar DEC-systems there are rarely planning criteria or optimised supervisory system concepts available. This deficit contributes to the fact that the distribution of this technology is far below its market potential. The development of the essentially needed expertise and design strategies shall contribute to the diffusion of the multivalent solar-DEC-systems. Therefore, solar DEC-systems with multivalent use of solar thermal heat were fundamental aspects within this research.

1.3 Research Objectives

The main aims and objectives are:

a. to devise system optimisations for solar DEC-systems in a multipurpose environment regarding hardware components, system commissioning and operation as a result of a detailed survey of measurement data and an in-depth failure and operation analysis;

b. to develop a simulation model of the solar DEC-system with multivalent use of solar thermal heat;

c. to deduce an advanced integral system design concept for solar DEC-systems with multivalent use of solar thermal heat;

d. to develop design criteria on system level as a result of simulation and sensitivity analysis in order to solve dimensioning problems in the planning process of future multivalent solar DEC-systems;

e. to evaluate the effectiveness of the solar DEC-Technology for diverse climatic conditions and devise appropriate planning recommendations.

1.4 Research Methodology

The procedural method of the research work is illustrated in Figure 1.3.

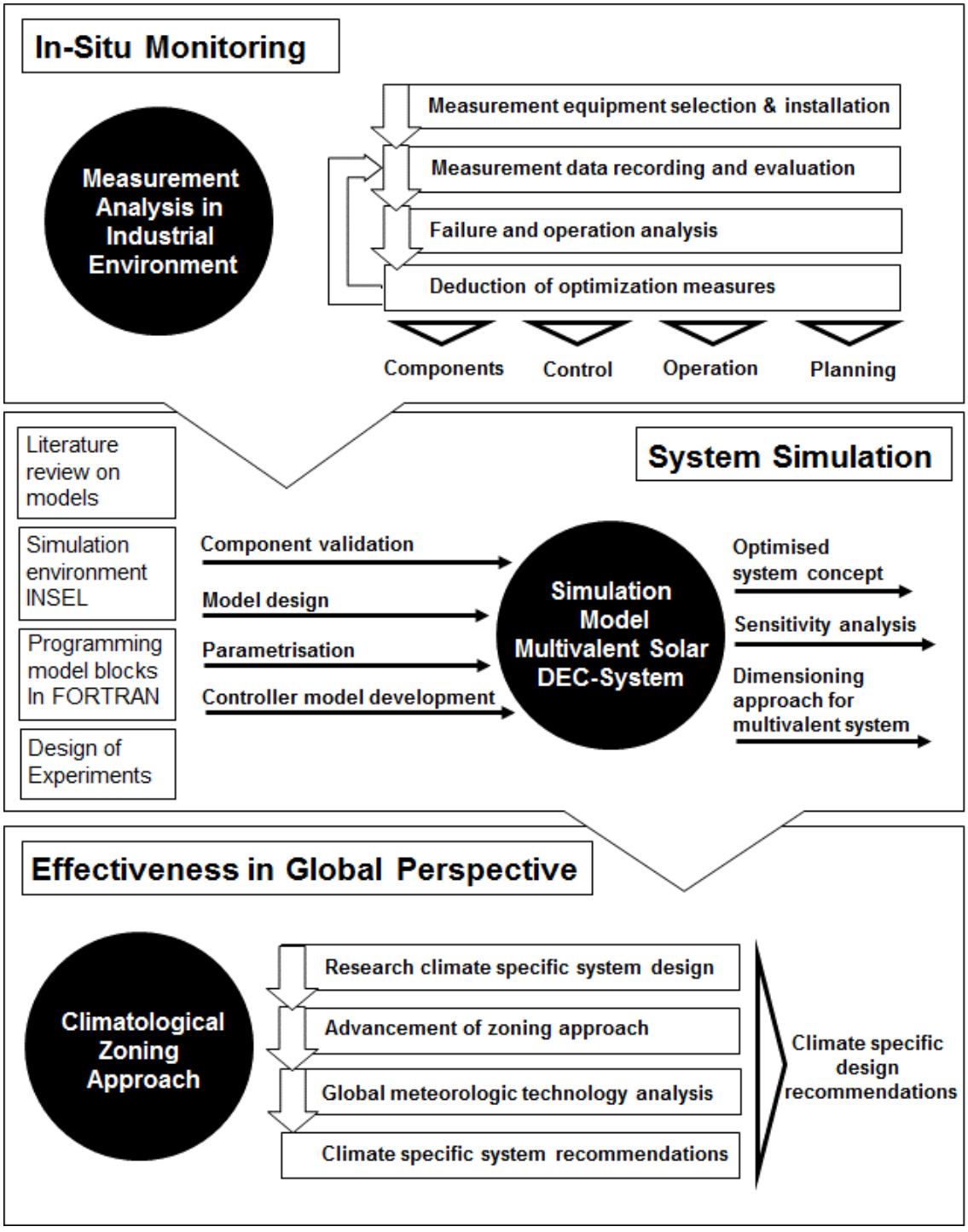

Figure 1.3: Research methodology

In order to achieve the research objectives, the methodology has been applied as follows:

a. Literature review of solar-DEC-system monitoring and simulation studies as well as of component modelling for solar-DEC-system simulation
b. Measurement sensor selection by means of Gauss error propagation
c. Discuss and reflect measurement results with system planner, plant manufacturer, component suppliers and system operator
d. Establish a system simulation model of a multivalent solar-DEC-system
e. Survey research projects on solar DEC-controllers and convey state-of-the-art controller for system simulation
f. Program model blocks and implement in INSEL system model
g. Carry out sensitivity analysis adopting the design of experiments method
h. Develop climatological zoning approach applying diverse standardisation work
i. Climatological analysis utilising Köppen Climate Classification

The following equipment and software have been applied to perform the work in this research:

a. Contemporary personal computers
b. Extensive measurement sensor equipment for in-situ monitoring
c. NI DIAdem for graphical analysis of measurement data and simulation results
d. Visual Basic for programming conversion of measurement data
e. INSEL 8 (Integrated Simulation Environment Language) system simulation programme for modelling the multivalent solar-DEC-system
f. FORTRAN 77 for developing new blocks for components and control-modules
g. JMP 11 statistical software to carry out design of experiments
h. Meteonorm 7.0 for global meteorological analysis
i. Microsoft Excel for graphical analysis
j. Microsoft Word for thesis writing and editing

1.5 Thesis Structure

The thesis consists of six chapters. Chapter one provides an introduction to the thesis and includes the research background to establish the research at hand in the overall global energy and air-conditioning context and to appraise the multivalent application of the solar DEC-technology. The introductory part further highlights the research objectives, the research methodology as well as the research objectives and the structure of the thesis.

Chapter two is dedicated to the in-situ solar DEC-System analysis. In this context this chapter describes the system investigated and gives a literature overview on previous measurement experiences. It describes the developed measurement concept and discusses the results and knowledge gained in system monitoring.

Chapter three is focused on a literature review on solar DEC-system simulation and modelling the developed simulation model of the multivalent solar DEC-system. The modelled multivalent system is described in detail and the developed controllers are introduced.

Chapter four presents an integral system design study based on the developed model, in order to optimise the multivalent solar DEC-system with regard to relevant objective functions. An optimised control strategy for multivalent solar DEC-systems is introduced. Subsequently a sensitivity analysis of the optimised system design is carried out by means the Central Composite Design being deduced as design of experiments (DoE) method relevant to this research. This leads to optimised dimensioning criteria on system level.

Chapter five focuses on the effectiveness of solar DEC-systems on a global perspective. In order to systematically assess the application of the solar DEC-technology at climatically diverse sites a developed simplified methodology is formulated. A subsequent meteorological analysis for 17 sites mapping the world climate creates a transparent understanding on the activity of the DEC-systems activity and allows the comprehension on the site-specific effectiveness of solar DEC-systems.

Chapter six summarises the research results and proposes future research themes.

The research ends with a list of research references and appendices. Details of component models of the multivalent simulation model are presented in Appendix A. Further appendices include a logical flow charts of the developed DEC-system controller (Appendix B) as well as a graphical overview of the simulation model in INSEL 8 (Appendix C). Appendix D includes the Legend to the Köppen climate classification and the complemented result of the meteorological analysis is shown in Appendix E. The researcher's own publications are listed in Appendix F.

.

2 In-Situ Solar DEC-System Analysis

2.1 Overall System Concept

The analysed solar-driven DEC-system is situated in a multipurpose building located in Ingolstadt (Germany) as illustrated in Figure 2.1.

Figure 2.1: Multipurpose building in Ingolstadt (Haller 2007)

The 10,000 m² gross floor area building is part of the biggest logistic centre in the region. The investigated building provides space for a training centre (ground floor), an office environment, a film studio (first floor) and a hotel (second floor). The floor plan shows an area of 4,100 m², the building has a capacity of approx. 45,000 m³. The diverse utilisation of the building has special requirements on the supply engineering (cf. Haller et al. 2005). Next to a ground-source heat pump for base-load heating and cooling, the building is equipped with two arrays of solar-thermal flat-plate collectors and a DEC-system. Due to high internal and external thermal loads active cooling is required. While base-load cooling is supplied by the heat pumps via the thermo-active building structure, peak-load cooling is realised by solar-driven DEC-technology.

The overall energy supply system of the building consists of two arrays of solar thermal flat-plate collectors, two DEC-plants, a heat pump system (heating power: 320 kW, cooling power: 240 kW), three domestic hot water storage tanks (1,500 l, each), a thermal ground storage (approximately 15,000 m pipes in the building base plate), 72 vertical closed geothermal loops of 40 m depth, a thermo-

active building structure combined with floor and wall heating and a façade-integrated thin-film photovoltaic-plant of 18 kWp that feeds into the grid only (cf. Haller 2007).

The solar-driven DEC-system in particular consists of two separate plants with a nominal air flow rate of 8,000 $m^3 h^{-1}$ and a nominal refrigeration capacity (ambient air to supply air) of 35 kW each. However, only one of both DEC-plants is in operation. Overall design data of the investigated solar DEC-system are summarised in Table 2.1.

Table 2.1: Design data of the solar-driven DEC-system (Haller 2007)

Design Data		
Geographic position of the building	48.78°N	11.40°E
Solar collector aperture area	262.5	[m²]
Active area air-conditioned (both plants)	2,040	[m²]
Nominal ventilation air flow rate	2 x 8,000	[$m^3 h^{-1}$]
Max. nominal cooling capacity	2 x 35	[kW]
Nominal capacity regeneration air heat exchanger	87	[kW]

The plant in Ingolstadt, as illustrated in Figure 2.2, uses a desiccant wheel with sorbent lithium chloride (LiCl; cf. section 2.2.1), a heat recovery wheel (cf. section 2.2.2) and a spray nozzle humidifier in the supply air duct and the return air duct (cf. section 2.2.3).

Figure 2.2: Solar collector array 1 (left) and investigated DEC-unit (right; Haller 2007)

An overall scheme of the solar driven DEC-system with its different components is illustrated in Figure 2.3. The solar DEC-system conveys ambient air from the outside, dehumidifies it by means of the desiccant wheel (DW), lowers its

temperature by the exchange of sensible heat (heat recovery wheel, HRW) and then lowers its temperature and enriches its humidity to the desired condition by evaporation by means of the supply air humidifier (SHUM). Therefore, the principle is in accordance with the process described in section 1.2 and the illustrated positions refer to the corresponding process steps.

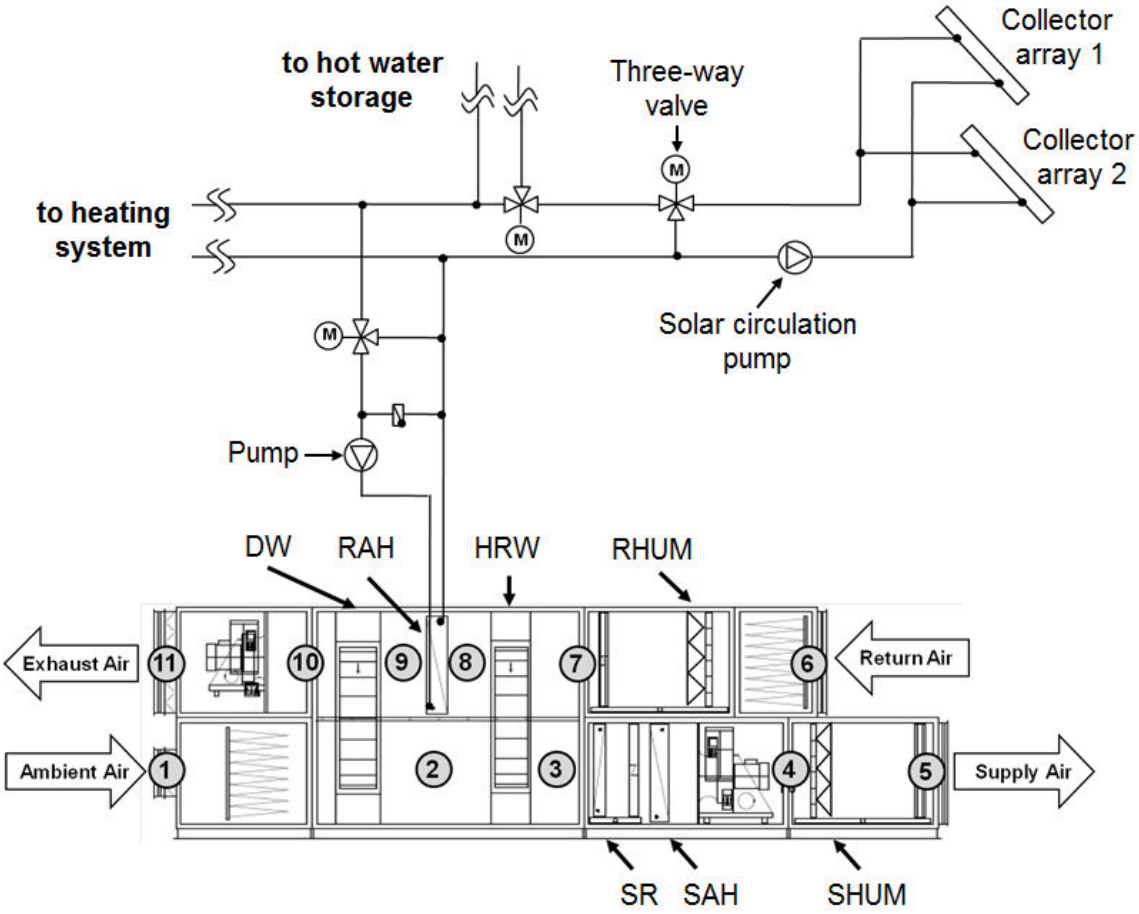

Figure 2.3: Solar DEC-system layout scheme

The regeneration heat to dehumidify the desiccant wheel on the return air side is provided by the installed solar thermal collector arrays via the regeneration air heat exchanger (cf. section 2.2.4) at a nominal capacity of 87 kW and a temperature of up to 70°C. The mass flow of the regeneration air heater (RAH) is regulated depending on the inlet temperature of the regeneration air heater. Besides the RAH, the DEC-plant is equipped with two more heat exchangers. An additional surface radiator (SR) with a nominal cooling power of 40 kW is

integrated as backup into the supply air duct and a supply air heater (SAH) with a nominal capacity of 34 kW accomplishes the system (Bader et al. 2009).

Due to a changed demand of the plant operator regarding room ventilation, only one DEC-plant has been in operation during the progress of this project. This plant has been operating with a reduced air flow. Furthermore, the surface radiator has been deactivated for the measurements, to solely analyse the solar DEC-process without interference of auxiliary cooling. In order to evaluate measurement results and to assess the performance of the investigated DEC-system the evaluation figures were defined, described in the following section.

When evaluating the DEC-process in form of an absolute figure, the calculation of the terms cooling capacity (supply air to return air) and refrigeration capacity (ambient air to supply air) are of importance. When calculating the refrigeration capacity $\dot{Q}_{cold}$ of a DEC-system, it is essential to consider the change of enthalpy within the supply air duct (Eq. 2.1, Erpenbeck 1999).

$$\dot{Q}_{cold} = \dot{V} \cdot \rho_{air} \cdot \left(h_{amb} - h_{sup}\right) = \dot{m} \cdot \left(h_{amb} - h_{sup}\right) \quad (2.1)$$

where,

$\dot{V}$	air volume flow [$m^3\ h^{-1}$]
ρ_{air}	density air [$kg\ m^{-3}$]
h_{amb}	enthalpy ambient air [$kJ\ kg^{-1}$]
h_{sup}	enthalpy supply air [$kJ\ kg^{-1}$]
$\dot{m}$	mass flow [$kg\ s^{-1}$]

While the refrigerating capacity $\dot{Q}_{cold}$ describes the heat capacity provided by the plant, the cooling capacity $\dot{Q}_{cool}$ describes the heat capacity provided to the room.

$$\dot{Q}_{cool} = \dot{m} \cdot \left(h_{ret} - h_{sup}\right) \quad (2.2)$$

where,

h_{ret}	enthalpy return air [$kJ\ kg^{-1}$]

Lavan et al. (1923) as cited by Erpenbeck (1999) discussed the basics of the calculation of the coefficient of performance (COP_{th}) in open-cycle DEC-processes.

Hence, according to Eq. 2.3 the COP_{th} is defined as the ratio of the capacity output of a DEC-plant $\dot{Q}_{cold}$ to the thermal driving heat $\dot{Q}_{RAH}$, provided to the process by the regeneration air heater RAH.

$$COP_{th} = \frac{\dot{Q}_{cold}}{\dot{Q}_{RAH}} \tag{2.3}$$

Analogue, for DEC-systems the electrical COP_{el} is calculated as the ratio of $\dot{Q}_{cold}$ to the effective electrical power P_{el} consumed by the DEC-process (Eq. 2.4). Thereby, P_{el} summarises the power to drive the different components such as wheels, fans and pumps.

$$COP_{el} = \frac{\dot{Q}_{cold}}{P_{el}} \tag{2.4}$$

In general, the refrigeration capacity of a DEC-system is defined as a combination of passive adiabatic cooling (humidifiers only) and active thermal driven cooling (sorptive dehumidification). Since the passive part is not completely taken into account as effort, its performance figures cannot be directly compared to those of other systems. Erpenbeck (1999) further defines the primary energy ratio for DEC-systems PER_{DEC} by Eq. 2.5.

$$PER_{DEC} = \frac{\dot{Q}_{cold}}{\frac{P_{el}}{\varepsilon_{el}}} \tag{2.5}$$

where,

ε_{el} conversion efficiency [-]

Of course, depending on climatic conditions at a targeted site, the consumed water amount is of importance, and defined in section 2.2.3.

2.2 DEC-System Composition

2.2.1 Desiccant Wheel

The desiccant wheel (DW) as key component of a DEC-plant is a common type of sorption dehumidifier based on the use of a desiccant. The purpose of the DW is to dehumidify the supply air isenthalpically. The basic principle is that the matrix of a slowly rotating wheel has two air volume flows in counter-flow in order to transfer humidity from the supply air into the return air across the DW. Desiccants abstract moisture from the air by creating an area of low vapour pressure at the surface of the desiccant.

As Harriman (1990) describes, the partial pressure of the water in the air is high, so the water molecules move from the air to the desiccant and the air is dehumidified. The desiccant material is coated or impregnated in a supporting structure, such as cellulose or different fibres, similar to that of a rotary heat exchanger (Henning 2004a). Commonly used desiccant materials include lithium chloride (LiCl), silica gels, aluminium silicates (e.g. zeolites or molecular sieves, Camargo et al. 2005).

A DW can be operated as dehumidifier in cooling mode or as enthalpy changer for a combined heat and humidity recovery in heating mode. The mode depends on the rotational speed of the wheel. A rotational speed of 20 h^{-1} is appropriate for the dehumidification mode, whereas a rotational speed of 600 h^{-1} makes the wheel operate as an enthalpy changer (Henning 2004a). Through its special sorptive properties and its comparably long exposure time in either the process air stream or the hot and dry return air stream, a high exchange in humidity between both air streams can be reached. Regeneration of DW is realised through hot air deriving from the regeneration air heating coil supplied by low temperature solar-thermal heat.

The investigated plant utilises a DW which consists of a honeycomb structure made of cellulose impregnated with lithium chloride. Therefore the process of dehumidification is based on the absorption principle. LiCl is characterised by its hygroscopic behaviour and its biocidal and germicidal properties leading to its hygienic innocuousness. The LiCl-wheel which is embedded into an aluminium housing is characterised by low expansion rates when exposed to humidity.

Table 2.2 summarises the overall design data of the installed desiccant wheel.

To dehumidify the air, the DW is driven with a rotational speed of 20 h^{-1}, whereas the regeneration temperature should not exceed 72°C (Eicker et al. 2002) as higher temperatures could damage the matrix of the wheel.

Table 2.2: Desiccant wheel design data

Desiccant Wheel Design Data		
Sorbent	LiCl	
Wheel diameter	1.41	[m]
Wheel depth	0.45	[m]
ω rotational wheel speed (dehumidification mode)	20	[h^{-1}]
ω rotational wheel speed (enthalpy exchange mode)	600	[h^{-1}]
Design supply and return air flow rate	8,000	[$m^3\ h^{-1}$]
Regeneration air temperature	70.0	[°C]
Pressure drop	236	[Pa]
Nominal dehumidification capacity Δx (T_1 = 32.0°C, φ_1 = 40%; T_2 = 46.6°C, φ_2 = 12%)	4.1	[g kg^{-1}]
Nominal electric power	0.4	[kW]

In times when the desiccant wheel is not in operation and therefore not rotating, a protection mode integrated in the desiccant wheel control is turning the wheel a half revolution every 30 minutes in order to avoid a one-sided oversaturation and thus a one-sided damage of the desiccant wheel due to displacement of the sorbent (cf. Haller 2007). LiCl impregnated desiccant wheels may not be exposed to liquid water and an operation with air streams of a relative humidity above 90% r.h. has to be avoided among conditions when the absorbed water is not driven out with the regeneration air flow (Franzke und Heinrich 1997).

The performance of the desiccant wheel is evaluated by means of the respective figures of merit, dehumidification capacity and dehumidification efficiency.

The dehumidification capacity Δx [g kg^{-1}] describes the amount of absolute humidity taken from the supply air by the desiccant wheel.

$$\Delta x = x_{sup,\, upstream\ DW} - x_{sup,\, downstream\ DW} \tag{2.6}$$

where,

$x_{sup,\, upstream\ DW}$ absolute humidity upstream DW in supply air [g kg^{-1}]
$x_{sup,\, downstream\ DW}$ absolute humidity downstream DW in return air [g kg^{-1}]

The dehumidification efficiency η_{dehum} [-] is defined as the ratio of the actually reached dehumidification capacity Δx to the theoretically maximum possible dehumidification capacity Δx_{max} (Henning 1993, Erpenbeck 1999 as cited by Hoefker 2001).

$$\eta_{dehum} = \frac{\Delta x}{\Delta x_{max}} \tag{2.7}$$

2.2.2 Heat Recovery Wheel

The effect of isenthalpic dehumidification of the process air stream raises its temperature downstream the desiccant wheel and therefore does not benefit the cooling aspect. This phenomenon is further accompanied by an additional rise in temperature due to released absorption heat. This rise in temperature requires a consequent sensible heat transfer by means of the heat recovery wheel (HRW). Therefore the HRW is essential for the operation of the DEC-system as it represents the only component reducing the enthalpy in the supply air duct. In cooling mode the return air upstream the HRW has a significantly lower temperature level than the process air downstream the desiccant wheel. This leads to a sensible heat transfer between the return and the supply air stream across the HRW, from the air stream of higher temperature to the air stream of

lower temperature. Combining the principle of sorptive dehumidification with the principle of heat recovery from the return air, it becomes possible to resupply the recovered energy into the DEC-process. The HRW is applied to cool the processed air after dehumidification and to preheat the return air prior to regeneration enabling an efficient operation of the overall process (Franzke and Heinrich 1997).

The HRW's mass storage is designed as a cylindrical rotor, which measures a diameter of 1.42 m and a depth of 0.40 m. Its structure is similar to the desiccant wheel, however in contrary it consists of a seawater resistant aluminium alloy matrix ($AlMg_3$). The heat recovery capacity is set in accordance with the frequency of the wheel, which is 600 h^{-1} in operation. The overall design data of the installed heat recovery wheel are shown in Table 2.3.

Table 2.3: Heat Recovery Wheel design data

Design Data Heat Recovery Wheel		
Design supply and return air flow rate	8,000	[$m^3\ h^{-1}$]
Heat recovery ratio among design conditions (T_1=46.6°C, T_3=19.1°C, T_2=26.7°C)	72.3	[%]
Pressure drop supply air duct	122	[Pa]
Pressure drop return air duct	106	[Pa]
Nominal electric power	0.18	[kW]

The efficiency of the HRW as determined by EN 308 (1997) and VDI 2071 (1997) is assessed by the heat recovery ratio Φ. Thus, Φ is defined as the ratio of the actual sensible heat transfer to the maximum possible sensible heat transfer.

$$\Phi = \frac{T_{sup,upstream\ HRW} - T_{sup,downstream\ HRW}}{T_{sup,upstream\ HRW} - T_{ret,upstream\ HRW}} \tag{2.8}$$

where,

$T_{sup,upstream\ HRW}$ supply air temperature upstream HRW [°C]
$T_{sup,downstream\ HRW}$ supply air temperature downstream HRW [°C]
$T_{ret,upstream\ HRW}$ return air temperature upstream HRW [°C]

The humidity recovery rate Ψ defines the ratio of transferred humidity across the HRW to the maximum possible humidity transfer (Franzke and Heinrich 1997).

$$\Psi = \frac{x_{sup,upstream\ HRW} - x_{sup,downstream\ HRW}}{x_{sup,upstream\ HRW} - x_{ret,upstream\ HRW}} \quad (2.9)$$

where,

$x_{sup,upstream\ HRW}$ absolute supply air humidity upstream HRW [g kg^{-1}]
$x_{sup,downstream\ HRW}$ absolute supply air humidity downstream HRW [g kg^{-1}]
$x_{ret,upstream\ HRW}$ absolute return air humidity upstream HRW [g kg^{-1}]

2.2.3 Humidifiers

Humidifier units are installed in the supply air duct and the return air duct of the DEC-system. Each unit consists of a high pressure pump and a humidification chamber.

Turbulators and spray nozzle sets are installed within the humidification chambers, whereas five spray nozzles are installed within the supply air duct and seven spray nozzles are installed within the return air duct. With aid of the nozzles, pre-treated water provided by an ion-exchanger is precisely sprayed into the duct at a pressure of 3 MPa to 7 MPa, depending on the operating point of the humidifier. The generated fine droplets expeditiously evaporate in the air-stream and the turbulators improve the intermixture with the air in order to enhance the humidification capacity.

The humidification capacity is controlled by a frequency adjustment of the high pressure pumps set by a frequency converter from 20% – 100%. A two-step aluminium matrix droplet separator accomplishes the humidifier unit together with a base plate of stainless steel with slope and a sidewise drain in order to prevent microbial growth and to avoid the application of chemicals (Haller 2007).

The overall design data of the installed humidifier units are summarised in Table 2.4.

Table 2.4: Design data humidifiers

Design Data Humidifiers		
Supply Air		
Number of spray nozzles	5	[-]
Relative humidity downstream humidifier	70.4	[%]
Humidification ratio	95	[%]
Nominal electric power pump	0.55	[kW]
Return Air		
Number of spray nozzles	7	[-]
Relative humidity after humidifier	95.0	[%]
Humidification ratio	95	[%]
Nominal electric power pump	0.55	[kW]

The performance of a humidifier can be evaluated by means of the figures for water consumption, humidification ratio and water consumption rate. Therefore the water consumption $\dot{m}_{cons}$ is regarded as absolute amount of water consumed per defined period of time.

The humidification ratio further describes the relation of realised humidification in absolute humidity Δx_{real} and the maximal possible humidification Δx_{max} considering an adiabatic humidification process along the isenthalpic lines reaching the saturated vapour line in the wet-bulb temperature.

$$\eta_w = \frac{\Delta x_{real}}{\Delta x_{max}} = \frac{x_{downstream\,HUM} - x_{upstream\ HUM}}{x_{sat} - x_{upstream\,HUM}} \tag{2.10}$$

where,

$x_{downstream\,HUM}$ absolute humidity downstream humidifier [g kg^{-1}]
$x_{upstream\ HUM}$ absolute humidity upstream humidifier [g kg^{-1}]
x_{sat} absolute saturation humidity (wet bulb temperature) [g kg^{-1}]

The water consumption rate f_w defines the proportion of the consumed amount of water $\dot{m}_{cons}$ in relation to the amount of water absorbed by the air $\dot{m}_{hum}$.

$$f_w = \frac{\dot{m}_{cons}}{\dot{m}_{hum}} = \frac{\dot{m}_{cons}}{\dot{V} \cdot \rho_{air} \cdot \Delta x_{real}} \quad (2.11)$$

2.2.4 Regeneration Air Heater

A plate heat exchanger is installed in the return air duct before the desiccant wheel. The overall design data of the installed regeneration air heater (RAH) is summarised in Table 2.5.

Table 2.5: Design data regeneration air heater

Design Data Regeneration Air Heater		
Design air flow rate	8,000	[m³ h^{-1}]
Register volume	15.20	[l]
Pressure drop air duct	122	[Pa]
Pressure drop fluid side	3000	[Pa]
Heat transfer capacity	87	[kW]

Supplied with solar thermal heat, the RAH creates a continuous heat exchange in dehumidification mode to heat the air before the desiccant wheel to its required regeneration air temperature T_{reg} and therefore to desorb the desiccant wheel in the return air stream. In the system under investigation, the RAH is directly fed by the solar circuit without intermediary buffer store. A return air mixing loop controls the RAH flow temperature $T_{RAH,fl}$ to a maximum of 70°C to avoid damage of the desiccant wheels' cellulosic honeycomb matrix. The transferred heat capacity is expressed with Eq. (2.12).

$$\dot{Q}_{RAH} = \dot{m}_{RAH} \cdot c \cdot \left(T_{RAH,fl} - T_{RAH,ret}\right) \quad (2.12)$$

where,

$\dot{m}_{RAH}$ mass flow fluid [kg s^{-1}]
c specific heat capacity fluid [kJ kg^{-1} K^{-1}]
$T_{RAH,ret}$ RAH return temperature [°C]

2.3 Solar Thermal System

As described in section 2.1, solar flat-plate collector arrays provide the required heat to drive the DEC-process in desiccant mode. The solar heat is directly provided by the collector arrays and is supplied to the DEC-process via the regeneration air heat exchanger.

The arrays of solar-thermal high-performance flat-plate collectors are installed on the flat roof of the building. The collectors are mainly supposed to supply the regeneration heat for the DEC-plant. Additionally, they supply heat to the hot water storages for domestic hot water preparation of the hotel, regenerate the heat pump energy source in the ground storage and supply the heating system during heating period.

Due to leakages, the plant operator decided to bypass two collectors, which therefore results in a total aperture area of 258.65 m^2 in use. An azimuth of the solar arrays of -20° is induced by the building position. Table 2.6 summarises key figures of the two collector arrays.

Table 2.6: Key figures of the solar flat-plate collector arrays

Design Data			
Total aperture area (designed)	262.50		[m²]
Total aperture area (currently in operation)	258.65		[m²]
Azimuth of solar array (South=0°, East=-90°)	-20		[°]
Slope of solar arrays	30		[°]
	Array 1	**Array 2**	
Aperture area (currently in operation)	167.40	91.25	[m²]
per module	1.860	1.901	[m²]
Optical efficiency η_0	0.801	0.841	[-]
Linear heat loss coefficient a_1	3.858	3.430	[W m^{-2}K^{-1}]
Quadratic heat loss coefficient a_2	0.0100	0.0185	[W m^{-2}K^{-2}]
Stagnation temperature (G = 1,000 W; T_{amb} = 30°C)	210	217	[°C]
Heat capacity	9.99	23.80	[kJ m^{-2}K^{-1}]

Regarding the hydraulic collector circuit design according to the Tichelmann principle (Kohlenbach and Jakob 2014), five collectors are connected in series, whereas the series circuits of each collector array are connected in parallel. With 50 collectors (48 currently in operation) in array 1 this results in 10 parallel series. The collector array 2 with 90 collectors makes up 18 parallel series. Downstream the collector arrays, both arrays are jointing in a common point of transfer.

According to the planning documentation, the circulation pump in the solar circuit is controlled depending on the absorber temperature and the collector mass flow is varied depending on the collector flow temperature, whereas the mass flow of the regeneration air heater is regulated depending on the inlet temperature of the regeneration air heater.

In order to evaluate the solar collector arrays in operation the following terms are applied. The collector efficiency η_{col} for example, is defined as the ratio of the useful heat output $\dot{Q}_{use}$ to the total global irradiation incident G on the collector surface A (Henning 2004a) and can therefore be applied to evaluate the performance of the solar collector circuit.

$$\eta_{col} = \frac{\dot{Q}_{use}}{G \cdot A} \tag{2.13}$$

Ileri (1997) as cited by Erpenbeck (1999) evaluates the solar fraction of the overall supplied energy using the Fraction of Non-Purchased Energy (FNP) to evaluate the efficiency of the solar energy use. FNP is an ideal figure of merit for solar heating applications to measure the solar use, since the heating load is directly reduced by the solar heat. However, to apply the FNP to a thermal driven cooling process this figure has to be modified, since the percentage of solar heat is determined by its fraction in the operation of the thermodynamic cooling process. Otherwise FNP would have the same value, no matter if the solar energy was used completely or partly for the cooling process.

Hence, Ileri (1997) introduced the solar performance coefficient (SPC) in order to determine the solar efficiency in a thermal cooling process.

$$SPC = 1 - \frac{\dot{Q}_{aux}}{\dot{Q}_{load,cool}} \tag{2.14}$$

where,

$\dot{Q}_{aux}$ auxiliary heat flux [kW]
$\dot{Q}_{load,cool}$ cooling load [kW]

The SPC describes the amount of auxiliary energy that has to be provided per energy unit cooling load. The figure SPC equals another known figure for solar driven applications, the solar fraction SF_{DEC}. Since the investigated system within this work does not utilize auxiliary energy in form of cold (Surface radiator inactive), the figure SF_{DEC} is used with regard to the electric power to drive the process.

$$SF_{DEC} = 1 - \frac{P_{el}}{\dot{Q}_{cold}} \tag{2.15}$$

where,

P_{el} effective electric power [kW]
$\dot{Q}_{cold}$ refrigeration capacity [kW]

The solar heat management efficiency ε_{sol_heat} (IEA SHC-Task 38 2011) describes the quantity of global irradiation that is utilized in the system. Therefore the heat supplied to the regeneration air heater $\dot{Q}_{RAH}$ is divided by the solar irradiation G on the collector area A.

$$\varepsilon_{sol\_heat} = \frac{\dot{Q}_{RAH}}{G \cdot A} \tag{2.16}$$

2.4 Control Strategy

In the scope of this research two control strategies were of superior relevance:

a) The overall system control on supervisory level to decide on the distribution of solar heat
b) The control of the solar driven DEC-process

The overall system control on supervisory level allows different operation modes regarding the use of the solar heat. Thereby, the solar heat can either be used as regeneration heat for the DEC-process, for the hot water preparation in the hotel or as support to the heating system during operation times with heating load. In times without heat demand for air-conditioning excess heat can therefore be used for hot water preparation to avoid stagnation in the collector arrays. It was striking that the in-situ investigated energy system was realised without solar buffer store (SBS). Furthermore the object under investigation was operated with an exclusionary control strategy according to the “either-or” principle. Therefore, a simultaneous supply of several heat sinks was not possible. Planning guidelines or descriptions regarding the supervisory control strategy of the overall system were not available for this research due to a lack of documentation. However, based on the experiences gained regarding the system operation and interviews with experts, a memory copy of the supervisory control has been developed accordingly as basis for the system simulation.

The control of the solar DEC-process is particularly important regarding the evaluation in the system monitoring phase. However, a documentation of the in-situ integrated DEC-systems’ control strategy has not been available throughout the research. Several expert interviews with the plant manufacturer and the system planner enabled the deduction of a control strategy scheme of the DEC-plant as it is implemented in the field. The control scheme is illustrated in Figure 2.4 and consists of three main operation modes:

- Cooling
- Ventilation
- Heating

Due to a mixed ventilation strategy the return temperature T_{ret} is assumed to represent the room air temperature T_{room}. A return temperature lower than 19°C initiates setting the plant into heating mode, while it starts its cooling cycle when T_{ret} exceeds its set value of 23°C. In between these two set points, the DEC-plant works in ventilation mode without any active air handling but operating fans.

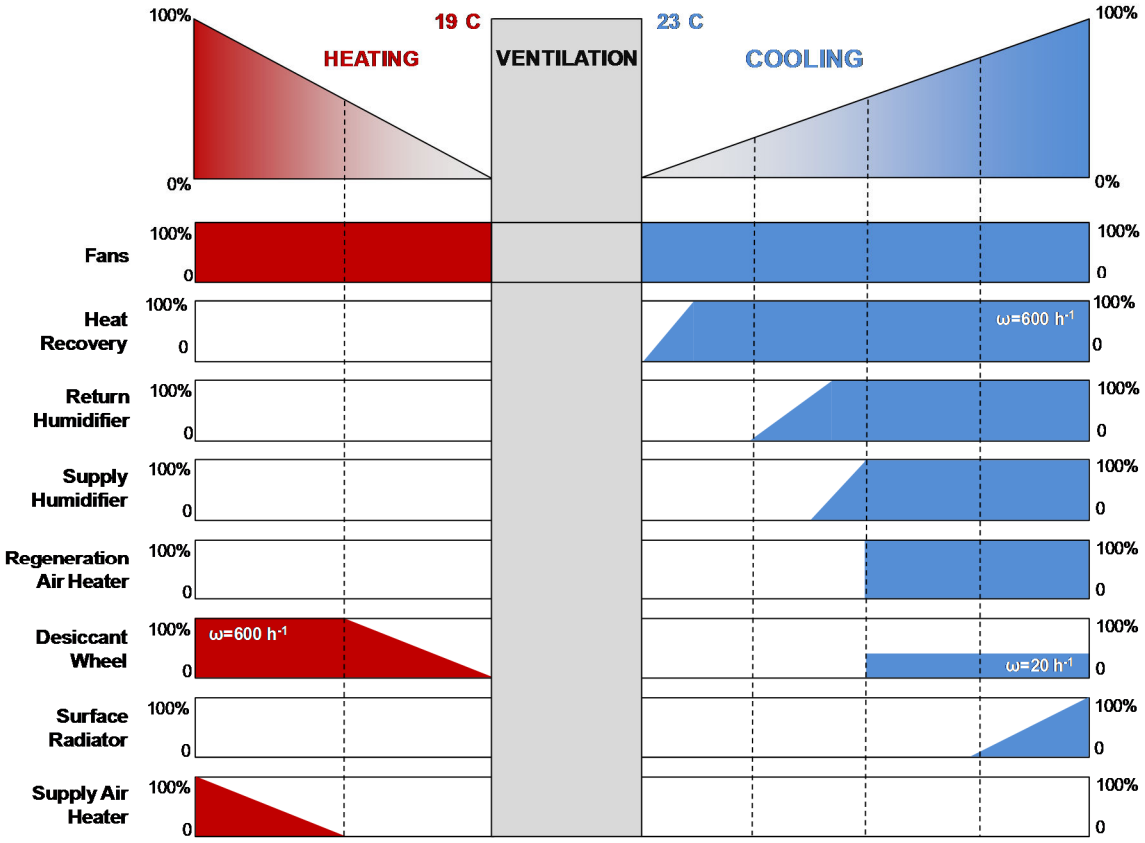

Figure 2.4: Control scheme of the solar-driven DEC-system

Thus, the DEC-system is controlled according to the following principle in cooling mode:

Level 1: Heat Recovery

In case of the return air temperature exceeding its maximum set point, the system control starts the heat recovery wheel if $T_{amb} > T_{ret}$. Its number of revolutions is then increased to a maximum value of 600 h^{-1}.

Level 2: Humidification of Return Air (adiabatic cooling)

If the return air still exceeds its maximum set point after the heat recovery has reached its maximum performance, the humidifiers in the return air start operation. The performance of the humidifiers is increased to its maximum performance by gradually increasing the frequency of the high-pressure pump.

Level 3: Humidification of Supply Air

If the return air temperature is still of a higher value than its set point, in spite of an operating heat recovery and a working return air humidifier, the supply air humidifier starts to operate. Similar to the return air humidifier, its capacity is regulated by increasing the frequency of the high-pressure pump steadily.

Level 4: Desiccant Cooling

Operation of the DEC-process only starts, if the relative humidity of the supply air exceeds its maximum set point. The start of the DEC-process goes along with the start of the regeneration air heater. After the regeneration air temperature is reached, the desiccant wheel starts operating.

As the performance of the desiccant wheel itself cannot be controlled, it is operated at a fixed rotational speed of 20 h^{-1}.The DEC-process is stopped if the minimum set point of the relative humidity of the return air or the minimum temperature of the return air falls below the set point.

Level 5: Surface Radiator

In case of an insufficient cooling capacity due to a too high return or supply air temperature (compared with the maximum set points) the additional surface radiator starts its operation in order to cool the supply air. Within this work, the surface radiator has been deactivated to solely analyse the solar DEC-process.

During periods of heating, the HVAC-System controls according an additionally implemented heating mode with the following principle:

Level 1: Enthalpy Exchange using the Desiccant Wheel

In case of the return air temperature falling below its minimum set point, the system control starts the desiccant wheel as enthalpy exchanger. Thereby, its number of revolutions is increased to the maximum value of 600 h^{-1}.

Level 2: Supply Heating Coil

In case of an insufficient heating capacity due to a too low return or supply air temperature (compared with its minimum set point), the additional supply heating coil starts its operation in order to heat the supply air.

2.5 Monitoring Approach

2.5.1 Previous Experiences and Monitoring Focus

Several monitoring research analyses have been conducted considering the solar DEC-technology. On the one hand, within the scope of different research projects on DEC-systems, single components of DEC-systems have been analysed in laboratory test stands. On the other hand, investigations have been accomplished on separate prototype plants regarding the performance of the entire air-conditioning plant.

Regarding component analyses, different tests on single components of a DEC-plant like humidifiers or desiccant wheels were conducted by Franzke and Stangl (2000) and Franzke and Seifert (2005). The results led to the development of simulation models of the investigated components. Similar research projects were performed by Möckel (2003) on a test rig, analysing an air-conditioning plant with sorption based dehumidification.

Considering the investigation of overall prototype plants, two solar-operated pilot DEC-plants in Althengstett (Germany) and Mataró (Spain) were analysed. Both plants were supplied with regeneration heat from solar air collectors and

metrological surveys were performed. A further plant operated with solar air collectors is situated in Freiburg (Germany) and was scientifically analysed by Hindenburg (2002). Kodama et al. (2002) carried out experimental testing of a solar DEC-plant with honeycomb rotor at Kumamoto University, Japan. Testing of different sorbents and desiccant wheels were conducted by Eicker et al. (2002) and Schürger (2007).

Another pilot plant is operated with fluid driven flat-plate collectors and is air-conditioning a seminar room in Riesa-Großenhain (Germany). This plant was scientifically analysed by Erpenbeck (1999) and resulted in a simulation model for the DEC-plant. The research, however, only concentrated on the DEC-plant and its combination with the solar collectors. Neither the integration in the further building technology nor the interaction with further cooling devices was part of this analysis. A further plant is located in Hartberg (Austria), which was analysed by Podesser and Stiglbrunner (2000) with focus on an energy efficient control strategy and minimisation of water consumption. A solar-assisted pilot plant was monitored in Palermo (Italy) by Beccali et al. (2008). The results show that improvements are still necessary, especially concerning air leakage reduction in the heat exchanger and the adjustment of set points in the plant control. Monitoring results of a solar-assisted DEC-unit in Lisbon (Portugal) by Mendes et al. (2009) emphasise the Primary Energy Ratio of the system and show that the required maintenance is not to be underestimated.

Since 2008, a solar-assisted DEC-system has been monitored in Vienna (Austria) by Preissler and Selke (2009). For this system a systematic simulation was based on measurement data from the Ingolstadt plant provided by Haller (2007). The monitoring results in principle were of major interest to investigate plant capacity and efficiency as well as on the PER of the overall system. Unfortunately, detailed information on relevant monitoring results is not available yet. Further experiences were gained in a monitoring of a DEC-plant integrated into a large solar heating and cooling network in an office building in Gleisdorf (Austria) by Thür and Vukits (2009).

So far, the research projects concentrated on the analysis of DEC-system components. The research neither focussed on the solar collector integration nor on the integration of further heat sinks into the overall system. It becomes obvious that in the previous research work on solar DEC-systems scientific measurements at pilot plants served to optimise a particular solar DEC- system in the first instance.

However, the efficient integration of a solar DEC-system into the further building environment has hardly been discussed, neither on component nor on control level. In this context Beccali and Nocke (2007) further underline the importance of integrating the DEC-technology on system level. This is of interest for the feasibility and the success of projects with solar DEC-systems as well as for the selection of suitable technical solutions in the planning phase.

Beyond the previously described background of intense monitoring efforts that have been carried out globally in recent years, a solar-driven DEC-system embedded into a multipurpose building with diverse needs has been investigated in in-situ operation in Ingolstadt (Germany).

This system showed massive problems during the first year of operation (2006). While the degree of comfort in the building was found to be satisfying during the cooling period, the solar-driven DEC-plant showed major deficiencies in cooling performance, hydraulics and control. Especially, a too high rotational speed of the desiccant wheel and an inadequate adjustment of solar collector arrays, DEC-plants and building structure were identified. Therefore, in an overhaul of the system, several problems in the hardware were identified and corrected such as blocked spray nozzles due to calcifications, leakages in the sealing of the desiccant wheel and an incorrect installation of a non-return valve in the hydraulic system of the regeneration air heater. Moreover, the control strategy regarding the cooling power of the plant and the speed of the desiccant wheel were checked (Haller 2007, Trinkl et al. 2007).

In the second year of operation (2007), some deficiencies of the first year were found to be removed, but still the plant did not work according to its capacity. Insufficient dehumidification by the desiccant wheel was identified as a major

problem. Based on a detailed analysis of the desiccant wheel, one-sided displacement of the sorbent was assumed to be the reason for insufficient cooling capacity. Obviously, control or mechanical malfunctions during operation led to a one-sided oversaturation and thus to a one-sided damage of the desiccant wheel as described by Trinkl et al. (2007). Consequently, the damaged wheel was removed prior to the 2008 cooling period.

During the third year of operation (2008), the DEC-plant was not permanently in operation throughout the cooling period due to organisational complications. However, as described by Bader et al. (2009) analyses on exemplary days proved that the one-sided damage of the desiccant wheel in 2007 could be solved by replacing the desiccant wheel during maintenance in spring 2008. Therefore, considering the concurrent plant settings in cooling period 2008 with a reduced volume flow, a maximum refrigeration capacity of around 24 kW was again expected to be reached during times of DEC-mode, as the difficulties with the desiccant wheel seemed to be resolved.

However, measurement results with the newly integrated desiccant wheel of the same type evidenced the contrary. Thus, in 2008 the refrigeration capacity (ambient air to supply air) was analysed with maximum values of around 15 kW (including the surface radiator) and thereby the expected value was by far not reached. The design conditions of the desiccant wheel regarding the altered mass flow conditions in the air duct have been taken into account. According to that, the decreased volume flow cannot be a reason for a decreased efficiency of the wheel.

Regarding scientific discussions and analyses as published by Beccali et al. (2008), arguing that DEC-systems are characterised by a limited dehumidification potential for given characteristics of the desiccant rotor beyond the flow rates, such as regeneration air temperature, ambient conditions etc. it became obvious, that a detailed investigation of the originate DEC-process is needed.

Therefore, the plant could not be further regarded as a black box, but supplementary measurement had to be integrated as described within the following section 2.5.2.

2.5.2 Measurement Concept

As described, previous monitoring investigations revealed that the solar DEC-system did not reach the expected cooling capacity. At the beginning of this monitoring analysis, the cause of the low refrigeration capacity was in principle searched within in the following areas:

- Solar integration: actually achieved regeneration air temperature upstream of the desiccant wheel in the return air duct and duration of availability of this condition.
- Component inspection: DEC-system component behaviour and efficiency within the DEC-plant.

The impact of the control strategy with respect to DEC-system control and supervisory control is considered and questioned throughout this work as far as it was possible.

In the first project phase, additional measurement equipment was installed within the DEC-plant (Figure 2.5) to closely monitor the DEC-process within the system and to evaluate the performance of its single components.

The additional measurement equipment that was integrated in the DEC-system prior to the 2009 cooling period measures temperature and relative humidity in order to analyse the single processes. Therefore six combined temperature and humidity sensors as well as four temperature sensors were installed in the DEC-plant.

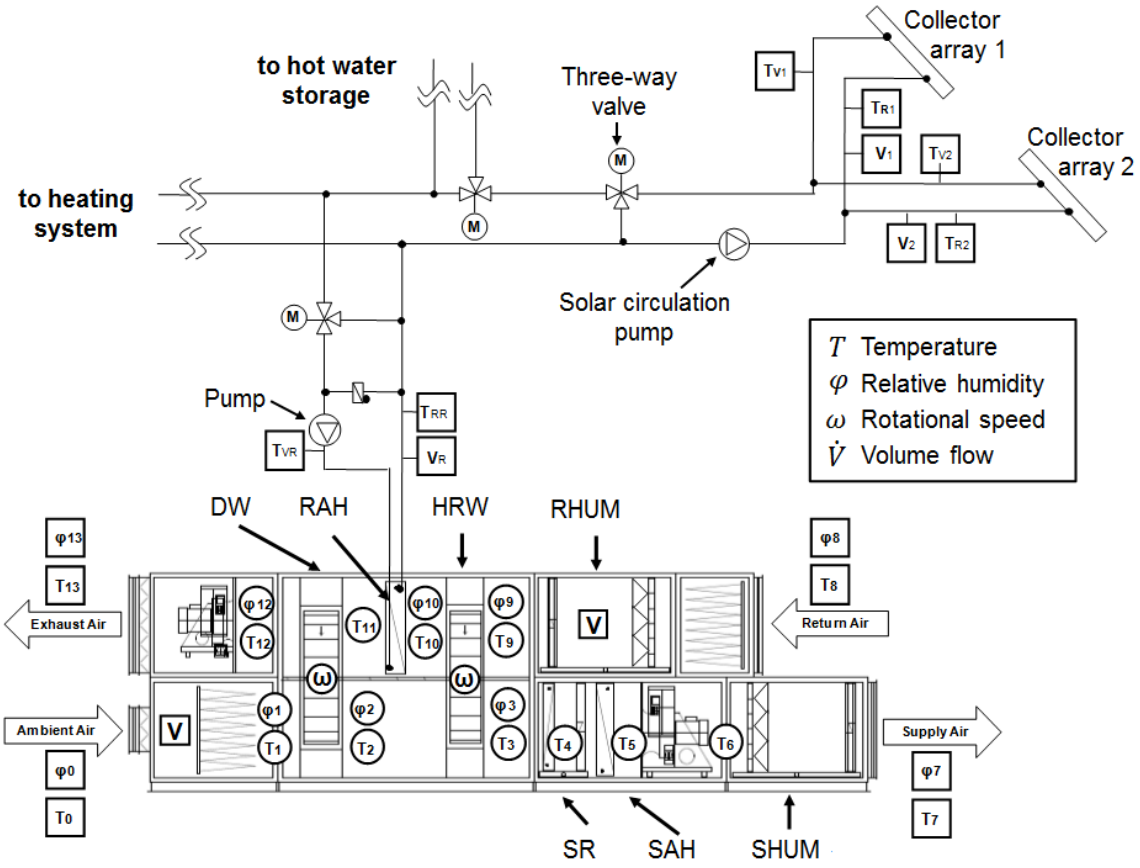

Figure 2.5: Schematic of the solar DEC-system with measurement points

In order to manage the problem of inhomogeneous air distribution in the duct, special measurement devices developed by Franzke (2008) were integrated as illustrated in Figure 2.6. Through seven pipes the air is sucked in with a fan and then mixed with a rotator, after which humidity and temperature are finally measured with the sensor.

Altogether seven measurement pipes were installed within the DEC-plant. In the supply air duct they were placed downstream of the desiccant wheel $(T_2; \varphi_2)$, downstream of the heat recovery wheel $(T_3; \varphi_3)$, downstream of the surface radiator (T_4) and downstream of the surface heater (T_5).

In the return air duct, measurement devices were placed downstream of the heat recovery wheel $(T_{10}; \varphi_{10})$, downstream of the regeneration air heater $(T_{11},$ no change in absolute humidity $x)$ and downstream of the desiccant wheel.

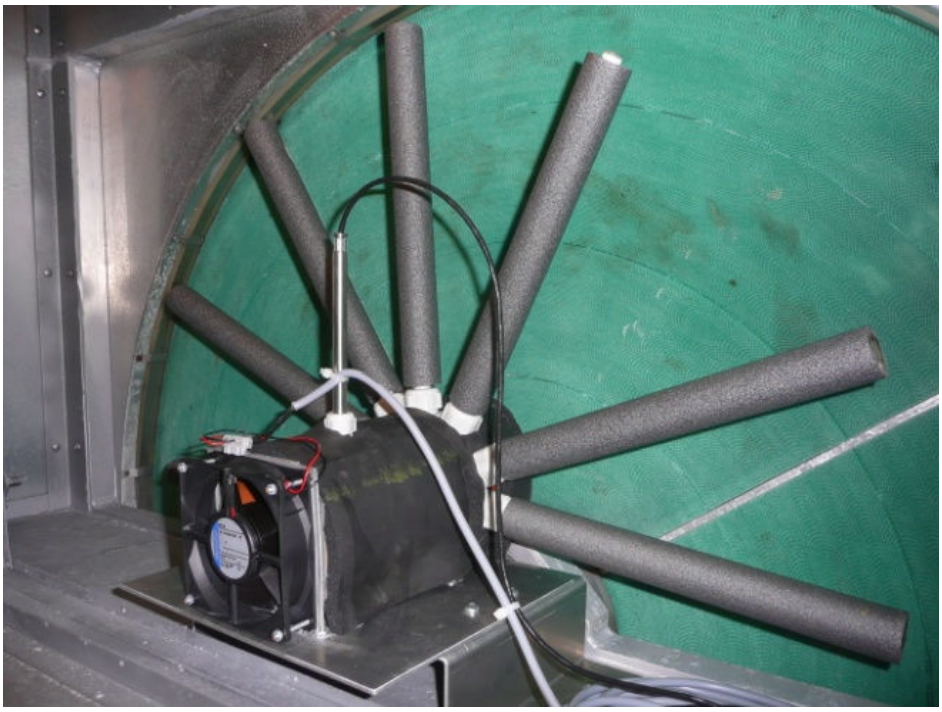

Figure 2.6: Measurement device downstream the desiccant wheel in the return air duct

As described, the existing measurement equipment was extended with additional sensors within the DEC-plant to enable an in-depth monitoring of the solar-driven DEC-process. To select reasonable sensors to be integrated for the system monitoring analysis and to determine the total measurement, an error propagation calculation was conducted. Therefore, the Gaussian error propagation law was applied (cf. VDI 2620 1973). From the quadratic sum of these measurement errors thus, the probable uncertainty $\Delta\Gamma$ was determined for the composite figure Γ.

$$\Delta\Gamma = \sqrt{\sum_{i=1}^{n} \left(\frac{\partial\Gamma}{\partial x_i}\Delta x_i\right)^2} \tag{2.17}$$

The error analysis was exemplarily carried out for the enthalpy h_{1+x} (Eq. 2.18).

$$h_{1+x} = c_p \cdot T + x\left(r_{0°C} + c_{pv} \cdot T\right) \tag{2.18}$$

This figure was expected to show the highest possible uncertainty since it is influenced by the relative humidity φ, the temperature T and the saturated vapour pressure $p_{sat}(T)$. The enthalpy is a key figure to evaluate thermal processes of open cycle systems as it implies both, temperature T and absolute humidity x and is calculated according to Cerbe and Hoffmann (1996). To determine the enthalpy, the absolute humidity x has to be deduced from the relative humidity φ and the saturated vapour pressure $p_{sat}(T)$ as described by Glück (1991). Thereby, 0.622 approximates the ratio of the gas constants of dry air and water vapour $R_{air}/R_{w,V}$ (R_{air} = 0.287 kJ kg^{-1}K^{-1}; $R_{w.V}$ = 0.4615 kJ kg^{-1}K^{-1}).

$$x = 0.622 \cdot \frac{\varphi \cdot p_{sat}}{p - \varphi \cdot p_{sat}} \tag{2.19}$$

The total error, calculated by the example of the enthalpy, was used as a selection criterion for the installed sensors measuring relative humidity φ and temperature T. In a first step, the probable error of the absolute humidity Δx is calculated.

$$\Delta x = \sqrt{\left(\frac{\partial x}{\partial \varphi}\Delta\varphi\right)^2 + \left(\frac{\partial x}{\partial p_{sat}}\Delta p_{sat}\right)^2} \tag{2.20}$$

The value of p_{sat} is identified with the corresponding temperature. Therefore the following equation is used (Glück 1991).

$$p_{sat} = 611 \cdot \exp(-1.91275 \cdot 10^{-4} + 7.258 \cdot 10^{-2} \cdot T - 2.939 \cdot 10^{-4} \cdot T^2 + 9.841 \cdot 10^{-7} \cdot T^3 - 1.92 \cdot 10^{-9} \cdot T^4) \tag{2.21}$$

Together with a total pressure of 100,000 Pa, it could be assumed, that T and p_{sat} are related linearly in the interval (T-ΔT ; T+ΔT). This linear relation allows to determine the resultant Δp_{sat} for each inaccuracy of the temperature ΔT.

$$\Delta h_{(1+x)} = \sqrt{\left(\frac{\partial h_{(1+x)}}{\partial T}\Delta T\right)^2 + \left(\frac{\partial h_{(1+x)}}{\partial x}\Delta x\right)^2} \tag{2.22}$$

$$\Delta h_{(1+x)} = \sqrt{\left[\left(c_p + x \cdot c_{pv}\right)\Delta T\right]^2 + \left[\left(r_0 + c_{pv} \cdot T\right)\Delta x\right]^2} \tag{2.23}$$

The sensors listed in Table 2.7 were selected as a result from the error calculation.

Table 2.7: Sensor details for temperature and humidity measurements

Measurand	**Sensor**		**Accuracy**
Temperature	Pt-100 (0 – 120°C)		± (0.15°C+0.002·T)
Relative Humidity	Hygro-Thermo-Meter (0 – 100°C)	<90% r.h.	± (1.3+0.3% MW)% r.h.
		>90% r.h.	± 2.3% r.h.

To give an impression of the measurement reliability of the selected sensor, the error propagation has been carried out for three significant air conditions within the DEC-process where both, adequate and high measurement errors were expected.

Thus, the calculation was performed for condition 1 ($T_{1;}\, \varphi_1$), condition 9 ($T_{9;}\, \varphi_9$) and condition 11 ($T_{11;}\, \varphi_{11}$). The calculated propagated error of the ambient air conditions upstream the DW (condition 1) give a perception of the dimensions of the error at moderate conditions. The effect of the highest possible humidity within the process is shown by the conditions of the return air downstream of the humidifier (condition 9), whereas an influence of the highest possible temperature on the measurement accuracy is determined in condition 11, regarding hot air conditions downstream of the regeneration air heater in the return air. Table 2.8 lists the results of the performed error calculation.

Table 2.8: Overview on measurement errors in diverse DEC-conditions

Measurand	Condition 1	Condition 11	Condition 9
T [°C]	30.00	60.00	17.00
ΔT [°C]	0.21	0.27	0.18
φ [%]	40.00	100.00	99.00
$\Delta\varphi$ [%]	1.40	1.30	2.30
x [g kg^{-1}]	10.70	12.60	12.20
Δx [g kg^{-1}]	0.40	1.70	0.30
$\Delta x\, x^{-1}$ [%]	3.68	13.58	2.61
$h_{(1+x)}$ [kJ kg^{-1}]	57.59	93.31	47.86
$\Delta h_{(1+x)}$ [kJ kg^{-1}]	1.01	4.30	0.82
$\Delta h\, h^{-1}$[%]	1.76	4.61	1.71

It becomes clear that the air in condition (1) at a temperature of 30°C and a relative humidity of 40% r.h., the absolute humidity is about 10.7 g kg^{-1}. With an accuracy of ±1.4% r.h. this leads to a relative humidity of between 38.6% and 41.4% whereas the absolute humidity reaches values between 10.3 g kg^{-1} and 11.1 g kg^{-1}. The enthalpy at a value of 57.6 kJ kg^{-1} shows a deviation of ±1.0 kJ kg^{-1} and ranges between 56.6 kJ kg^{-1} and 58.6 kJ kg^{-1}. The measurement deviation for the conditions of the air of 30°C and 40% r.h. therefore lies in an acceptable range. The error in condition (9) shows similar acceptable results. A high humidity up to 100% r.h. downstream the return air humidifier required a special humidity sensor with an accuracy of ± 2.3% r.h. as the conventionally adopted sensor was not approved for extreme conditions. As shown in Table 2.8 the measurement errors are unacceptably high in condition (11). This is due to the measurement of the relative humidity φ_{11} downstream of the regeneration air heater (RAH) at a high temperature of 70°C and a high absolute humidity. Thus, it was decided only to measure temperature T_{11} and to calculate the absolute humidity in condition (11) as following (Glück 1991):

$$\varphi = \frac{x}{x + 0.622} \cdot \frac{p}{p_{sat}} \tag{2.24}$$

This is applicable as the RAH only leads to a change in sensible heat but not in latent heat and therefore does not alter the amount of absolute humidity in g kg^{-1} in the air.

Apart from the additional integrated sensors, the following further sensor environment as listed in Table 2.9 was of use within this monitoring research.

Table 2.9: Additional existing sensor environment according to sensor data sheets

Measurand	Sensor	Accuracy	Annotation
G	Pyranometer (0 – 1400 W m^{-2})	15 W m^{-2}	inclined 30°
T_{amb}	Pt-100 (-30 – +70°C)	1/3 (0.3°C + 0.005 T)	radiation shielding
φ_{amb}	Hygro-thermo-meter (0 – 100°C)	2% r.h.	comb. with T_{amb}
T_{col}	Pt-100 (0 – 120°C)	1/3 (0.3°C + 0.005 T)	-
$\dot{V}_{col}$	Turbine flow-meter (0 – 120°C)	1%	-
$\dot{V}_{air}$	Flow sensor (< 80°C)	< 3 – 5%	-
$P_{el,eff}$	Effective power transmitter (AC)	< 0.2%	motors DW, HRW, fans, pumps

2.6 Operational System Analysis

Based on the measurement results, an extensive failure and operation analysis has been carried out for the diverse components of the solar-DEC-system.

The measurements and the analyses have been carried out in the cooling periods 2009, 2010 and 2011. In the following sections, the observed component behaviour is described on the basis of exemplary daily analyses. The results were verified with data from other days and years.

2.6.1 Thermal Comfort in Investigated Building

In order to acquire information on the condition within the air conditioned space, a thermal comfort analysis was carried out for the hotels breakfast and dining room in 2009 cooling period based on the comfort regulations given in DIN 1946-2 (1994)

The thermal comfort analysis of this exemplarily selected hotel room in the entire month of August 2009 showed a “comfortable” or “still comfortable” room condition (Bader et al. 2010 and Bader et al. 2010b). Only approximately two percent of the measured values could be ranked as “uncomfortably warm” during the occupied time. The temperatures within this time period ranked between minimum 20.92°C and maximum 25.92°C. The relative humidity measures its lowest value at 47.1% and reaches its maximum value at 67.94%.

However, when regarding the thermal comfort in the same hotel room only during DEC-operation on an exemplary day (August 20th, 2009), 68% of the measured values were “uncomfortably warm”. The temperatures ranged between values of 24.94°C and 25.88°C while the relative humidity reached values between 60.08% and 63.35%.

This phenomenon mainly occurred because within the entire month of August also air-conditions of cooler days and nights had an impact on the thermal comfort, while the comfort during DEC-operation exclusively reflected the thermal comfort of the room on a hot summer day.

This analysis of thermal comfort therefore showed, that the DEC-plant obviously sets the room temperature to conditions that do not meet the air condition required for thermal comfort. Also the humidity at that point is above the comfortable level. A probable reason for that might be an insufficient refrigeration capacity of the DEC-plant which therefore could not reach the targeted supply air conditions. Hence, the refrigeration capacity of the solar DEC-system was analysed and is described in the following section.

2.6.2 DEC-Plant Refrigeration Capacity

As described in section 2.1 the solar DEC-system was in operation with a reduced volume flow. The reduced air-flow rate reduced the nominal capacity of the DEC-plant to around 24 kW. To solely analyse the solar DEC-process, it has to be noted that the surface radiator has been deactivated in cooling period 2009.

The monitoring of the DEC-plant in cooling period 2009 showed that the expected refrigeration capacity of around 24 kW was not reached. The DEC-plant, which was supposed to supply peak-load cooling, only shortly reached a maximum refrigeration capacity of 15 kW. As shown for an exemplary day (August 20th, 2009), the average refrigeration capacity measured around 6 kW – 8 kW (Figure 2.7).

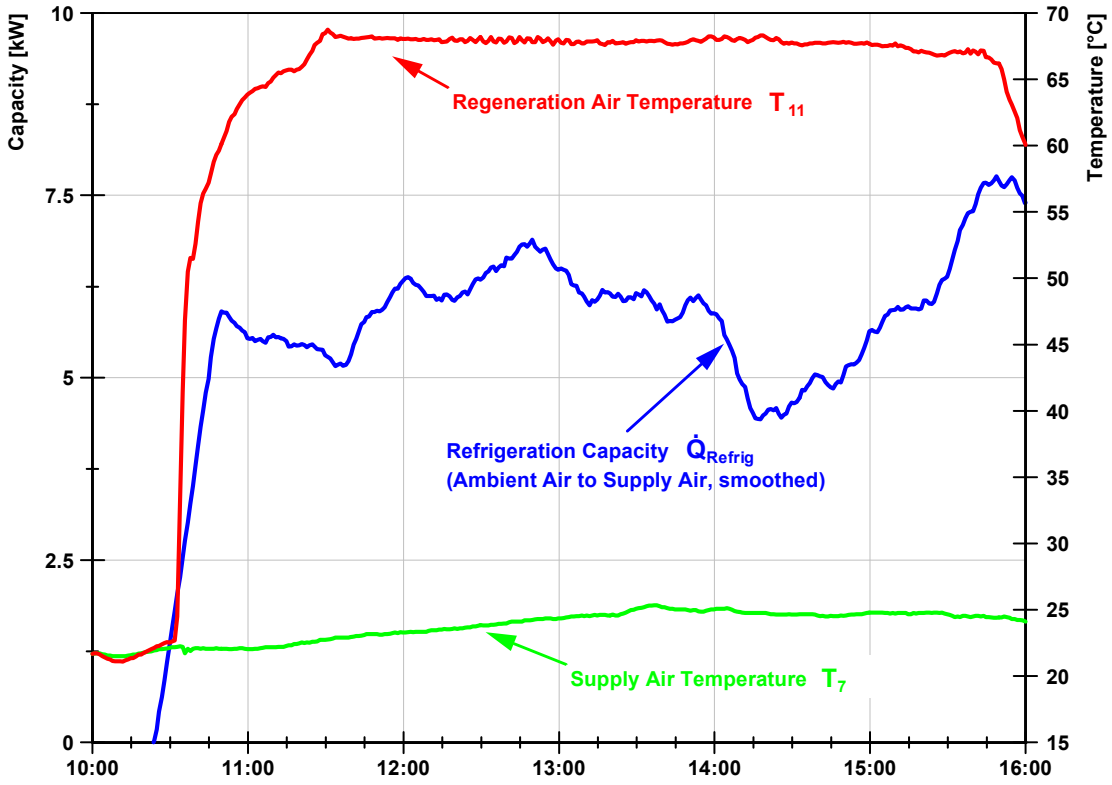

Figure 2.7: Solar DEC-plant performance for an exemplary day (August 20th, 2009)

However, the regeneration air temperature measured as stable at around 68°C throughout the entire DEC-process and therefore provides appropriate conditions for the DEC-process. On the exemplary day August 20th 2009, the supply air temperature of up to 25°C during DEC-operation has to be evaluated as too high. Especially the uncomfortable high room temperature showed that there was a higher cooling demand (Bader et al. 2010).

Analyses on diverse investigated days with DEC-operation in cooling period 2009 and 2010 (e.g. August 17th, 2009; July 22nd, 2010; August 01st, 2010) revealed a

similar result. Therefore, to investigate the reason for the considerable low refrigeration capacity in spite of a sufficient regeneration air temperature, the operation of the critical components in the DEC-process, such as desiccant wheel and heat recovery wheel was investigated in detail.

2.6.3 Desiccant Wheel Efficiency

Regarding the desiccant wheel (DW), the problem of an insufficient refrigerating capacity could derive from an inadequate dehumidification of the ambient air. Therefore, the dehumidification capacity Δx was analysed and compared to manufacturer data indentified with DW-manufacturer software. The measure dehumidification efficiency η_{dehum} was not applicable for the comparison as this figure was not available from the manufacturer.

The DW analysis on the same exemplary day August 20th, 2009 shows that the RAH heated the return air upstream the DW relatively constantly to around 68°C. (Figure 2.8, upper diagram). Therefore, reasonable regeneration conditions for the dehumidification of the DW were available throughout the entire duration of the DEC-operation.

A closer investigation of the desiccant wheel's dehumidification capacity (Figure 2.8, lower diagram) at a volume flow ratio of 1.14 (supply air to return air), shows that the desiccant wheel initially dehumidified the process air by around 4.3 g kg^{-1} dry air. Thus, at the beginning of the process the dehumidification capacity reached a value as it would be expected according to manufacturer information. However, the dehumidification capacity steadily decreased with ongoing DEC-process to around 2.5 g kg^{-1} dry air, even though the boundary conditions like the regeneration air temperature were measured as stable (Bader et al. 2011a).

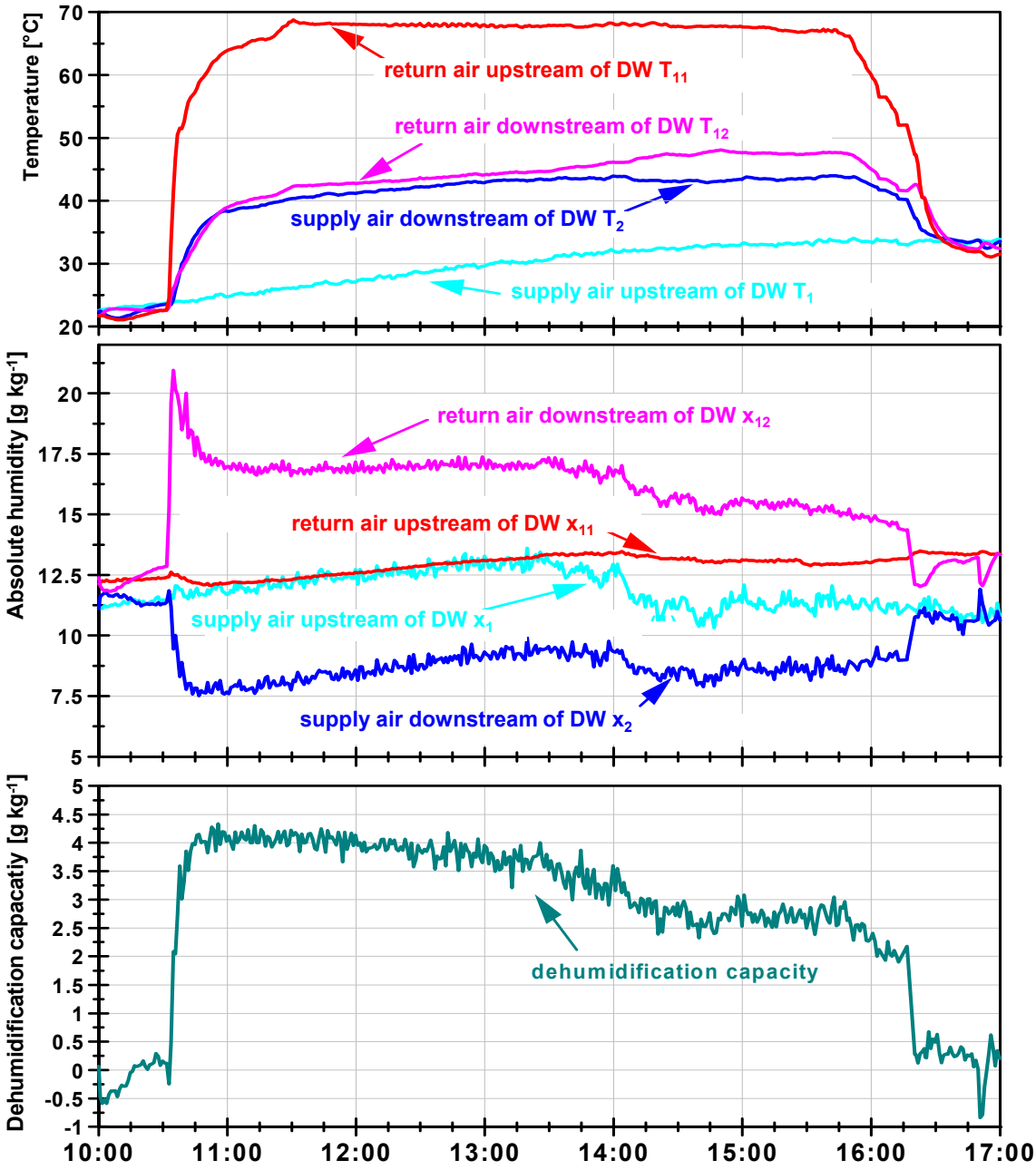

Figure 2.8: DW analysis (August 20th, 2009)

A temporary adjustment of the volume flow ratio from 1.14 to 1.05, as suggested by the manufacturer of the desiccant wheel did not result in an improved dehumidification capacity. As illustrated in Figure 2.9, the raised volume flow up to 4,750 $m^3 h^{-1}$ at 14:10 o'clock did not improve Δx. Even though all input

conditions (T_1,φ_1 ; T_{11},φ_{11}) were measured stable, Δx remained constant and rather declined slightly with time.

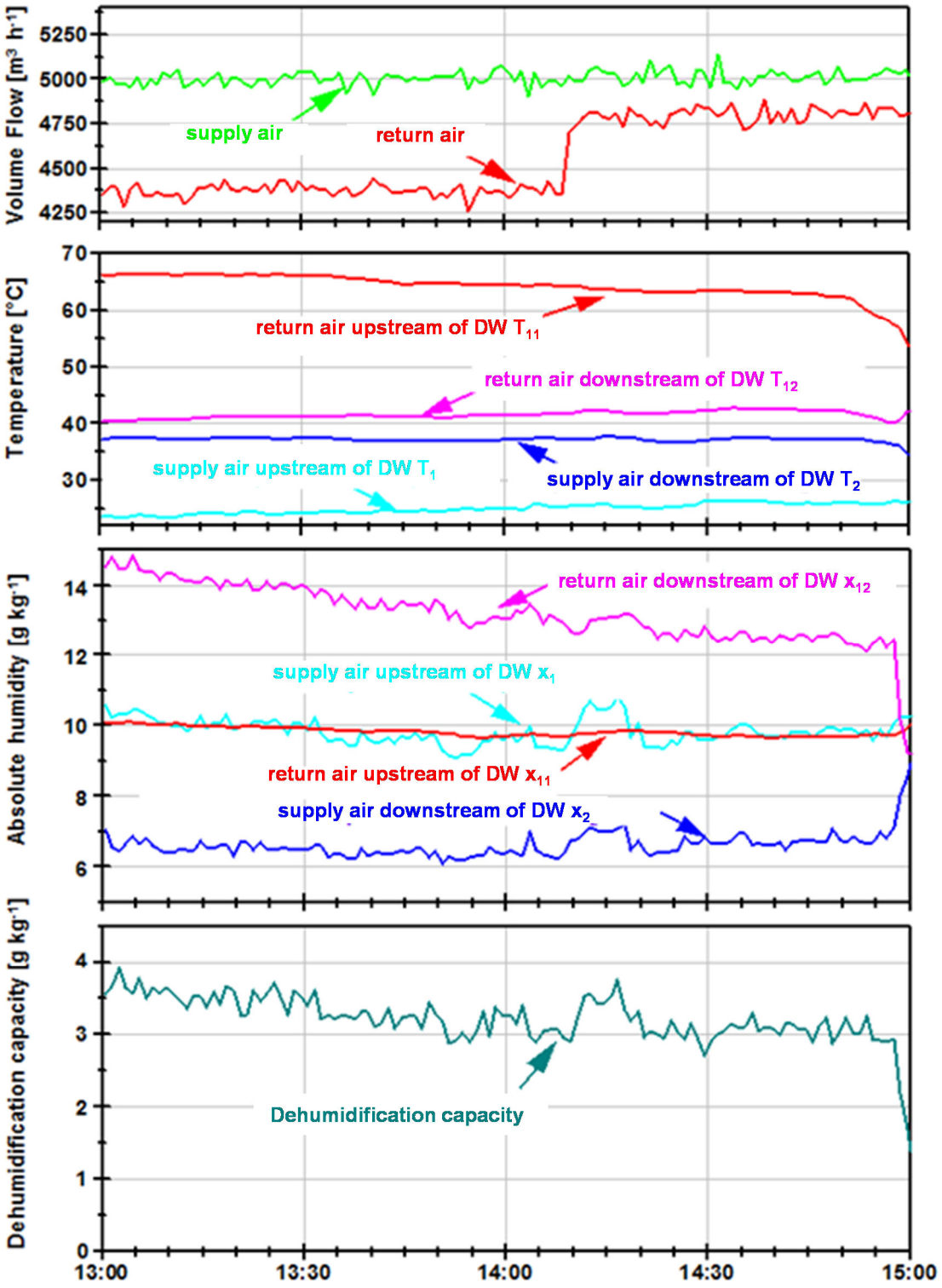

Figure 2.9: DW analysis with adjusted air flows (September 22nd, 2009)

Hence, the results are in line with those gained by Schürger (2007) in laboratory tests and could be proved under in-situ conditions.

Due to more prone measurement errors at a low relative humidity downstream of the DW in the supply air duct, higher measurement errors were in principle likely to occur at this point. In order to verify the absolute humidity downstream of the DW, the absolute humidity was as well calculated after the HRW and compared to the latter one. As the results matched and the HRW theoretically only leads to a sensible heat exchange, this proved the reliability of the measured data downstream of the DW.

As the rotational DW wheel speed was calculated from the motor frequency in cooling period 2009, it was questioned, whether another possibility for the low capacity could for instance be an unexpected varying rotational speed of the desiccant wheel, which was subject to investigations in 2010 cooling period. Therefore, the desiccant wheel was thoroughly adjusted in order to reduce leakages to a minimum and the wheel's flat drive belt was shortened in order to minimise the probability of its rotational speed varying due to a loose belt. Furthermore, frequency sensors were integrated to measure the rotational speed of the DW.

In 2010 cooling period, despite of the described implemented operational optimisations the refrigeration capacity of the solar DEC-system was re-measured beyond its expectations, as it could be proven by investigating diverse exemplary days, when the system was operating in DEC-mode (e.g. July 22nd, 2010 and August 01st, 2010).

The analysis of the desiccant wheel performance shows results comparable to 2009 cooling period. The dehumidification capacity decreased with ongoing DEC-process and did not reach the expected values according to manufacturer data. However, it could be proven that this is not caused by an inadequate wheel speed, as the newly integrated frequency measurements showed an appropriate constant wheel speed of 21 h^{-1} throughout the entire operation of the DEC-process on various days. According to the results of Schürger (2007) the dehumidification capacity of the lithium chloride desiccant wheel only decreases

with rotational speeds of above 25 h^{-1}. Therefore, the wheel speed cannot be regarded as a reason for the decreasing dehumidification capacity. The decrease in dehumidification capacity could be partly explained by a decreasing absolute humidity of the ambient air upstream the desiccant wheel as there is a trend of a higher dehumidification capacity with a higher water content of air upstream of the desiccant wheel. However, this trend does not explain the apparent decrease in dehumidification capacity in periods when the absolute humidity of the ambient air upstream of the desiccant wheel increases conspicuously. The phenomenon rather could be explained with the oversaturation of the desiccant wheel matrix. While on the one hand, the manufacturer recommends as a possible solution to raise the regeneration temperature up to 80°C, Schürger (2007) on the other hand, argues that temperatures significantly above 70°C may damage the desiccants wheel matrix.

2.6.4 Process Water Analysis

As already described by Haller (2007), calcification had been observed in previous investigations. A thorough visual inspection of the DEC-plant also revealed within this project, that calcification has not only been a major problem at the humidifier spray nozzles but proved that it affects the complete plant.

Although the whole system was cleaned thoroughly and renewed during maintenance in May prior to 2009 cooling period, already in July 2009 severe deposits of calcification were observed as shown in Figure 2.10.

Consequently, the humidifier process water was analysed with regard to water hardness in order to evaluate the effectiveness of the currently realised water treatment by an ion-exchanger.

A general hardness (GH) of the humidifier process water of max. 7°dH German degrees (corresponds to 8.87°e, English degrees; EH) is acceptable in the investigated case. The manufacturer of the humidifier unit even requires treated water with a general hardness of 3°dH (3.8°e) and a maximum electrical conductivity of 20 µS cm^{-1}. The analysis of the supplied water, however showed

a general hardness of 16°dH (20°e) and the analysis of the process water directly upstream of the humidifiers disclosed a general hardness of 11°dH (13.8°e).

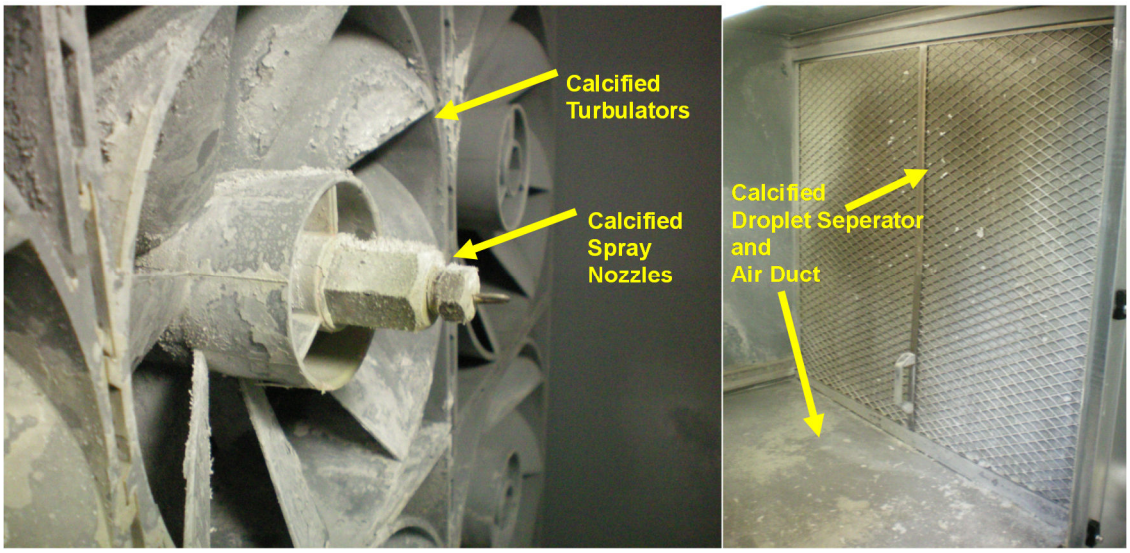

Figure 2.10: Exemplary calcification of the DEC-plant

This denotes that the water treatment was insufficient for the operation of a DEC-process. Hence, it was decided to integrate a reverse-osmosis system in addition to the ion-exchanger.

2.6.5 Heat Recovery Wheel Efficiency

As the only enthalpy reduction within the entire DEC-process is achieved by the heat recovery wheel, it represents a core component when investigating the reason for the lack of refrigeration capacity. Therefore, the behaviour of the HRW was also analysed in detail.

Figure 2.11 illustrates the process conditions for the heat recovery on the exemplary day August 20th, 2009. It was found that the heat recovery ratio only reached 58% at a rotational speed of 600 h^{-1} and a volume flow ratio (supply air to return air) of 1.14. According to information of the component manufacturer, a heat recovery ratio of 75% would be expected under the given conditions.

Hence, this component did not reach the planned efficiency. Comparable in-situ measurements carried out by Eicker et al. (2002) at the DEC-plant in Althengstett

(Germany) showed a similar difference between the measured heat recovery ratio and the expected value (Bader et al. 2011a).

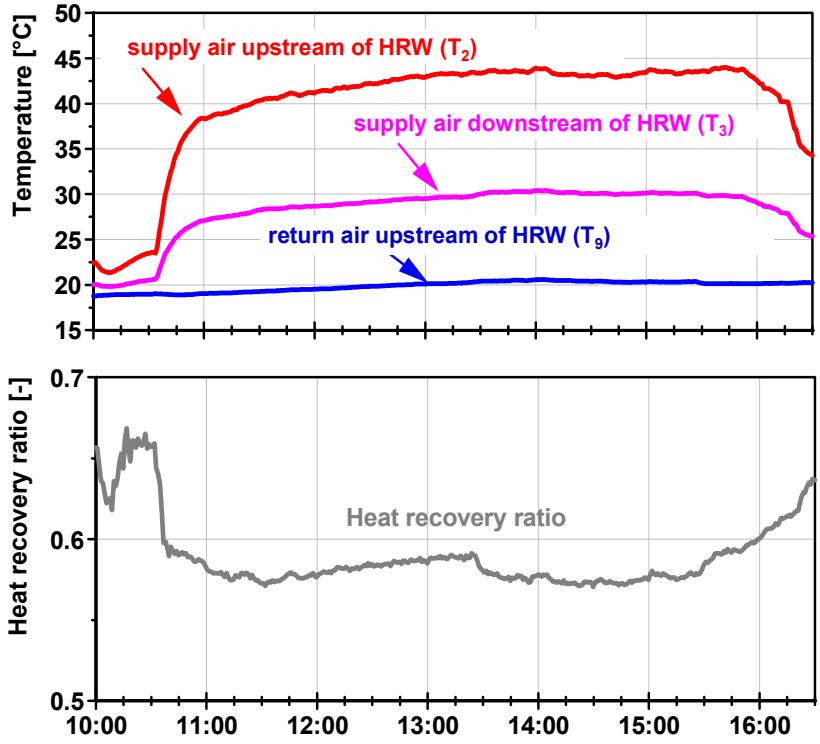

Figure 2.11: Heat recovery wheel analysis (August 20th, 2009)

In order to clean the HRW from possible calcification and dirt prior to the 2010 cooling period and to improve its heat recovery properties the heat HRW's aluminium alloy matrix was cleaned with high pressure hot water as shown in Figure 2.12.

Moreover, the calcified steel droplet separators at the humidifier unit were replaced by newly fibrous web droplet separators to filter calcifications from the air and thus minimize the impact of the hard water on further components within the DEC-process especially with regard to the cleaned HRW. This provisional measure became inevitable, as the system operator was not in the position to implement the highly recommended reverse-osmosis system straightforwardly.

Despite the implemented operational optimisation measures in the 2010 cooling period, the refrigeration capacity of the solar-assisted DEC-system was again measured far below the level of expectation on diverse investigated days

(e.g. July 22nd, 2010; August 01st, 2010). The thoroughly cleaned HRW again only reached heat recovery ratios below 60% on days with DEC-operation and, therefore, did not reach its expected efficiency as illustrated in Figure 2.13 for the exemplary day, July 16th, 2010.

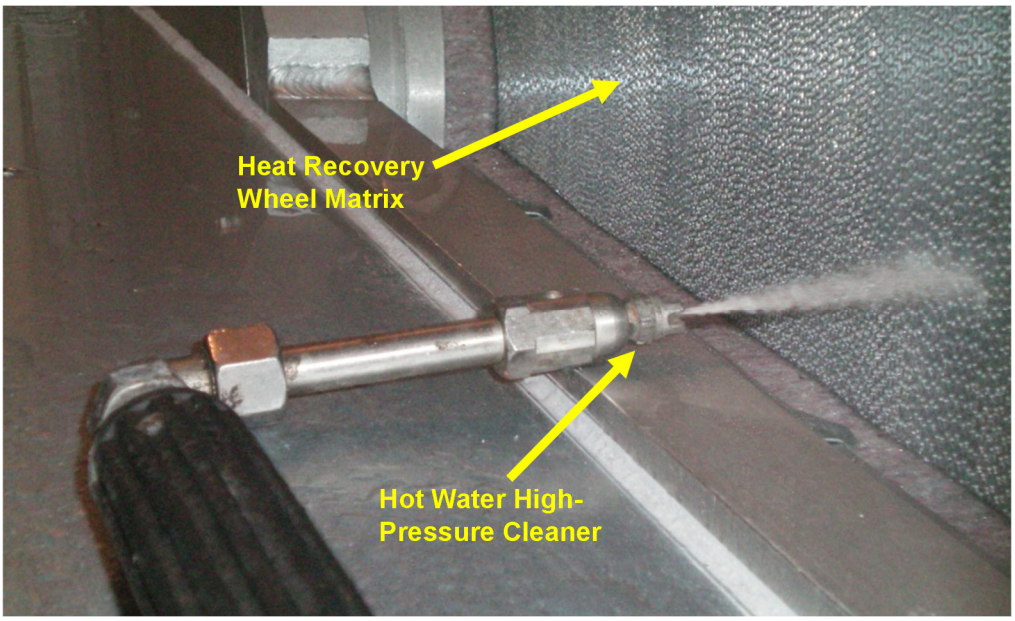

Figure 2.12: Cleaning of the HRW in May 2010

To further investigate the reasons for this deficit and to verify the effectiveness of the hot water cleaning process, the pressure drop across the wheel was measured during operation.

Considering the currently set operational volume flow rates in the supply air duct ($\dot{V}_{sup}$= 4,600 m^3 h^{-1}) and the return air duct ($\dot{V}_{ret}$=4,060 m^3 h^{-1}) the pressure drop was expected to be Δp_{sup} = 40 Pa in the supply air and Δp_{ret}= 27 Pa in the return air. The real concurrent decrease in pressure across the wheel, however, was measured as Δp_{sup}= 85 Pa in the supply air and Δp_{ret}= 62 Pa in the return air stream and is thus more than two times higher than expected.

Following these results, it was obvious that the calcification deposits in the wheel could not be reduced by hot water cleaning. In fact, the calcification may still reduce the cross section of the HRW´s aluminium alloy matrix and cause a higher pressure drop. This is clearly not only the effect of reduced heat transfer

characteristics due to declined material properties, but also due to a reduced cross section that leads to an increased air velocity reducing the heat transfer through convection.

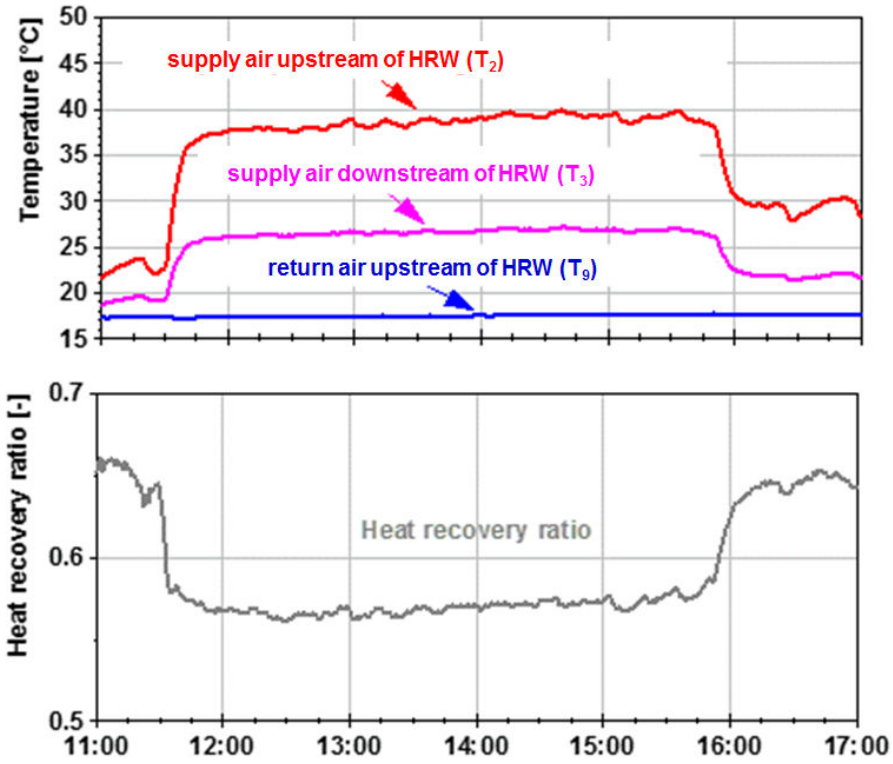

Figure 2.13: HRW Analysis (July 16thth, 2010)

Consequently, a new epoxy coated, highly anti corrosive heat recovery wheel was selected and integrated into the DEC-system (Figure 2.14). A reverse osmosis system to provide a complete water desalination for improved process water conditions was additionally recommended in order to minimise the calcification and corrosion of DEC-components. It was unfortunate to this research that a continuative monitoring could not be carried out to verify the effect of the system optimisations, because the system operator did not allow further measurement activities in the building.

As illustrated in Figure 2.15 the measured supply air temperature downstream of the HRW was compared to the corresponding simulated values. For this purpose, the simulation of the heat recovery wheel was carried out using a simple

efficiency model as implemented in the simulation environment INSEL 8 (Doppelintegral 2009).

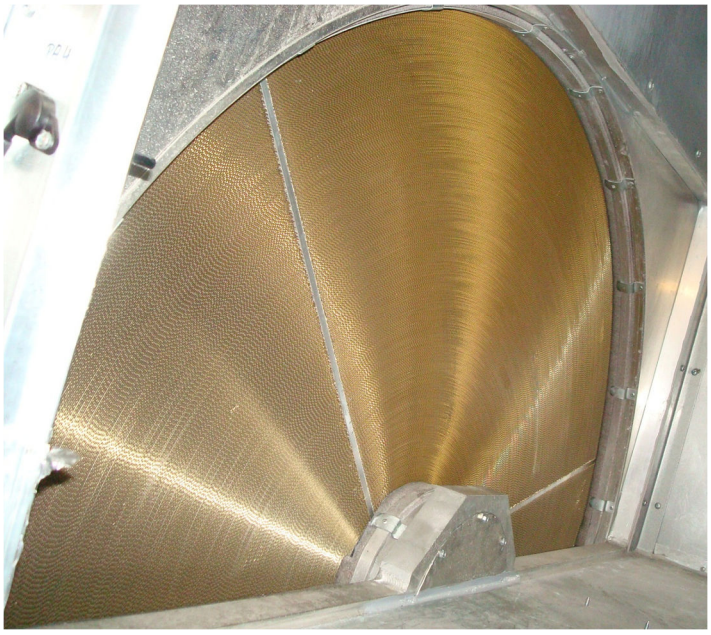

Figure 2.14: Epoxy coated HRW with anticorrosive material properties

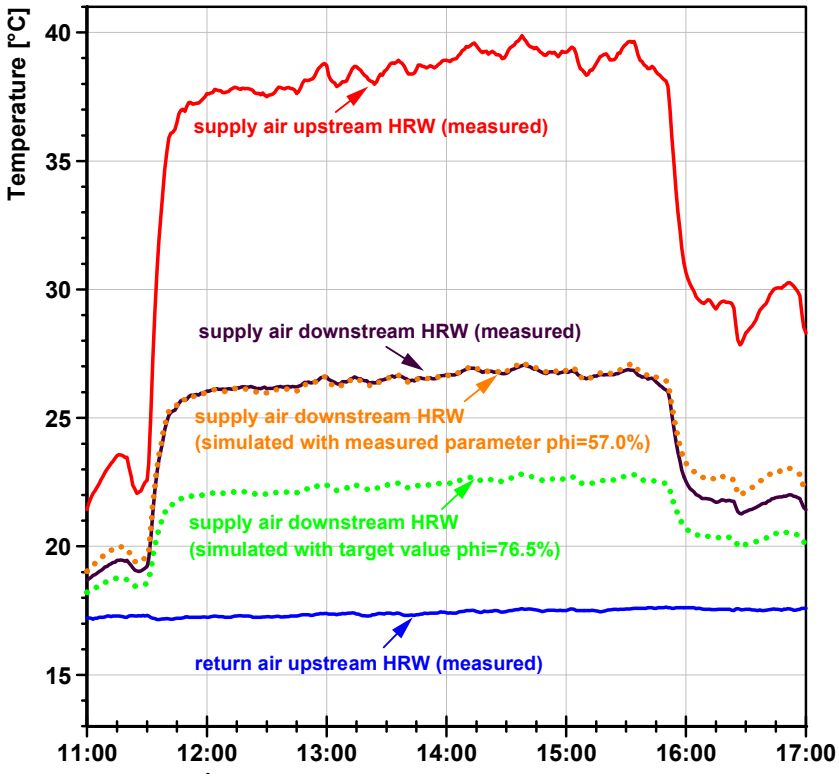

Figure 2.15: HRW Monitoring and Simulation (August 01st, 2010)

2.6.6 Solar System Integration Analysis

Both solar-thermal flat-plate collector arrays have originally been designed for the operation of a solar air-conditioning system including two DEC-plants with a nominal refrigeration capacity of 35 kW each. When evaluating the solar integration, it must be considered that only one of both DEC-plants is in operation at a reduced air flow (cf. section 2.2). According to available design information, the currently realised hydraulics and the control strategy allow the use of the solar heat either for the preparation of hot water for the hotel or alternatively for the supply of regeneration heat for the DEC-plant. As a third option, the solar heat can be used for the regeneration of the heat pump source in the building's base plate or for the heating support if required. At present, a simultaneous utilisation of the solar heat for diverse consumers is not possible with the implemented hydraulics and control strategy. Due to the dimensioning of the collector array for originally two DEC-plants, however, this would in principle be interesting from an energetic and operational point of view.

Figure 2.16 illustrates the daily operation of the solar collectors on a day with DEC-operation (August 20th, 2009). The lower diagram in Figure 2.16 shows that the flow temperature of the regeneration air heater constantly reached a temperature of 72°C to 73°C during DEC-operation. Therefore, the DEC-process was provided with an adequate regeneration temperature of around 68°C (cf. Figure 2.7). The collector arrays, however, provided flow temperatures of up to 110°C. As these temperatures are far too high for the DEC-process, they were consequently adjusted using the flow temperature mixer of the regeneration air heater, in order to reach reasonable temperatures for the DEC-process and to avoid a damage of the desiccant wheel. This indicates an existing potential of an integration of further heat sinks in the hydraulics and control of the overall solar system and furthermore shows the importance of flow temperature control of the collectors. However, it can be detected that there was obviously no interdependence between the insufficient refrigeration capacity of the DEC-plant and the integration of the solar collectors in the DEC-process in the cooling

period 2009, as solar regeneration heat was sufficiently available at a reasonable temperature level (Figure 2.16, lower diagram) during DEC-mode.

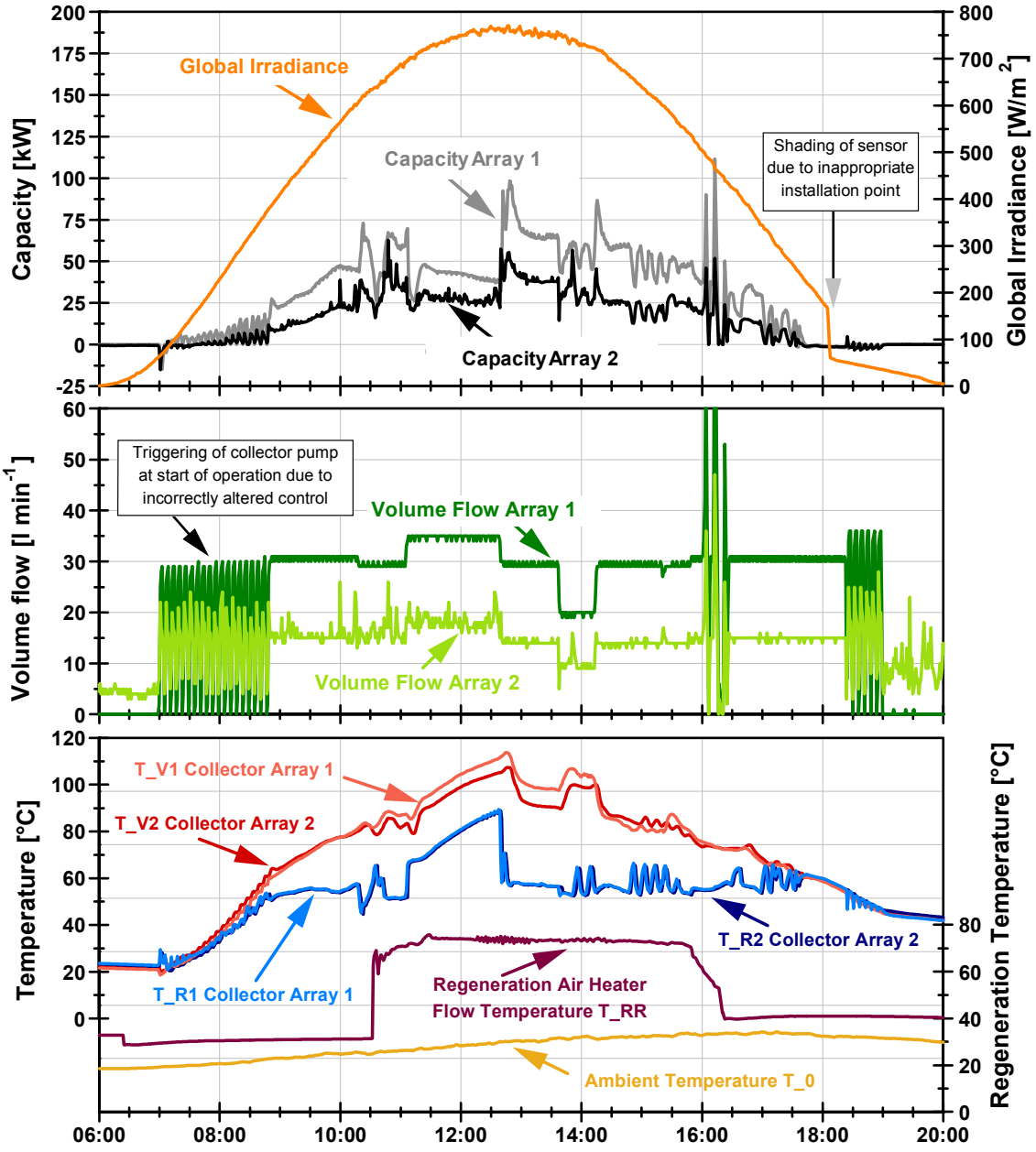

Figure 2.16: Daily operation of solar collector arrays on a day with DEC-operation (August 20th, 2009)

Regarding the collector arrays at the start of operation, it became evident that the collector pumps start is not anymore controlled depending on the absorber temperature of the hotter array. As Figure 2.16, middle diagram shows, the pump

starts at 07:00 and triggers switching on and off in 5 minute intervals until the flow temperature of collector array 2 $T_{fl,2}$ (Figure 2.16, lower diagram) finally exceeds a temperature of 60°C at around 08:50. Analyses of various additional days in cooling periods 2009/10 showed a similar behaviour and proved that the originally implemented control was obviously replaced by an insufficient time switch control (Bader et al. 2011).

The collector arrays' end of operation reveals a similar pattern of the volume flow when the collector pump is triggering again in five minute steps from 18:25 until 19:00. Due to this described control malfunction with its fixed initial time switch, it was observed that the pump triggers from 07:00 until 19:00 on days with little global irradiance without any permanent running. This control characteristic does not only contribute to the lifetime reduction of components but also causes unnecessary electricity consumption.

The collector arrays' end of operation is conspicuous for another reason. The approach of the collector flow temperatures ($T_{fl,1}$, $T_{fl,2}$) and their corresponding return temperatures ($T_{ret,1}$, $T_{ret,2}$) at 17:40 indicate that the solar heat consumption of all available heat sinks stopped at a collector flow temperature of 60°C. However, the set point which starts triggering the pump to switch off is only reached at 18:25. This proves on the one hand, that the collector fluid was unnecessarily circulated through the solar collector system for 45 min and reveals on the other hand that the currently hydraulics and control cannot use these heat quantities, e.g. to regenerate the heat pump source in the ground storage. After the end of operation at 19:00, the flow rate within collector array 1 remains at an average level of around 10 l min^{-1} (Figure 2.16, middle diagram) and therefore leads to negative collector capacities at night time since the circulating collector fluid is of a higher temperature than the ambient temperature T_{amb} at night time.

Figure 2.17 illustrates the end of the DEC-process on July 22nd, 2009 which can be regarded as representative for this kind of system condition.

At around 15:50 the DEC-process stops operating as the regeneration air heater flow temperature drops below its critical set point caused by insufficient collector flow temperatures (Bader et al. 2011 and Bader et al. 2012).

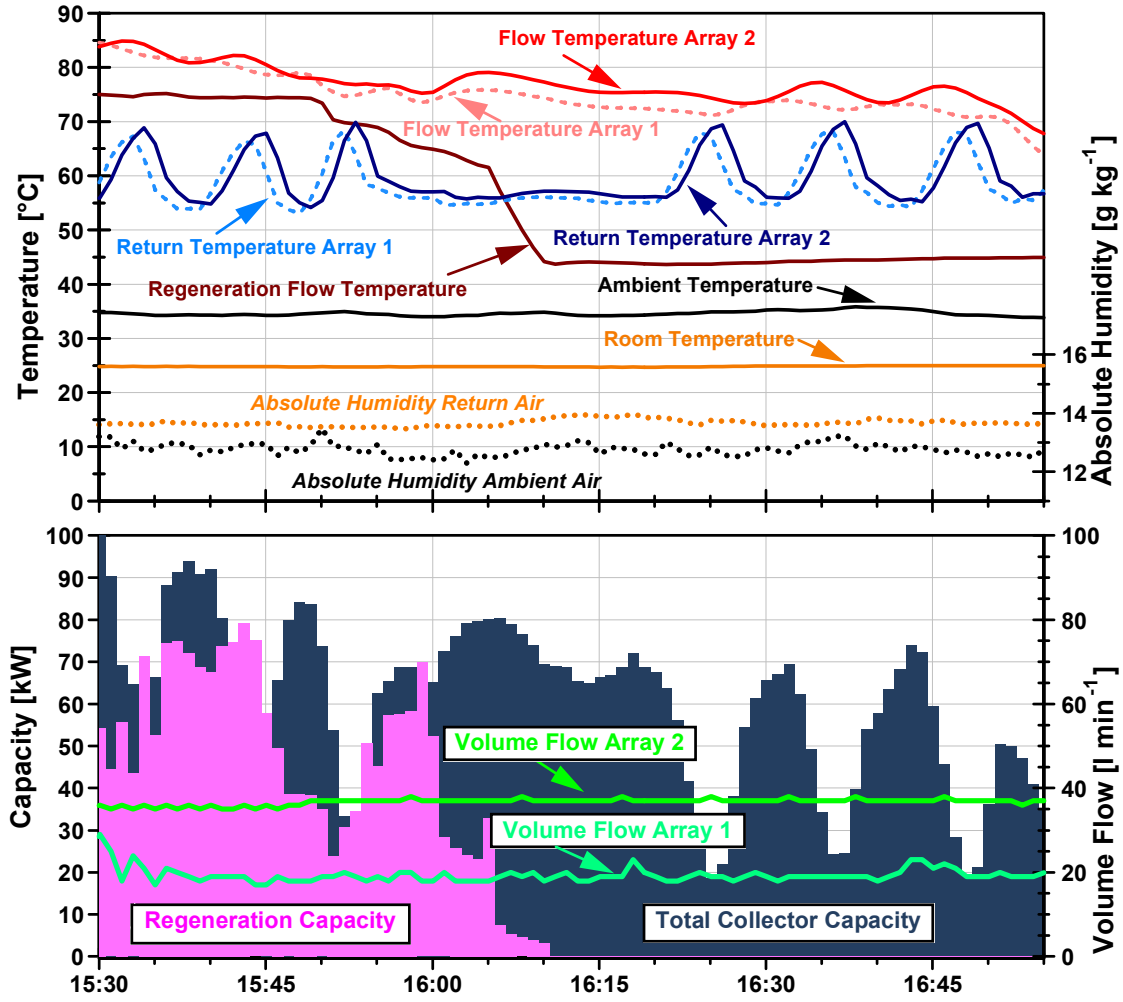

Figure 2.17: Solar integration analysis at DEC-process end (July 22nd, 2010)

The room air conditions with a room temperature of T_{room} ≈ 25°C and an absolute humidity of the room air (approximates T_{ret} due to mixed ventilation) x_{room} ≈ 13.7 g kg^{-1} at the end of the DEC-operation can be seen as inappropriate for a conference room of building category II according to EN 15251 (2007). Together with the unaltered high ambient air conditions (T_{amb} ≈ 25°C; x_{room} ≈ 13.0 g kg^{-1}) within the same time period it becomes evident that the DEC-process stop was not actuated by the DEC-control due to a change of air-

conditions respectively cooling load but in fact by insufficiently provided regeneration conditions in form of heat at a reasonable temperature of above 75°C.

The volume flows, as illustrated in Figure 2.17 lower diagram, of both collector arrays remain constant throughout the entire time span at levels of around 20 l min^{-1} (collector array 1) and 40 l min^{-1} (collector array 2). However, a decrease of collector volume flows by means of an intelligent solar DEC-integration control lowering the pump power would be expected in order to lengthen the DEC-systems operation in sorption mode. The total solar collector capacities of above 70 kW after 16:00 indicate a continuous availability of solar heat after the end of DEC-operation, which then partly supply other heat sinks (e.g. hot water storage, ground storage) and cannot be utilised by the DEC-process (Bader et al. 2012).

2.7 Conclusions and Recommendations

The focus of the first part of this research was a detailed in-situ monitoring of the solar-driven DEC-plant and an associated continuous failure and operation analysis to deduct optimisations for future systems. The results have been verified for different exemplary days in different cooling periods. Thereby the monitoring experiences disclosed that this technology was not mature, neither on component level nor on system level.

Franzke and Heinrich (1997), Franzke and Seifert (2005), Henning (2004a, 2004b), Schürger (2007), Solair (2009) as well as Eicker (2001, 2009) give basic recommendations for solar DEC-air-conditioning. In addition to those guidelines, the recommendations derived from the in-situ monitoring analysis by means of measurement results and experiences with a system in operation in a real industrial installation are summarized below. Thereby, recommendations are dedicated to component selection, system planning and system operation.

As described, the water quality at a site is crucial for the successful operation of a solar DEC-system. Therefore, it is strongly recommended to carry out a site-specific raw water analysis before further planning of a solar DEC-system. This initial water analysis shall be carried out to meet the requirements of guideline VDI 3803-3 (2014) and hence to create a well-founded basis for selecting the needed appropriate water treatment appliances.

With regard to the monitoring results and experiences, the integration of a reverse-osmosis system downstream the ion-exchanger is indispensable for solar-DEC-systems to ensure a complete desalination of the process water. This is essential for an accurate operation of the humidifier spray nozzles as well as to avoid the calcification of the plants air-ducts and the matrix of the heat recovery wheel.

In addition to a thoroughly designed water treatment system, future systems are recommended to be planned with an epoxy coated heat recovery wheel. The epoxy coating of the heat transfer aluminium alloy matrix creates a greater resistance towards surface corrosion and hence bears less corroding surface for calcification.

The in-situ investigations showed that the diverse suppliers of sub-systems to the multivalent solar-DEC-system individually planned the respective sub-systems (e.g. DEC-plant or solar collector array). However there was no holistic approach and involvement of component and subsystem suppliers. This obviously led to a deficient adjustment of subsystems and therefore to a suboptimal composition of the overall system, which was observed to be the cause for diverse system failures during system operation.

For future system planning, the design and definition of the supervisory control strategy of the overall system must be of high priority during the system planning phase.

In this context, it is suggested that for the system planning, the adaption of the different subsystems should go beyond the conventional approach of system integration, integrating the solar subsystem into the DEC-process. The planning

of future systems is rather recommended to follow an approach of system inclusion, where all system parts are subject to adaption with regard to an optimal overall system concept.

It should be noted that uncoordinated interventions of the system user and operator, e.g. in the system control and system adjustment reduced the system efficiency and contributed to unnecessary energy consumption. Therefore, the development of system concepts that consider a minimum of possibilities for manual intervention are recommended.

Further recommendations regarding planning of multivalent solar DEC-systems are:

- design a fresh air regeneration of the desiccant wheel with ambient air in operation times when the absolute ambient humidity is less than the absolute humidity after the HRW in the return air duct;
- integration of an optional air re-circulation for operation times at high absolute outdoor humidity or very low outdoor temperature;
- design the return air humidifier as a circulating water humidifier in order to reduce water consumption; and
- consideration of the user behaviour and the room occupancy as relevant parameters in the system control.

Considering the operation of the DEC-system, recommendations are:

- consider inspection of the DWs' and HRWs' drive belt and the adjustment of leakage panels as a standard part of any system maintenance;
- implement a continuous automated monitoring of the water quality at the humidifiers and thus secure the operational capability of the water treatment appliances e.g. ion exchange in series with a reverse osmosis system;
- consider an automated monitoring of the DW and HRW rotational speeds; and
- carry out intensive training and supervision of the system operators in taking care of complex energy systems.

3 Multivalent System Simulation Model

3.1 Literature Review

3.1.1 Simulation Studies on Solar DEC-Technology

Within the scope of existing research on solar DEC-systems, a number of investigations by means of simulation studies have been accomplished.

Already Dunkle (1965) published a method of solar air conditioning and describes the use of desiccants as a promising alternative air-conditioning technique, being combined with evaporators and heat exchangers. Nelson et al. (1978) carried out simulation studies regarding the feasibility and performance of open cycle desiccant systems using solid desiccants and solar energy. Barlow (1981) conducted an analysis of solar desiccant systems and concepts and Duffie and Mitchell (1982) performed a component and system evaluation study of solar desiccant cooling systems.

Pesaran et al. (1992) carried out an assessment of the desiccant cooling technology for the National Renewable Energy Laboratory (United States). The report gives a detailed overview on the existing component and system models for the simulation of DEC-systems. In another assessment of the desiccant cooling and dehumidification technology for the US department of energy, the Oak Ridge National Laboratory (1992) states numerical simulation activities at the University of Illinois at Chicago. The developed simulation program contains routines to calculate a solid desiccant wheel, a constant-effectiveness heat exchanger, a regenerative heat exchanger and both direct and indirect evaporative coolers.

Jain et al. (1995) conducted simulation studies on various DEC cycles for Indian climates. Erpenbeck (1999) carried out a theoretic analysis on the potential and system behaviour of solar DEC-air-conditioning based on simulations in TRNSYS. Davangere et al. (1999) simulated a solid desiccant air-conditioning

system with a backup vapour compression system and evaluated the performance of the system with regard to its feasibility in four cities in the United States. Beggs and Halliday (1999) carried out a theoretical evaluation of solar-powered desiccant cooling technology in the United Kingdom. Thereby, they investigated the potential for exploiting solar energy to drive desiccant cooling systems in the UK. Parametric energy studies were accomplished using a solar desiccant computer model developed at the University of Leeds. Optimised control strategies for DEC-plants without solar integration were analysed by Rathey (2000).

Henning et al. (2001) analysed the potential of solar energy use in desiccant cooling cycles. The overall simulation model including building load, solar cycle and DEC-system were modelled using the simulation software TRNSYS 1994 with the subroutines Type 275 and Type 276. A parametric study showed that combined solar assisted DEC-systems (desiccant and chiller) are feasible from an energetic and economic point of view, especially in warm-humid climates and reach primary energy savings up to 50 %.

Hoeffker (2001) published a thesis regarding desiccant cooling. The simulation study was carried out using modular simulation tool for dynamic thermal building simulations in the MATHEMATICA 1996 environment. Simulations for a DEC-system combined with solar air collectors were conducted for the sites of Stuttgart, Phoenix, Seville and Djakarta.

Mavroudaki et al. (2002) investigated the potential of solar powered desiccant cooling in southern Europe. The study demonstrates that single-stage solar desiccant cooling is feasible in parts of southern Europe, provided that the latent heat gains are not excessive. System simulations regarding the development of control strategies for solar-assisted DEC-systems with air collectors are published by Eicker (2002) and Eicker et al. (2006). Möckel (2003) developed a simulation model for an open-cycle DEC-plant and carried out numerical analyses. Ginestet et al. (2003) performed simulation studies of DEC-system with the SIMBAD library in the Matlab/Simulink environment. The analyses were

carried out with regard to the design of control of the open-cycle process to reduce the energy consumption.

Hirunlabh et al. (2007) conducted a feasibility study of desiccant air-conditioning systems in Thailand. Wurtz et al. (2005) performed a parametric analysis of a solar DEC-system using the SIMSPARK environment linked with Energy Plus. Simulations results show that humidifiers efficiencies and rotating heat exchanger efficiency have a major influence on the system performance. Franzke and Seifert (2005) developed the simulation tool SOLAC for the design of solar air-conditioning applications.

Beccali and Nocke (2007) emphasize the role of selecting an adequate computer based design tool being applied in the system planning phase. However it is further mentioned, that there is not yet a tool available unifying the diverse requirements at the different levels of the planning phase.

Daou et al. (2006) give an extensive overview on feasibility and performance studies of desiccant cooling systems focussing on system simulation. Schürger (2007) carried out investigations into solar powered adsorption cooling systems and developed a simulation model for desiccant wheels. Kohlenbach et al. (2007) discuss modelling and simulation of the DEC-system performance in particular systems or applications. Vitte et al. (2007) developed a proposal for a new hybrid control strategy for a solar DEC-system based on the modelling of the system in TRNSYS. Further studies by Vitte (2007), Pietruschka et al. (2009) and Pietruschka (2010) investigate the control of the DEC-process. Ruivo et al. (2007) analyse the modelling of DEC-components like the desiccant wheel. Chung et al. (2008) conducted numerical simulations regarding the optimisation of desiccant wheel speed and the area ratio of regeneration to dehumidification as function of regeneration temperature.

A solar-assisted pilot plant was simulated in Palermo (Italy) by Beccali et al. (2009a) and Beccali et al. (2009b). Fong et al. (2010) carried out a comparative study of different solar cooling systems for buildings and developed optimisations of solar-assisted desiccant cooling systems for subtropical Hong Kong based on system simulations. They further investigated in simulation studies a solar hybrid

air-conditioning system for high temperature cooling in a subtropical city. Ouazia et al. (2009) describe the performance of a DEC-system based on simulation results in TRNSYS. Simulation results are discussed with regard to energy efficiency and thermal comfort and show that the investigated system is especially well suited for areas with a high latent load. Besides an experimental analysis Panaras et al. (2010a) present a theoretical investigation of the performance of a DEC-system. A theoretical model to simulate the operation of a DEC-system is described and the results confirm the potential of the technology.

In further simulation work Panaras (2011) deducts design parameters for DEC-systems and investigates their effect on the system performance. Pietruschka (2010) carried out model based investigations on the control optimisation of renewable energy based open DEC-system. Heidarinejad and Pasdarshahri (2010) developed a mathematical model of a DEC-plant based on the transient coupled heat and mass transfer to predict the performance of the system under various design and operational conditions. Simulation results show the availability of an optimum regeneration temperature and rotational speed in which the supply temperature reaches a minimum value. Oorschot (2010) carried out a simulation study on a DEC-system. The goal of this research is to find the optimal strategy for controlling of the DEC-components in the Dutch climate.

Concina et al. (2011) simulated the solar assisted DEC-air-conditioning technology for different climate zones of the United States. Rachman et al. (2011) conducted a feasibility study and performance analysis of the solar assisted desiccant cooling technology in hot and humid climates. The study investigated the impact of ambient conditions and the efficiency of the key components DW and HRW on the supply air conditions of a solar desiccant cooling system. Parmar et al. (2011) provided an extensive review on the solar desiccant system including simulation studies and parametric studies on component and system basis. Vukits et al. (2011) carried out a simulation study of the solar DEC-technology in TRNSYS based on a model validation with measurement data gained in an in-situ monitoring in Gleisdorf (Austria).

Using a mathematical model to simulate the physical properties of air Hatami et al. (2012) carried out a study on the optimisation of the solar collector surface in a solar DEC-system. The typical configuration with a desiccant wheel, a heat exchanger, a spray nozzle humidifier and a solar thermal driven regeneration air heater showed that the necessary solar collector surface decreases with increased supply air temperature, supply air humidity ratio and increases with an increased regeneration air temperature.

The research on simulation of solar DEC-systems, however, solely concentrated on the DEC-plant and its combination with the solar collectors. Most research studied the impact of diverse component and system parameters on the performance of a solar DEC-system. Several research groups also model and study the performance of DEC-system components, whereas the modelling and investigation of the desiccant wheel plays a central role.

Regarding simulation studies that target the investigation of the entire solar DEC-system most analyses are carried out to research the effect of parameters on the system performance. Apart from performance analyses a number simulation studies investigate the feasibility of the technology and its potential for various applications and climates.

The simulation studies neither discussed the integration of the solar DEC-technology in the further building environment nor the interaction with further solar heat sinks in a system approach where solar heat is utilised for DEC-air-conditioning, hot water supply and heating. Previous research did not focus on the research of design and dimensioning multivalent systems. However this is the subject of the simulation study carried out in this research.

3.1.2 Solar DEC-System Component Modelling

3.1.2.1 Solar Collector Array

A simulation model for the modelling of solar flat plate collectors is described in the report of IEA SHC-Task 26 (2002) and was developed for the simulation

environment TRNSYS. The model was developed based on flexible physical equations which can be adapted to different collector characteristics and weather conditions as well as to a dynamic mode of operation.

Other physical solar collector models are described by Gniewosz (1999). Based on the characteristic collector data (material, dimensions, technology), the physical correlation function and the input parameters solar radiation, ambient temperature, wind speed, mass flow and inlet temperature the simulation model determines the collector outlet temperature. Two different modelling approaches are introduced that are applied to two different types of collectors. The first model defines the heat transfer to the collector fluid as a function of the incident solar energy. Based on the usable heat capacity, a differential equation is defined for the collector return temperature. This enables the specification of the time response of the solar collector. However, this first model does not allow the evaluation of measures relating to the elimination of convection. Therefore, a second model was developed to assess measures to eliminate convection. The detailed physical equations of the described models are based on Duffie and Beckman (1991) as cited by Gniewosz (1999).

The solar collector model available in the simulation environment INSEL 8 is based on physical relationships of the efficiency curve of a flat plate collector according to EN 12975-1 (2001) and is presented in detail in section 3.5.1. Reiter (2008) developed a model of a flat-plate collector in Carnot toolbox of the simulation environment Matlab Simulink. The model has been specially developed for the analysis of heat transfer characteristics and collector component development. Various simplifications have been made in order to determine the boundary conditions of the model.

In addition to these physical models of solar collectors other models are based on mathematical approaches being dissolved with numerical methods. The mathematical model of Shpilrain et al. (1989), for example, describes the behaviour of a flat plate collector for practical optimisation calculations. Another mathematical approach for the dynamic simulation of flat plate collectors is given by Wolf et al. (1981). This model is based on fundamental physical laws and

parameters of solar collectors and in particular reproduces the interaction of the several collector parts on its efficiency and on the return temperature. The model is based on differential equations and was implemented with CSMP-simulation language (Continuous System Modelling Program). It was used to analyse the mode of operation of different solar collector designs as it even allows to simulate measures such as the heat transfer coefficient between absorber and fluid. The numerical model approach by Hilmer et al. (1999) also provides a dynamic calculation of the solar collector characteristics taking into account varying mass flows. A further numerical model was developed by Oliva et al. (1991) in order to predict the thermal behaviour of solar collectors, especially with regard to the heat transfer inside the collector. The model is able to take into account various parameters, such as for example a non-uniform distribution of the fluid or collector shading.

An empirical collector model that was developed by means of characteristic curves derived from experimental results is available in the Carnot toolbox in Matlab Simulink (Hafner et al. 1999). The model divides the collector into finite nodes and calculates the energy balance for each node by means of a differential equation taking into account the specific heat capacities of fluid and collector.

3.1.2.2 Desiccant Rotor

Most publications on simulation models of DEC-system components apply the desiccant wheel. In the 70s, it was possible to model the heat and mass transfer of the sorption process using the finite difference method. These models require extensive input parameters and were characterized of a high computing time. Therefore, these models were not very suitable to model a sorption wheel for the simulation of complex solar DEC-systems. In addition, the application of the models was challenging as the required detailed input variables were often not available in practice (Pesaran et al. 1992)

Banks (1972) already developed a simpler method for calculating the heat and mass exchange of rotating storage masses. Thereby, the potentials for

temperature and humidity transfer are deduced from the material properties of the applied storage materials. Banks used mainly the sorbent silica gel to validate the models. Gutermuth (1980) carried out investigations for storage materials based on lithium chloride and developed a model that dissolves the transport and balance equations for heat and mass transfer numerically using the characteristics method. The model was used to analyse the impact of varying process air input parameters on the outlet air conditions. Henning (1993) applies a similar modelling approach as Banks, where the process outlet conditions are dependent on a gradient similar to an isenthalpic and limited by an isoplethe curve (air states of constant relative humidity), which is determined by the condition of the regeneration air. Jurinak (1982) as cited by Dumont et al. (2013) uses the approach of the potential functions to model the desiccant wheel. Both potentials are expressed as a function of temperature and absolute humidity and allow the affiliation of the desiccants wheel efficiency figures. In this modelling approach the functions are solved iteratively.

Pfeiffer (1986) developed a model that calculates a maximum dehumidification capacity. The results of this modelling approach can be regarded as a point of reference of the real value. Franzke (1990) devised a numerical model describing a coupled heat and mass transfer for a desiccant wheel impregnated with lithium chloride. The model assumes resistances for transfer of material only with the air, where temperature and absolute humidity are considered as the driving potential of the dehumidification process. Thereby, the model assumes the humid air as ideal mixture and the material properties are kept constant over the entire process. The storage behaviour of the wheel is modelled homogeneously. Diffusion and heat transfer in the axial direction can be neglected. The humidity transfer is set proportional to the gradient of the absolute humidity.

The physical desiccant wheel model of Erpenbeck (1999) is based on the supposition of the mass and enthalpy balance inside the wheel. The dehumidification procedure is modelled in the h-x-diagram as a function of temperature and humidity, whereas the course of this dehumidification function is determined by the change of these variables. The inlet conditions of supply and

exhaust air into the rotor form the boundaries of the dehumidification course. Thus, the model determines the supply air conditions downstream of the wheel based on the conditions upstream of the wheel in the supply air and in the return air. Therefore, the conditions of the dehumidification function are calculated until the relative humidity of the supply air downstream of the desiccant wheel equal the limit state of the relative humidity upstream of the desiccant wheel in the return air duct.

The base of a further numerical model of Franzke and Stangl (2000) is the calculation of mass and energy balances for a volume element. This numerical model is to be considered one-dimensional. The air-sided heat and mass transfer coefficients determine the resistance of the heat and mass transport. Furthermore, the thermodynamic properties of the storage material are regarded homogenous without radial transfer of the moisture and temperature. In addition, the air is considered as an ideal mixture. Heat conduction and diffusion in axial direction are neglected. Moreover, the humidity transport and the gradient of humidity are considered to be proportional.

A further numerical simulation model for the desiccant wheel is described by Ginestet et al. (2003). The entire simulation of the air conditioning system was carried out using Matlab Simulink. Thereby, the components of the air conditioning system were specifically modelled for this simulation environment. The model of the sorption wheel is based on the theory of Banks. The detailed calculation approaches can be taken from Banks (1972) and Banks (1985).

Beccali et al. (2003a) developed a parameter model for the desiccant wheel based on available measurement data provided by desiccant wheel manufacturers. Using the measured data, the empirical relationships of different fabricate and sorbent could be deduced. With the input data of ambient air conditions and regeneration air the model calculates temperature, humidity and enthalpy of the supply air using a linear approach. With the help of field data Beccali et al. (2003b) derived the corresponding parameters for the specification of the model properties for three sorption wheels with different manufacturer and material (Seibu Giken: sorbent silica gel; Munters: silica gel; Klingenburg: lithium

chloride). The model had been validated for different air flow rates. An empirical correlation of the absolute humidity and temperature of the supply air downstream the desiccant wheel was deduced. In addition, model variants were created to simulate different supply and return air volume flows and bypasses.

The model of Casas et al. (2005) depicts a homogenous, unified desiccant wheel consisting of a supporting structure and the sorption material and taking into account the corresponding specific heat capacities. Similar to the model of Franzke (1990) this model neglects an axial heat transfer. The heat and mass transfer of the matrix is modelled with global transfer coefficients. The model was implemented in the Modelica library and enables both stationary and dynamic calculations. Joos et al. (2008) further developed and improved the model of Casas et al. (2005) with special consideration of the wheel rotation. The structurally improved model allows faster computation times and is thus offering the possibility for long-term simulation.

Nia et al. (2006) developed a model to simulate the combined nonlinear heat and mass exchange of a desiccant wheel with solid sorbent based on correlation functions with temperature and humidity as input parameters. The model enables the investigation of the desiccant wheel performance and its optimal rotational speed.

Brychta and Pol (2007) describe approaches to model individual components of solar-DEC-systems. In this context the TRNSYS model "Type 275" developed at the *Fraunhofer Institute for Solar Energy Systems* is referenced. The overall model allows the simulation of desiccant wheels as well as heat exchangers and humidifiers. The desiccant wheel model is based on simple physical correlations. Both, the specific heat capacity and the air mass flow of supply air and return are equated. The maximum achievable dehumidification capacity Δx_{max} results from the difference of the absolute humidity of supply and return air upstream the desiccant wheel. Thereby, the model considers a defined sensible and latent efficiency.

The mathematical model of De Antonellis et al. (2010) considers the effect of various input variables on the operation of the desiccant wheel in order to identify

an optimal rotational speed. The model assumes a one-dimensional air flow and a uniform, homogenous wheel matrix. Temperature, humidity and air velocity at the inlet are assumed to be homogenous and the heat and mass transfer between adjacent matrix tubules is assumed to be negligibly low. Furthermore, specific heat and thermal conductivity of dry air and water vapor is considered to be constant. An air exchange between supply and return air stream is neglected.

In addition, there are numerous researchers who have also dealt with the modelling and the analysis of desiccant wheels. These are Charoensupaya and Worek (1988a, 1988b), Zheng and Worek (1993), Nia et al. (2006), Zhang et al. (2003), Simonson and Besant (1997), Chung et al. (2008), Chung et al. (2009) and Chung and Lee (2009). Thereby, the investigation of the impact of the rotational speed on the dehumidification was a main aspect of most research. Ge et al. (2008) give a summarizing overview of existing numerical desiccant wheel models.

The desiccant wheel model available in INSEL 8 is based on the assumption that the supply air can maximally be dehumidified to the same level of the relative return air humidity upstream of the desiccant wheel. In addition, it is assumed that the dehumidification process is ideally isenthalpic. The INSEL model is described in detail in section 3.3.1.

3.1.2.3 Regenerative and Recuperative Heat Exchangers

In comparison to the many existing models for desiccant wheels only a small number of models is available to specially depict the regenerative heat recovery of a HRW.

The model of "Type 760", developed by *Thermal Energy System Specialists* is a TRNSYS type for the simulation of the heat recovery based on simple physical correlations. The model of "Type 760" is very similar to "Type 91", the model of a heat exchanger. However, "Type 760" in addition considers a pressure drop during the heat recovery process.

TRNSYS model of "Type 94" is suitable for both the modelling of a desiccant wheel as well as of a heat recovery wheel (Rathey 2000). The model is based on the theory developed by Franzke (1990). The model includes a linear pressure drop due to a laminar flow of the air in the pores of the regenerator matrix. However, for these calculation algorithms the required numerous material parameters for porosity, density, specific surface area and heat storage capacity can only be researched at great expense. To address this difficulty, Bernd (1997) developed an empirical calculation method for the heat and humidity recovery.

The simulation model for the heat recovery implemented in INSEL8 is solely based on the parameter heat recovery efficiency and does not consider the influence of different supply air and return air volume flows. This model is described in detail in section 3.3.2.

With regard to the modelling of the regeneration air heater, the following physical simulation models for recuperative heat exchangers were reviewed.

The physical heat exchanger model "Type 275" was developed by the *Fraunhofer Insitute for Solar Energy Systems* (Brychta and Pol 2007). The model determines the regeneration temperature based on the assumption of similar mass flows at a constant specific heat capacity of air.

Another physical approach for a regenerative heat exchanger is provided by Möckel (2003). In order to calculate precisely the heating and cooling down of the mass flows the model accesses the manufacturers' software for component dimensioning of Klingenburg GmbH. This facilitates the calculation of component specific figures such as the heat recovery ratios and therefore the degree of quality of the modelled heat exchanger to determine the consequent temperatures.

In addition, Madjid (1996) describes a physical model that takes into account the heat transfer capacity for both the air mass flow and the water mass flow. The heat output is calculated by means of the mass flow, the specific isobaric heat capacity and the temperature difference between inlet and outlet. Hence, the required outlet temperatures are those determined with the identified heat

recovery efficiencies. Moreover, the model considers the occurring pressure drop.

3.1.2.4 Air Humidification

The humidifier model implemented in "Type 275" gradually calculates the air conditions of the humidified air with respect to a maximum saturation of the air based on defined inlet conditions. The model regards the humidification process to be ideally isenthalpic. The enthalpy of the process is calculated in the first step based on the inlet conditions. Thereafter, the absolute outlet humidity is calculated considering a full saturation of 100% relative humidity. Finally, the outlet temperature after the humidification process is calculated (Brychta and Pol 2007). In the same publication they describe the TRNSYS model "Type 641", a further physical humidifier model to specially simulate an adiabatic return air humidifier.

The TRNSYS model "Type 94" is a model enabling the simulation of a complete ventilation system described by Rathey (1999). This model provides several sub-models to simulate various types of humidifiers such as trickle humidifiers, contact humidifiers, steam humidifiers or spray humidifiers. When calculating the air conditions of the spray humidifier for example, initially a water-air number and the degree of humidification is determined. The evaporated water mass flow is calculated by the increase of the air water content. In addition, the model includes the calculation of the pressure drop over the humidifier unit as it is mainly occurring at a droplet separator.

Pietruschka (2010) developed a simple numerical model of a humidifier. In order to simulate the humidification process, the contact matrix of the humidifier is sub-divided into finite elements. The water mass stored in the contact matrix is usually lower than the air mass conveyed through the humidifier unit. Therefore, for reasons of simplification it is assumed that the water temperature is equal to the temperature of the chilled air by means of evaporative cooling. Regarding the energy balance both water mass and heat capacity of the matrix are neglected.

The model used for the simulation of the humidifier units in the course of this research is based on basic physical equations and described in detail in section 3.3.3.

3.2 Simulation Environment

The simulation study has been carried out with the simulation environment INSEL 8 (Doppelintegral 2009). As the research at hand was inspired by the solar DEC-research activities at Stuttgart University of Applied Sciences, the software tool INSEL 8 was recommended to be applied for the system simulation. This was regarded as budding solution because this simulation software and several of its component models have already been successfully applied by Pietruschka (2010) in his PhD thesis at the Institute of Energy and Sustainable Development at De Montfort University Leicester. The INSEL 8 software setup is briefly introduced in this section.

INSEL 8 (Integrated Simulation Environment Language) is a block diagram oriented simulation software for the quantitative analysis of renewable energy systems from the company Doppelintegral GmbH. This modular simulation environment enables the planning, visualization and monitoring of the diverse energy systems in the field of renewable energies. Therefore INSEL provides numerous "state-of-the-art" functions as graphical blocks (Doppelintegral 2009). These serve for example to simulate meteorological data or thermal and electrical energy components. In addition, INSEL provides the opportunity to access extensive databases for photovoltaic modules, inverters, thermal collectors and meteorological parameters (Doppelintegral 2010). Furthermore, INSEL includes a programmable environment based on the programming languages FORTRAN 77 or C/C++ to implement self-created model code as graphical user block (Wiemken et al. 2008). An INSEL simulation model consists of a series of interdependent blocks that are linked. In principle, the structure of all the blocks is similar. Each block has a fixed or an arbitrarily expandable number of inputs and outputs. The blocks are parameterised with individual parameter sets and

thus characterise a respective block. The characteristic parameters are either real or string values (Martin 1997). Figure 3.1 illustrates the general structure of an INSEL block.

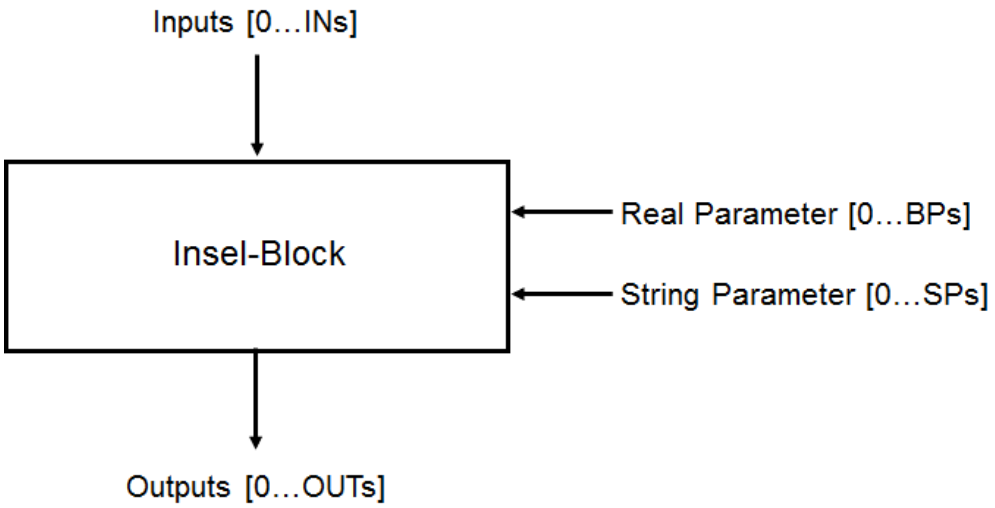

Figure 3.1: Principal structure of an *INSEL*-Block (Martin 1997)

Being executed within a model, a block initially requires input information or input data from the output of a predecessor block. When the calculation within a block is completed, the results are available at the respective block output interfaces to be passed to the subsequent block.

The statistical analysis tool JMP was used to carry out the parametric variation study based on a design of experiments' full factorial design.

3.3 DEC-System Model

A multivalent solar DEC- system was modelled for simulation based on the object under investigation and with consideration of appropriate planning guidelines and state-of-the-art information.

To assess the applicability of the diverse component models for the modelling of the solar DEC-system, the simulation results of the DEC-component models were compared with available measurement data. Therefore, measurement data of the August 1st, 2010 were exemplarily used.

To confirm the results, an additional day was simulated and evaluated for each model. Thereby, the assessment of the INSEL models is mainly based on the calculated relative error and evaluated regarding the capability of a respective model. The absolute error corresponds to the difference between the measured value and the simulated value and the relative error is calculated as the difference between the measured and the simulated value divided by the measured value, which is considered as the true value. The measured values of temperature and relative humidity which are recorded upstream and downstream of a component are subject to measurement uncertainty (see Table 2.8 in section 2.5.2). The sensor accuracy affects both, the simulation results as well as the calculated deviations between measured values (measured values downstream a respective system component) and simulated values.

Thus, during this validation, the model input parameters (measured values upstream a respective system component) used for the simulation of a component possess a certain error band. Therefore any arbitrary value within the measurement uncertainty of the used sensors gives a slightly different simulation result.

The following section presents the simulation models used in this study and describes the validation regarding the applicability in the context of this research where appropriate. A screenshot of the developed overall model in INSEL 8 is illustrated in Appendix C.

3.3.1 Desiccant Wheel Model

The employed desiccant wheel model available in INSEL 8 ideally takes the fact that the sorption isotherms coincide independent of temperature as a basis. Thus, the approach assumes that the ambient air humidity (supply air upstream DW) can be maximally reduced to the value of the absolute humidity of the regeneration air (Eicker 2001).

In a real object, however, this ideal maximum dehumidification is not achieved due to non-steady conditions and deficiencies. Reasons are irreversible effects, such as heat loss and heat exchange between the supply and return air duct at the desiccant wheel. In order to take this non-ideal behaviour into account the model implies the parameter dehumidification efficiency η_{dehum} as the ratio between the effectively achieved dehumidification and the ideally expected dehumidification Eqs. (3.1) and (3.2).

$$\eta_{dehum} = \frac{x_{amb} - x_{sup,eff}}{x_{amb} - x_{sup,ideal}} \tag{3.1}$$

$$x_{sup,eff} = x_{amb} - \eta_{dehum} * (x_{amb} - x_{sup,ideal}) \tag{3.2}$$

where,

η_{dehum}	dehumidification efficiency [-]
x_{amb}	absolute humidity of ambient air [g kg^{-1}]
$x_{sup,eff}$	effectively absolute supply humidity output downstream DW [g kg^{-1}]
$x_{sup,ideal}$	ideally expected absolute supply humidity downstream DW [g kg^{-1}]

For the calculation of $x_{sup,ideal}$ the enthalpy content of the supply air is simplified assumed to remain constant during the dehumidification process (isenthalpic change of condition). In addition, it is assumed that the relative supply air humidity downstream the desiccant wheel φ_{sup} is equal to the relative humidity of the regeneration air upstream the desiccant wheel φ_{reg}. Thereby, the relative humidity φ_{air} is defined by Eq. (2.24) in chapter 2. The specific enthalpy of the

supply air h_{sup} is calculated according to Glück (1991) as shown in Appendix A1. Hence, the actual values of the absolute humidity of the dehumidified supply air are calculated with Eq. (3.2, Pietruschka 2010).

Based on the input variables T_{sup} and φ_{sup} (supply air condition upstream DW) and T_{reg} and φ_{reg} (regeneration air condition upstream DW) as well as the parameter dehumidification efficiency η_{dehum} the output values downstream the DW are calculated for both air streams.

In order to assess the suitability of this DW model for the modelling of the solar DEC system its simulated results were compared with the corresponding measured values of the investigated object, for different operational times of the DW, e.g. July 16th, 2010. Consequently, a respectively reduced dehumidification efficiency of 62% was included in order to reproduce the actual in-situ DW operation. Thereby, the relative humidity $\varphi_{sup,out}$ shows a very low average relative error of 2.4% (0.4% r.h.).

In the real plant operation, the wheel causes a short-term humidification of the supply air $T_{sup,out}$ immediately after the DW start. This is a result of a non-regenerated matrix in the start phase and in contrary to the DW's essential dehumidification function while the simulation is based on the ideally modelled isenthalpic dehumidification process. This initially causes a relatively high deviation of the simulated data to the measured data which attenuates significantly in the further course of operation, so that the average relative divergence is 3.5% (1.5 K).

This shows that the model is suitable to simulate the supply air conditions downstream the DW with relatively little deviation. Thus, the model is evaluated as sufficiently accurate to reproduce the DW's supply air conditions for the targeted simulation study on system level. Furthermore it is noted, that due to a relatively short time delay the components of a DEC-system are mainly operated in a quasi-stationary operational state. Thus, it is anticipated, that static DW models are expected to provide quite reliable results for annual simulations of a solar DEC-system at the system level (Dumont et. al 2013). The described DW

model is thus used for the simulation calculations within the framework of this research.

3.3.2 Heat Recovery Wheel Model

The INSEL model to simulate the heat recovery function in the DEC-system consists of a simple parameter model based on the HRW's heat recovery ratio.

This model is suitable to calculate a HRW operated at a constant speed and does generally not consider divergent mass flows in the supply and return air. In conformity with Eq. (2.8) the model defines the supply air sided heat recovery ratio ϕ_{HRW} according to Eq. (3.3).

$$\phi_{HRW} = \frac{T_{sup,in} - T_{sup,out}}{T_{sup,in} - T_{ret,in}} \tag{3.3}$$

where,

$T_{sup,in}$ supply air temperature upstream HRW [°C]
$T_{sup,out}$ supply air temperature downstream HRW [°C]
$T_{ret,in}$ return air temperature upstream HRW [°C]

Pietruschka (2010) analysed this HRW model and carried out a validation with measured values. The results indicate a good accordance between the measured and the simulated behaviour and the model was therefore evaluated to be sufficiently accurate for the simulation of a DEC-system. In addition to that the applicability of the model for the simulation of the multivalent system was checked by a comparison of simulation and measurement data, analogue to the practise with the DW model. For this purpose, the arithmetic mean of the measured heat recovery ratio of 0.61 was used in the simulations.

The comparison of the measured and simulated supply air temperatures downstream HRW for the sample day (July 16th, 2010) showed a relative deviation between 3% and 4% (0.8 K to 1 K) in DEC-mode. During the operation

of the HRW only, the error ranges between minus 0.5% and minus 2% (-0.2 K to -0.5 K).

The reason for a higher deviation of the supply air temperature during the DEC-operation (measured heat recovery ratio in DEC mode $\phi_{HRW} = 0.57$) is due to the statically included average heat recovery ratio $\phi_{HRW} = 0.61$ which remains constant for the entire operational time of the HRW and is not dynamically adjusted to the respective operating state.

Throughout the reference period, this results in an average relative error of the supply air temperature of 0.4%. This means that the simulated values deviate from the actual measured values by 0.5 K in average. This deviation can be interpreted by the measurement uncertainty of ±(0.15°C+0.002 T) in the temperature measurement up- and downstream the HRW. The applicability of the INSEL model for the system simulation has been tested for further exemplary sample days.

3.3.3 Humidifier Model

The parameter-based INSEL model for the modelling of humidifiers (Schumacher 2011) describes the humidification process on the basis of fundamental physical equations.

In the first instance the model determines the value of the absolute humidity upstream of the humidifier by the corresponding values for temperature and relative humidity. Humidification of the process air occurs only, if the relative humidity upstream of the humidifier is less than the assumed humidification efficiency and if the absolute humidity upstream of the humidifier is lower than the maximum saturation humidity. The ideally modelled isenthalpic humidification process can then be carried out up to a maximum of 100% relative humidity. Thereby, the model uses an iterative approximation method according to Eq. (3.4) to calculate the absolute humidity downstream of the humidifier.

$$x_{air,n} = x_{air,n-2} + \frac{1{,}0 - \varphi'_{air,n-2}}{\varphi'_{air,n-1} - \varphi'_{air,n-2}} * \left(x_{air,n-1} - x_{air,n-2}\right) \quad (3.4)$$

where,

$x_{air,n}$	current iterated absolute humidity downstream humidifier [g kg^{-1}]
$x_{air,n-1}$	absolute humidity after previous calculation step [g kg^{-1}]
$x_{air,n-2}$	absolute humidity after penultimate calculation step [g kg^{-1}]
$\varphi'_{air,n-1}$	relative humidity after previous calculation step [-]
$\varphi'_{air,n-2}$	relative humidity after penultimate calculation step [-]

In the next step, the simulation model calculates the absolute humidity downstream of the humidifier $x_{air,out}$ based on the parameter humidification efficiency η_{hum}.

$$x_{air,out} = x_{air,in} + \eta_{hum} * (x_{air,100\%} - x_{air,in}) \quad (3.5)$$

where,

$x_{air,100\%}$	absolute humidity after iteration at 100% relative humidity [g kg^{-1}]
$x_{air,in}$	absolute humidity upstream humidifier [g kg^{-1}]

Based on $x_{air,out}$ and ideally assuming a constant enthalpy during the adiabatic humidification process, the model subsequently calculates the temperature and relative humidity downstream of the humidifier.

In addition, the model calculates the humidifiers water consumption m_{cons} which is determined by the effective absolute humidification as well as by the water consumption factor f_w (Eq. 2.11, chapter 2).

$$m_{cons} = m_{hum} * f_w \quad (3.6)$$

$$m_{hum} = \int \dot{m}_{hum}\ dt = \rho_{air} \int \left[\dot{V}_{air}(t)\ \Delta x \right]\ dt \tag{3.7}$$

In order to evaluate the applicability of this humidifier model for the simulation of the return air humidifier the simulation results of the model were verified with corresponding measurement data (August 01st, 2010) for the complete operation of the humidifier unit. Therefore, the parameter humidification efficiency η_{hum} is determined as defined in section 2 (Eq. 2.10) and included in the model based on monitoring data. The assessed values depict the stable operation of the humidifier at full capacity. The necessary maximum absolute humidity in saturation was identified using the software *ILK-h,x-Dia* of the *Institut für Luft- und Kältetechnik ILK Dresden* (ILK 2005). Accordingly, the humidification efficiency of the return air humidifier in operation is 86%. In real operation the water consumption parameter is $f_w = 4.3$. Considering the measured water consumption of 358 l in the reference period the effectively absorbed quantity of water by the air m_{hum} is 84 l.

The comparison shows a very small deviation of the simulation results to the measured values of the air conditions downstream the humidification process. Accordingly, the average relative error regarding the relative humidity is below 1% (0.8% r.h.) and less than 2.7% (0.3 g kg^{-1}) with regard to the absolute humidity. As a result the temperature values show an average deviance of 2.8% (0.5 K). The difference between the simulated and measured values is merely distinctive at the beginning of the humidifier operation. This is due to the fact that in real operation the humidifier performance is increased stepwise, while the model does not simulate this accelerating in steps. The calculated water consumption over the entire reference period is 371 l. Thus, the relative deviation between the actually measured and simulated water consumption is -3.6%.

The same procedure has been carried out targeting the supply air humidifier and shows average deviations downstream the humidifier of 2.3% (1.6% r.h.) for the relative humidity and 4.5% (0.9 K) regarding the temperature. In terms of the humidifiers water consumption the simulated value deviates 1.5%.

On the whole, the humidifier model allows a simulation of both the supply air humidifier and return air humidifier with acceptable small deviations from the measured values in average. This result was confirmed with data of further exemplary test periods and the model was therefore evaluated appropriate for the simulation of the humidifier units within the system model.

3.3.4 Ventilation and Heating Function

Following the design of the monitored system, the implemented DEC-control is modelled with ventilation fans with fixed volume flow rate of $V_{DEC} = 8{,}000$ m^{3}h^{-1}. This corresponds to a rotational speed of the drive motor of $\omega = 1{,}440$ min^{-1} with a nominal electrical power of $P_{el} = 4.0$ kW per fan (Wolf Anlagen-Technik 2005). A variable adjustment of the systems volume flow as final cascade to the complete DEC-process can be neglected as the research focus is the comparative evaluation of different multivalent designs on system level.

The systems heating function was modelled by means of a supply air heating (SAH) in the supply air duct. This heating function is temporarily limited to the heating period from October 1st until April 30th.

At first, the supply air is preheated with solar heat from the solar buffer store (SBS) by means of a water/air cross flow heat exchanger, whereby the flow temperature to the heat exchanger is limited to 25°C by means of a mixing loop with the return flow.

In addition, an auxiliary electric backup was included to sustain the supply air temperature in heating mode at $T_{sup,set} = 22$°C in order to compensate for operation times with insufficiently available solar heat.

The heating mode does not reproduce the operation of the desiccant wheel (DW) as enthalpy exchanger. The DW model is limited to the dehumidification function in cooling mode. In addition, the DEC-system model does not consider an anti-frost protection of the DW matrix in winter period as it is recently argued scientifically. Moreover, for simplification reasons the winter heating function does not include supply air humidification.

3.4 DEC- System Control Algorithm

The control algorithm of a solar DEC-process has the primary functions to maintain the room air within the desired set values for temperature and humidity as well as to operate the system energy efficiently. However, INSEL 8 lacked an applicable DEC-controller model. Therefore, an appropriate state-of-the-art DEC control strategy was modelled with FORTRAN 77 and implemented in INSEL 8.

As shown in section 2.4, there were neither planning documents nor descriptions of the DEC-control strategy or its parameters available for the object under investigation. The sketched documentation in section 2.4 therefore shows a reconstructed control strategy as it was obviously implemented according to the information of system planner, manufacturer and operator. Due to different information and observed inconsistencies of the given information with gained measurement results and operating experiences, the current state of the art of DEC-system control was reviewed with regard to the system simulation. Therefore, an intensive literature research was conducted in order to create a broad basis for the modelling of the DEC-controller. General principles regarding the control of solar DEC-systems and especially particular published control strategies of solar DEC-prototype plants were analysed. In addition to the control strategy the focus was on control parameters and the respective set values.

3.4.1 State-of-the-Art of Solar DEC-Control

Handbooks for air-conditioning Baumgarth et al. (2003) and Fitzner (2008) provide general information regarding the control of DEC-systems. According to that, a room air-supply air temperature cascade control characterises the adjustment of the set point of the supply air control in dependence of the room temperature and is thus taking into account the particular cooling load. Thereby, the temperature difference between room and supply air is only to vary within a determinate interval (Recknagel et al. 2007).

With regard to the cooling period DIN 1946-2 (1994) and VDI 3525 (2007) regulate a proportional adjustment of the room temperature set points between 22°C and 26°C with increasing ambient temperature in the range of 22°C to 32°C.

The planning guide “Solar Cooling for Planners, Building Designers and Installers” provides an overview of solar technologies for air conditioning and serves as guideline for the conception of solar DEC-systems (Wiemken and Petry 2013). This guideline however does neither focus on DEC-control strategies nor on the adjusting of essential control parameters. Another guideline summarizes the requirements for the design and configuration of small and medium-sized plants for solar air-conditioning (Solair 2009). However, also this guide does not describe aspects and rules considering the control of solar DEC-systems.

Franzke (2008) distinguishes a sensible and a latent control loop in dependency of the ambient air conditions for temperature and humidity. The sensitive loop thereby describes the regulation of the supply air temperature with the modes return air humidification with heat recovery and supply air humidification. The latent loop determines the setting of the supply air humidity by activating the sorption unit consisting of desiccant wheel and regeneration air heater. A basic classification of the solar DEC-control strategy in the phases free ventilation, indirect adiabatic cooling (heat recovery with return air humidifier), combined adiabatic cooling (with additional supply air humidification) and desiccant cooling through further activation of the desiccant wheel is described in Henning (2004a). From an energy efficiency point of view, this control principle recommends a variable increase of the volume flow rate to its maximum value as the last option, only if the room temperature set points cannot be reached in the desiccant cooling mode (cf. Fitzner 2008, Pietruschka 2010). The control strategy does not consider a pure heat recovery phase. All control modes are set according to the supply air temperature. The sorptive dehumidification mode is activated when either the supply air temperature or the supply air humidity exceed a critical set value. The presented control schemes however do not give recommendations on the

definition of the respective set values for the supply air temperature in dependence of the actual room air conditions.

Erpenbeck (1999) describes the cooling control cascade comprising the steps of free cooling, adiabatic return air humidification with heat recovery and finally the full DEC dehumidification mode. In contrast to Henning (2004a), the activation of the supply air humidification and the activation of the DEC-mode are regarded as one control step, whereas the efficiency of the desiccant wheel and the humidifier are designed adjustable. The supply air flow is thereby regulated depending on the room air parameters. Different from Henning (2004a), an adjustment of the air flow is possible in each operating mode for a continuous capacity control.

Hoefker (2001) distinguishes the control modes free ventilation, return air humidification with heat recovery and sorptive dehumidification with active operation of all components. As DEC-systems are characterized by its dehumidification function in order to condition the humidity level, a control according to the room air parameters is recommended to consider the interaction with the building load. A control according to the supply air temperature is only appropriate, if the room humidity can be neglected. Also Fong et al. (2010) describe the control of the DEC-system according to the room air humidity level.

Kaelke et al (2003) describe the control of a solar DEC-plant in Brückberg (Germany) by means of a control cascade consistent with Erpenbeck (1999). However, the modes are solely controlled according to the return air temperature. The room or return air humidity is not taken into account as control parameter in this system, whereupon exactly the inclusion of the room air humidity as control parameter together with the room air temperature is recommended.

3.4.2 Comparative Study on Solar DEC-Controls in Operation

Due to the limited availability of elementary literature and the diverse researched approaches to control solar DEC-systems, several solar DEC-systems in operation have been comparably analysed with regard to the system dimensioning and the respectively implemented control strategy.

Figure 3.2 shows the dimensioning of the nominal cooling capacity of six European solar DEC-systems that have been scientifically studied in recent years, in relation to the specific and absolute collector area. The overview reveals an obvious variation of the dimensioned specific collector area in relation to the nominal cooling capacity reaching values between 1 $m^2\,kW^{-1}$ and 9.8 $m^2\,kW^{-1}$. In the first instance, different overall system configurations with additional heat sources and a varying range of heat sinks are a reason for these differences. However, also a barely existing basis for the dimensioning of multivalent systems leads to this significant discrepancy in the dimensioning of the collector area.

At the plants in Palermo (Italy) and Hartberg (Austria) solar heat is for example solely used as regeneration heat for the DEC-system, while the systems in Gleisdorf and Vienna (both Austria) supplementary use solar heat for hot water preparation and heating. Furthermore the system in Gleisdorf is combined with a biomass cogeneration plant serving as additional heat source. All system designs include a solar buffer store in the system design except Ingolstadt (Germany). The system in Althengstett (Germany) has to be considered separately as it is equipped with solar air collectors.

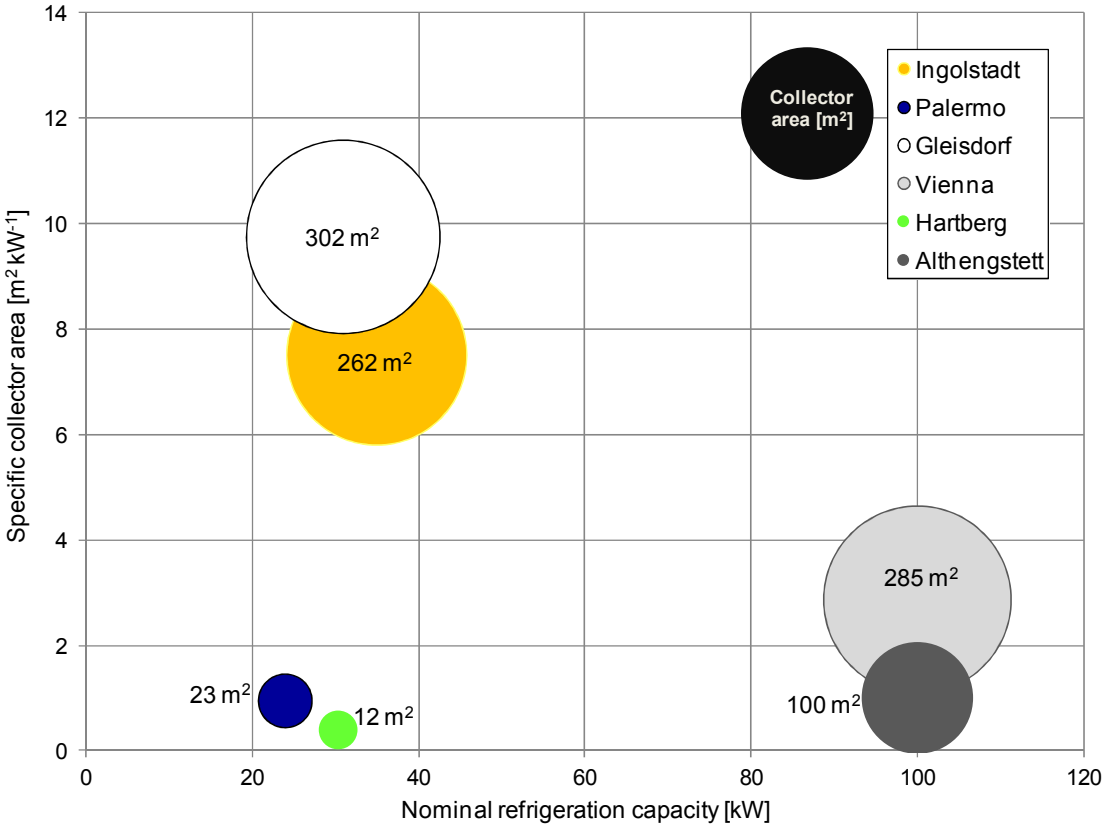

Figure 3.2: Dimensioning of collector area in relation to the nominal refrigeration capacity with solar DEC-plants in operation

Based on this outline of systems in operation the solar DEC-control strategies were comparatively analysed with focus on the cooling phase, taking into account additional information based further scientific research work (Franzke and Heinrich 1997, Ginestat et al. 2002, Vitte 2007, Eicker 2009, Pietruschka 2010, Panaras et al. 2011, Wrobel et al. 2013, Preisler and Zucker 2013, Podesser and Stiglbrunner 2000, Nelson et al. 1978). The control strategies of systems in operation having been investigated and compared in detail are illustrated in Table 3.1. It was found that all investigated DEC-control strategies are based on a sequence or cascade control realised by switching on and off of individual components (cf. Henning 2004a). Thus, the principal structure of the control strategy of the system under investigation in Ingolstadt is similar to the investigated control strategies.

Table 3.1: Outline of control strategies in operation

System	Control sequence	Parameters and set values	
Palermo	O. $\dot{V}$ (ventilation only)	T_{amb}	$20°C \leq T_{amb} \leq 24°C$
Lab room	I. (O) + HRW (600 h^{-1}) +RHUM	T_{amb}	$T_{amb} > 24°C$
$\dot{V} = 1{,}500\ m^3h^{-1}$	II. (I) +DW (15 h^{-1}) +RAH	$T_{amb},\ x_{sup}$	$T_{amb} > 24°C,\ x_{sup} \geq 8\ g\ kg$
Finocchiaro et al. (2010)	III. (II) + 2 $HX_{cool,aux}$	$T_{sup},\ x_{sup}$	$T_{sup} > T_{sup,set},\ x_{sup} \geq 8\ g\ kg$
Vienna	O. $\dot{V}$ (ventilation only)	T_{sup}	$T_{sup,set} = 22°C$
Office building	I. (O) + HRW (600 h^{-1})	$T_{sup}, T_{ret}, T_{amb}$	$T_{sup} > 22°C;\ T_{ret} < T_{amb}$
$\dot{V} = 8{,}240\ m^3h^{-1}$	II. (I) + HRW (600 h^{-1}) +RHUM	$T_{sup}, T_{ret}, T_{amb}$	$T_{sup} > 22°C;\ T_{ret} > T_{amb}$
(2 DEC- plants)	III. (II) + DW (20 h^{-1}) + RAH +SHUM	T_{sup}, φ_{sup}	$T_{sup} > 22°C; \varphi_{sup} > 80\%$ v $\varphi_{ret} > 45\%$
Preissler and Zucker. (2013)		*Different set values published for* $\varphi_{sup,max} = 60\%$ *(or* 80%*) and* $\varphi_{ret,max} = 42\%$ (or 45%)	
Gleisdorf	O. $\dot{V}_{min}$ (ventilation only)		
Town hall	I. (O) + HRW (900 h^{-1}) +RHUM	T_{sup}	$T_{sup,set} = 18°C \pm 1K$
$\dot{V} = 6{,}250\ m^3h^{-1}$	II. (I) + DW (18 h^{-1}) +RAH + SHUM	T_{sup}	$T_{sup,} > T_{sup,set} + 1K$
Thür and Vukits, (2009)	III. (II) $\dot{V}_{min} \rightarrow \dot{V}_{max}$	T_{sup}	$T_{sup,} > T_{sup,set} + 1K$
		T_{sup}	$T_{sup,} > T_{sup,set} + 1K$
		DEC-Mode (II) not controlled by a humidity threshold	
Hartberg	O. $\dot{V}_{min}$ (ventilation only)		
Ecocpark	I. (O) + HRW +RHUM	T_{amb}	$20°C \leq T_{amb} \leq 22°C$
$\dot{V} = 6{,}000\ m^3h^{-1}$	II. (I) + DW + RAH +SHUM	T_{amb}	$T_{amb} > 22°C$
	III. (II) + $\dot{V}_{min} \rightarrow \dot{V}_{max}$	T_{amb}, ω_{HRW}	$T_{amb} > 22°C,\ \omega_{HRW} = 100\%$
		T_{amb}	$T_{amb} > 22°C$
Podesser and Stiglbrunner (2000)		$\dot{V}_{min}$ *controlled according to* CO_2*-level*	
Althengstett	O. $\dot{V}$ (ventilation only)	T_{amb}	$19°C \leq T_{amb} \leq 23°C$
Industry hall	I. (O) + SHUM	T_{amb}, x_{ret}	$T_{amb} > 23°C, x_{ret} < 11.7 gkg^{-1}$
$\dot{V} = 18{,}000\ m^3h^{-1}$	II. (O) + HRW +RHUM	T_{amb}, x_{ret}	$T_{amb} > 23°C,\quad x_{ret} > 11.7 gkg^{-1}$
Eicker (2009)	III. (II) + DW + RAH	T_{amb}	$T_{amb} > 23°C$
Stuttgart	O. $\dot{V}_{min}$ (ventilation only)	$T_{room},\ x_{sup}$	$T_{room} < 23.5°C,\ x_{sup} < 10.0\ gkg^{-1}$
Lecture room	I. (O) + HRW +RHUM	$T_{room},\ x_{sup}$	$T_{room} > 23.5°C,\ x_{sup} < 10.0\ gkg^{-1}$
$\dot{V} = 3{,}000\ m^3h^{-1}$	II. (O) + SHUM	$T_{room},\ x_{sup}$	$T_{room} > 24.5°C,\ x_{sup} < 10.0\ gkg^{-1}$
Pietruschka (2010)	III. (II) + DW + RAH	$T_{room},\ x_{amb}$	$T_{room} > 25.5°C$ v $x_{amb} > 10.0\ gkg^{-1}$
	IV. (II) + $\dot{V}_{min} \rightarrow \dot{V}_{max}$	$T_{room},\ x_{amb}$	$T_{room} > 26.5°C$

All control strategies thereby include an initial free ventilation mode without explicit air treatment (mode O) for sufficiently comfortable ambient air conditions. The sequence then proceeds slightly different in all strategies. While in Vienna,

the sequence is in principle designed with a pure heat recovery phase (HRW only), the strategies in Palermo. Gleisdorf, Hartberg and Stuttgart respectively start the sequence with the adiabatic cooling mode (HRW + RHUM). In Althengstett in turn, the cooling cascade begins with the direct adiabatic cooling by supply air humidification. While in Althengstett and Stuttgart a phase of combined cooling (HRW + RHUM + SHUM) occurs before the full DEC-mode (DW and RLGH), this combined mode is not implemented in the control of the other four systems. In these control sequences the indirect adiabatic cooling phase is directly followed with the DEC-mode, where besides DW and RAH usually also the SHUM is activated. Only the control strategy in Palermo does not consider the humidification of the supply air (SHUM) due to high humidity levels of the ambient air. Further cooling is realised by means of two additionally integrated chillers. The control sequences of the systems in Gleisdorf, Hartberg and Stuttgart include as last step the increase of the air flow rate to its maximum value $\dot{V}_{max}$, while other control strategies operate the system with the maximum nominal flow rate throughout. However, the increase in flow rate sequentially after the activation of the full DEC-mode is discussed as optimised control option in terms of primary energy efficiency (Pietruschka 2010).

The analysed control strategies show not only differences in terms of the sequence order. In particular, according to available scientific publications the respective systems are controlled with largely different parameters and set values, without noting outstanding climatologic or load specific reasons.

While the sequences in Gleisdorf, Hartberg and Althengstett control the sequence according to the ambient air temperature T_{amb}, the systems in Vienna and Gleisdorf control the phases according to a set value for the supply air temperature T_{sup} . In Vienna the activation of the HRW and the activation of the indirect adiabatic cooling mode is additionally controlled by the temperature difference between T_{amb} and T_{room}. In contrast, the sequence in Stuttgart is controlled to set values of the room air temperature T_{room} and therefore takes into account the room load. In Stuttgart, the set values are thereby varied between $23.5°C < T_{room} < 26.5°C$ in dependence of the respective control mode.

While the system in Palermo activates the DEC-sequence when $T_{amb} > 24°C$, the corresponding control parameters are set in Hartberg to $T_{amb} > 22°C$ and in Althengstett to $T_{amb} > 23°C$. Also the control strategies that consider T_{sup} as control variable use different set values (Vienna: $T_{sup} > 22°C$; Gleisdorf: $T_{sup} > 19°C$).

In fact, the various systems also control the actual activation of the full DEC mode (DW + RAH) differently. The control strategies for Gleisdorf and Hartberg activate the DEC-mode according to the same temperature thresholds that are considered to activate the other phases and do not consider a maximum tolerable humidity condition. The control sequence in Palermo starts the DEC mode in dependence on the absolute supply air humidity $x_{sup} \geq 8\ g\ kg^{-1}$, while the strategy in Vienna activates the DEC-mode either if the relative supply air humidity $\varphi_{sup} > 80\%$ or if the relative return air humidity $\varphi_{ret} > 45\%$, whereas φ_{ret} corresponds to φ_{room}. The sequence in Althengstett controls according to the absolute room or return air humidity $x_{room} \geq 11.7\ g\ kg^{-1}$. Conversely, the control strategy in Stuttgart activates this mode according to the absolute humidity of the ambient air $x_{amb} \geq 10\ g\ kg^{-1}$.

Thus, it is found that apart from the principal sequential cascade approach, all investigated control strategies are based on different sequential arrangements, parameters and set values. However, reasons for these differences in system control regarding the selection and quantification of the corresponding parameter set values are not discussed in the respective publications. Therefore, aside from unrequired supply air humidification due to significant high ambient air humidity levels in Palermo, climatologic conditions can obviously not be regarded as cause for the diverse approaches to control the solar DEC-systems.

It can be further noted that none of the control strategies considers the specifications the control of air conditioning systems as defined in guideline VDI 3525 (2007). Regarding the control of air-conditioning systems such as a DEC-system, this guideline basically envisages a proportional adjustment of the set room temperature in dependence of the respective ambient air temperature.

Accordingly, it is recommended for ambient temperatures ranging in the interval $22°C \leq T_{amb} \leq 32°C$ to linearly and continuously raise the room air set value from $T_{room,set} = 22°C$ to $T_{room,set} = 26°C$. At ambient air temperatures above $32°C$ the adapted $T_{room,set}$ is defined to remain constant again.

3.4.3 Defined DEC-Control Strategy

Considering the carried out analysis of solar DEC-control strategies and taking into account the control cascade described in section 2.4, a state-of-the-art control strategy was defined in order to model the DEC-controller for simulation. The developed control strategy is summarized as truth table in Table 3.2 and the detailed controller flow chart is found in Appendix B of this thesis. The formulated control sequence was programmed as subroutine using the numerical programming language FORTRAN 77. The compiled code was implemented as block module in the INSEL 8 simulation environment.

Table 3.2: Truth table of the defined DEC-control strategy

Mode		$\dot{V}$	HRW	RHUM	SHUM	DW	RAH	SAH
10	Heat and heat recovery	1	1	0	0	0	0	1
9	Heat	1	0	0	0	0	0	1
8	Heat recovery	1	1	0	0	0	0	0
1	Free ventilation	1	0	0	0	0	0	0
2	Heat recovery	1	1	0	0	0	0	0
3	Adiabatic Cooling	1	1	1	0	0	0	0
4	Combined Cooling	1	1	1	1	0	0	0
5	DEC-mode	1	1	1	1	1	1	0
0	Plant off	0	0	0	0	0	0	0

Regarding the simulation of the existing reference system the cooling cascade (modes 0 to 5) is considered as well as the heating cascade (modes 8-10), whereas the focus of the simulation is on the control of the cooling process. Thereby, the function of a variable volume flow with the option to increase the volume flow to the maximum value as last optional sequence of the cascade was not modelled. In order to comparatively evaluate preferable system options of

multivalent systems on an overall system basis, this can be assumed with reasonable certainty. For the control of systems in real operation, however, this is to be considered in terms of improved primary energy efficiency, as discussed in detail by Pietruschka (2010).

The parameters room air temperature and absolute room air humidity are defined as command variables of the cascade control to account for the room load. Thereby, an undesirable variation in supply air temperature, possibly caused by system failure as it occurs in real operated plants, is not immediately detected and controlled. As the defined sequence is controlled according the room air temperature a failure would have to affect the room before the control responds. However, an additional supply air temperature set value can be neglected in a simulated controller, as unlike to real plants, the effects of unplanned system failure, such as the failure of components is not subject to an ideal system simulation. A direct control of the DEC-sequence according to the room respectively the return air was therefore assessed to be sufficiently accurate for the simulation of multivalent solar DEC-systems.

Based on the definition of the thermal room comfort in section 5.2.2 and in consideration of the fundamentals of air conditioning given by Recknagel et al. (2007), the maximum room air temperature set point is defined as $T_{room,max} = 22°C$. The room humidity value for the activation of the desiccant mode is set to $x_{room,max} = 10.4\ g\ kg^{-1}$and therefore $1.0\ g\ kg^{-1}$ lower than the in principal admissible value according to standard. Thereby, this should avoid that the supply air dehumidification is not activated when the room air humidity already exceeds its maximum set value. For both control variables the hysteresis is defined by the half width of the comfort zone $dT = 2°C$ and $dx = 2.5\ g\ kg^{-1}$. The required flow temperature of the regeneration air heater is included as a constant value ($T_{reg} = 68°C$) and is not dynamically adjusted according to the actual dehumidification demand or the heat supply. The function of the DW to operate as enthalpy exchanger during heating demand is not included in the model.

3.5 Solar Collector Circuit

3.5.1 Solar Thermal Collector Model

The employed solar collector model utilizes a steady state approach and is based on Doppelintegral (2010). The model simulates a solar thermal flat plate collector array with the basic collector given by ISO 9806-1 (1994) and is presented in detail in Appendix A.2. The collector specific model parameters were quantified according to the manufacturer's data sheet (Table 3.3; Solahart Industries 2004).

Table 3.3: Parameter of Solahart collector array

Model parameter	Value
Absorber area per module A [m²]	1.86
Maximal efficiency η_0 [-]	0.801
Linear heat loss coefficient $U_{\mathrm{eff},1}$ [W m^{-2}K^{-1}]	3.858
Quadratic heat loss coefficient $U_{\mathrm{eff},2}$ [W m^{-2}K^{-2}]	0.01
Specific heat capacity of collector fluid $c_{p,WG}$ [kJ kg^{-1}K^{-1}]	3.827

Thereby, $c_{p,WG}$ is assumed for a water-glycol mixture with a glycol content of 30% at an average collector temperature of 60°C (Eq. 3.8, Haller 2007) resulting in a value of 3.827 kJ kg^{-1} K^{-1} included as constant parameter in the model.

$$c_{p,WG} = 4.1868 * (0.866803 + 0.000789 * T'_m) \quad (3.8)$$

The two physically divided solar collector arrays in the object under investigation are modelled as one complete array with an overall collector aperture area of 262 m^2 in the system simulation model. Accordingly, 5 serial connected collectors were arrayed in 28 parallel strings. The solar heat exchanger to the solar storage that has been included in improved system models has been modelled as a brine-water counter flow heat exchanger, configured according to Peuser et al. (2001) with a heat transfer coefficient of 100 W K^{-1} per m^2 aperture area. Piping losses in the collector array are not taken into consideration in the model and can be neglected due to the comparative analysis of different design approaches.

In order to validate the solar collector model for the reproduction of the solar collector arrays in the system simulation, the simulation results of the Solahart array were exemplarily compared to measurement data of August 1st, 2010. As a result the course of the measured flow temperature shows a good conformity with the simulated flow temperature values (Figure 3.3). For the regarded simulation period this results in an average deviation of 5.3% (2.6 K) between simulated and measured values. The additionally performed comparison for July 16th, 2010 shows a deviation of 5.2% and hence confirms this result.

The main reason for the deviation is primarily due to simplifications in the static model including the parameter collector efficiency. Furthermore the model does not consider pipe losses or a reduction in power due to the aging of the collectors under measurement. However in general it can be evaluated, that the INSEL collector model reproduces the solar collector array with sufficient accuracy.

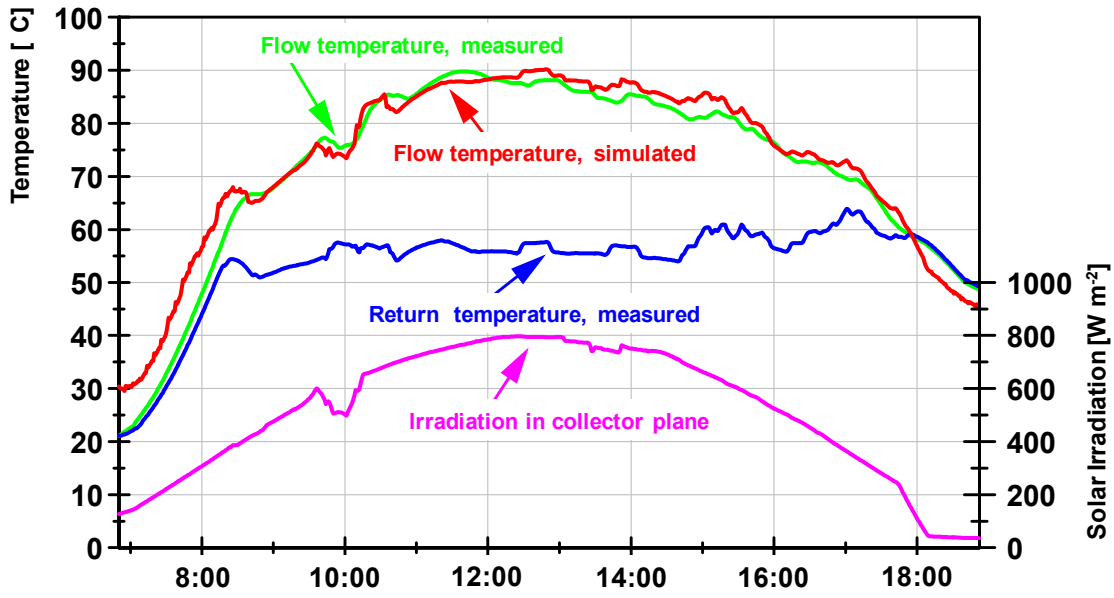

Figure 3.3: Comparison of simulated and measured flow temperatures Solahart collector array (August 1st, 2010)

Table 3.4 provides an overview of the detected average deviations in supply air output between simulation results and measured values for various component models implemented in the system model.

Table 3.4: Summarized results of validated component models

Component Model		DW	HRW	HUM	Solar Collector
cf. section		3.3.1	3.3.2	3.3.3	3.5.1
$T_{sup,out}$	Avg. abs. error [K]	1.5	0.5	0.5	2.6
	Avg. rel. error [%]	3.5	0.4	2.8	5.3
$\varphi_{sup,out}$	Avg. abs. error [% r.h.]	0.4	n/a	0.8	n/a
	Avg. rel. error [%]	2.4	n/a	1.0	n/a

3.5.2 Collector Circuit Control

The collector circuit control was implemented with matched-flow function of the collector volume flow. Thus, the control adjusts the collector mass flow in dependence of the temperature difference between collector flow $T_{col,fl}$ and the temperature at the bottom of the solar buffer $T_{SBS,bottom}$. The implemented control steps have been modelled according to the recommendations of Bollin (2009) as listed in Table 3.5. Thereby, the respective maximum mass flow rate was designed for a low-flow application and thus configured with 1.2 kg s^{-1} (equivalent to 16 l m^{-2} h^{-1}). The controller further takes into account a shutdown of the collector pump at a maximum buffer temperature of $T_{SBS,top}$ = 95°C and a hysteresis of T_{hyst} = 4 K.

Table 3.5: Matched-flow control steps

Temperature difference dT [K]	0	8	13	18	23	33	43
Fraction of maximum mass flow [%]	0	30	40	50	70	80	100
Power consumption solar pump [W]	0	105	115	140	160	165	170

In order to simulate the annual electricity consumption of the solar circuit pump a respective pump consumer was determined following DIN 4701-10 (2002). The consumption profile of the selected solar pump Wilo Top STG 25/7 was included in the model, considering array dimensions, maximum designed flow rate and pumping head. With respect to the varying collector flow rates, the calculation of the electric energy consumption considers the alternating power consumption of the solar pump on the basis of the component-specific characteristic curve of the manufacturer with the values listed in Table 3.5.

3.5.3 Stratified Storage Model

In the multivalent system model both the solar buffer storage as well as the hot water storage are based on the stratified tank model available in the INSEL 8 library (Eicker 2001). The model is shown in detail in Appendix A.3.

In contrast to the developed system options with solar buffer storage, the hydraulic system of the simulated original reference system does not include a buffer store. Thus, to simulate the reference system, this tank model was converted into a hydraulic switch between the solar circuit and the various heat sinks and parameterised accordingly.

In addition to the tank model the logic of a SBS discharge function was modelled to allow for sink specific varying return temperatures and mass flows at storage discharge. As a discharge of different SBS layers is not included in the existing model this function was programmed, whereas the return to the SBS is restricted to the bottom layer.

The heat loss behaviour of the storages was taken into consideration according to the component related heat transfer coefficients a_n measured by ITW Stuttgart (2003) for the reference tank product OSKAR of manufacturer ratiotherm (storage cap: $a_1 = 0.27\ W\ m^{-2}K^{-1}$, storage base: $a_2 = 0.95\ W\ m^{-2}K^{-1}$, lateral area: $a_3 = 2.52\ W\ m^{-2}K^{-1}$). Thereby, an effective vertical heat conductivity $\lambda = 0.90\ W\ m^{-1}K^{-1}$ is taken into account.

3.5.4 Store Discharge Supervisory Control Strategy

With regard to the utilization of solar thermal energy a multivalent system provides a variety of different operation modes. This creates specific requirements for the discharge strategy of the solar buffer on supervisory control level. Thus, the simulation model distinguishes the use of solar heat to drive the regeneration process of the DEC-system on the one hand and the utilisation for hot water preparation and heating support during the heating season on the other hand.

In the investigated system for optimisation, a sequential either-or control strategy without buffer storage is implemented for that matter. This strategy solely allows the load circuits to be fed directly via the solar heat exchanger. Buffering of solar heat or a simultaneous supply of multiple heat sinks with solar heat is not possible. This is reproduced in an initial model by converting the sub-model of the buffer store into a hydraulic switch by means of accordingly adapted default parameters.

In the simulation model, this original basic hydraulic scheme is used as a starting point for the simulation analysis. This initially implemented control is characterized by a distribution priority of solar heat for hot water preparation, as it was realised in-situ. In the further selection of a heat sink this first priority is followed by the utilization as DEC-regeneration heat followed by the use for heating as last option.

The respective control modes are shown in Table 3.6.

Table 3.6: Store discharge supervisory control modes

Modes of control sequence	**mode_supvis**
No discharge of solar heat	0
Charge hot water storage for hot water preparation	1
Feed regeneration air heater DEC-system	2
Feed heat exchanger heating function	3
Check regeneration heat demand DEC-system	22

Due to a lack of planning documentation of the control strategy in the investigated system, the control strategy was reproduced based on the results of interviews with the system planner and accordingly considered literature and norms.

The detailed flow chart of the formulated control strategy as illustrated in Figure 3.4 was programmed using FORTRAN 77. The compiled subroutine was implemented as block module in the INSEL 8 simulation environment and thus integrated in the multivalent system model.

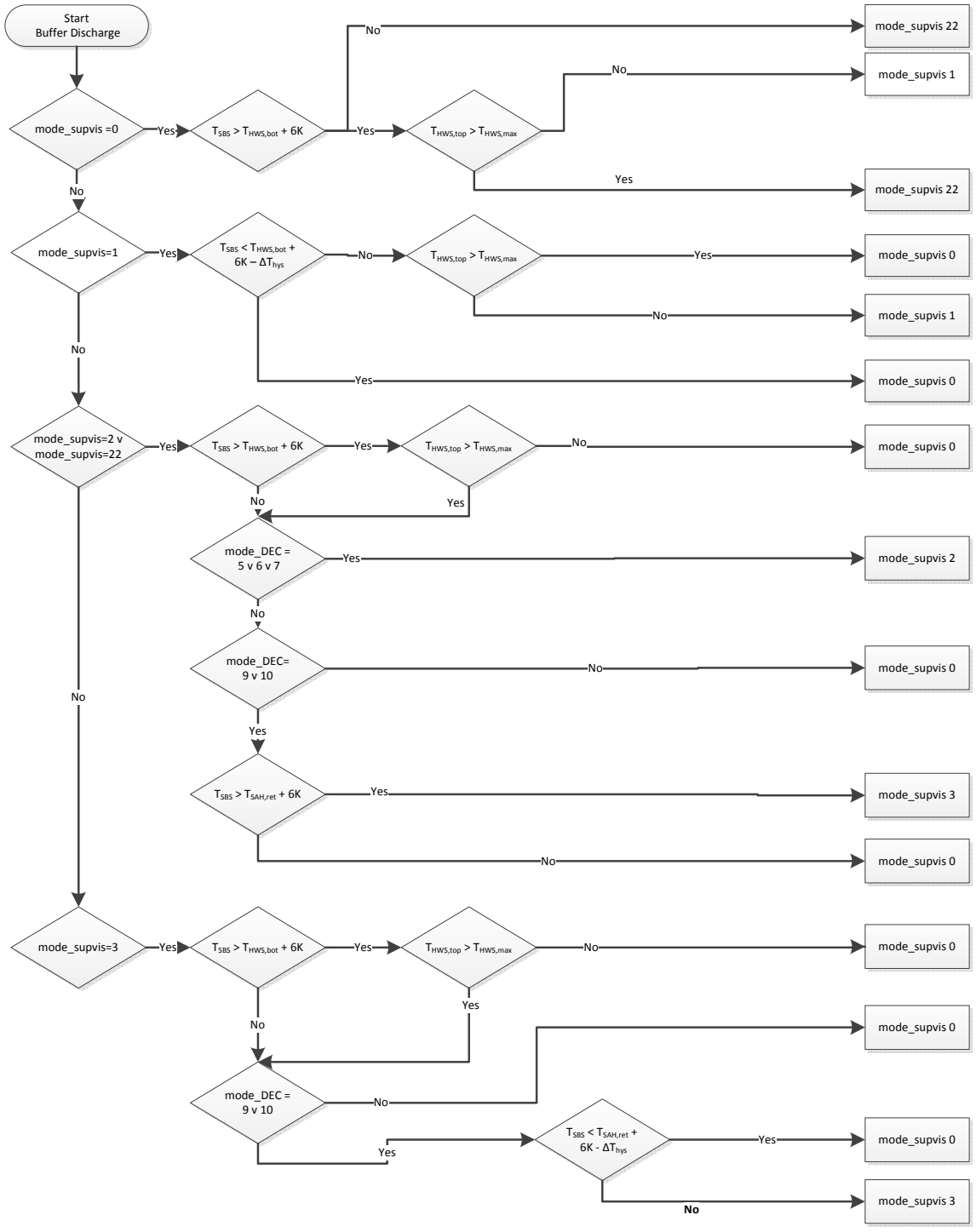

Figure 3.4: Developed supervisory control flow chart of initial multivalent system (sequential Integration)

In the simulated first optimised system variant the integration of a buffer store was examined based on this sequential discharge control with principally

concurrent heat sink demand profiles. Building on that, an advanced approach considering a simultaneous integration of the multivalent heat sinks is studied. The appropriately developed refined control strategy is introduced in chapter 4.

3.6 Hot Water Circuit Modelling

Besides the solar DEC-air-conditioning the preparation of solar hot water is a key function of the multivalent solar system. The modelled hot water circuit is supplied with solar thermal heat and equipped with an electric heating rod (heating element) as system backup.

The hot water circuit (Figure 3.5) has been modelled with a stratified storage tank model as described in section 3.5.3. The storage was dimensioned according to Schwenk (1999) as shown in section 4.4.2 and the storage heat loss behaviour is modelled similar to the solar buffer storage. Thereby, the hot water storage was subdivided into 7 nodes and is preferentially charged with solar thermal heat from the solar circuit. The charge control is part of the supervisory control strategy as described in section 3.5.4.

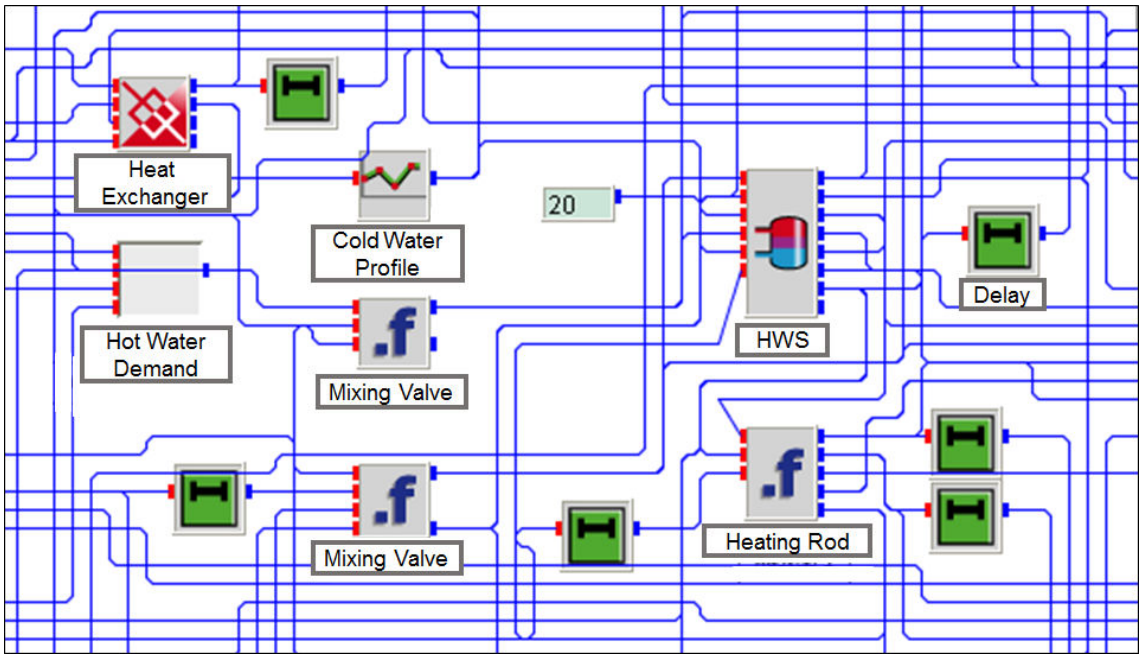

Figure 3.5: Detailed view of the hot water circuit sub-model in INSEL 8

In order to compensate for times with high discharge loads and low solar gains the system was equipped with an electrically driven heating rod (HRD) which was implemented as a model block. If the temperature of the tank sinks below 48°C in node 2 (hysteresis $dT = 2K$) the heating rod is activated with a maximum heating capacity of $\dot{Q}_{HRD}$ = 36 kW (electrical efficiency $\varepsilon = 0.95$) and supplies heat to the hot water storage additionally to the supply of the solar circuit with $\dot{m}_{HRD}$. Thereby, the implemented hydraulics and control allows to feed in available solar heat $\dot{Q}_{sol,in}$ in addition to the backup $\dot{Q}_{HRD}$ at any time. This is realised by means of a programmed simplified mixing valve. The mixing valve is assumed as node without mass. Therefore, the mixing temperature T_{out} can be determined by means of the law of conservation of energy (Eq. 3.9).

$$0 = \dot{Q}_{sol,in} + \dot{Q}_{HRD,in} - \dot{Q}_{MIX,out} = \dot{m}_{sol,in} \cdot c_p \cdot T_{sol,in} + \dot{m}_{HRD,in} \cdot c_p \cdot T_{HRD,in} - \dot{m}_{out} \cdot c_p \cdot T_{out} \quad (3.9)$$

Simplified assuming a temperature- independent specific heat capacity c_p the capacities in the valve can be solved for T_{out} with (Eq. 3.10).

$$T_{out} = \frac{\dot{m}_{sol,in} \cdot T_{sol,in} + \dot{m}_{HRD,in} \cdot T_{HRD,in}}{(\dot{m}_{sol,in} + \dot{m}_{HRD,in})} \quad (3.10)$$

Regarding the hot water demand, the hotel capacity was considered with 70 persons, following the dimensions of the monitored object. According to Recknagel et al. (2007) the maximal hot water demand at 45°C was considered with 0.12 m^3 per person and day for rooms of luxury category with shower. Hence, the reference system for the system simulation was dimensioned with for a daily hot water consumption of 8.4 m^3 (45°C).

The diurnal variations of the hot water demand were adapted with regard to recommendations based on measurement data of Orth and Martenka (2005) and (Schwenk 1999) and corresponding draw off patterns were included as daily profiles for simulation (Figure 3.6). Compared to the draw-off pattern of a typical

household, it is conspicuous that the draw-off in the morning time between 06.00 and 10.00 is significantly more distinct.

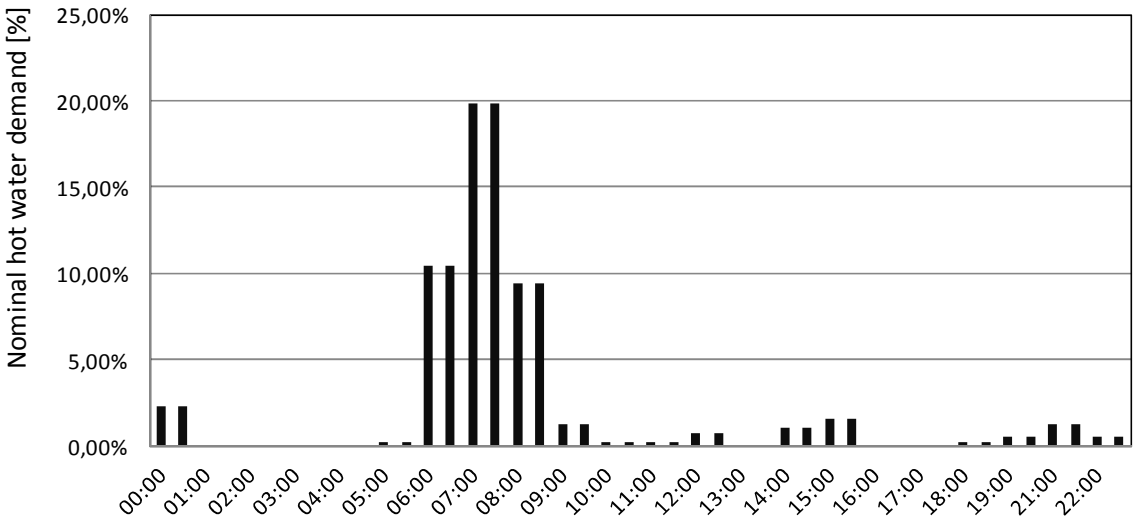

Figure 3.6: Draw-off pattern hotel hot water demand

The cold water supply of the tank follows an annual sinusoidal course between 8°C in February and 12°C in August and has been included in the model as profile based on the accordingly deduced Eq. (3.11).

$$T_{cw} = 10 - 2\ \sin\frac{\pi}{6}\ (moy + 1) \tag{3.11}$$

where,

T_{cw} supplied cold water temperature [°C]
moy month of the year, $m = 1, 2, \ldots, 12$

3.7 Thermal and Latent Room Model and Load

The air conditioned room is modelled using the building model by Schumacher et al. (2012), as it was applied for the simulation of a solar DEC-system by Pietruschka (2010). The model was implemented into the simulation environment INSEL 8 in the course of this research. This dynamic building model includes sub-models for an external wall and three inner walls as well as for floor and ceiling. In addition, the mode is complemented with a room node block, a

block to calculate exchange of long-wave radiation of the walls and a block to calculate the input of short-wave radiation through the window area. The model as it is visualized in Figure 3.7 thereby considers on the one hand the heat conduction and storage in walls, ceilings and floors, but on the other hand also the interaction of the building mass with the room air temperature through convection, long-wave radiation, solar gains, internal loads or ventilation.

The thermal conduction through the wall is explicitly calculated for each individual wall unit solving the one-dimensional heat transfer equation by means of the transfer function method in the corresponding wall block, whereas inner walls (block WALL) and external walls (WALLX) are distinguished. Thereby, the structure of the different walls can be included in the model with parameters thickness D, thermal conductivity λ, density ρ, and heat capacity c for each of the various wall layers.

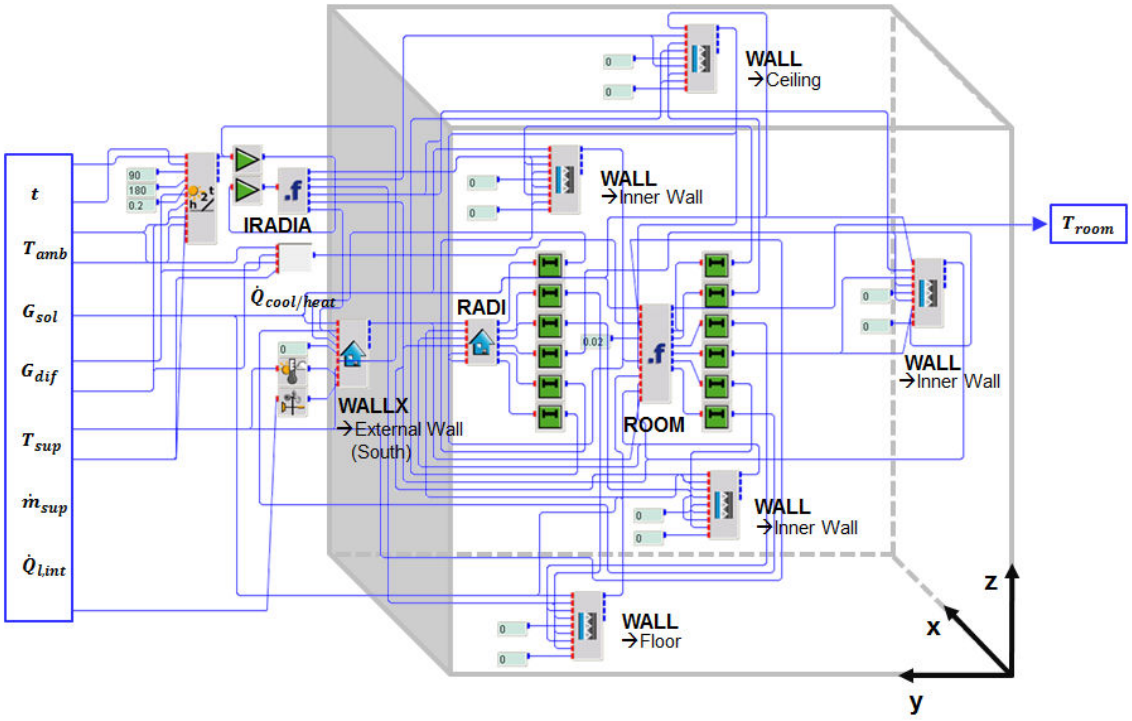

Figure 3.7: Thermal room model

For this purpose, the material parameters required for the model were determined for the room type category m based on VDI 2076 (2003) sheet 11 as it is summarized at a glance in Table 3.7.

The surface temperatures of the walls T_{wall} are completely calculated from the heat flux balances of each layer with the respective values of the previous time step. As boundary conditions short-wave solar gains, convective heat fluxes from the room air node and long-wave heat fluxes from the surrounding wall surfaces (from block RADI) are included in the calculation of the respective wall temperature T_{wall}. Additional constraints, especially required for the calculation of the external wall, are ambient temperature T_{amb}, sky temperature T_{sky} and wind speed v_{wind}.

Table 3.7: Wall material parameter

Element	**Layer**	D [m]	λ [W m^{-1}K^{-1}]	ρ [kg m^{-3}]	c [J kg^{-1}K^{-1}]
External wall	concrete	0.240	2.035	2100	920
	polystyrene insulation	0.062	0.047	75	840
	façade plate	0.025	0.045	1300	1050
Ceiling/Floor	metal ceiling	0.001	58.000	7800	480
	Rock wool	0.020	0.047	75	840
	armoured concrete	0.120	2.035	2100	920
Internal walls	aerated concrete	0.120	0.400	1200	1050

The solar gains into the room are included in the model with the block IRADIA. Thereto, the solar radiation on the vertical window area is multiplied with the transmission coefficients of window pane and external shading device. Thus, the IRADIA block calculates the distribution of the short-wave solar radiation input on the inner surfaced of the room walls. Thereby, the solar radiation is distributed on a percentage basis to the individual walls in accordance with the particular products of wall surface and respective absorption coefficient, which is ascertained individually for each wall.

The exchange of long-wave thermal radiation between the inner sided wall surfaces with different temperatures is modelled with the block RADI. Thereby,

the self-emission of each wall surface is balanced with the long-wave absorption of the residual surfaces and the net radiant flux is calculated for every wall surface. Boundary conditions for the block are the respective wall surface temperatures and the parameters of room length, width and height as well as the particular emission coefficients of the wall surfaces. For all walls the emission coefficient is uniformly assumed for concrete with 0.94 (Recknagel et al. 2007)

The block ROOM subsequently balances the convective heat fluxes and the convective fractions of the internal loads as well as the additional convective heating or cooling capacities to condition the room, taking into account the wall surface temperatures from the blocks WALL/WALLX. By means of the parameters room volume, the individual wall surfaces and a start value for the temperature of the room air node, the block eventually calculates the room air temperature T_{room} and the convective heat fluxes to the particular wall surfaces.

The described thermal room model determining the room temperature T_{room} exclusively accounts for sensible cooling loads. In order to calculate the absolute room humidity content and the resulting relative humidity of the room air, this thermal model is thence supplemented by a simple static humidity model according to Pietruschka (2010). According to that, the average absolute room air humidity x_{room} is calculated from the latent internal loads as well as the humidity input due to ventilation and infiltration (Appendix A.4).

The dimensioning of the air conditioned room was designed for an air-conditioning system with a supply air flow rate of 8.000 $m^3\ h^{-1}$ in accordance with the object under investigation. The utilization of the floor area is divided into 50% office area and 50% conference room. Based on a specific room area of 10 m^2 per person according to EN 13779 (2007) with EN 15251 (2007) and an occupancy rate of 0.9 according to a cooling load estimation as per VDI 2078 (2012) this results in a room occupancy of $n_{pers} = 40$ people and a corresponding room floor area of 900 m^2. Additional parameters of the room model are summarized in Table 3.8.

Table 3.8: Room model parameters

Dimensioning			
room volume V_{room}	2,700 m³	geometry:	quadratic
round area A_{room}	900 m²	room height:	3 m
room length	30 m	room width:	30 m
External loads			
proportion of window area	35%	window area	31.5 m²
absorbance coefficient window $b = b1 \cdot b2 \cdot b3$ = 0.05			(according to VDI 2078)
where: $b1 = 0{,}65$ *(double absorbance glazing),* $b2 = 0{,}15$ *(jalousie),* $b3 = 0{,}5$ *(bright curtains)*			
infiltration	0.02 V_{room} h⁻¹		54 m³ h⁻¹
Internal loads – room use			
occupation	40 persons (07:00 – 19:00)		
persons (sensible)	75 W p. pers.	VDI 2078, Tab. A1	3000 W (07:00 – 19:00)
PC's (sensible)	200 W per PC	VDI 2067, Tab. A2	8000 W (07:00 – 19:00)
			1000 W (07:00 – 19:00)
light	20 W m⁻²	VDI 2078, Tab. A2	2102 W (07:00 – 19:00)
	assumption: in average max. 20% of installed capacity in use		
persons (latent)	50 g h⁻¹ p. pers.	EN 13779, Tab. A13	2000 g h⁻¹ (07:00 – 19:00)
plants (latent)	overall	EN 13779, Tab. A13	300 g h⁻¹ (24 / 7)

3.8 Model Limitations and Boundary Conditions

In the course of this research planning documents were neither available for the DEC-control nor for the supervisory control or the collector circuit control of the investigated building. All of them have been developed in this research based on respective standards and expert interviews with system planner and manufacturer.

Aside from that, the modelled system simplifies the air-conditioned part of the building as a representative single room. While the monitored building is equipped with a thermal activation of the building structure supplied by heat pumps, the system model simplifies the basic heating function by means of a

supply air heater (SAH) in order to exclude the modelling of the thermally activated building structure and heat pumps from the system model. As a consequence, the validation of the overall system model with measurement data was not possible. In fact, the system model was validated on component level and the overall system was tested for plausibility.

Due to the fact that the simulation result foremost serves for the comparison of various system designs the system model allows the neglecting of pipe losses. In this context it must be additionally noted that apart from the electricity consumption of the solar pump, the consumption of circulating pumps in the heat distribution circuits is not regarded in respective energy balances.

Against the background of the described comparative evaluation of different concepts this consumption is assumed to occur similarly and can therefore be neglected. However, under real conditions additionally occurring thermal losses in the pipe system and the electricity consumption of further circulating pumps are to be considered.

As the overall research targeted the cooling process, the DEC-control does not include a winter supply air humidification for simplification reasons. Therefore, the evaluation of the thermal room comfort refers to the cooling period. Thereby, the respective set points for room air humidity are implemented as steady values as discussed in section 5.2.2. Due to the rising comfort demand of occupants in hotels and office buildings a dynamic linear adjustment of the room air temperature set point with increased ambient air temperature as it is introduced in VDI 3525 (2007) is avoided. As the system operation is limited from 07:00 to 19:00 the evaluation of the room comfort is limited to this time span.

The entire simulation study was carried out for the climatic boundary conditions of Ingolstadt (Germany), a site with multivalent heat demand for hot water, cooling and heating. Thereby, the study is based on meteorological weather data from the meteorological database Meteonorm (2013) including all typical weather conditions of a year in Ingolstadt. This test reference year (TRY) as illustrated in Figure 3.8 represents a statistical average year with time increment in minutes,

which was relevant for the simulation and evaluation of the systems control behaviour.

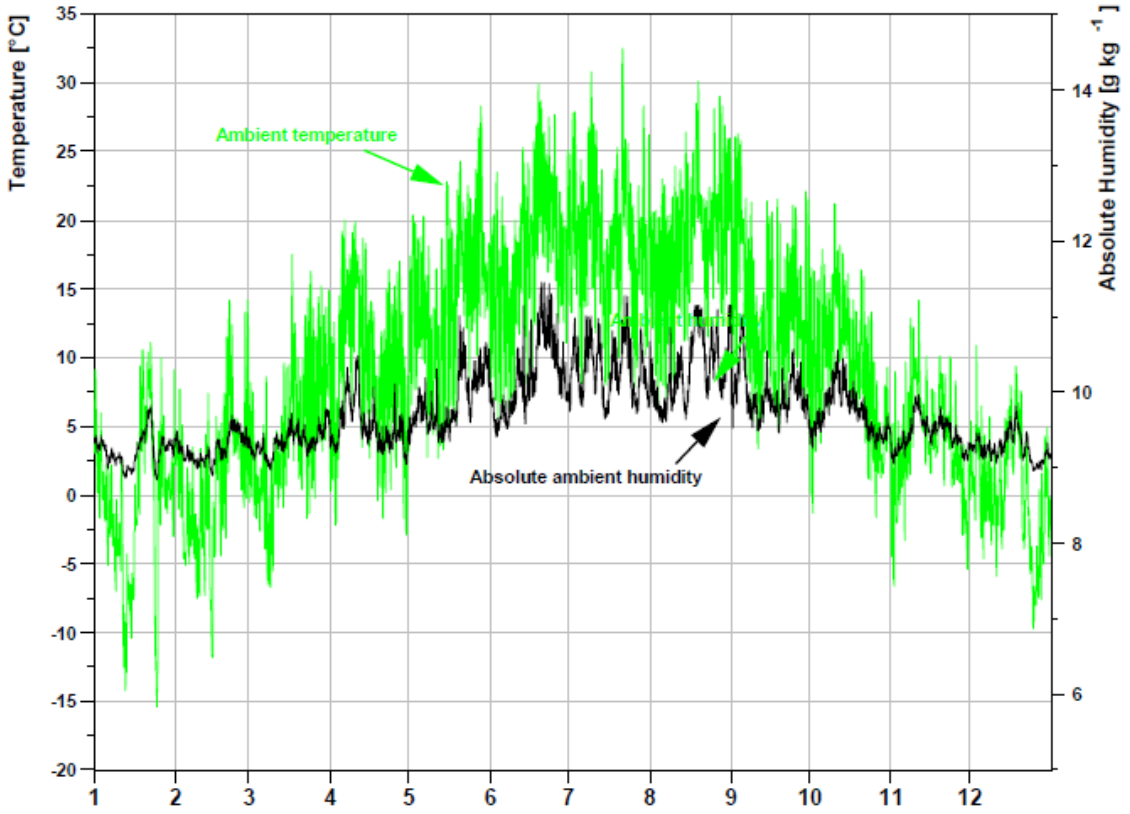

Figure 3.8: Weather data at site Ingolstadt (Germany)

4 Integral System Design Study

In order to investigate optimisations on the multivalent solar DEC-system the developed model is employed in a subsequent system design study. Thereto, appropriate objective functions are defined to create a common base of comparison.

In the first instance, the initial system configuration with direct sequential supply of heat sinks, as it was monitored in-situ, is enhanced by integrating a solar buffer store. Both system designs are hence analysed and evaluated in a primary base case. Thereby, as against the findings in the monitoring, the simulation study was carried out with the component parameters given by component manufacturers for the respective components in mint condition.

Based on the results of the initial base case, an optimised control strategy for solar DEC-systems with multivalent use of solar heat for air-conditioning, hot water preparation and heating is introduced. This advanced strategy is predicated on a simultaneous sink integration concept. The behaviour of this system with optimised control strategy is analysed and discussed by means of system simulations. Thereby, the system performance is systematically evaluated on the basis of preassigned objective functions.

Subsequently, a sensitivity analysis of the system with optimised control strategy is carried out. The sensitivity analysis is based on the central composite design approach which is deduced as an appropriate design of experiments (DoE) method relevant to this research. An experimental space for the parametric study is deduced defining ranges of the system parameters intended to be varied. Finally, the sensitivity analysis with parameter variation leads to optimised dimensioning criteria at a system level with regard to an improved configuration of multivalent systems in the system planning phase.

4.1 Objective Functions for Optimisation

Objective functions for system optimisation describe the aimed state of output regarding system dimensioning and either describe a minimization or a maximization problem. In contrary to problems with the pursuit of a single objective, within this research, multiple and partly concurrent objectives have to be defined in the search for system optima.

Hence, for a year-round assessment of the performance of the investigated system approaches of a multivalent solar DEC-system for air conditioning, hot water preparation and heating, the following optimisation objectives were regarded in particular:

- minimise the total auxiliary electrical energy consumption $E_{el,TOT}$,
- maximise the primary energy ratio PER,
- maximise the solar fraction f_{sol},
- maximise the specific annual collector yield $Q_{col,spec}$.

The operation of the multivalent solar thermal system requires the use of auxiliary electrical energy. Therefore, a main objective is to reduce and minimize this cumulative annual total electricity consumption (Eq. 4.1).

$$minimize\, E_{elTOT} = \sum_{i=1}^{8760} (E_{elDEC,i} + E_{elSAH,i} + E_{elHRD,i} + E_{elSPU,i}) \tag{4.1}$$

$$E_{elDEC,i} = E_{elHRW,i} + E_{elDW,i} + E_{elSHUM,i} + E_{elRHUM,i} + E_{elFANS,i} \tag{4.2}$$

where,

$E_{el\,TOT}$	total auxiliary electric energy consumption [kWh]
$E_{elDEC,i}$	hourly electric consumption DEC-system [kWh]
$E_{elSAH,i}$	hourly electric consumption supply air heater [kWh]
$E_{elHRD,i}$	hourly electric consumption HW-heating rod [kWh]
$E_{elSPU,i}$	hourly electric consumption solar circulation pump [kWh]

$E_{elHRW,i}$ hourly electric consumption motor HRW [kWh]
$E_{elDW,i}$ hourly electric consumption motor DW [kWh]
$E_{elSHUM,i}$ hourly electric consumption high pressure pump SHUM [kWh]
$E_{elRHUM,i}$ hourly electric consumption high pressure pump RHUM [kWh]
$E_{el,FANS,i}$ hourly electric consumption fans in supply and return air [kWh]

In addition to the total auxiliary electric energy consumption $E_{el\,TOT}$, the primary energy ratio PER serves as additional evaluation criterion in the course of the system optimisation. The PER expresses the units of effectively useful cooling and heat energy output in relation to the expended primary energy. Thus, PER provides the comparison of multivalent solar cooling systems considering potential primary energy savings and broadens the energetic evaluation with an environmental dimension. The corresponding objective function (Eq. 4.3) was defined in due consideration of the monitoring procedure for solar heating and cooling systems defined by the IEA Task 38 (Sparber et al. 2008).

$$maximize\ PER = \varepsilon_{el} \frac{\sum_{i=1}^{8760}\left(\left|\Delta H_{AHU,i}\right| + Q_{HWuse,i}\right)}{E_{elTOT}} \tag{4.3}$$

where,

$\left|\Delta H_{AHU,i}\right|$ absolute hourly enthalpy difference ambient air to supply air [kWh]
$Q_{HWuse,i}$ hourly heat consumption hot water preparation [kWh]
ε_{el} conversion factor [-]

In line with IEA Task 38, the absolute value of the hourly supply air enthalpy difference $\left|\Delta H_{AHU,i}\right|$ accounts for the absolute heating and refrigeration capacity of the DEC-system depending on the mode of operation. The conversion factor ε_{el} as ratio of usable electrical final energy to primary energy is assumed with $\varepsilon_{el} = 0.4$ representing the average value for electricity generation within the EU-17 states (Faninger 2009).

The maximisation of the evaluation figure annual solar fraction f_{sol} was assigned as further objective regarding the optimisation of the multivalent solar DEC-

system (Eq. 4.4). The solar fraction f_{sol} illustrates the contribution of used solar yields to the overall energy demand. According to Duffie and Beckman (1991), the total load of the multivalent system can be expressed as sum of the solar yields Q_{col} and the auxiliary electric energy consumption E_{elTOT}, regardless of the size of the solar thermal system in terms of its aperture area A_{col}. Thus, maximizing f_{sol} leads to a reduced consumption of auxiliary electric energy E_{elTOT} if the overall energy consumption is kept constant.

$$maximise\, f_{sol} = \frac{\sum_{i=1}^{8760} Q_{col,i}}{E_{elTOT} + \sum_{i=1}^{8760} Q_{col,i}} \tag{4.4}$$

$$Q_{col,i} = c_{pWG} \int_{1}^{60} \dot{m}_{col}(t)\,[T_{out}(t) - T_{in}(t)]\,dt \tag{4.5}$$

where,

f_{sol}	annual solar fraction [-]
$Q_{col,i}$	hourly solar yields [kWh]
c_{pWG}	specific heat capacity collector fluid [kJ (kgK)$^{-1}$]
$\dot{m}_{col}\ (t)$	mass flow collector circuit at a time step t (minute) [kg s^{-1}]
$T_{in}\ (t)$	collector return temperature at time step t (minute) [°C]
$T_{out}\ (t)$	collector flow temperature at time step t (minute) [°C]

The evaluation criterion $Q_{col,spec}$ denotes the annual collector yield in relation to the installed collector area A_{col}.

$$maximise\, Q_{col,spec} = (A_{col})^{-1} \sum_{i=1}^{8760} Q_{col,i} \tag{4.6}$$

Apart from an energetically efficient mode of operation, the achievement of thermally comfortable room air conditions is the elementary objective of the solar DEC-system. Therefore, as an additional constraint to the energetically focused objective functions, the impact of the parameter variation on the continuous variables room air temperature T_{room} and room air humidity φ_{room} was observed.

4.2 Impact of Buffer Store Integration towards Original Design

The in-situ monitored system to be optimised did not include a solar buffer storage (SBS). However, buffering of solar heat was identified to be state-of-the-art of solar DEC-systems. Hence, in an initial base case the original system design was compared to a modified system design with SBS.

4.2.1 System Designs under Investigation

The initial base case simulation study compares the behaviour and performance of the following two system designs using TRY weather data as described in section 3.8:

- System design A: Direct sink integration without SBS (cf. Figure 4.1)
- System design B: Buffered sink integration with SBS (cf. Figure 4.2)

Thereby, system design A (Figure 4.1) is based on the initial situation at the system under in-situ investigation. The thermal interface between collector circle and heat sinks was designed by means of a hydraulic switch, as illustrated symbolically in Figure 4.1. As implemented in-situ, the supervisory control strategy follows a sequential distribution of solar heat to the heat sinks DEC-system (RAH), hot water preparation (HWS) and heating (SAH) and hence represents the actual situation. In this context, the control follows the sequence as described in section 3.5.4. This sequence follows a sequential “either-or” strategy with priority of solar heat supply to hot water preparation.

In contrast to system design A, the modified system design B (Figure 4.2.) represents a sequential hydraulic integration of the heat sinks with SBS. The SBS was dimensioned with a volume V_{SBS} =10.68 m^3, representing a buffer volume to supply solar heat in order to extend the DEC-operation by two additional hours compared to a system without buffer store. The supervisory control strategy of system design B is similar to the strategy of system design A and also follows a sequential “either-or” strategy with priority of solar heat supply to hot water preparation.

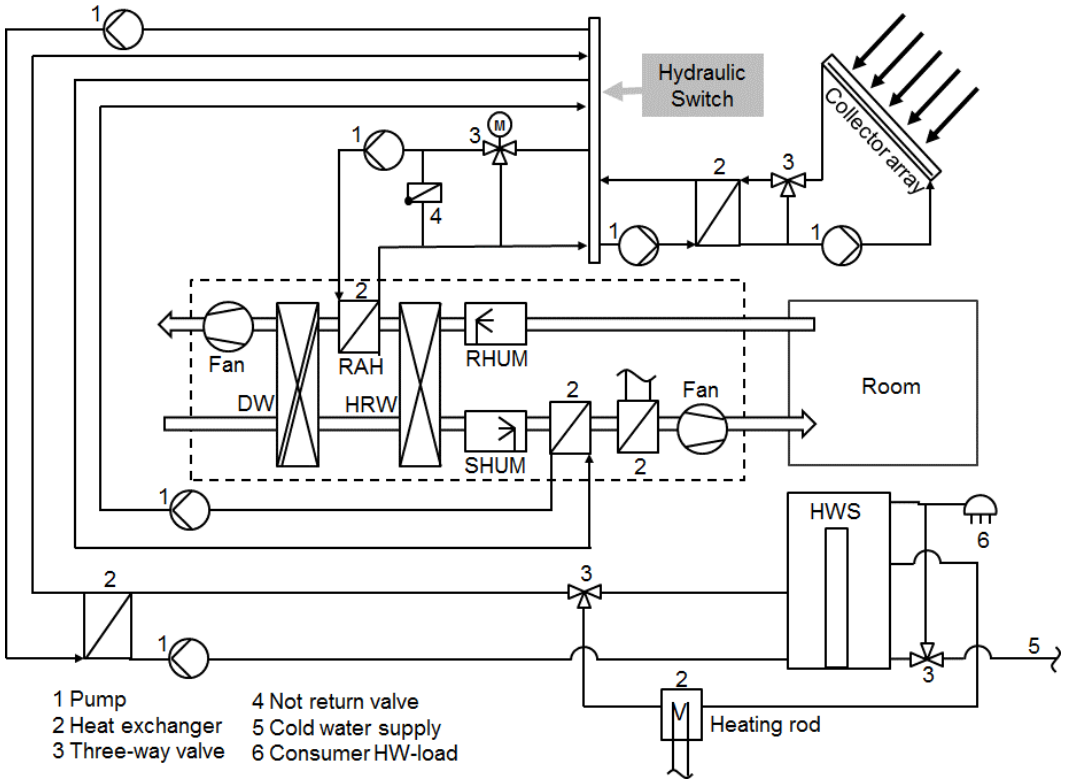

Figure 4.1: System design A - sequential direct sink integration without SBS

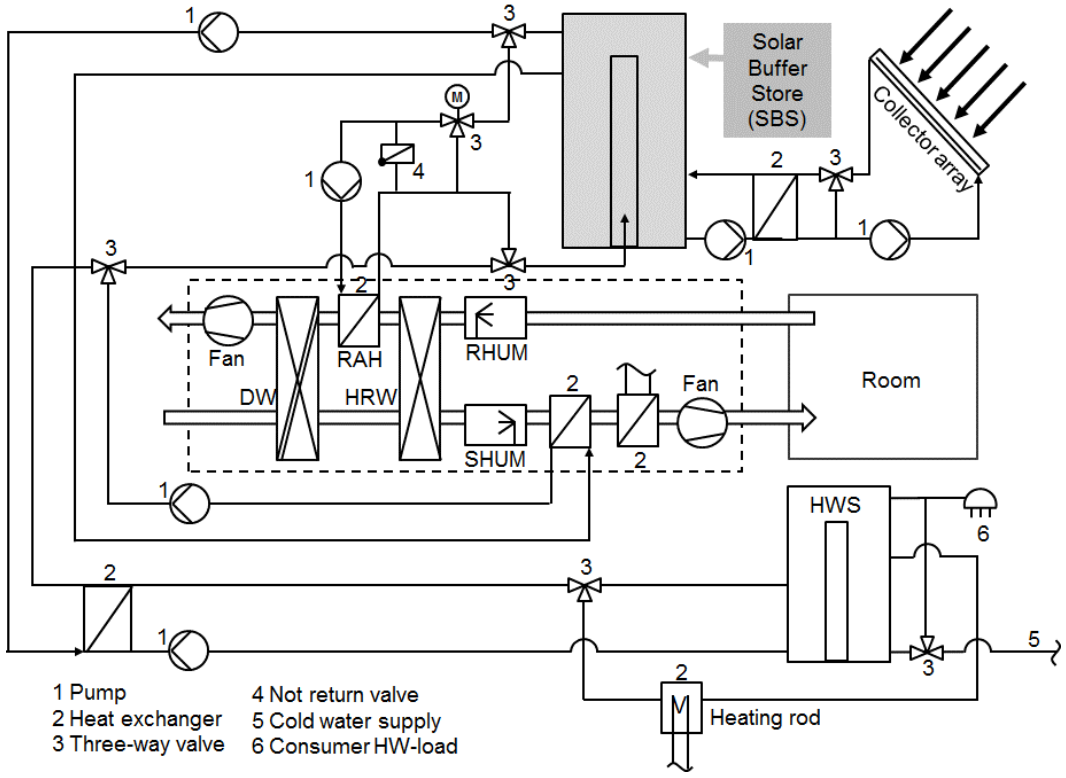

Figure 4.2: System scheme B - sequential buffered sink integration with SBS

To ensure comparability of results, this base case for both systems A and B is performed with the system dimensions of the in-situ object, defined as follows: flat-plate collector area $A_{col} = 260.40°m^2$, inclination angle $\alpha = 30°$ and volume hot water storage $V_{HWS} = 4.5\ m^3$.

4.2.2 Direct Sequential Sink Integration

Analysing the system behaviour of the initial system with sequential direct sink integration without SBS (system design A) it became evident that the DEC-system can operate in full DEC-mode including dehumidification on 17 operation days. It can be noted, that on all respective operation days the system cannot maintain a stable operation in full DEC-mode (mode 5).

As shown for a considered exemplary cooling day in June at around 12:10 the supervisory control facilitates the DEC-system to start its operation in full DEC-mode (Figure 4.3, lower diagram). Due to the fact, that the room air humidity x_{room} measures 12 g kg^{-1} and already exceeds the implemented threshold for the room air humidity $x_{room,set}$ (c.f. section 3.4.3), the DEC-system starts its operation in DEC-mode and hence can create comfortable room air conditions (Figure 4.3, middle diagram).

However, the DEC-process can only be maintained for approximately 80 minutes. As the collector flow temperature decreases, the hydraulic switch cannot maintain the supply of regeneration heat at a sufficiently high temperature level above $T_{reg,set}$ = 75°C and thus stops the dehumidification mode (Figure 4.3, upper diagram). Indeed a further sorptive dehumidification would be required, but due to the lack of a solar buffer storage the available regeneration heat directly depends on the actual heat flux provided by the collector array.

Apart from the discontinuous unstable DEC-operation, the simulation analysis of system A provides further understanding of the system behaviour which is characterized by extensive operation times with stagnation in the solar circuit. During operation times with limited or no solar heat demand the absence of a solar buffer storage leads to a standstill of the solar pump and thus to excessive

temperatures of up to 180°C in the solar circuit. According to the simulation results it is worth noting that the problem of stagnation occurs on 86 operation days in the course of the year. Thus, in a real system the observed stagnation would not only cause excessive pressures and temperature loads on the system components. In fact, high times of system stagnation obviously lead to a reduced annual collector yield. Overall, the annual collector yield reaches 80.5 MWh which corresponds to 308 kWh m^{-2}.

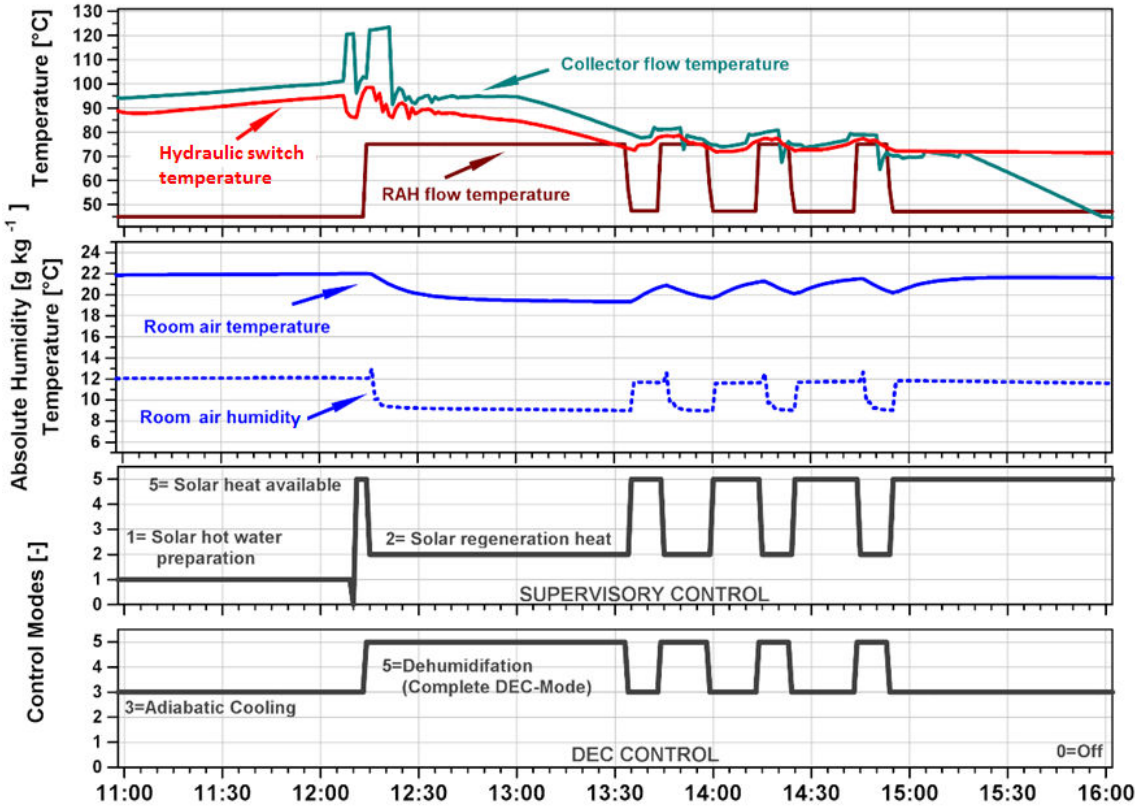

Figure 4.3: Instable DEC-operation of solar DEC-system with sequential direct sink integration without SBS (system design A)

This simulation result supports the integration of a solar buffer store (SBS) in the system design.

4.2.3 Sequential Sink Integration with Solar Buffer Store

A comparison on an annual basis was carried out comparing the yearly performance figures of the system without buffer store (system design A) with the results of the system with solar buffer store (SBS, system design B).

The improved system with SBS achieves an annual collector yield of 100.5 MWh and thus the specific annual collector yield can be increased by 24.9% to 386 kWh m^{-2}. Due to the substantially increased collector yield, the system's solar fraction is augmented from 42% to 51% (+21.4%). In terms of the year round total auxiliary electric energy consumption E_{elTOT}, the comparison to the system with direct sink supply revealed savings in auxiliary energy consumption of 16.1 MWh (-14.5%). This leads to a raised PER from 0.82 to 0.97 (+18.3%). The results for the overall annual performance figures of the two design alternatives are summarized in Table 4.1.

Although the integration of a SBS leads to increased solar gains, both system alternatives provide the bulk of the solar thermal heat for hot water preparation. On a yearly basis, more than 90% of the solar heat provided to the system is distributed to hot water preparation in both system designs. This is due to the priority of this heat sink in the supervisory control strategy.

Table 4.1: Overview overall year round performance figures

Performance Figure	System A	System B
Total auxiliary electricity consumption	111.1 MWh	95.0 MWh
DEC-operation	0.9%	1.0%
Ventilation	31.6%	36.9%
Supply air heating back up	17.0%	17.3%
Hot water back up	50.3%	44.5%
Solar pump	0.2%	0.3%
Annual solar collector yield	80.5 MWh	100.5 MWh
Specific solar collector yield	308 kWh m^{-2}	386 kWh m^{-2}
to DEC-process	1.6%	2.2%
to hot water preparation	94.8%	92.4%
to supply air heating	3.6%	5.4%
Primary Energy Ratio	0.82	0.97
Solar Fraction	42%	51%

In order to further investigate the behaviour of the multivalent system with SBS and the impact of the supervisory control strategy on the system performance, the system operation is analysed on a daily basis for selected representative days. Figure 4.4 illustrates the modes of DEC and supervisory control as well as relevant air conditions for an exemplary cooling day in June. It can be observed that the room air humidity exceeds the maximum threshold of 10.4 g kg^{-1} already with start of DEC-system operation at 07:00 (Figure 4.4, middle diagram).

The system, however, complies with the high morning hot water demand in the hotel and the supervisory control regulates the system to mode 1 to provide solar heat for hot water preparation (Figure 4.4, lower diagram).

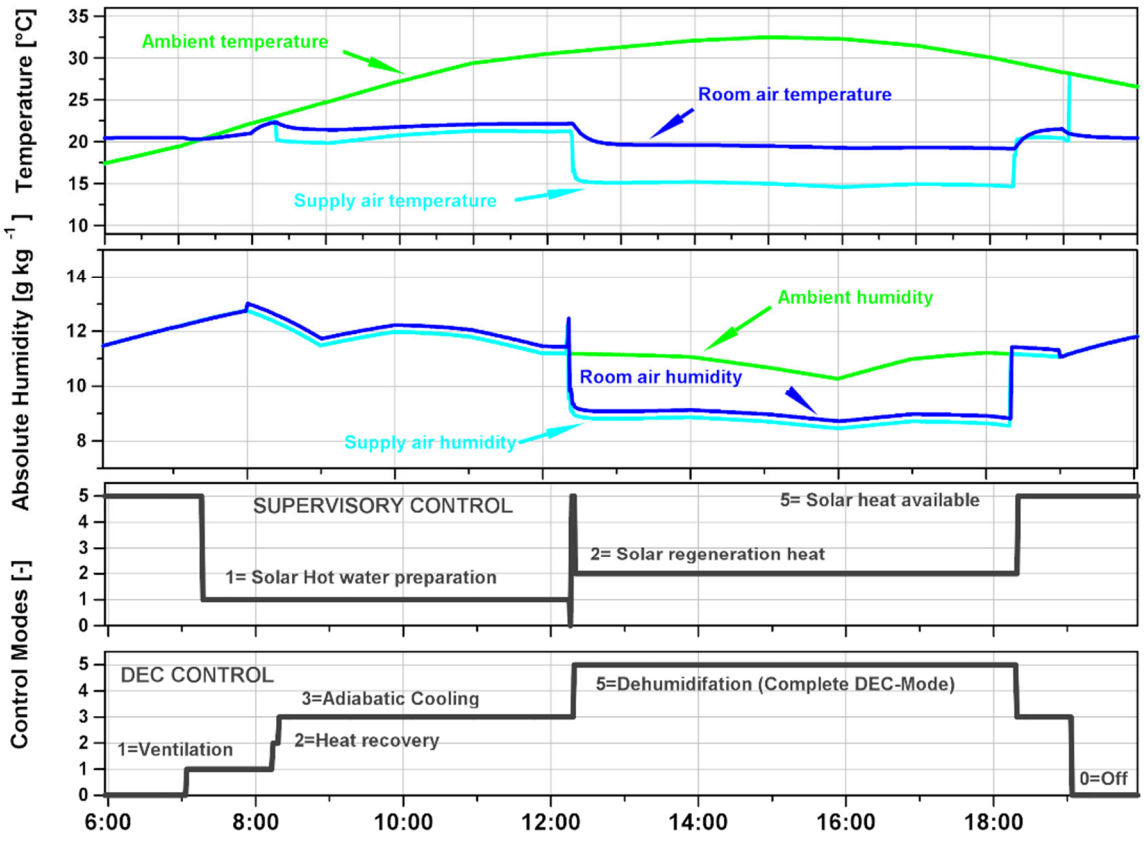

Figure 4.4: System design with SBS - control modes and thermal comfort conditions on a representative cooling day

Due to the priority of hot water preparation in the original supervisory control and the fact that the SBS discharge does not allow any parallel supply of more than one heat sink, the DEC-process is not sufficiently provided with solar heat.

Because of the unavailable solar heat the DEC-control has to remain in its adiabatic cooling mode 3. Thus, the required sorptive dehumidification of the supply air in order to lower the room air humidity level cannot be activated. Hence, the system cannot realise appropriate thermal comfort conditions.

As illustrated in Figure 4.5 the mass flow (lower diagram) and thus the heat flux to the HWS (upper diagram) stops at around 12:10 as the HWS top temperature reaches its maximum set point. Accordingly, the supervisory control indicates the availability of solar heat (mode 5; Figure 4.4, lower diagram). Due to that effect the DEC-control is able to activate the dehumidification mode (mode 5; Figure 4.4, lower diagram), as the SBS is now capable of supplying the required regeneration heat at a temperature level above 75°C (Figure 4.5, middle diagram). Thus, the solar DEC-system can take its complete operation and create comfortable room air conditions (Figure 4.4, upper and middle diagram).

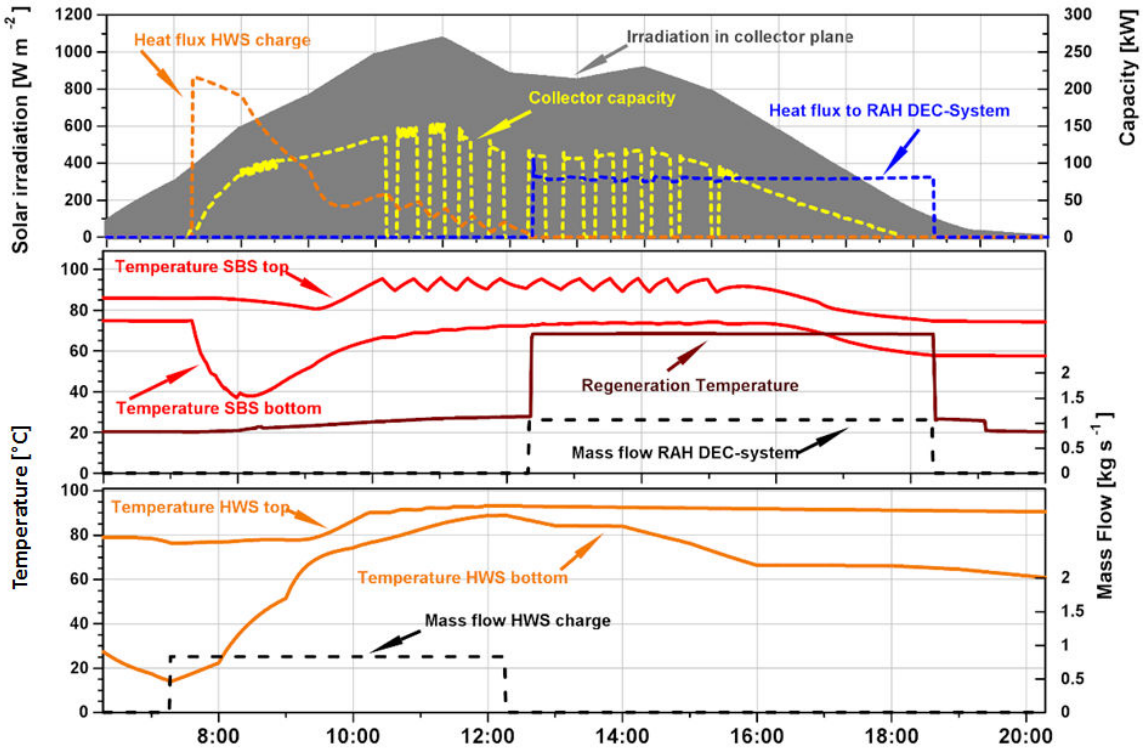

Figure 4.5: System design with SBS – Storage behaviour and heat distribution on a representative cooling day

The simulation results before 12:10 further show that the exclusive priority of the hot water preparation hinders the system's ability to provide the required regeneration heat to the DEC-system. Even though the discharged capacity from the SBS decreases with increasing HWS temperature level, the supervisory control is not able to provide solar heat for a further heat sink.

Altogether, the data show that the DEC-system could not operate in the required DEC-mode, either because of the direct interference with the hot water preparation or because of a decreased SBS temperature after a respective exhaustive hot water preparation which is then insufficient to operate the RAH in the DEC-system. The detailed investigation of the simulated data shows that, in summary, the hot water preparation interferes with the DEC-process on 29 days for approximately 230 operating hours.

As the data show, a contemporaneous high heat flux from the collector array leads to the complete charge of the SBS (Figure 4.5, middle and upper diagram). In consequence, the collector circuit stagnates periodically after 10:00. For the exemplary cooling day this demonstrates very clearly that on the one hand, the implemented supervisory control strategy cannot comply with the systems heat requirements and on the other hand, as a consequence, this reduces the collector yield.

The observed control problem of the competing heat sinks arises again during heating periods. As illustrated in Figure 4.6 (lower diagram), the results for an exemplary heating day in February show that the DEC-control indicates the requirement of supply air heating (mode 10) throughout the analysis period. However, due to the supervisory control's priority on solar hot water preparation (mode 1), solar heat cannot be utilized for room heating.

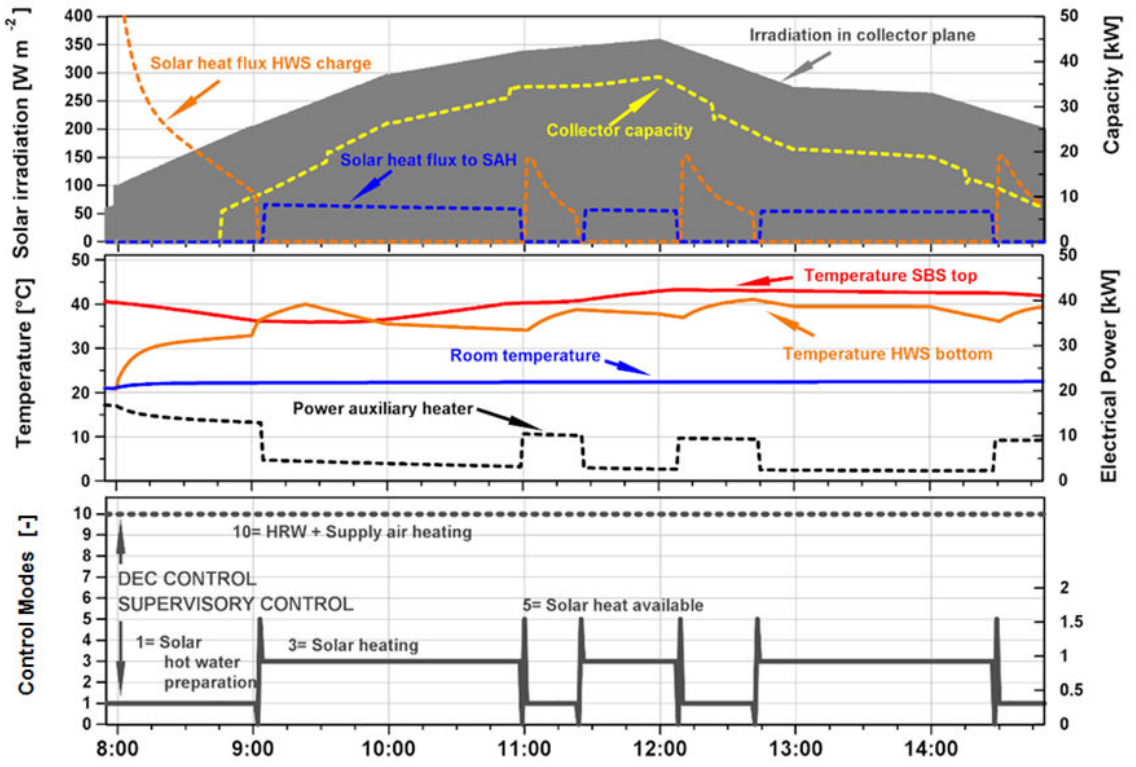

Figure 4.6: System design with SBS – System behaviour and heat distribution on a representative heating day

In consequence, the capacity of the auxiliary heating backup in the supply air duct increases in order to compensate for the unavailable solar heat, even though the SBS shows a sufficiently high temperature of above 30°C for room air heating (Figure 4.6, middle diagram).

It can be further observed that the solar heat flux to supply air heating is interrupted repeatedly Figure 4.6 (upper diagram). When the temperature difference between $T_{SBS,top}$ and $T_{HWS,bottom}$ exceeds 6 K, the supervisory control prioritizes the hot water preparation and temporarily stops the solar air heating process Figure 4.6 (middle diagram). The sequential control strategy therefore causes auxiliary energy consumption in times of operation, when the system would in principle be capable to operate with solar thermal heat only.

A detailed review of the simulation data reveals that the described interference of the system modes heating and hot water preparation occurs during 63% of the operational days with heating demand.

4.3 Development of Optimised Control Strategy for Multivalent Systems

The simulation results of the two design alternatives in section 4.2 showed that the system with SBS can significantly increase the solar fraction and the annual collector yield and thus reduce the auxiliary primary energy consumption of the multivalent system compared to the system without SBS. Therefore, the design option without SBS was not further involved in the ongoing study. However, it must be noted that the sequential control strategy hinders the system to fully utilize the available solar heat and thus causes unnecessary consumption of auxiliary primary energy. Therefore it is relevant to further develop the system with SBS with an optimised supervisory strategy.

4.3.1 Simultaneous Supervisory Control Strategy Development

The following new approach consists of a supervisory control strategy based on a comprehensive concept which allows a simultaneous supply of heat sinks. The simultaneous SBS discharge concept hence allows the provision of solar thermal heat for cooling or heating contemporaneous to the hot water preparation.

This advanced optimised control strategy aims at creating a stable solar-driven DEC-cooling and heating process while maintaining the solar hot water preparation at the same time. The hydraulic scheme of the simultaneous concept (system design C) is illustrated in Figure 4.7.

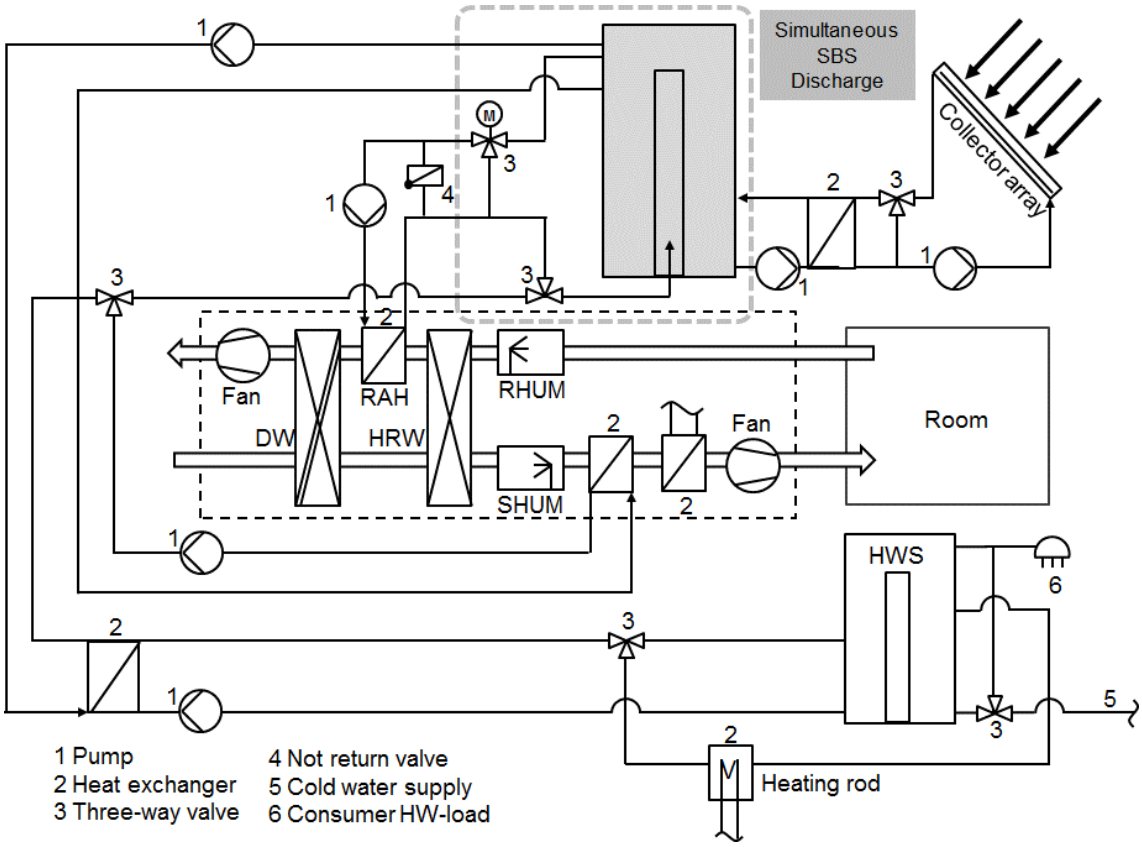

Figure 4.7: System design C - simultaneous sink integration with SBS

The operation modes (mode_supvis) of the developed simultaneous control strategy are shown in Table 4.2 and its decision scheme is illustrated in detail in Figure 4.8 and Figure 4.9. The control strategy was programmed as subroutine using FORTRAN 77. The compiled code was implemented as block module in the INSEL 8 simulation environment.

Table 4.2: Store discharge supervisory control modes

Modes of simultaneous control sequence	**mode_supvis**
No discharge of solar heat	0
Hot water preparation (HW)	1
Feed DEC-system regeneration air heater (RAH)	2
Feed supply air heater (SAH)	3
Simultaneous DEC-cooling (RAH) with HW-preparation	4
Simultaneous supply air heating (SAH) with HW-preparation	5

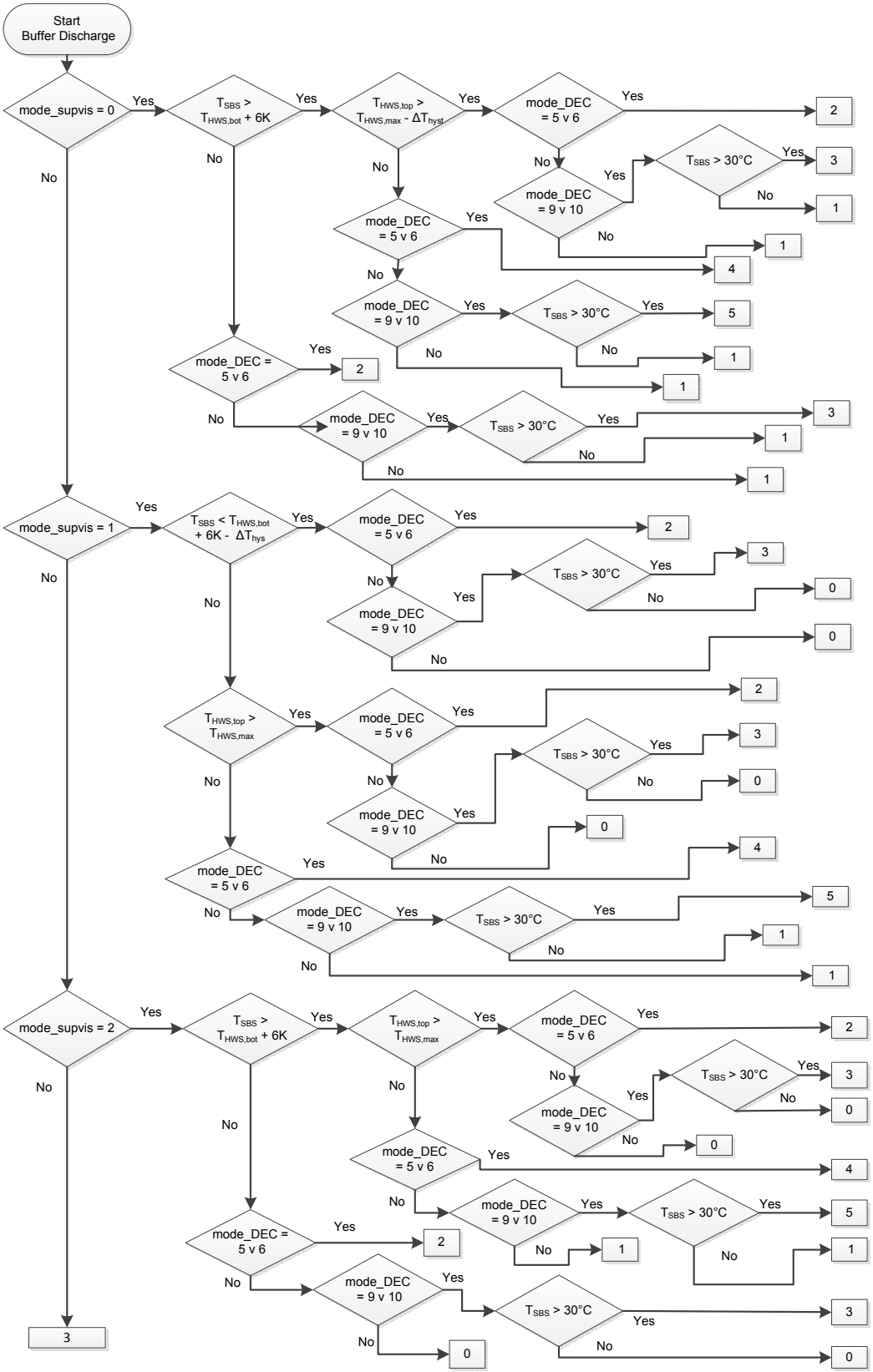

Figure 4.8: Developed simultaneous supervisory control strategy (mode_supvis 0 - 2)

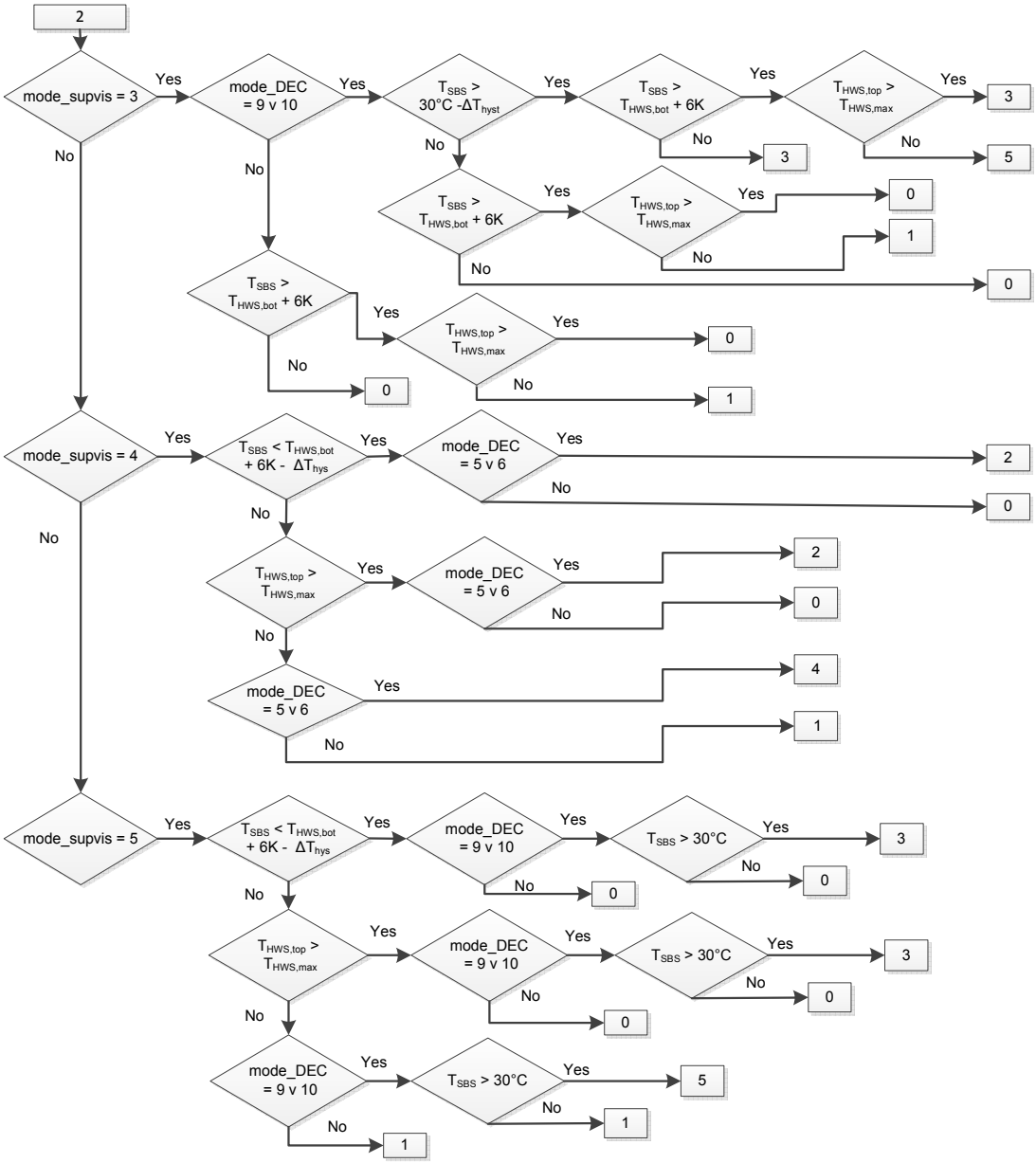

Figure 4.9: Developed simultaneous supervisory control strategy (mode_supvis 3 - 5)

4.3.2 Optimised System Behaviour and Design Evaluation

In order to verify the effect of the advanced simultaneous supervisory control strategy on the system performance, the simulation results are discussed in the following. Regarding the comparability of results the multivalent system behaviour is investigated for the same selected exemplary days that have been analysed with the prior sequential control strategy.

Figure 4.10 outlines the multivalent system operation for the exemplary cooling day in June. The results show that the supervisory control is discharging the SBS providing heat for hot water preparation when the DEC-system starts its operation at 07:00 (Figure 4.10, lower diagram).

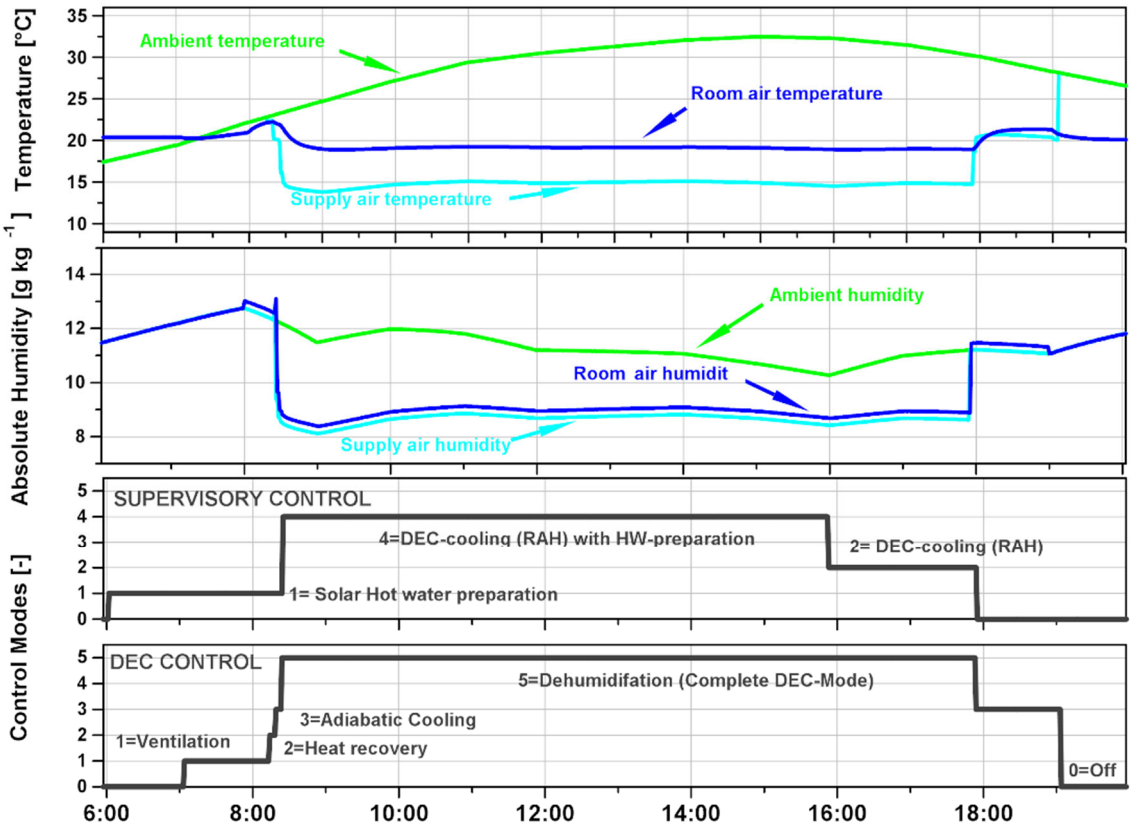

Figure 4.10: Simultaneous supervisory control strategy - control modes and thermal comfort conditions on a representative cooling day

At around 08:10, the room air temperature T_{room} exceeds its upper threshold of 22°C (Figure 4.10, upper diagram) and thus the DEC-control starts its cooling cascade (Figure 4.10, lower diagram). Due to the fact that the room air humidity level already requires dehumidification with start of the cooling cascade, the DEC-control regulates the cascade to mode 5 (complete DEC-mode).

In contrast to the discussed behaviour of the sequential control strategy, the newly implemented simultaneous supervisory control strategy is in the position to provide regeneration heat for the DEC-process even though the hot water preparation (HW) indicates a continuing solar thermal heat demand. Therefore,

the advanced system enables the simultaneous operation of both DEC-process in dehumidification mode and HW-preparation as defined by the respective control modes (Figure 4.10, lower diagram) and the respective mass flows to the heat sinks (Figure 4.11, upper diagram). Shortly before 16:00, the temperature difference between SBS-top node and HWS bottom node decreases below its lower threshold (Figure 4.11, upper diagram). This terminates the solar HW-preparation and the supervisory control continues regulating the system in DEC-cooling-mode only (mode 2, Figure 4.10, lower diagram).

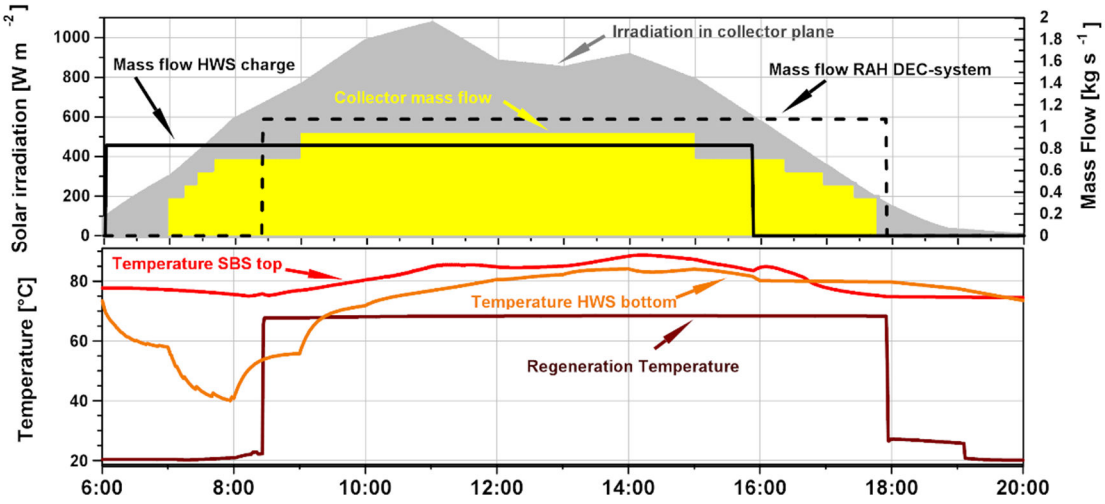

Figure 4.11: Simultaneous supervisory control strategy – storage behaviour and mass flows on a representative cooling day

Hence, the obtained simulation results show that the introduced simultaneous control strategy has a positive impact on the thermal room comfort on the one hand and on a stable operation of the multivalent solar system on the other hand.

In addition, it can be seen that the modified supervisory control strategy also improves the system behaviour in heating mode. As illustrated in Figure 4.12 (lower diagram) the control allows the system to provide solar heat for HW-preparation while maintaining the solar heating function with the heat supply to the supply air heater (SAH). In contrast to the original control strategy, e.g. at 11:05 or at 12:10, the solar thermal heating is not interrupted by the occurrence of solar heat demand for HW-preparation. In fact, solar thermal heat is provided for both heat sinks as indicated by the mass flows in Figure 4.12 (middle

diagram). Due to this increase in utilization of solar heat, the supply air auxiliary heating back-up does not have to be operated with full power in times of solar HW-preparation (Figure 4.12, middle diagram).

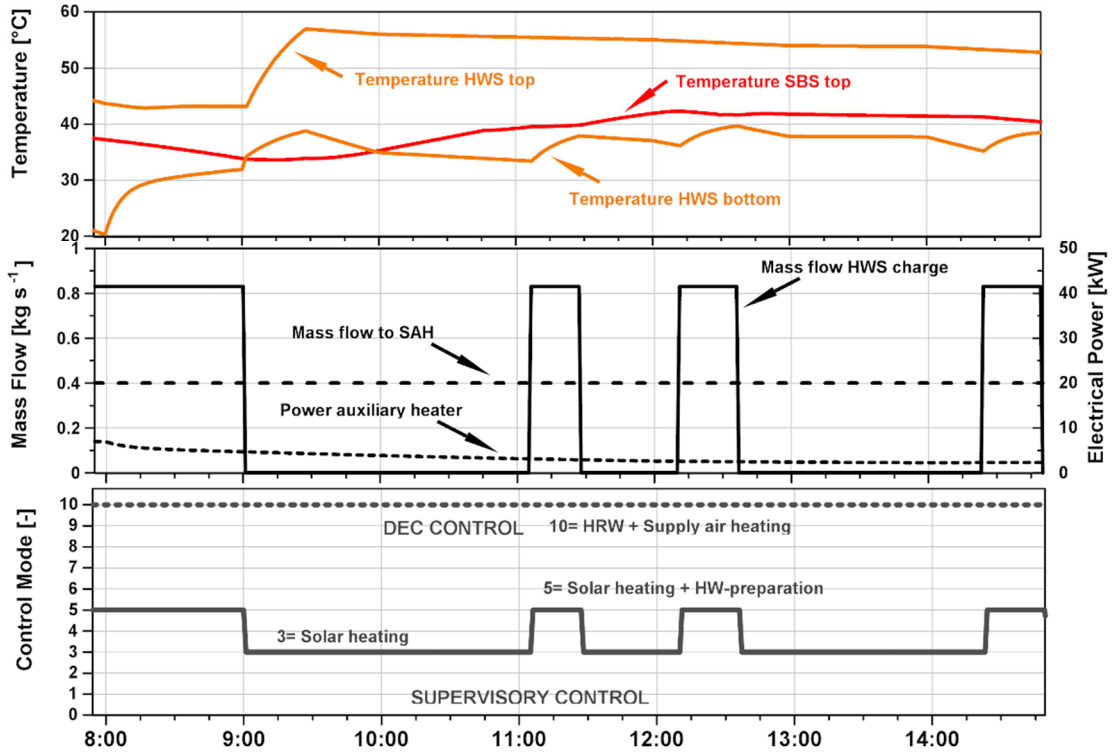

Figure 4.12: Simultaneous supervisory control strategy - system behaviour on a representative heating day

From this improved system behaviour it follows that the new simultaneous design can further reduce the total auxiliary electric energy consumption E_{elTOT} and increase the solar fraction, compared to the sequential solar buffer discharge strategy.

As depicted in Figure 4.13, the concept with simultaneous sink integration is capable to further reduce E_{elTOT} by 5.2% to 90.1 MWh. This implies that merely the optimisation of the control strategy to a simultaneous heat sink supply increases the PER of the multivalent system by a further 6.2% to 1.03. The data further show that the solar fraction f_{sol} can be increased by 3.9%, whereas the specific annual collector yield $Q_{col,spec}$ increased by 1% to 390 kWh m^{-2} (Figure 4.14).

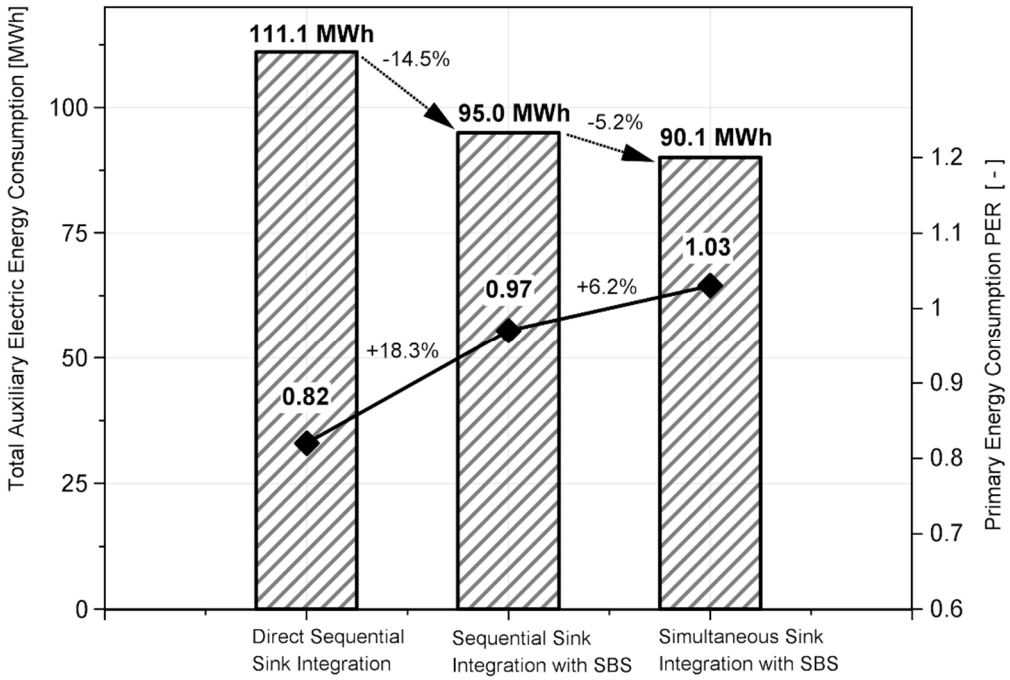

Figure 4.13: System comparison – E_{elTOT} and PER

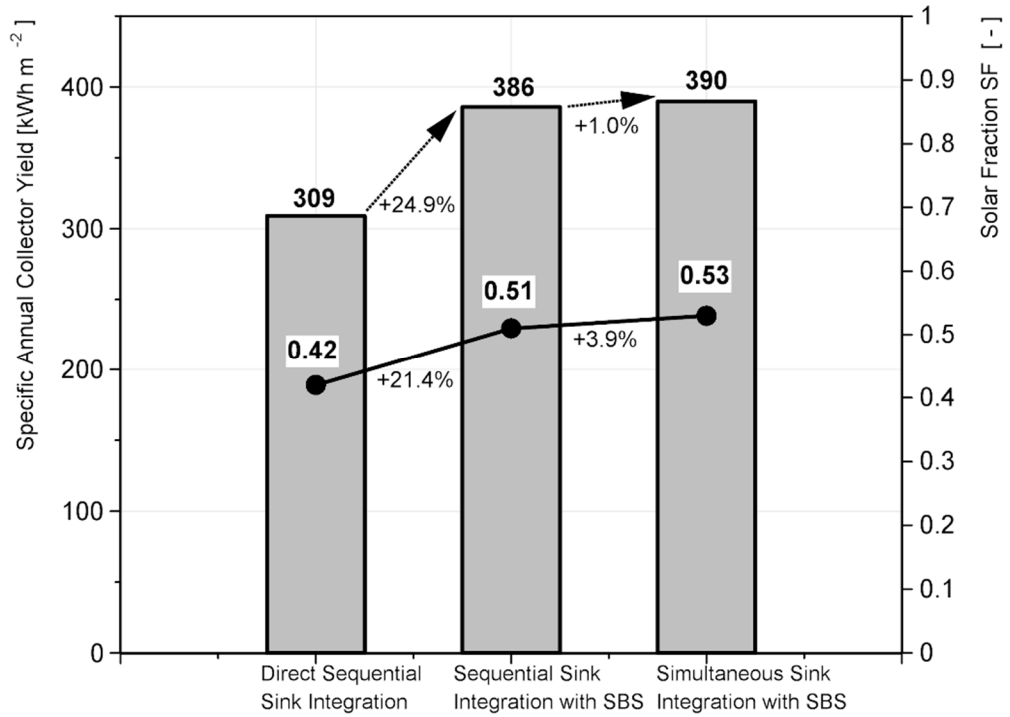

Figure 4.14: System comparison - $Q_{col,spec}$ and f_{sol}

Through this comparative simulation study it was found that the simultaneous SBS discharge concept (system design C) obtained improved energetic indicators compared to the concepts with sequential SBS discharge (system designs A and B). Due to the fact that a simultaneous heat sink supply by trend necessitates a generously dimensioned SBS it was expected that the performance of the system could be further increased with properly adjusted system dimensions. As a result, the most promising system design C was selected for a subsequent parameter variation in order to deduce optimised dimensioning parameters on system level.

4.4 Sensitivity Analysis of Optimised System Design

After having confirmed the effectiveness of the simultaneous supervisory control strategy, this section presents the parametric simulation study on this optimised new multivalent design. This leads to the most promising system dimensioning setup.

4.4.1 Design of Experiments Methodology

Design of Experiments (DoE) is regarded as an efficient and reliable statistical method for simulation based system optimisations in order to approximate system optima with a limited number of simulation runs. DoE is defined as a set of tests with altering selected system factors to investigate the effects in the response variables resulting in valid and objective conclusions (Dixon et al. 2006, Montgomery 2009). By means of the simulation results for selected parameters DoE determines a regression function for each response variable (objective function) which is considered valid over the entire defined experiment space.

Therewith, arbitrary function values as well as minima and maxima can be calculated. Hence, DoE can maximise the amount of information gained in an experiment (Adam 2004). Compared to conventional local sensitivity analysis methods, such as one factor at a time (OFAT), DoE reduces the testing effort

requiring minimum resources and gives more precise results as it is capable of considering relationships between the varied factors.

There is a variety of approaches to carry out DoE analyses: full factorial design (FD), fractional factorial design (FFD), Box-Behnken design (BBD), latin hypercube design (LHD) and central composite design (CCD).

FD investigates all factors levels combinations and all possible interactions. A FD is very powerful in investigating linear relationships, however, it lacks the ability to discover higher order, e.g. quadratic relationships. Applying a FD, with an increasing number of factors, the experiment turns out to be comparatively complex leading to an augmented number of simulation runs to be conducted.

FFD carries out a subset of the runs of a full factorial design. Compared to FFD, BBD is optimised to cover a pure calculation of main effects and two-factor interdependencies (Box and Behnken 1960). However, BBD is mostly relevant to test categorial parameters when the number of factor levels is limited due to technical reasons (Kleppmann 2011).

LHD is a space-filling method which covers design points randomly in the entire design space. Each factor has as many levels as there are runs in the design. Thereby, the randomly determination of factors is less efficient than specially elaborated designs and a homogenous coverage of the design space requires a high number or runs (Siebertz et al. 2010). LHD cannot investigate quadratic relationships and is difficult repeatable (Trottenberg 2008).

A central composite design (CCD) consists of a full factorial design with 2^k factorial runs, $2k$ axial runs and n_c centre runs (Montgomery 2009). Figure 4.15 illustrates the principle of CCD design for k=3 factors. A CCD can investigate non-linear effects and the number of required runs increases moderate with the number of factors. Hence, the CCD is discussed as a commonly used design (Siebertz et al. 2010).

Regarding the eventual selection of a best design, Siebertz et al. (2010) further highlights that there is no universal solution. A comparison of CCD and LHD by means of an exemplary experiment shows only remarkably little differences in the

result of both designs. Based on this profound assessment of designs in combination with the advantages of the CCD and an own pre-testing of different designs, the CCD was selected as appropriate methodology to carry out the parametric study within this research. This made selection was confirmed by scientifically acknowledged experts with experience on DoE methods (Adam 2004).

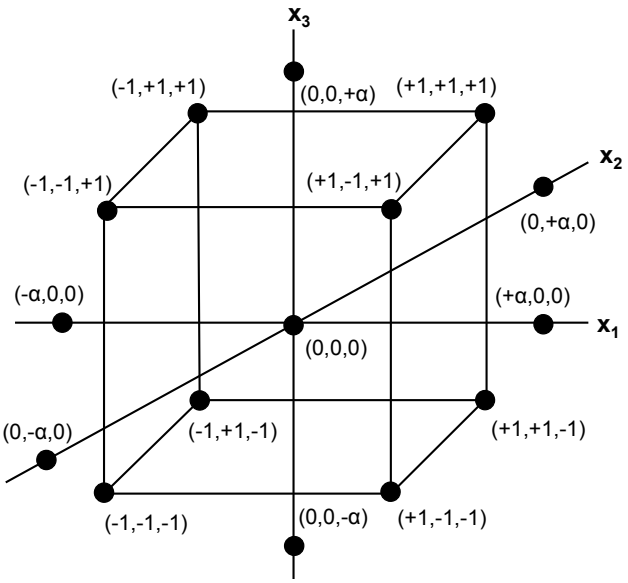

Figure 4.15: Principle experimental set-up of a 2^3 central composite design

In order to define the parametric space to carry out the CCD, parameters and problem variables are defined in the subsequent section. A detailed description regarding the implementation of the CCD follows in section 4.4.3.

4.4.2 Parameter and Problem Variables

The primary objective of the parametric study is the optimisation of the performance of the multivalent solar DEC-system with reference to the objective functions introduced in section 4.1. The following discrete parameters were considered as relevant dimensioning variables with significant impact on the performance of the overall multivalent system.

- Solar collector array aperture area A_{col}, expressed in direct relationship with the following model parameters:

  - number of parallel collector strings $n_{col//}$ according to the Tichelmann method (Kohlenbach and Jakob 2014);
  - maximum collector mass flow $\dot{m}_{col}$ in dependency of A_{col}; and
  - heat transfer coefficient of collector circuit heat exchanger $a_{HX,col}$ in dependency of A_{col}.
- Collector array inclination angle α
- Solar buffer store size expressed by volume V_{SBS} and diameter d_{SBS}
- Hot water storage dimensions depicted by volume V_{HWS} and diameter d_{HWS}

Figure 4.16 outlines the relations of sub-models and parameters to the system output in a cause-effect diagram. With respect to a clear arrangement, only the selected parameters for variation are listed in detail while all other parameters are depicted on subsystem level.

In order to define the limits of the scope for the parameter variation, minimal and maximal thresholds were ascertained for the parameters A_{col}, α, V_{SBS} and V_{HWS}. Thereto, it was taken into account that this research on multivalent solar DEC-systems first and foremost focuses on the heat sinks DEC-air-conditioning (RAH) and HW-preparation. Additional solar yields serve to cover heating load.

Thus, the minimal value of the collector area $A_{col,min}$ is determined according to planning guidelines for solar cooling (Henning 2004a), assuming an area that is minimally required for a solar DEC-system primarily designed for solar cooling. Thereunto, $A_{col,min}$ is defined via an efficiency approach based on the solar DEC-system's nominal refrigeration capacity $\dot{Q}_{cold,nom}$ (Eq. 4.7)

$$A_{col,min} = \frac{\dot{Q}_{cold,nom}}{G * \eta_{col} * COP_{th}} \tag{4.7}$$

where,

G	solar irradiation in inclined plane [kW m^{-2}]
η_{col}	collector efficiency under reference conditions [-]
COP_{th}	thermal coefficient of performance DEC-System [-]

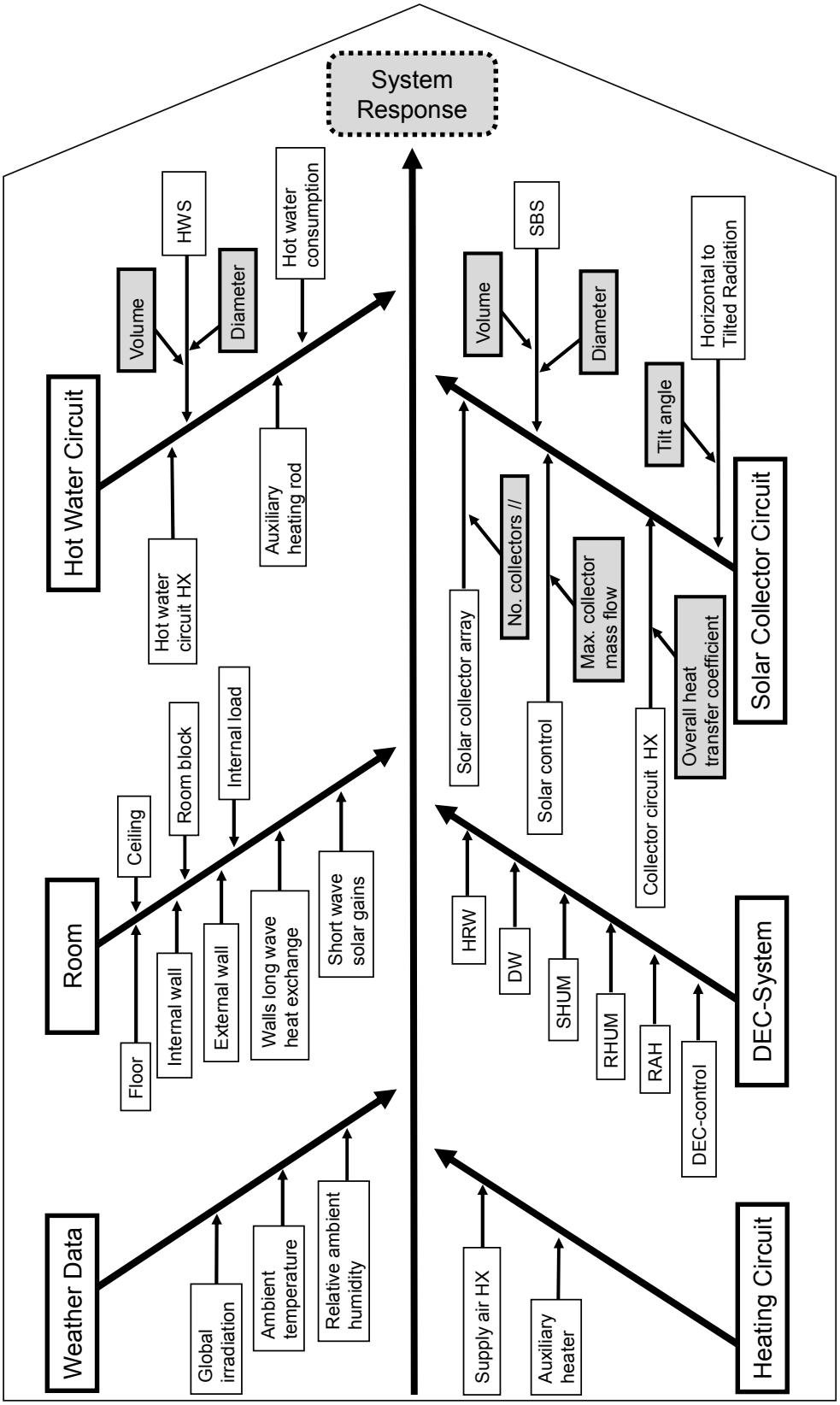

Figure 4.16: Selected system parameters for variation at a glance

Assuming the nominal refrigeration capacity of $\dot{Q}_{cold,nom} = 35$ kW, an averaged available solar irradiation $G = 0.6$ kW m^{-2} (average solar irradiation on the inclined plane on June 21st from 06:00 until 18:00) together with $\eta_{col} = 0.45$ and $COP_{th} = 0.6$, the minimal aperture area is arranged with $A_{col,min} = 216$ m^2. The assumed values, thereby, refer to the in-situ investigated system.

In order to deduce $A_{col,max}$ (Eq. 4.8) the minimum value $A_{col,min}$ is increased by the collector area $A_{col,HW}$ (4.9) which derives from the dimensioning of a collector array for solar hot water preparation according to VDI 6002 (2014) and Schwenk (1999). Defining these maximum limits, synergistic effects regarding the heat distribution for both heat sinks are intentionally not considered.

$$A_{col,max} = A_{col,min} + A_{col,Hw} \tag{4.8}$$

$$A_{col,HW} = \frac{\left(n_{pers} \cdot v_{gst} \cdot \bar{\zeta}\right)^{0,75}}{6,05} \qquad (0,3 < f_{sol} < 0,6) \tag{4.9}$$

where,

n_{pers}	number of beds of hotel [-]
v_{gst}	average of daily hot water consumption per guest at 60°C [l]
$\bar{\zeta}$	average hotel occupancy [-]
f_{sol}	solar fraction [-]

At a hot water consumption of 120 l (45°C) per person and day in a hotel of class 1 (Recknagel et al. 2007) with an occupation of $n_{pers} = 70$, the additionally considered collector area for hot water preparation results in $A_{col,HW} = 110$ m^2. This leads to $A_{col,max}$ = 326 m^2. In order to parameterise the collector area A_{col} the number of parallel collector strings $n_{col//}$ is determined with Eq. (4.10).

$$n_{col//} = \frac{A_{col}}{A_{spec} \cdot n_{col,s}} \tag{4.10}$$

where,

A_{spec} aperture area of one Solahart collector [= 1.860 m^2]
$n_{col,s}$ number of collector in series [= 5]

In the simulations with parameter variation, the maximal collector mass flow $\dot{m}_{max}$ is considered in dependency of A_{col} and is included in the model with an average value of $\dot{m}_{col}$ = 16 kg (m^2 h)$^{-1}$ according to Peuser et al. (2001).

Proportionately to the variation of A_{col}, accordant varying heat transfer capacities of the solar heat exchanger in the collector circuit are respected with $a_{HX,col}$ =100 W (K m^2)$^{-1}$, as recommended by Peuser et al. (2001) and Bollin (2009).

Considering the inclination angle α, the parameter limits were assumed with α_{min} = 30° and α_{max} = 60°, being regarded as descriptive parameters for a system dimensioned either for an exclusive cooling or heating purpose at the site of Ingolstadt. Thus, the centre value of α is chosen to be in the dimension of the sites latitude.

With regard to the definition of the limits of the solar buffer store (SBS), the lower boundary level $V_{SBS,min}$ represents a storage size as it is recommended for an exclusive hot water preparation. According to VDI 6002 (2014) and Peuser et al. (2001), a targeted solar fraction for hot water preparation of $f_{sol,HW}$ = 0.5 requires an average specific store volume of V_{spec} = 0.06 m^3 per m^2 collector. Thus, $V_{SBS,min}$ was defined to be 6.6 m^3, neglecting any buffer volume for additional heat sinks.

The maximally simulated level $V_{SBS,max}$ arose from $V_{SBS,min}$ increased by the store volume $V_{SBS,DEC}$, representing the required amount of heat necessitated to maximally extend the duration of the DEC-process by 6 hours. This approach which expresses the SBS size in hours of cooling load was applied following SACE (2003). In due consideration of a default RAH capacity of 85 kW and a presumed temperature difference at the RAH of 15K, the additional $V_{SBS,DEC}$ results in 29.2 m^3.

Due to the static collector model provided by INSEL 8 both $V_{SBS,min}$ and $V_{SBS,max}$ additionally include a certain volume representing the capacity of the collector array, as it was utilized to simulate the original system. As a result $V_{SBS,min}$ = 7.3 m^3 and $V_{SBS,max} = 36.5$ m^3 are included in the simulation study.

The parameter limits $V_{HWS,min}$ and $V_{HWS,max}$ to parameterise the hot water storage were deduced on the basis of a hot water storage pursuant to the maximum hourly peak load at a full room occupancy in the hotel (Schwenk 1999). Accordingly, the stand-by HWS was dimensioned in order to meet the highest possible peak withdrawal. As illustrated in Figure 3.6 in section 3, the maximum hourly peak load of 18.7% occurs between 07:00 and 08:00. Thus, the mean HWS volume was defined with $V_{HWS} = 1.176$ m^3. The lower limit $V_{HWS,min}$ = 0.588 m^3 and the upper limit $V_{HWS,max} = 1.764$ m^3 were assumed to range symmetrically around this mean value.

Table 4.3 summarizes the defined boundaries for the parameter variation.

Table 4.3: Defined parameter thresholds for parameter variation

Parameter		**min**	**max**
collector array area	A_{col}	216 m^2	326 m^2
Parallel collector strings	$n_{col//}$	24	36
collector mass flow	$\dot{m}_{col}$	0.96 kg s^{-1}	1.45 kg s^{-1}
heat transfer coefficient	a_{col}	21,600 W K^{-1}	32,600 W K^{-1}
inclination angle	α	30°	60°
buffer store volume	V_{SBS}	7.3 m^3	36.5 m^3
buffer store diameter	d_{SBS}	2.16 m	4.82 m
hot water store volume	V_{HWS}	0.588 m^3	1.764 m^3
hot water store diameter	d_{SBS}	0.61 m	1.06 m

The following parameters and influencing variables were regarded constant throughout the system simulations:

- All parameters regarding the thermal and latent room model
- Climate data set central Europe: Ingolstadt (Germany)
- DEC-system component parameters
- Air change and fresh air content: 100%
- Air volume flow DEC-system 8,000 $m^3\ h^{-1}$
- Regeneration temperature level: 75°C
- Hot water consumption and daily demand profile

4.4.3 Central Composite Design Set-Up for Parametric Study

As described in section 4.4.1 the parametric study is carried out by means of the DoE approach of a central composite design (CCD) with $k = 4$ factors and $n = 1$ centre point.

An orthogonal CCD design was chosen in order to ensure that the coefficients of the associated regression model are independent. This is obtained by the adjustment of $\varkappa$, expressing the distance of the star points to the centre. According to Kleppmann (2011), a CCD design is defined as orthogonal by Eq. (4.11).

$$\varkappa^2 = \frac{\sqrt{N \cdot N_C} - N_C}{2} = \frac{\sqrt{(2^k + 2k + n) \cdot 2^k} - 2^k}{2} \tag{4.11}$$

where,

N	number of total simulation runs
N_C	number of factorial cuboidal runs
k	number of varied parameters (factors)
n	number of centre points

Due to the given four-dimensional experimental space, the number of total simulation runs results in $N = 25$ from which $\varkappa = 1.414$ follows.

Table 4.4 comprises the values of natural parameters and appendant coded variables used to implement the respective CCD response surface model.

Eq. (4.12) exemplarily shows the response variable total auxiliary electricity consumption E_{elTOT} in dependence of the factors by means of the respective second-order regression model. The model comprises the direct effects of each individual factor, pair-wise interaction effects and quadratic effects of each parameter.

Table 4.4: CCD set-up for parametric study

Factor	Coded		Levels	-1.414	-1	0	+1	+1.414
α	X_1	-	°	23.79	30	45	60	66.21
V_{SBS}	X_2	V	m^3	1.30	7.30	21.90	36.5	42.50
		d	m	0.91	2.16	3.73	4.82	5.20
A_{col}	X_3	$n_{col//}$	-	22	24	30	36	38
		a_{col}	W K^{-1}	20,460	21,600	27,900	32,600	35,340
		$\dot{m}_{max}$	kg s^{-1}	0.86	0.96	1.24	1.45	1.55
V_{HWS}	X_4	V	m^3	0.35	0.59	1.18	1.76	2.01
		d	m	0.74	0.61	0.87	1.06	1.13

$$E_{elTOT} = \beta_0 + \beta_1 X_1 + \beta_2 X_2 + \beta_3 X_3 + \beta_4 X_4 + \beta_5 X_1 X_2 + \beta_6 X_1 X_3 + \beta_7 X_1 X_4 + \beta_8 X_2 X_3 + \beta_9 X_2 X_4 + \beta_{10} X_3 X_4 + \beta_{11} X_1^2 + \beta_{12} X_2^2 + \beta_{13} X_3^2 + \beta_{14} X_4^2 \quad (4.12)$$

Table 4.5 outlines the complete design of the conducted CCD to create the base for a surface response model to identify the regression coefficients $\beta_0, \beta_1 - \beta_{14}$.

In this research, the CCD was implemented using JMP statistical software (SAS 2010). JMP is a contemporary computer tool designed to investigate complex statistical problems. The software comprises several design of experiments methods and can compute response surface models. For the regression analysis associated with the CCD analysis, JMP applies the least square method.

Table 4.5: Interactions & Quadratic Effects based on parameters Main Effects

E_{tot}	X_1	X_2	X_3	X_4	X_1X_2	X_1X_3	X_1X_4	X_2X_3	X_2X_4	X_3X_4	${X_1}^2$	${X_2}^2$	${X_3}^2$	${X_4}^2$
y_1	-1	-1	-1	-1	+1	+1	+1	+1	+1	+1	+1	+1	+1	+1
y_2	-1	-1	-1	+1	+1	+1	+1	-1	-1	-1	+1	+1	+1	+1
y_3	-1	-1	+1	-1	+1	-1	+1	+1	+1	+1	+1	+1	+1	+1
y_4	-1	-1	+1	+1	+1	-1	-1	-1	-1	+1	+1	+1	+1	+1
y_5	-1	+1	-1	-1	-1	+1	+1	-1	-1	+1	+1	+1	+1	+1
y_6	-1	+1	-1	+1	-1	+1	-1	-1	+1	-1	+1	+1	+1	+1
y_7	-1	+1	+1	-1	-1	-1	+1	+1	-1	-1	+1	+1	+1	+1
y_8	-1	+1	+1	+1	-1	-1	-1	+1	+1	+1	+1	+1	+1	+1
y_9	+1	-1	-1	-1	-1	-1	-1	+1	+1	+1	+1	+1	+1	+1
y_{10}	+1	-1	-1	+1	-1	-1	+1	+1	-1	-1	+1	+1	+1	+1
y_{11}	+1	-1	+1	-1	-1	+1	-1	-1	+1	-1	+1	+1	+1	+1
y_{12}	+1	-1	+1	+1	-1	+1	+1	-1	-1	+1	+1	+1	+1	+1
y_{13}	+1	+1	-1	-1	+1	-1	-1	-1	-1	+1	+1	+1	+1	+1
y_{14}	+1	+1	-1	+1	+1	-1	+1	-1	+1	-1	+1	+1	+1	+1
y_{15}	+1	+1	+1	-1	+1	+1	-1	+1	-1	-1	+1	+1	+1	+1
y_{16}	+1	+1	+1	+1	+1	+1	+1	+1	+1	+1	+1	+1	+1	+1
y_{17}	$-\varkappa$	0	0	0	0	0	0	0	0	0	$\varkappa^2$	0	0	0
y_{18}	$\varkappa$	0	0	0	0	0	0	0	0	0	$\varkappa^2$	0	0	0
y_{19}	0	$-\varkappa$	0	0	0	0	0	0	0	0	0	$\varkappa^2$	0	0
y_{20}	0	$\varkappa$	0	0	0	0	0	0	0	0	0	$\varkappa^2$	0	0
y_{21}	0	0	$-\varkappa$	0	0	0	0	0	0	0	0	0	$\varkappa^2$	0
y_{22}	0	0	$\varkappa$	0	0	0	0	0	0	0	0	0	$\varkappa^2$	0
y_{23}	0	0	0	$-\varkappa$	0	0	0	0	0	0	0	0	0	$\varkappa^2$
y_{24}	0	0	0	$\varkappa$	0	0	0	0	0	0	0	0	0	$\varkappa^2$
y_{25}	0	0	0	0	0	0	0	0	0	0	0	0	0	0

4.4.4 Optimised System Dimensioning

The simulation results of the CCD parametric study are shown in Table 4.6 and discussed in the following.

Table 4.6: Response values of CCD parametric study

RUN		α	V_{SBS}	$n_{col//}$	V_{HWS}	E_{elTOT}	PER	f_{sol}	$Q_{col,spec}$
1	−−−−	30	7.3	24	0.588	99.7	0.91	0.48	409
2	−−−+	30	7.3	24	1.764	98.2	0.93	0.48	409
3	−−+−	30	7.3	36	0.588	90.4	1.01	0.54	312
4	−−++	30	7.3	36	1.764	89.1	1.03	0.54	311
5	−+−−	30	36.5	24	0.588	93.0	0.98	0.53	471
6	−+−+	30	36.5	24	1.764	92.4	0.99	0.53	467
7	−++−	30	36.5	36	0.588	83.2	1.11	0.59	364
8	−+++	30	36.5	36	1.764	82.5	1.12	0.59	360
9	+−−−	60	7.3	24	0.588	101.3	0.89	0.47	398
10	+−−+	60	7.3	24	1.764	99.5	0.92	0.47	400
11	+−+−	60	7.3	36	0.588	91.2	1.00	0.53	306
12	+−++	60	7.3	36	1.764	89.2	1.03	0.54	307
13	++−−	60	36.5	24	0.588	92.9	0.98	0.52	458
14	++−+	60	36.5	24	1.764	91.7	1.00	0.53	455
15	+++−	60	36.5	36	0.588	79.7	1.16	0.61	368
16	++++	60	36.5	36	1.764	78.7	1.18	0.61	365
17	-$\varkappa$000	23.7	21.9	30	1.176	88.7	1.03	0.55	384
18	$\varkappa$000	66.2	21.9	30	1.176	86.7	1.06	0.55	385
19	0-$\varkappa$00	45	1.3	30	1.176	116.2	0.76	0.37	245
20	0 $\varkappa$00	45	42.5	30	1.176	83.8	1.10	0.58	421
21	00-$\varkappa$0	45	21.9	22	1,176	94.0	0.97	0.51	478
22	00 $\varkappa$0	45	21.9	38	1.176	79.5	1.16	0.60	339
23	000-$\varkappa$	45	21.9	30	0.345	87.8	1.04	0.56	408
24	000 $\varkappa$	45	21.9	30	2.007	85.4	1.08	0.56	397
25	0000	45	21.9	30	1.176	85.2	1.08	0.57	397

According to the conditions computed in the CCD analysis, the total auxiliary electric energy consumption $E_{el,TOT}$ varied between 78.7 and 116.2 MWh, the primary energy ratio PER ranged from 0.76 to 1.18, the solar fraction f_{sol} went

from 0.37 to 0.61 and the specific annual collector yield $Q_{col,spec}$ varied between 245 and 478 kWh m^{-2}a^{-1}.

Based on the results, a second-order regression model was applied to describe the multiple response variables. The quality of approximation of the regression model was observed adequate by means of the coefficients of determination R^2. R^2 indicates the statistical fitness of the data (simulation results) to the regression model and reaches values between 0.88 and 0.95. Thus, according to Chin (1998) the fitness can be assessed as substantial since all R^2 reach values above 0.67. Figure 4.17 to Figure 4.20 illustrate the coefficients values for the response variables $E_{el\,TOT}$, PER, f_{sol} and $Q_{col,spec}$. All regression coefficients carry the units of the respective response since the coded factors are included dimensionless.

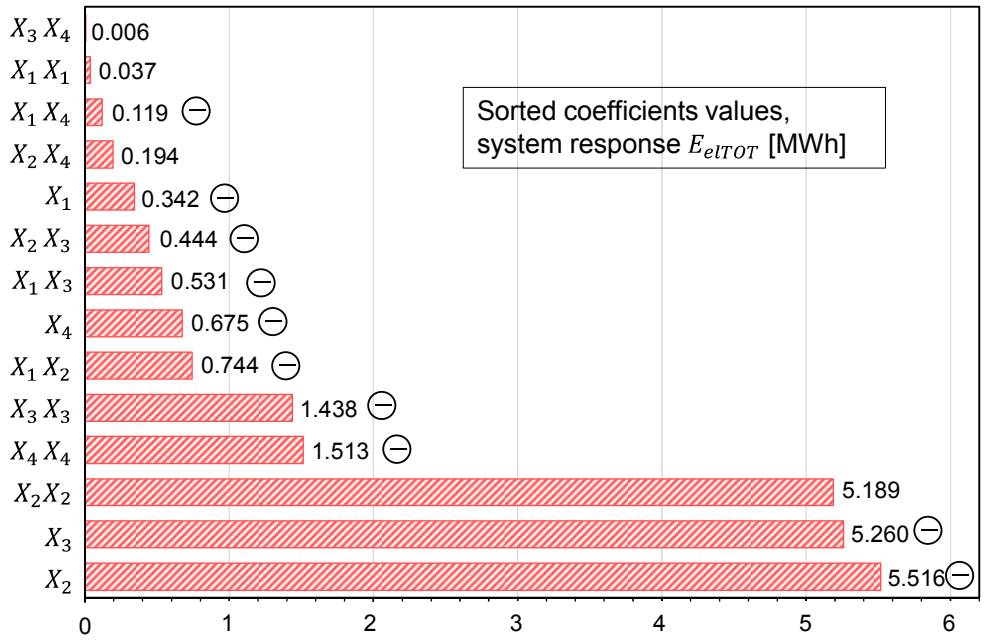

Figure 4.17: Estimated coefficient values of the system response total auxiliary electrical energy consumption $E_{el\,TOT}$ (R^2=0.88)

The effects of the variables on the response $E_{el\,TOT}$ are shown in Figure 4.17. The parameter V_{SBS} (X_2) has the highest coefficient indicating -5.516 MWh. The second-strongest effect reveals the collector area A_{col} (X_3) showing -5.260 MWh. This implies that $E_{el,TOT}$ decreases with increasing buffer store volume V_{SBS} as

well as with increasing A_{col}. Beside these main effects, it is also noticeable that the quadratic effect of V_{SBS} (X_2X_2) shows the highest significant second order relationship. The estimated coefficients of the factors α (X_1) and V_{HWS} (X_4) only denote minor effects on the response. It further became apparent that interactions have an inferior impact on the system design. Interactions include whether the effect of a parameter on the response alters with the change of another parameter. The significance of each effect was investigated by the p-value using JMP software. The p-value is an estimate of the confidence that the effect is due to a relationship rather than one which occurs by chance and determines an effect the more significant the smaller its value. Thus, the parameters X_2, X_3 and X_2X_2 were the factors with the most significant effects on $E_{el\,TOT}$, whereas the further effects were found to be statistically not significant (p > 0.05). From Figure 4.18 it can be seen that A_{col} (X_3) and V_{SBS} (X_2) have again a strong positive effect on PER, whereat the effect of A_{col} (X_3) is slightly dominant.

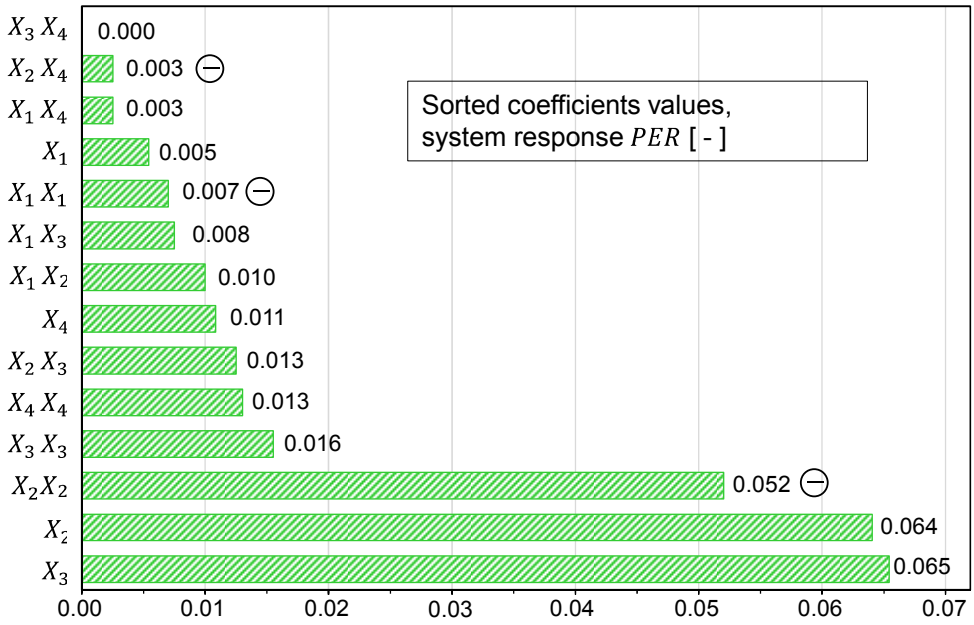

Figure 4.18: Estimated coefficient values of the system response Primary Energy Ratio PER (R^2=0.92)

Both effects favour the optimisation of the PER while the quadric relationship of V_{SBS} (X_2X_2) shows an inverse impact. Analogous to the regression model for

$E_{el,TOT}$, solely the coefficient terms X_2, X_3 and X_2X_2 were significant with appropriately small p-values (p < 0.05).

The estimated coefficients of the responses f_{sol} and $Q_{col,spec}$ are shown in Figure 4.19 and Figure 4.20.

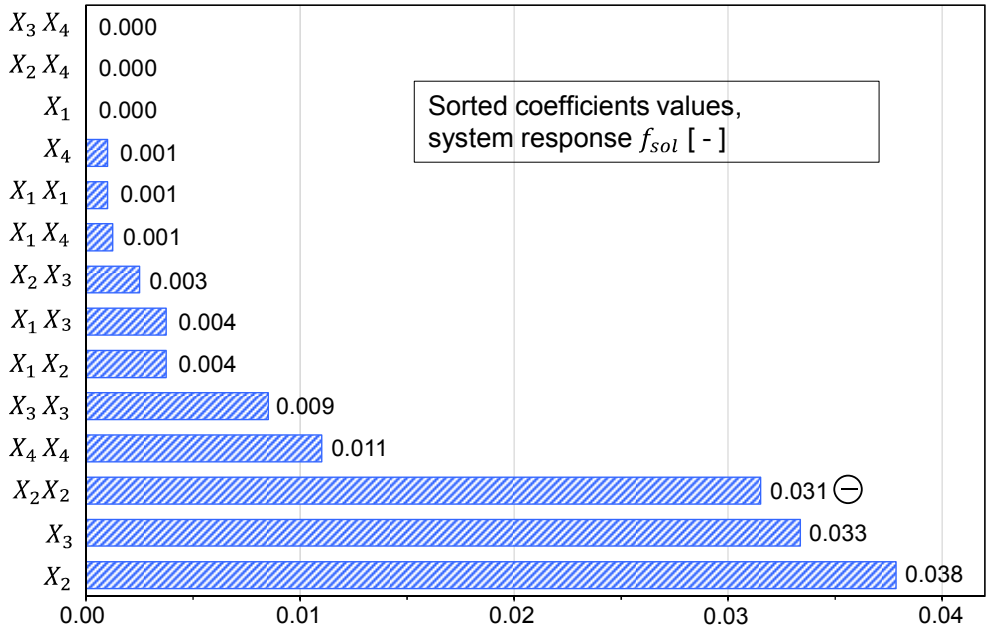

Figure 4.19: Estimated coefficient values of the system response solar fraction f_{sol} (R^2=0.89)

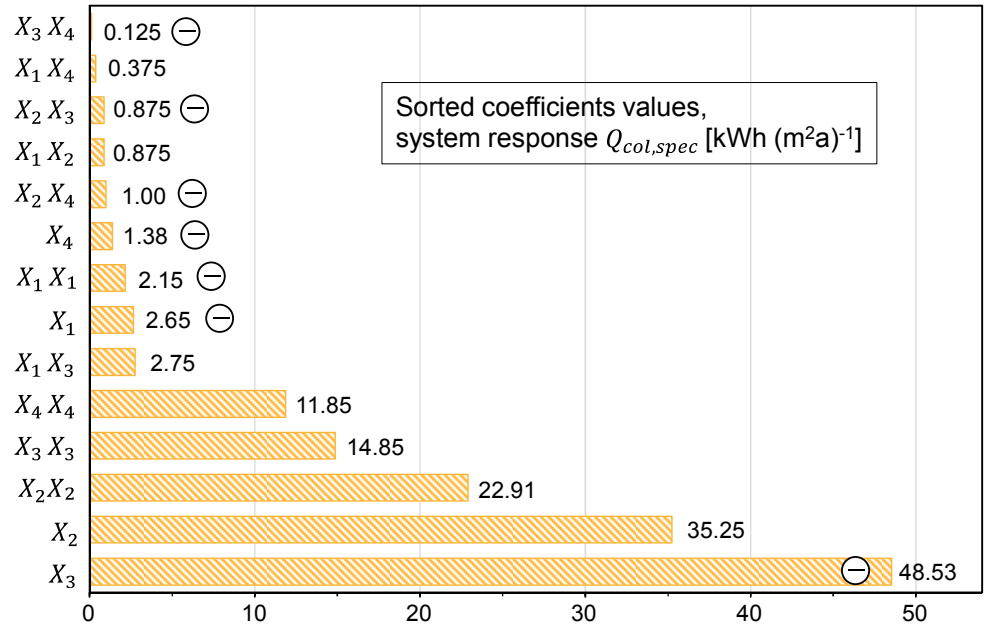

Figure 4.20: Estimated coefficient values of the system response specific annual collector yield $Q_{col,spec}$ (R^2=0.95)

It becomes evident that the main influence on these system response variables are the linear main effects V_{SBS} (X_2) and A_{col} (X_3) with the nonlinear trend V_{SBS} (X_2X_2). Again the main effects of α (X_1) and V_{HWS} (X_4) as well as other interactions were found to be insignificant (p > 0.05). This means that the effect of α (X_1) and V_{HWS} (X_4) is insignificant for all response variables.

Thus, α (X_1) and V_{HWS} (X_4) can be set constant in the further analysis.

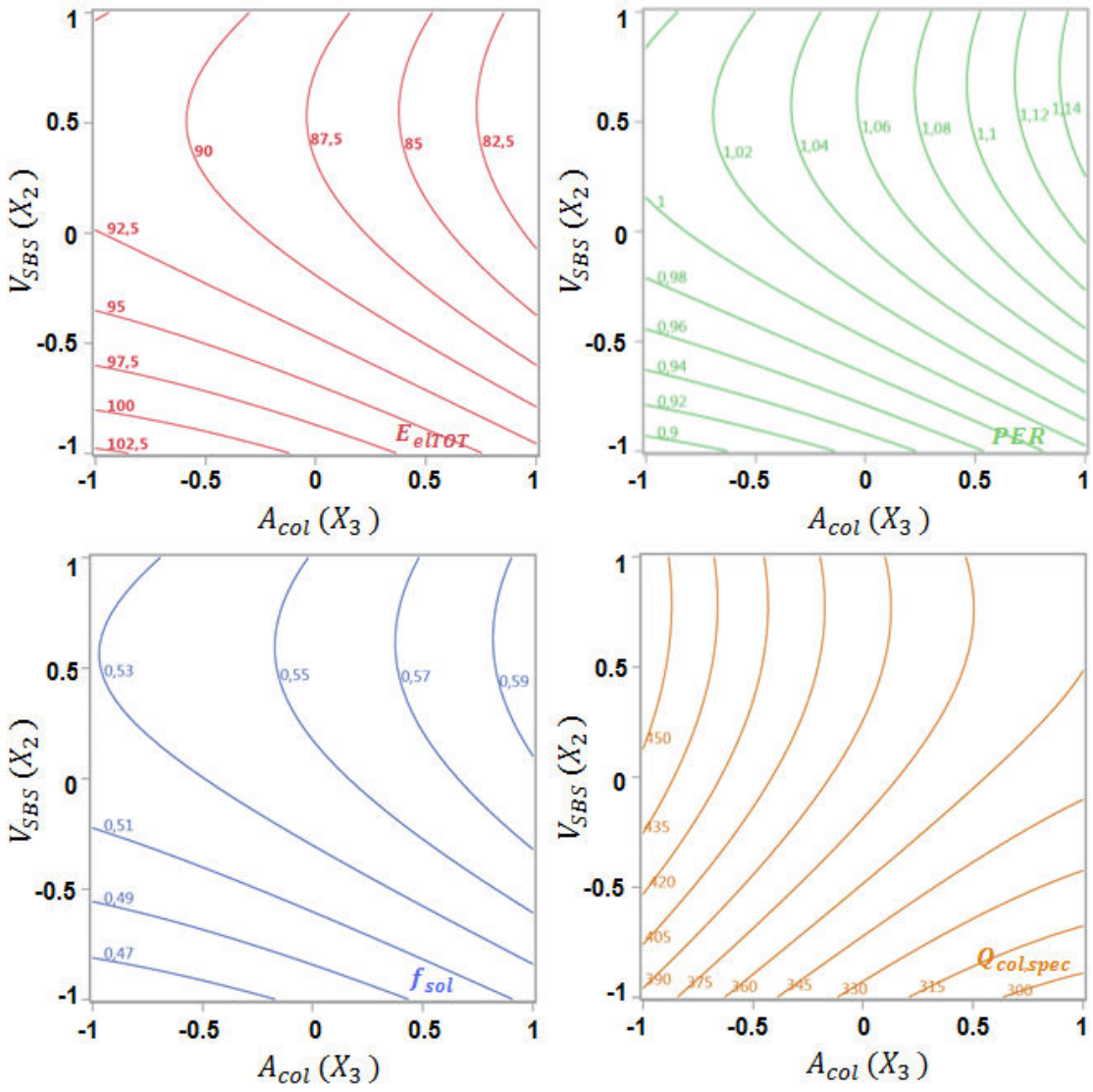

Figure 4.21: Contour plots of the multiple system responses in dependence of V_{SBS} (X_2) and A_{col} (X_3) with $X_1 = 0$ and $X_4 = 0$

Thereby, V_{HWS} is considered at 1.176 m^3 (X_4=0). This represents a minimum storage size to cover the highest possible peak withdrawal as it is described by

Schwenk (1999). It can be further inferred that a deviation of α from 45° is without impact on the system response. Consequently, this parameter is kept at 45° (X_1=0) in the further analysis.

Hence, contour plots for each system response were generated to illustrate the effects of V_{SBS} (X_2) and A_{col} (X_3) on the system responses. The individual contour plots are shown in Figure 4.21, illustrating the difficulty of optimising system responses with opposing behaviours. For instance, an increasing collector area A_{col} serves, on the one hand, to minimize the total auxiliary electricity consumption $E_{el,TOT}$ (minimization objective) and also to increase the PER (maximization objective). On the other hand, the specific annual collector yield $Q_{col,spec}$. (maximization objective) represents a concurrent objective and decreases respectively.

Multiple response optimisation seeks a compromise between the responses. However, it is not always possible to find a solution optimising all of the responses simultaneously (Montgomery 2009). In order to approach this multi-response optimisation problem, the technique of overlaying contour plots (Figure 4.22) was employed to identify a compromise in terms of a polyoptimum (Adam 2004).

Figure 4.22 shows the overlaying contour plot analysing the effect of V_{SBS} (X_2) and A_{col} (X_3) on the multiple responses $E_{el,TOT}$, PER, f_{sol} and $Q_{col,spec}$ at $X_1 = 0$ and $X_4 = 0$. Regarding the targeted optimisation, the respective objective functions were defined in section 4.1. These objectives were further refined taking into account the results of the system with simultaneous control strategy. Accordingly, all system responses of the optimised system should minimally reach the performance figures of this initial system. In order to visualise the potential areas with improved system responses, the particular areas below or above the minimum or maximum objectives were shaded for each response. This conduces to further narrow down the target area to locate an optimum. The resulting unshaded white intersection, where $E_{el,TOT} < 90.1$, $PER > 1.03$, $f_{sol} > 0.53$ and $Q_{col,spec} > 390$ kWh m^{-2}a^{-1} represents the area in which all given system responses reach improved values compared to the initial system.

As labelled in Figure 4.22 two corresponding optima were identified regarding the dimensioning of the multivalent system. Optimum 1 pursues, on the one hand, the optimisation of the primary energy consumption through maximizing PER.

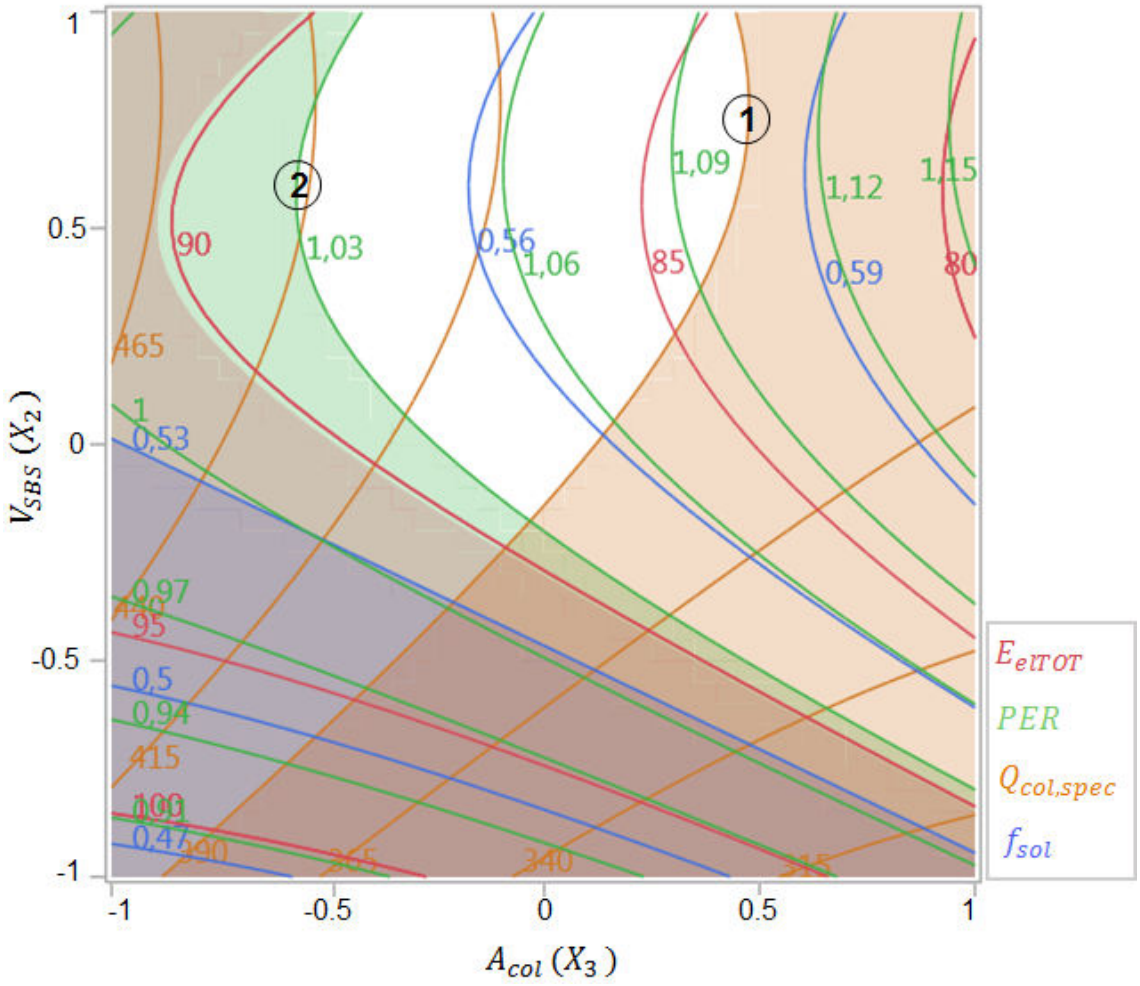

Figure 4.22: Multi-response analysis with overlaid contour plots

Thus, this optimum focuses on the primary energy saving potential rather than on the highest economic possible specific annual collector yields $Q_{col,spec}$. As a contrast to that, optimum 2 aims, on the other hand, at maximizing $Q_{col,spec}$ and, therefore, emphases on system dimensions that can principally be related to an optimised amortization of a possible initial investment in the solar thermal system (Brandstetter 2007). The system dimensions for the derived optima are outlined in Table 4.7 and can be used for design purposes.

Table 4.7: Summarized design criteria at the identified system optima

Optimum	α	V_{SBS}	A_{col}	V_{HWS}	E_{elTOT}	PER	f_{sol}	$Q_{col,spec}$
1 (0.47;0.70)	45	32.1	305	1.176	83.5	1.11	0.58	390.0
2 (-0.57;0.55)		29.9	247		89.0	1.03	0.55	441.6

4.5 Conclusions

In-depth, optimised concepts and control strategies for the multivalent solar DEC-system were developed and evaluated applying the system simulation model described in chapter 3. Alternative supervisory control concepts were considered and analysed systematically taking particular account of the solar DEC-system approach with multiple integrated heat sinks.

In order to assess the different systems, a set of objective functions was introduced as a basis for comparison: total auxiliary energy consumption E_{elTOT}, primary energy ratio PER, solar fraction f_{sol} and annual specific collector yield $Q_{col,spec}$.

In an initial base case, the original system design with direct sequential supply of heat sinks was compared to an advanced system with solar buffer store. On the one hand, the results clearly show that a buffer store can significantly increase the systems PER by 18.3% and reduce the consumed total auxiliary electric energy E_{elTOT} by 14.5%. Also, the system's solar fraction f_{sol} (+21.4%) and annual specific collector yield $Q_{col,spec}$ (+24.9%) are improved substantially.

On the other hand, the behaviour with sequential supervisory control strategy reveals room for improvement with regard to the system control. The unsatisfactory system behaviour is discussed for both cooling and heating periods.

Based on this initial base case, an optimised store discharge supervisory control strategy was formulated and proposed for future systems. This improved control strategy is based on a comprehensive concept which allows for the simultaneous supply of heat sinks. The analysis of the daily systems performance shows that the established simultaneous approach stabilizes the solar DEC-process in the

first place. This has a positive impact on the thermal room comfort and improves the overall system performance. Compared to the system with sequential heat sink supply, the total auxiliary electricity consumption E_{elTOT} can again be reduced by 5.2%. This goes along with the increase of the primary energy ratio PER (+6.2%) and a slight increase of the solar fraction f_{sol} (+3.9%) and the annual specific collector yield $Q_{col,spec}$ (+1.0%). Thus, aside from hardware optimisation, particularly the advancement of the systems supervisory control strategy reveals a notable potential in the context of the optimisation of multivalent solar DEC-systems.

Due to the fact that the optimised system design with simultaneous buffer discharge concept is expected to provide a further improved performance with optimised system dimensions, this system was chosen for a subsequent parametric study. Aiming at this investigation of optimised system dimensions for the multivalent solar DEC-system, the design of experiments (DoE) method of central composite design (CCD) was selected.

It was found out that the collector area A_{col} and the solar buffer store volume V_{SBS} are the critical parameters for system dimensioning in order to improve the systems performance with regard to E_{elTOT}, PER, f_{sol} and $Q_{col,spec}$. On the contrary, the roles of the inclination angle α and the hot water store volume V_{HWS} were detected to have no significant effect on the performance of the multivalent solar DEC-system. In order to identify a compromise in terms of a polyoptimum, the technique of overlaying contour plots revealed to be a promising procedure.

As the aimed responses describe concurrent optimisation objectives, two system optima can be derived. On the one hand, the first optimum represents a system design that favours the minimisation of the total auxiliary electricity consumption E_{elTOT}, hence the maximisation of PER and f_{sol}. According to this assumption, the optimal system dimensions are found to be $A_{col} = 305$ m² and $V_{SBS} = 32.1$ m³. This system design achieves a lower total auxiliary electricity consumption E_{elTOT} by 7.9% as compared to the initial simultaneous approach and by 33.1% compared to the modelled original system monitored in-situ. This goes along with

an increase of the PER by 7.8% (35.4% compared to the original system) and f_{sol} by 9.4% (38.1%). However, it must be noted that this system design optimum does not improve the specific annual collector yield $Q_{col,spec}$ any further, as compared to the initial simultaneous system.

On the other hand, the second identified optimum accordingly results in a system with maximised specific annual collector yield $Q_{col,spec}$. Thus, at system dimensions of $A_{col} = 247$ m^2 and $V_{SBS} = 29.9$ m^3, this multivalent solar DEC-system increases $Q_{col,spec}$ by 13.2% as compared to the initial simultaneous approach and by 42.9% as compared to the modelled original system monitored in-situ.

Thus, based on the study conducted, the implementation, simultaneous embedding and generous dimensioning of the solar buffer store prove to be considerable measures towards both system optima. In fact, the substantial reduction of E_{elTOT} in optimum 1 is generally recommended regarding the saving of primary energy in operation, while optimum 2 is related to an optimised amortization of a possible initial investment in the overall solar thermal system. Both optima represent system dimensions recommended for the erection of a future multivalent solar DEC-system of given load and size.

5 Effectiveness of Solar DEC-Systems on a Global Perspective

The previous chapters of this research discuss the investigation of a multivalent solar DEC-system by means of an extensive in-situ monitoring analysis and an in-depth system simulation study. Especially the monitoring at the site Ingolstadt (Germany) revealed that the prevailing heating dominated climatic conditions only require a very limited operation time of the system in full DEC-mode. The associate literature review moreover demonstrated that the bulk of pilot plants being investigated in the course of the development of the solar DEC-technology are also located in moderate European climates. However, the application and effectiveness of solar DEC-systems is certainly predominantly dependent on the climatological conditions at the respective site.

Thus, this section of this research aims at analysing the climate specific effectiveness of solar DEC-systems in order to create a basis for relevant preferable adaptations of the system design. In order to systematically deduce design-specific outline data for the application of the solar DEC-technology at climatically different sites a methodological zoning approach is further developed. A subsequent meteorological analysis for 17 sites mapping the world climate creates a transparent understanding on the activity of the specific system components. This results in an understanding of the site-specific effectiveness of solar DEC-systems and provides insights on how this information could be applied to pre-design principally relevant and efficient system configurations prior to system simulation.

5.1 Review on Solar DEC-Systems for Diverse Climates

Worldwide, the demand for air-conditioning of buildings is growing rapidly. Solar air-conditioning with DEC-systems utilises solar-thermal heat to drive the air-conditioning process (Figure 5.1). The open cycle DEC-process conditions the air directly and comprises the air-treatments cooling, heating, humidifying and

dehumidifying. In times of high ambient air humidity in the summer cooling period, the system cannot achieve a thermal room comfort level with adiabatic cooling only. The supply air needs to be additionally dehumidified, which in case of a DEC-system can be assured by means of a desiccant wheel. Only this dehumidification mode requires solar heat at a relevant high temperature level (e.g. 70°C for sorbent lithium chloride) to regenerate the wheels' matrix. Hence, the effectiveness of solar DEC-systems does not only depend on the available global irradiance at a respective site. In particular, additional climate descriptive parameters, such as the ambient air conditions and the required thermal comfort, are of significant relevance to draw a conclusion on the effectiveness of solar DEC-systems in climatically different regions.

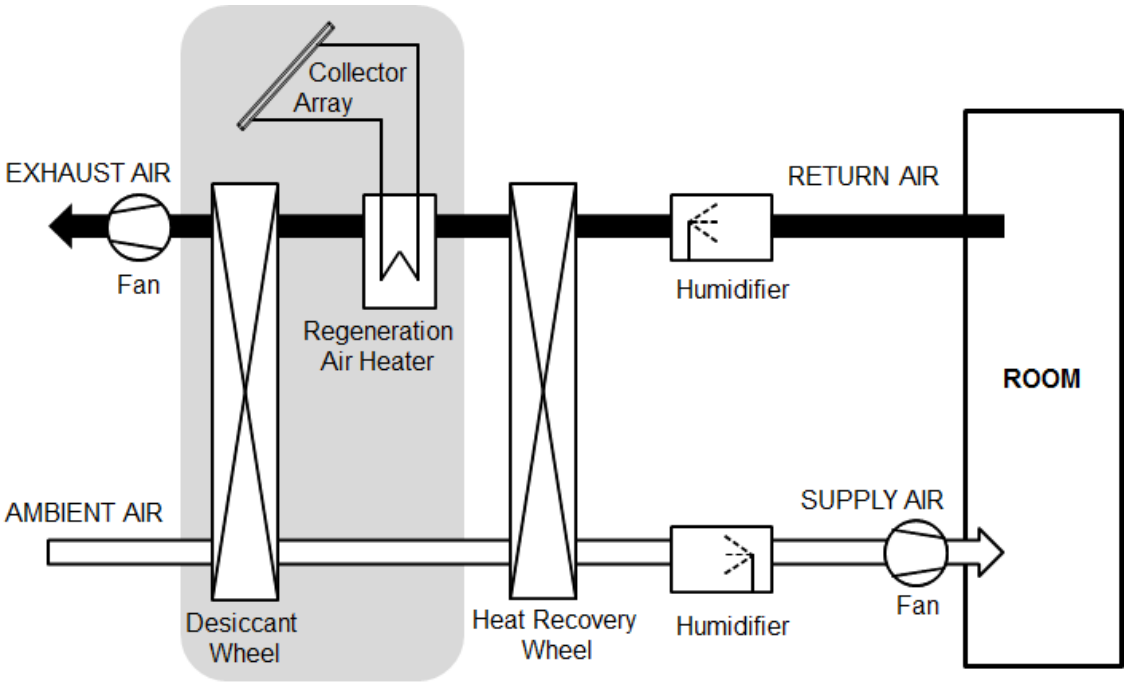

Figure 5.1: Active components of a solar DEC-system in dehumidification mode

To date, the assignability of the solar DEC-technology for diverse climatic conditions has not been investigated systematically. In fact, its potential for different climates has been most notably analysed in particular simulation studies. Individual system configurations were simulated for different climatic conditions and their adaptability to climates was investigated.

Smith et al. (1994) exemplarily examined in computer simulation the performance of the DEC technologies for different sites in the United States. Different open-cycle DEC-process configurations were analysed by Dhar et al. (1995) considering its application under various Indian climates. Jain et al. (1995) developed recommendations regarding the operation of diverse DEC-cycles with solid sorbents under hot humid climatic conditions and analysed the potential of the technology for 16 relevant Indian sites. Thereby, the DEC-design according to the Dunkle-cycle often arose as a suitable configuration.

Hoefker (2001) conducted simulations for a solar DEC-system with solar air collectors by using climate data for Stuttgart, Phoenix, Seville and Jakarta. Mavroudaki et al. (2002) investigated the use of solar powered single DEC-systems in Southern Europe and its potential in relation to non-excessive humidity loads.

Mandegari and Pahlavanzadeh (2009) assessed the performance of a certain proposed hybrid desiccant cooling systems at various climates in a laboratory plant. Bakmedeeniya (2010) modelled and simulated a DEC-system to evaluate the performance of the system for tropical and subtropical climates with special focus on Sri Lanka. Wrobel et al. (2013) carried out a simulation based energetic and economic evaluation of a solar assisted air conditioning at different geographical locations.

Beyond individual simulation studies Henning (2004a) describes a general methodology for the site-specific correlation of expected global irradiance and cooling loads to deduce the heat requirement for thermally driven cooling systems. Selection schemes for planning solar air-conditioning systems of Solair (2009) roughly distinguish between temperate or extreme climates.

Previous studies therefore confine to investigations and testing of certain systems under different climate conditions. In contrast, the developed integrated methodological approach does not aim to test a specific system design for a certain selected climate, but rather presents a procedure to give basic recommendations for the application of solar DEC-systems regarding the general

system effectiveness and the structural configuration depending on the particular climatic boundary conditions (Bader et al. 2013a).

5.2 Development of Refined Zoning Methodology

5.2.1 Approach and Methodological Basis

The developed advanced methodological zoning approach builds on the principle idea presented in the guideline for ventilation and air conditioning VDI 2067 (2003). The approach shall provide a thorough understanding of the activity of the air-treatment components within a solar DEC-plant and their demand profile. The method indicates the principle appropriateness and effectiveness of solar DEC-systems for a particular climatic site or region. It further helps to deduce relevant efficient plant optimisations.

The principle of zoning is to group the Mollier-diagram of humid air into distinct zones, defined according to its thermodynamic properties: temperature ϑ, absolute humidity x, relative humidity φ and enthalpy h. Therefore, the diagram is subdivided into zones according to the available air-conditioning functions in a solar DEC-System. Each zone is specified by a definite combination of air-treatment to condition the ambient air to its required state. Solely air conditions with dehumidification demand require the operation of the desiccant wheel and its according solar-thermal regeneration.

5.2.2 Thermal Comfort Requirements

A preferably high satisfaction of the users and therefore a high productivity and achievement potential is strived for, especially in the context that comfortable room conditions improve physical and psychological well-being. Thereby, the thermal comfort of human beings depends on numerous factors categorised in physical, physiological and intermediate scales and therefore showing the complexity of ’well-being’.

In the view of abundance of influencing factors a complete acceptance of all users cannot be reached generally. In this context it further has to be considered that the satisfaction of the users is very much an individual matter. That is why for example next to the measureable physical factors, also the compliance with the user expectations plays a role (Voss et al. 2005). Four physically defined and therefore measurable thermal comfort factors are air temperature, air humidity, temperature of enclosing surfaces and air velocity.

Within this work, the thermal comfort is evaluated by the room air temperature ϑ_{room} [°C] and the relative and absolute values of the room air humidity φ_{room} [% r.h.] and x_{room} [g kg^{-1}]. However, apart from an individually sensed comfort, governmental regulations and norms provide standardised thermal comfort definitions of thermal comfort in an office environment contemplated in diverse guidelines. Thereby, the definitions differ slightly depending on the particular standard (Bundesministerium für Arbeit und Sozialordnung 2001).

Physical environmental conditions at the work place leading to satisfaction with thermal comfort can for example be calculated via the heat balance equation for the human body. The methodological procedure is described in ISO EN 7730 (2005) and calculates acceptable air temperatures and air movements in dependence of the physical activity and the insulation performance of clothing.

Another common way to determine thermal comfort conditions is based on the PMV/PPD testing-method. PMV is the Predicted Mean Vote and PPD is the Predicted Percentage Dissatisfied. The PMV index by Fanger (1970) derives from Eq. (5.1).

$$PMV = (0.303\, e^{-0.036M} + 0.028)\, L \tag{5.1}$$

where L is the thermal load, and M is the metabolic heat production depending on occupancy and the activity level of the occupants (ASHRAE 2009). In accordance with ASHRAE thermal sensation scale, a PMV of +3 is hot, -3 is cold and thus 0 (neutral) is the aim.

As the application focus of solar DEC-systems is predominantly office buildings or hotels, the zoning analysis is approximately based on the thermal comfort requirements of a landscaped office space with a conference room as defined in standard EN 15251 (2007). Hence, the building is categorized as new building with normal level of expectation (PPD < 10%, -0.5 < PMV < +0.5).

Based on that standard, a room temperature range of 23°C to 26°C is assumed during the cooling period for a standard clothing level of 0.5 clo, where 1 $clo = 0.155$ (m²°C)W^{-1}.

Slightly divergent from this, the design criteria for the room temperature given in EN 13779 (2007) aim for a range of 22°C to 26°C. Accordant to recommendations in DIN V 18599 (2007) a maximum acceptable room temperature of 26°C is assumed during cooling period for all types of usage, while guideline VDI 3525 (2007) recommends a room temperature in the range of 22°C to 26°C in direct proportion to the actual ambient temperature from 22°C to 32°C.

As it sets a union for the fundamental standards giving recommendations on thermal comfort, the zoning model is based on a room temperature lower limit $\vartheta_{room,l} = 22$°C and an upper limit $\vartheta_{room,u} = 26$°C.

Regarding the room humidity, as second considerable comfort measure, the reference EN 15251 (2007) recommends a relative humidity of 25% to 60%. The standard EN 13779 (2007) limits the permitted maximum humidity during cooling period to 12 g kg^{-1} which equals 60% r.h. at the upper temperature limit $\vartheta_{room,u} = 26$°C. Thus, the humidity range is defined with a lower limit $\varphi_{room,l} = 25\%$. Based on a procedure given in VDI 2067 (2003) part 21, the relative humidity limits are transferred into absolute values, by determining the intersections of the average room temperature $\vartheta_{room,m}$ (arithmetic mean of $\vartheta_{room,l}$ and $\vartheta_{room,u}$) with the relative humidity limits $\varphi_{room,l}$ and $\varphi_{room,u}$. This leads to the absolute room humidity limits $x_{room,l} = 4.7$ g kg^{-1} and $x_{room,u} = 11.4$ g kg^{-1}.

Considering the standard EN 13779 (2007) which recommends the threshold values of 6.0 g kg^{-1} to 12.0 g kg^{-1}, the restrictive intersecting set of values $x_{room,l} = 6.0$ g kg^{-1} and $x_{room,u} = 11.4$ g kg^{-1} is used to define the absolute

humidity levels limiting the comfort zone. The complete thermal comfort zone is described by the following intervals:

$$\vartheta_{room,l} < \vartheta_{room} < \vartheta_{room,u} \text{ and } x_{room,l} < x_{room} < x_{room,u}.$$

5.2.3 Definition of Zones

Subsequently, a zone of required conditions of the air to be supplied to the room (zone 0) is deduced taking into account appropriate internal sensible and latent cooling loads. Ambient air conditions ranked within this zone do not necessitate any air-treatment. Therefore, a fresh air supply can be realised with operating ventilation only. Based on zone 0 the zones Ia to IV are designed in accordance and based on the air treatment possibilities of a solar DEC-process as illustrated in Figure 5.2.

Due to a too low absolute humidity and high enthalpy values, the combination of cooling and humidifying is requested in zone Ia, while heating and humidifying is required to treat the ambient air in zone Ic, where the air reveals too low values of both enthalpy and humidity. In zone Ib adiabatic cooling can reach appropriate supply air conditions. As a result of an inconvenient high temperature together with an acceptable humidity level, sensible cooling is required in zone II. Zone III is characterized with a sensible heating demand and acceptable humidity values analogue to zone II.

Solely, the air states in zone IV show a demand for a dehumidification of the supply air as the high absolute humidity content needs to be reduced to reach comfortable conditions. In this zone, the solar DEC-system operates in full mode including heat recovery, combined humidification and the desiccant wheel to cool and dehumidify the air.

In order to quantify the respective thresholds of zone 0, the values of the supply air temperature $\vartheta_{sup,l}$, $\vartheta_{sup,u}$ and the absolute supply air humidity $x_{sup,l}$, $x_{sup,u}$ are calculated. The supply air temperature limits can in principle be derived from the rooms' energy balances. However, besides internal loads caused by persons and office equipment this approach does not include external cooling loads due to

radiation through windows, as it is site dependent and can highly be influenced by passive solar architecture and the type of building.

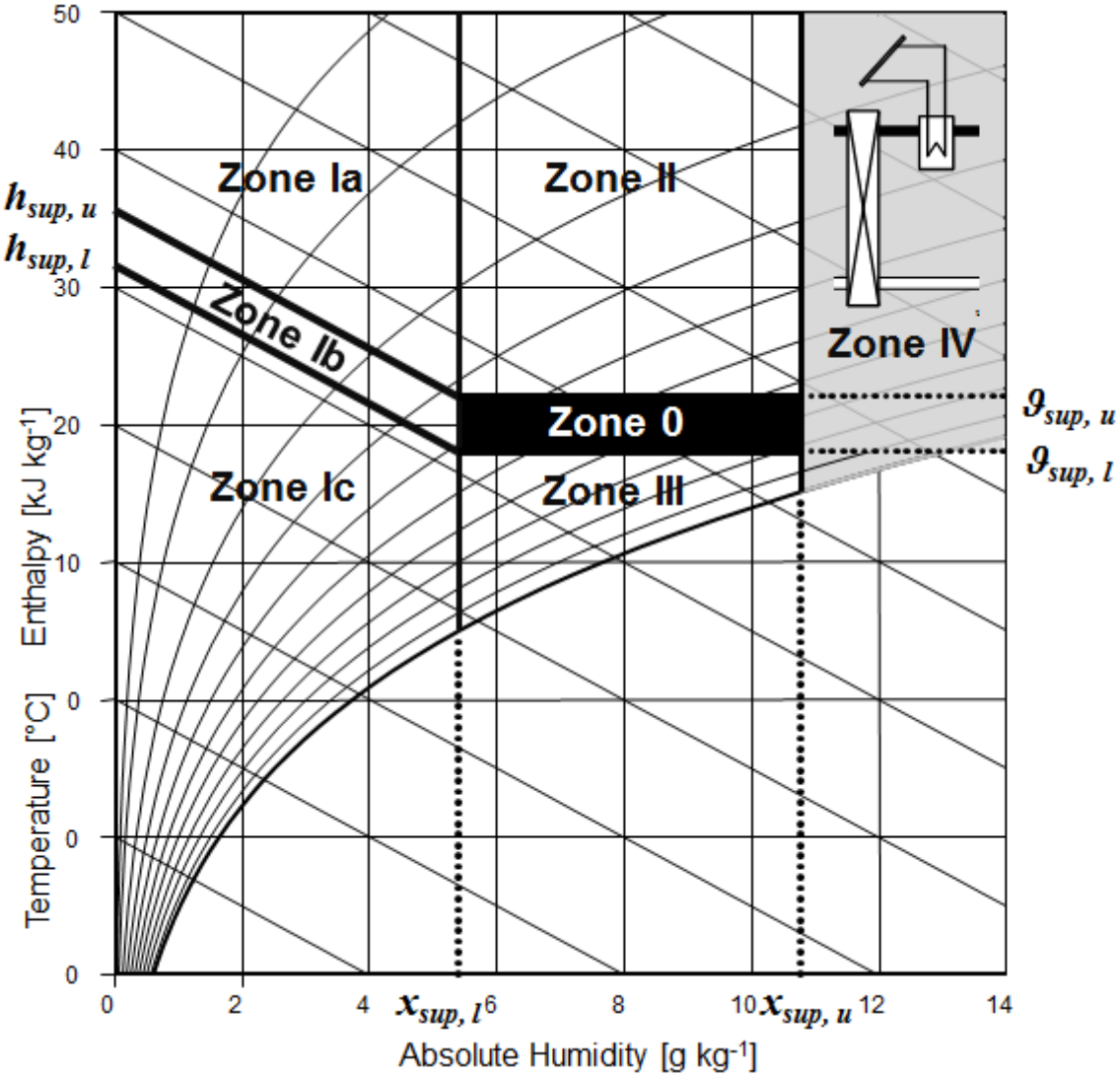

Figure 5.2: Zoned Mollier-diagram with respect to air treatment functions in a solar DEC-process

Hence, to ensure the comparability of the zoned results for climatically different sites, the loads are not determined site specifically. In fact, the determination of the temperature thresholds is complemented with recommendations regarding supply air conditions that are in principle tolerable for an air-conditioning plant. Recknagel et al. (2007) proposes as planning criterion to deduce the airflow volume by means of the supply air temperature. However, the supply temperature

cannot be lowered arbitrarily without restriction and is rather determined in dependence on the maximum permitted room temperature. The temperature difference ΔT between the upper limit of the room temperature $\vartheta_{room,u}$ and the lower limit of the supply air temperature $\vartheta_{sup,l}$ should not exceed 8 K for normal air-conditioning systems. Therefore, with $\vartheta_{sup,l} = \vartheta_{room,u} - \Delta T$ the lower limit of the supply-air temperature $\vartheta_{sup,l}$ is 18°C, calculated for the upper room temperature threshold $\vartheta_{room,u}$. Based on this value the width of zone 0 $(\Delta\vartheta)$ is defined in conformity with the thermal comfort zone (5.2).

$$\vartheta_{sup,u} = \vartheta_{sup,l} + \Delta\vartheta = \vartheta_{sup,l} + (\vartheta_{room,u} - \vartheta_{room,l}) \tag{5.2}$$

Thus, with $\vartheta_{sup,l}$ = 18°C the upper limit of zone 0 results in $\vartheta_{sup,u} = 22$°C.

The absolute humidity limits $x_{sup,l}$ and $x_{sup,u}$ are determined from the humidity balance of the air-conditioned room with Eq. (5.3) considering the water material effort of a DEC-system $\dot{m}_w$ and its air mass flow $\dot{m}_{air}$.

$$x_{sup} = x_{room} + \frac{\dot{m}_w}{\dot{m}_{air}} \tag{5.3}$$

As the analysis emphasizes the dehumidification function of a solar DEC-system the referred water effort for the DEC-system $\dot{m}_w$ can be assumed equal to the dehumidifying demand $\dot{m}_D$. $\dot{m}_D$ is defined in dependence of the human occupancy in persons as expressed by Eq. (5.4). Further latent load from equipment or potted plants are not taken into consideration.

$$\dot{m}_D = \dot{m}_{D,spec} \cdot \frac{A_{floor}}{n_{pers}} \tag{5.4}$$

Finally, the upper and lower limits of zone 0 ($x_{sup,l}$; $x_{sup,u}$) can be determined in dependence of the humidity boundaries of the thermal comfort zone as expressed by Eq. (5.5)

$$x_{sup} = x_{room} + \frac{\dot{m}_{D,spec}}{\rho_{air} \cdot \frac{\dot{V}_{sup}}{A_{floor}} \cdot n_{pers}} \tag{5.5}$$

Recommendations for specific air flow rates $\dot{V}_{sup}/A_{floor}$ and human occupancy n_{pers} are given by DIN V 18599 (2008) with regard to the type of room. According to the defined building $\dot{V}_{sup}/A_{floor}$ is defined with 7.2 $m^3(h\ m^2)^{-1}$ and n_{pers} is assumed with 9.8 $m^2\ pers^{-1}$. The specific dehumidifying demand $\dot{m}_{D,spec}$ is determined with 50 g h^{-1} according to VDI 2067 (2003) part 11. Therewith, based on the determined limits of the thermal comfort zone, the limits of zone 0 are quantified with $x_{sup,l} = 5.4$ g kg^{-1} and $x_{sup,u} = 10.8$ g kg^{-1}. Finally, based on the ascertained humidity and temperature limits of zone 0, the appropriate enthalpy boundaries are deduced according to ASHRAE (2009). To obtain an affine form for the respective psychometric analysis, the equation is reduced with regard to recommendations by El-Shawaari (1994) in the ASHRAE transactions. Thus, the lower limit of the supply-air enthalpy $h_{sup,l}$ and the upper limit of the supply-air enthalpy $h_{sup,u}$ is calculated with Eq. (5.6).

$$h_{sup} = \vartheta_{sup} + 2500 \cdot x_{sup} \tag{5.6}$$

Eventually the boundaries defining zone 0 and the resulting further proceeding zones have been devised by Bader et al. (2013) and Bader et al. (2013a) and are presented in Table 5.1.

Table 5.1: Defined zone boundaries and thresholds

Zone	Required function	Defined zone boundaries
0	ventilation only	$x_{sup,l} < x_{sup} < x_{sup,u}$; $\vartheta_{sup,l} < \vartheta_{sup} < \vartheta_{sup,u}$
Ia	cooling and humidifying	$h_{sup} > h_{sup,u}$; $x_{sup} < x_{sup,l}$
Ib	humidifying	$h_{sup,l} < h_{sup} < h_{sup,u}$; $x_{sup} < x_{sup,l}$
Ic	heating and humidifying	$h_{sup} < h_{sup,l}$; $x_{sup} < x_{sup,l}$
II	cooling	$x_{sup,l} < x_{sup} < x_{sup,u}$; $\vartheta_{sup} > \vartheta_{sup,u}$
III	heating	$x_{sup,l} < x_{sup} < x_{sup,u}$; $\vartheta_{sup} < \vartheta_{sup,l}$
IV	solar dehumidification	$x_{sup,l} < x_{sup} < x_{sup,u}$; $\vartheta_{sup} < \vartheta_{sup,l}$
upper thresholds	$\vartheta_{sup,u}$ = 22°C,	$x_{sup,u}$ = 10.8 g kg^{-1}, $h_{sup,u}$ = 35.5 kJ kg^{-1}
lower thresholds	$\vartheta_{sup,l}$ = 18°C,	$x_{sup,l}$ = 5.4 g kg^{-1}, $h_{sup,l}$ = 31.5 kJ kg^{-1}

5.3 Global Solar DEC-Potential Analysis

5.3.1 Climate and Site Selection

To analyse the principle effectiveness of the solar DEC-technology in a global perspective, the selection of appropriate climatically different sites is based on the Köppen climate classification (Köppen 1923). This classification of world climates describes climatic zones according to their appearance and is based on measurements and observations. It distinguishes five basic climate zones according to the annual and monthly arithmetic means of temperature and precipitation: tropical climates, dry climates, temperate climates, continental climates and polar climates.

In additional categories the Köppen classification further differentiates into specific seasonal characteristics of temperature and precipitation as well as the quantitative precipitation. The identified sites and their climates are illustrated at a glance in Table 5.2. Köppen sites in climates without potential requirements for cooling are not considered in this study. Appendix D gives an overview of the legend to the Köppen climate classification.

Table 5.2: Selected sites and climates

Sites / Climate	Zone	Type	Subtype
Singapore (Singapore) /Af	tropical	wet	tropical rainforest climate
Miami (USA) /Am		tropical monsoon climate	
Mumbai (India) /Aw		winter dry	savanna climate
Maun (Botswana) /BSh	dry	semiarid	hot, avg. annual temperature > 18°C
Denver (USA) /BSk			cold, avg. annual temperature < 18°C
Cairo (Egypt) /BWh		arid	hot, avg. annual temperature > 18°C
Ashgabat (Turkmenistan) /BWk			cold, avg. annual temperature < 18°C
Houston (USA) /Cfa	temperate	wet	hot summer, warmest month avg. > 22°C
Ingolstadt (Germany) /Cfb			warm summer, warmest month avg. < 22°C
Los Angeles (USA) /Csa		semiarid	hot summer, warmest month avg. > 22°C
Santiago (Chile) /Csb			warm summer, warmest month avg. < 22°C
Hong Kong (China) /Cwa		winter dry	hot summer, warmest month avg. > 22°C
Johannesburg (S. Africa) /Cwb			warm summer, warmest month avg. < 22°C
Chicago (USA) /Dfa	polar	wet	hot summer, warmest month avg. > 22°C
Helsinki (Finland) /Dfb			warm summer, warmest month avg. < 22°C
Beijing (China) /Dwa		winter dry	hot summer, warmest month avg. > 22°C
Vladivostok (Russia) /Dwb			warm summer, warmest month avg. < 22°C

5.3.2 Global Meteorological Technology Analysis

Based on the zoning approach, a climatologic analysis was carried out for the selected 17 international sites shown in Table 5.2.

The analysis is based upon test reference year (TRY) data from the meteorological database Meteonorm 7.0 (2013). These data represent a stochastically developed typical average year that is statistically representative for the site in terms of temperature, humidity and global radiation. According to Gansler et al. (1994) a satisfactory accuracy of the Meteonorm data is given for application in scientific simulation studies.

The analysis was performed for two varying operational periods of solar DEC-system (a. operation 24 hours a day without restriction, b. Operation from 07:00 until 19:00 every day). This thesis presents the results of the latter alternative

which is assumed to be representative for the operation of the investigated solar DEC-system.

First, the pairs of values determined by temperature and absolute humidity are classified in the zoned Mollier-diagram based on hourly annual data. The resulting mapping provides an overview of the distribution of the ambient air conditions to the zones Ia to IV within the reference year and accordingly reveals the bandwidth of the different corresponding air-states at a site.

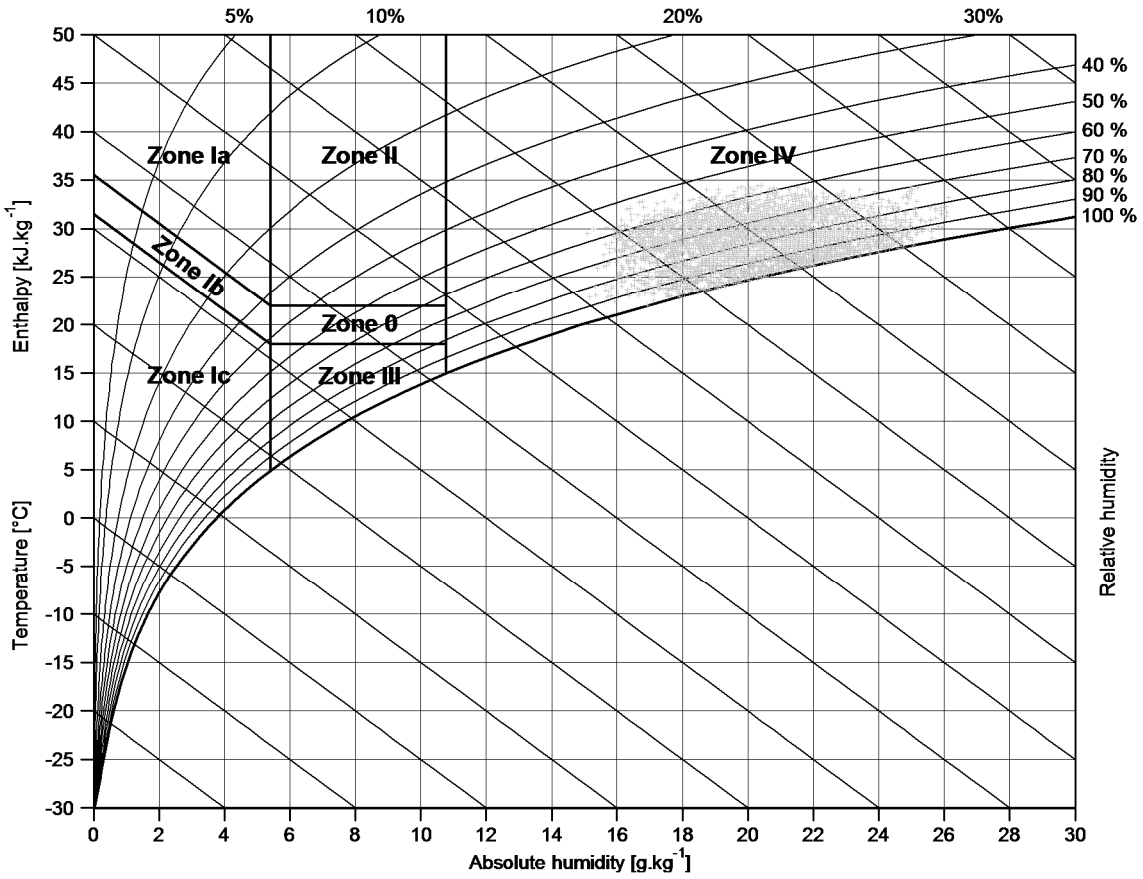

Figure 5.3: Zoned meteorological ambient air conditions in Singapore (tropical rainforest climate)

As Figure 5.3 exemplarily shows for Singapore (tropical rainforest climate), all annual air states solely range in zone IV with an absolute humidity of 14 g kg^{-1} to 28 g kg^{-1} and within a temperature range from 20°C to 35°C. This means that the dehumidification mode is required during the entire operation time of a solar DEC-system to provide comfortable room conditions.

In Cairo (Egypt, Figure 5.4), exemplary representing hot arid climates, the ambient air conditions range in bandwidths of 2 g kg^{-1} to 22 g kg^{-1} and 5°C to 45°C. Under these conditions, zone IV (full DEC-operation; 37%) and zone II (cooling only; 27%) occur as the most prevalent zones. This means for about 63% of the operating times no dehumidification function is required to adjust comfortable room conditions.

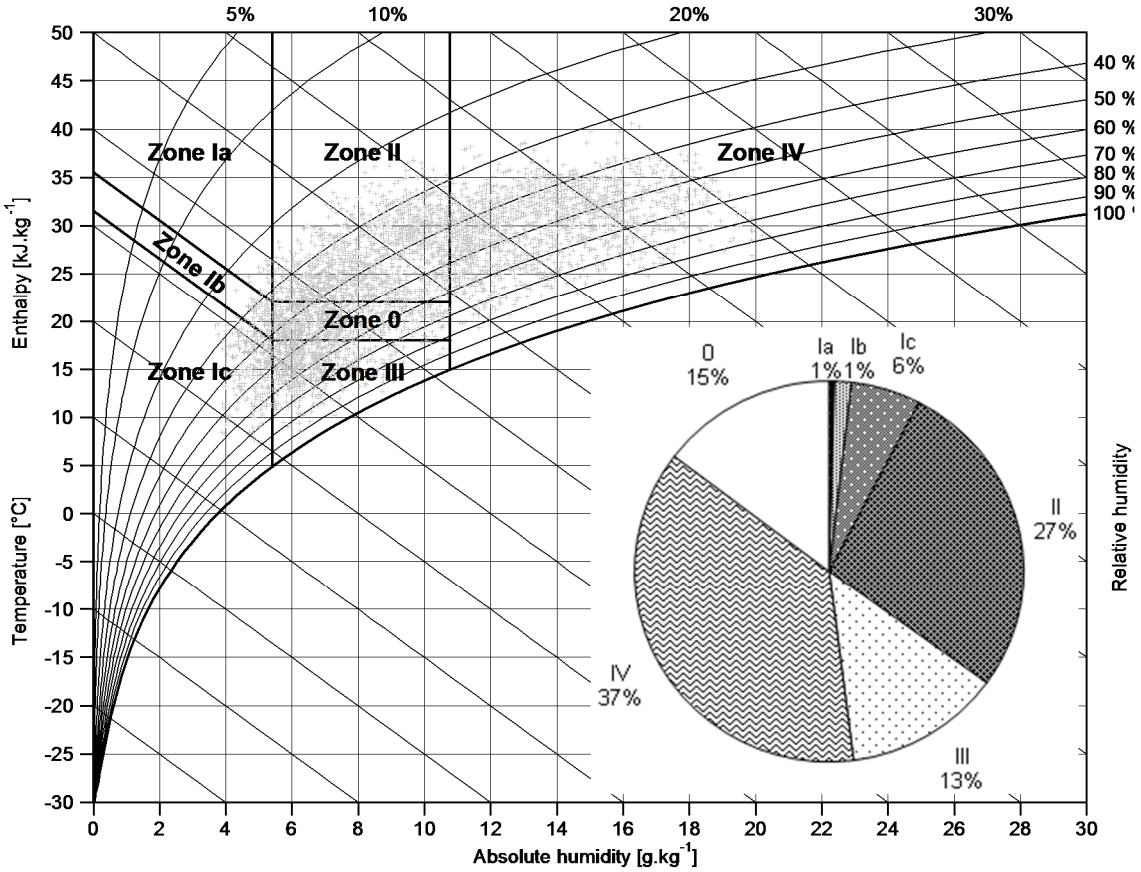

Figure 5.4: Zoned meteorological ambient air conditions in Cairo (dry arid climate)

In addition, the results of Chicago site (USA, Figure 5.5) show that during the predominant DEC-system operation times a dehumidification of the air is hardly needed in humid boreal climates with hot summers. Only 15% or around 661 hours per year of the operation time requires a full DEC-mode with solar dehumidification (zone IV).

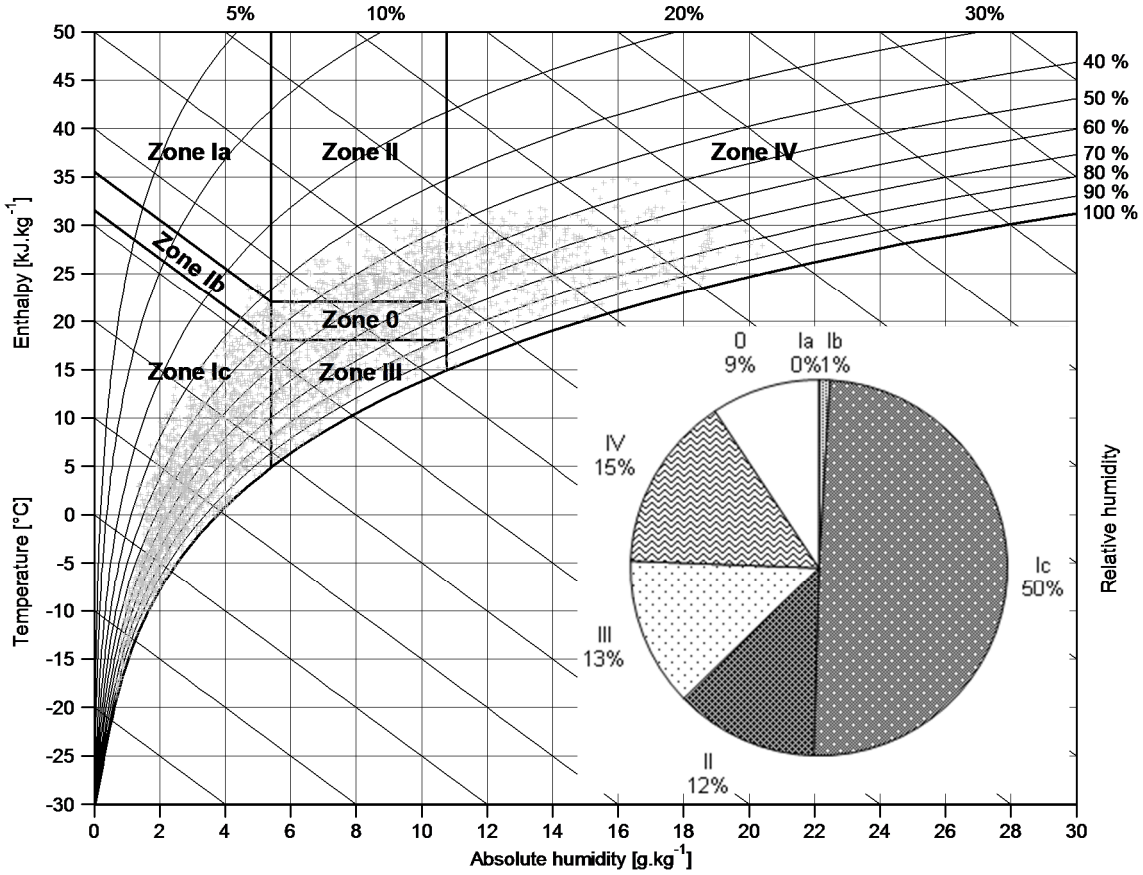

Figure 5.5: Zoned meteorological ambient conditions in Chicago (polar wet climate)

In Ingolstadt (Germany) for example, the climate can be classified as temperate and humid with moderate summers (warmest month < 22°C). As illustrated in Figure 5.6, the absolute outdoor humidity reaches values from 0 g kg^{-1} to 22 g kg^{-1} and the temperature varies between -20°C and 35°C. A bulk of the ambient air conditions thereby lies in the zones with heating demand Ic (humidification and heating, 50%) and III (heating). 7% of the ambient air conditions can be classified to zone II (cooling); the air treatment functions humidifying (zone Ib) as well as cooling and humidifying (zone I) are to some extent not relevant in Ingolstadt. Only about 8% of the states are located in zone IV and therefore in the area where solar driven dehumidification is required. Hence, in Ingolstadt air conditions that require a full DEC-process driven with solar regeneration heat only occur for about 342 hours per year, distributed across 56 days with at least one hour of operation in zone IV.

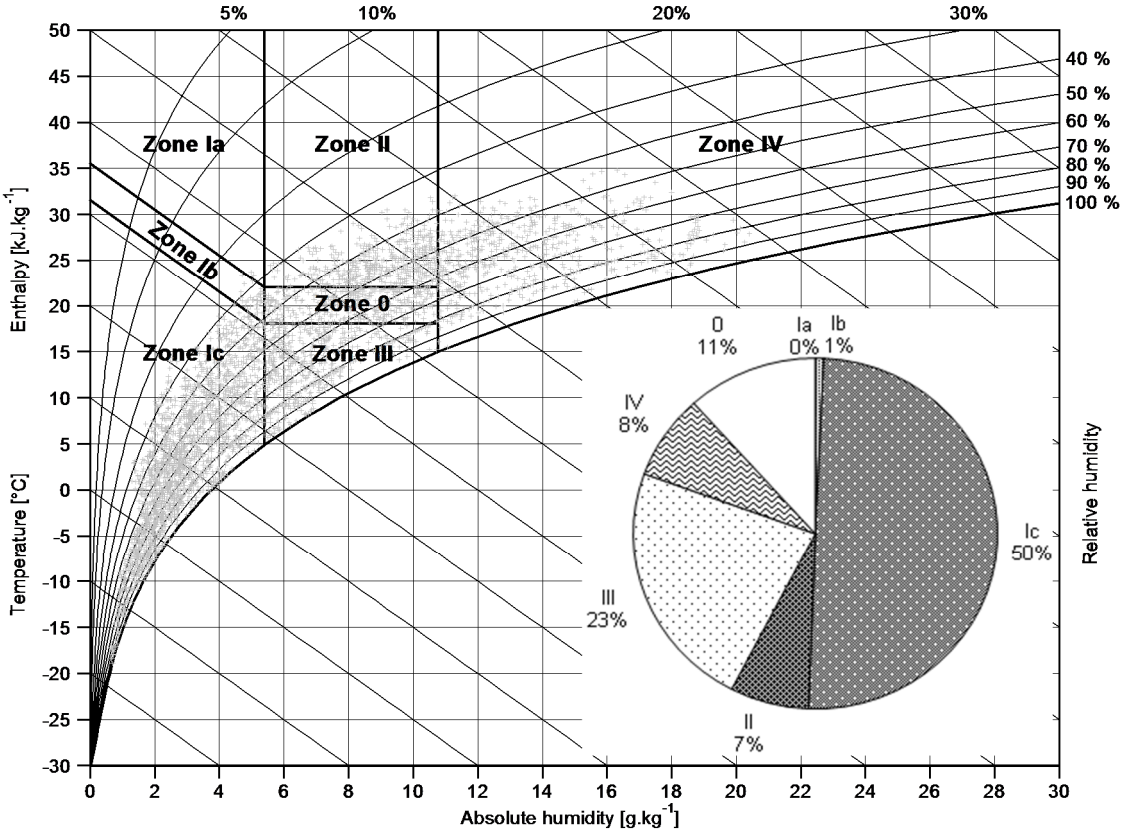

Figure 5.6: Zoned meteorological ambient air conditions in Ingolstadt (temperate wet climate)

As exemplified for the four climates of Singapore, Cairo, Chicago and Ingolstadt, the ambient air conditions of all of 17 analysed international climates have been zoned accordingly. The results, as summarized in Figure 5.7, reveal the particular air-treatment requirements for the application of solar DEC-systems at a specific site (Bader et al 2013a).

Moreover, based on the zoned ambient air conditions, the analysis provides a relation of the available global solar irradiation to the particular zones of required air treatment. In this connection, Figure 5.8 exemplifies the particular average global irradiation intensity per zone with cooling demand for the climates Cfb (Ingolstadt, Germany), BWh (Cairo, Egypt) and Dfa (Chicago, USA).

The results for Ingolstadt (Figure 5.8, upper diagram) for instance show an average available global solar irradiation amounting to 525.1 W m^{-2} during system operation in zone II (sensible cooling demand). In operation times, when the air

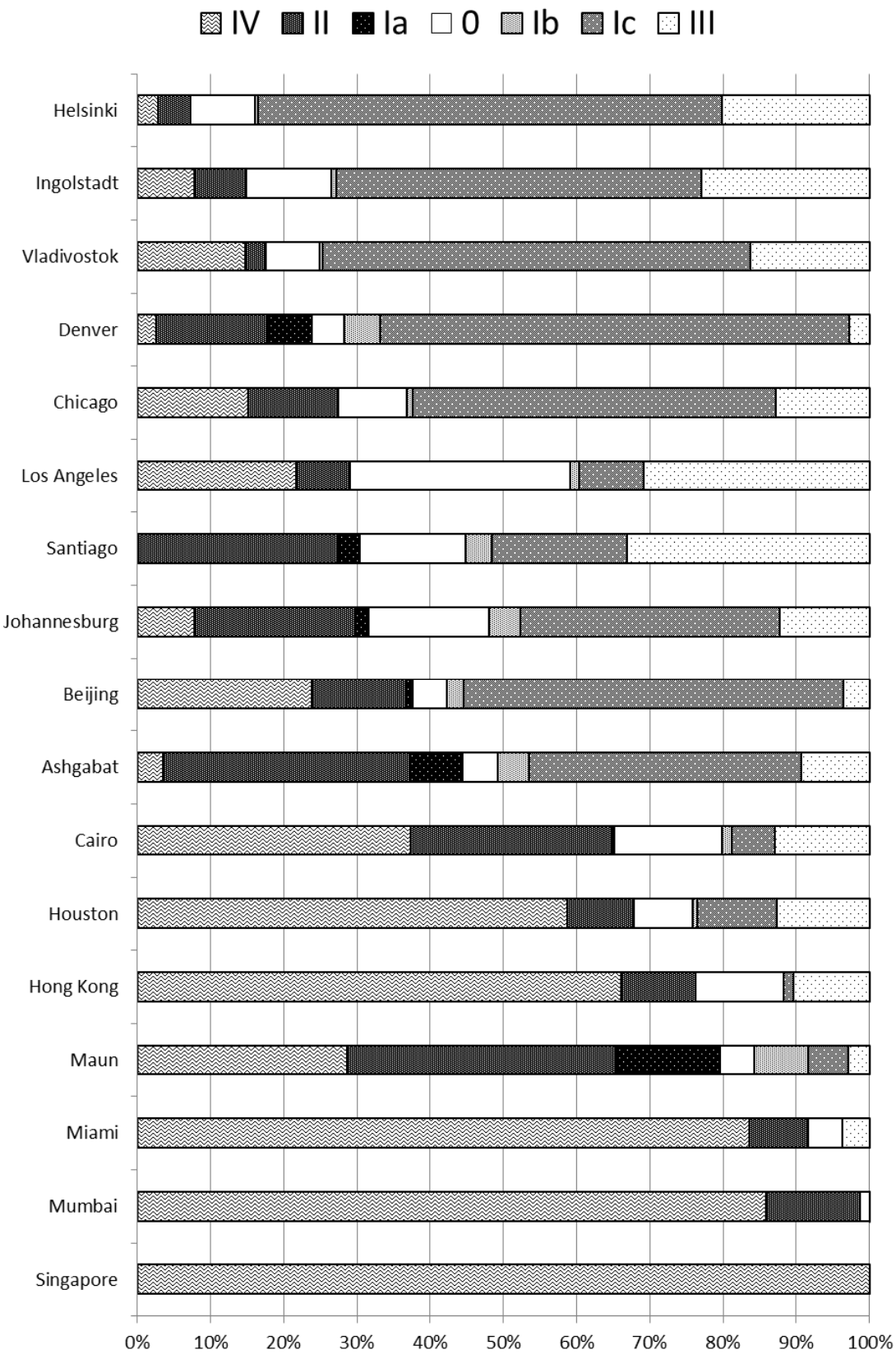

Figure 5.7: Classified air treatment requirements of the 17 investigated climates

conditions require a solar dehumidification (zone IV) the solar irradiation however is notably lower with an average value of 272.5 W m^{-2}.

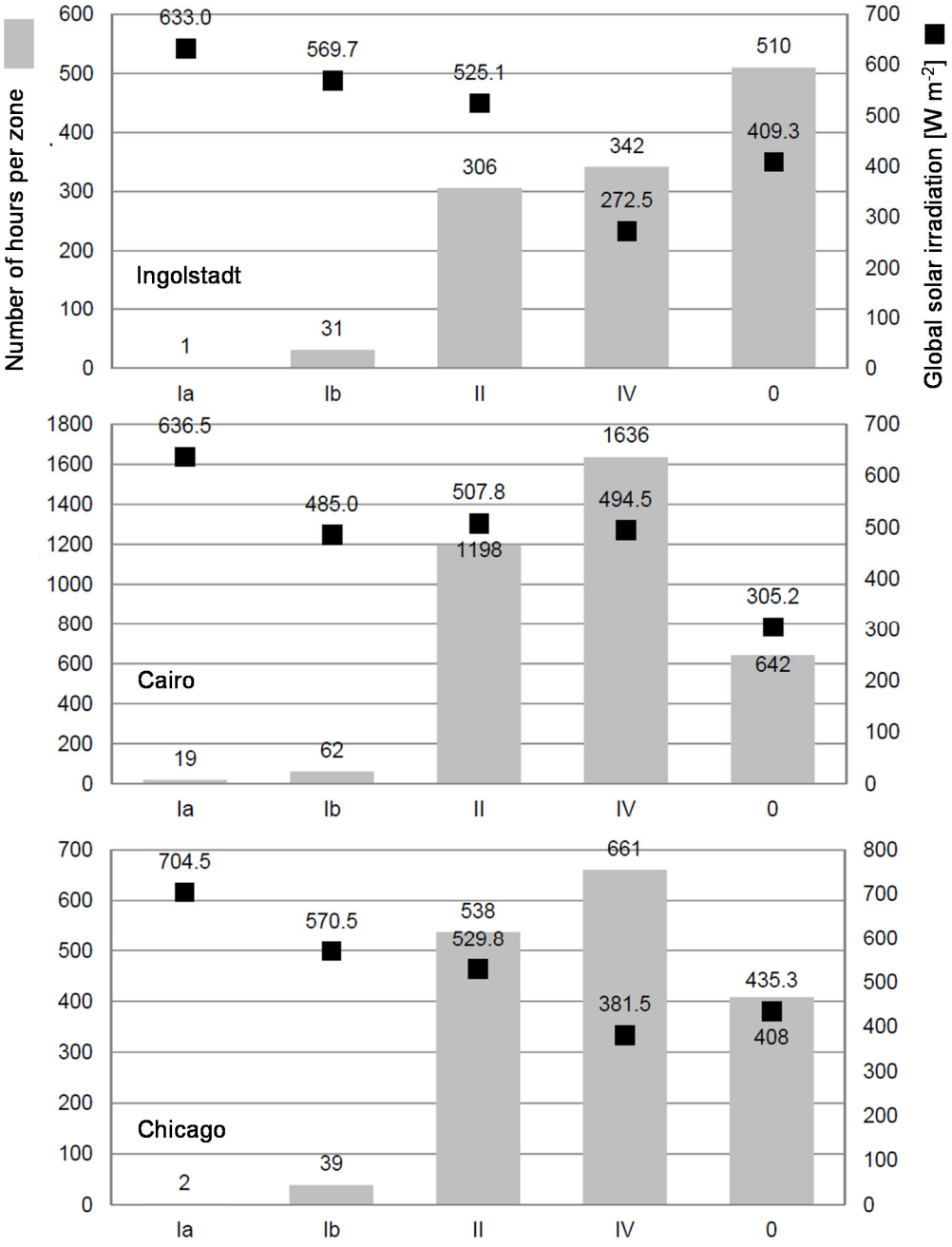

Figure 5.8: Average global irradiation intensity per zone with cooling demand for the climates Cfb (Ingolstadt), BWh (Cairo) and Dfa (Chicago)

By contrast, the solar irradiation during times of DEC-cooling demand (zone IV) is significantly higher in Cairo and Chicago. Thus, a contemporaneous utilisation

of solar gains is in principal more advantageous in these climates while the consideration of a solar buffer store concept is obviously of special significance under conditions of climate Cfb in order to retain additional solar heat at disposal for conditions in zone IV.

As shown in Figure 5.9 and Figure 5.10 the technology specific analysis further provides knowledge on the monthly occurrence of the different operation modes of a DEC-system (zone 1 to IV) in the course of the test reference year (TRY) together with the expected global solar irradiation yields per month.

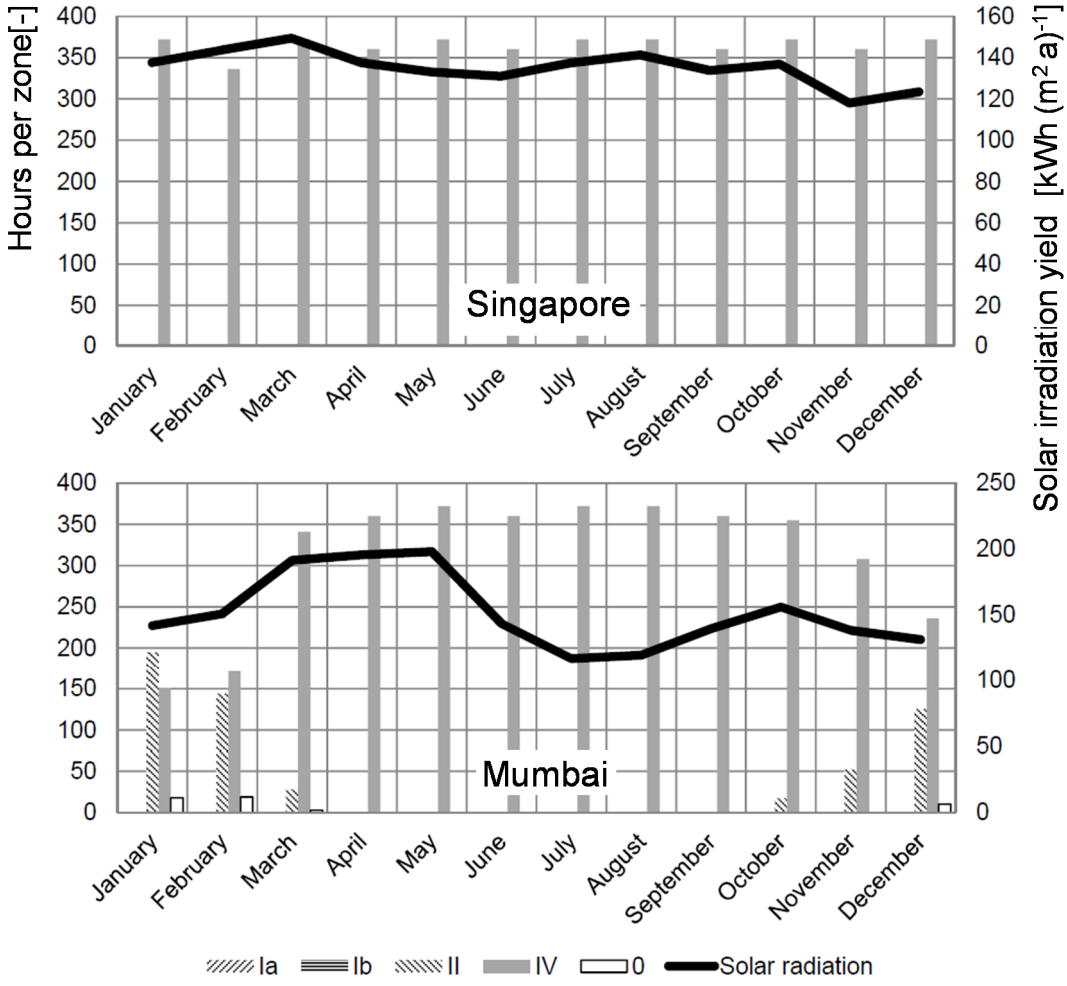

Figure 5.9: Monthly zone occurrence and expected global solar irradiation yields in Singapore (climate Af) and Mumbai (Aw)

In tropical climate of Singapore (Af Figure 5.9, upper diagram), all ambient air values coincide with a requirement for dehumidification (zone IV). The respective

solar yields are also expected homogenously throughout the year. This indicates one the one hand that the available solar yields can be completely harnessed for the DEC-process. On the other hand this shows, that the system obviously operates in a similar way throughout the year which simplifies the system dimensioning.

Also in the climate Aw, represented by Mumbai (Figure 5.9, lower diagram) the full DEC-mode with dehumidification (zone IV) is the dominant required air treatment throughout the year with slightly reduced occurrence from December to March. However, in contrary to Singapore, the data for Mumbai shows that the months with a maximum operation time in zone IV and thus with maximal solar heat requirement for the DEC-process (July, August) offer the least available solar yield at this site. Assuming that the entire latent cooling load is targeted to be covered with solar energy, it can be derived that the system design of a system in Mumbai is rather to be configured with the general requirements in the months of July and August, when heat demand and global irradiation are opposed.

Figure 5.10 shows the monthly solar fit analysis for the climates of Ingolstadt (Cfb) Cairo (BWh) and Maun, Botswana (BSh). Unlike the climates of Singapore and Mumbai, the data shows that the dehumidification mode IV is not required throughout the year but in fact limited to the respective summer months in northern or southern hemisphere. However, especially in the arid and semiarid climates of Cairo and Maun (Figure 5.10, upper and middle diagram) substantial solar yields between 250 and 330 kWh m^{-2} are available per month during these operational periods. This suggests that additional heat sinks are supposed to be integrated in the overall system in order to dissipate the solar heat in operational months without requirement of DEC-cooling.

In Ingolstadt, in the predominant months with DEC-cooling requirement the expected monthly solar yield ranges between 100 and 130 kWh m^{-2}. Due to the fact, that the overall DEC-cooling time is limited to 342 hours in total, and neglecting possibilities of short-term solar heat storage, only a maximum of about 50 kWh m^{-2} of the expected annual solar irradiance of 1,080 kWh m^{-2} are available for the DEC-process under these climatic conditions.

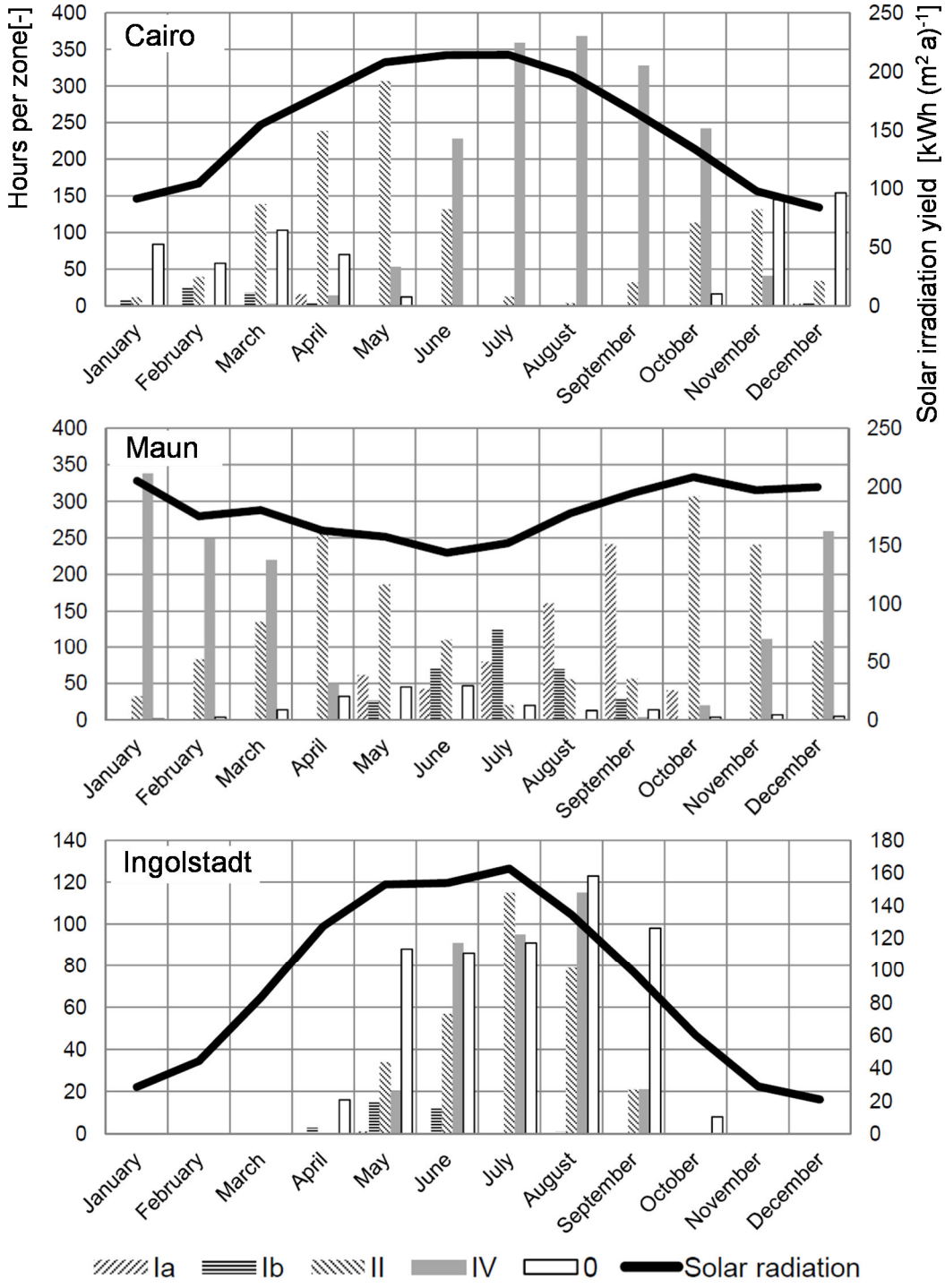

Figure 5.10: Monthly zone occurrence and expected global solar irradiation yields in Cairo, Chicago and Ingolstadt.

Thus, the average solar yield per day with DEC-operation (zone IV) provides additional detailed information with regard to the detailed system dimensioning. For instance in Ingolstadt, an average solar irradiation of approximately

3.86 kWh m^{-2} can be expected per day with DEC-operation according to the Meteonorm data. This information can be used for the overall pre-design of the solar DEC-systems buffer store at the particular site.

The complete analysis of the remaining sites and climates is found in Appendix E. As a result of this systematic analysis, basic recommendations for the climate specific design of solar DEC-systems can be derived, as it is discussed in the following section.

5.3.3 Climate Specific Design Recommendations

The gained technology-specific climate information for the diverse global sites, as presented in section 5.3.2, can serve as novel basis for the effective climate-specific preplanning of solar DEC-systems prior to system simulation. In the following, possible deduced pre-design approaches and recommendations as discussed by Bader et al. (2013b) are outlined.

Thus, the climates have been clustered according to the particular solar heat requirements considering that heat is only recommended in zone IV for dehumidification (DEC-cooling) as well as in zone III and Ic for heating respectively for heating and humidification. Thereby, the yearly distribution of the heat demand and accordantly expected solar gains were taken into consideration. In this manner, climate-dependent overall strategies for the operation DEC-systems (S1–S6) have been identified as shown in Table 5.3.

Solely the climates ranked in strategy S1 (Af, Aw, Am, Cwa, Cfa) indicate a demand for DEC-cooling (dehumidification) throughout the year with an average expected solar irradiation between 302 W m^{-2} and 410 W m^{-2} in zone IV. Accordingly, these climates principally provide the conditions for an application of the DEC-technology as a DEC stand-alone system.

Due to the generally high external loads it may be advised to consider the design of the DEC-unit as return-air design, as illustrated in Figure 5.11. As discussed by Fong et al. (2010) for the climate of Hong Kong, the excessive ambient humidity loads in the climates S1 generally cause a high energy consumption.

Table 5.3: Clustered climates and assigned overall DEC-strategy

Climate		II	IV	III	Ic	Overall DEC-Strategy
		Sensible Cooling	Cool + De-humidify	Heat	Heat + Humidify	
Af	Singapore	0%	100%	0%	0%	DEC stand-alone (S1)
Aw	Mumbai	13%	86%	0%	0%	
Am	Miami	8%	84%	4%	0%	
Cwa	Hong Kong	10%	66%	10%	1%	
Cfa	Houston	9%	59%	13%	11%	
BWh	Cairo	27%	37%	13%	6%	DEC + HW (S2)
BSh	Maun	37%	29%	3%	5%	
Dwa	Bejing	13%	24%	4%	52%	DEC + Heating (S3)
Csa	Los Angeles	7%	22%	31%	9%	
Dfa	Chicago	12%	15%	13%	50%	DEC Multivalent (S4)
Dwb	Vladivostok	3%	15%	16%	58%	
Cfb	Ingolstadt	7%	8%	23%	50%	
Cwb	Johannesburg	22%	8%	12%	35%	
BWk	Asgababat	34%	3%	9%	37%	No DEC / Adiabatic Cooling (S5)
Csb	Santiago	27%	0%	33%	18%	
BSk	Denver	15%	2%	3%	64%	
Dfb	Helsinki	4%	3%	20%	63%	Passive Cooling (S6)

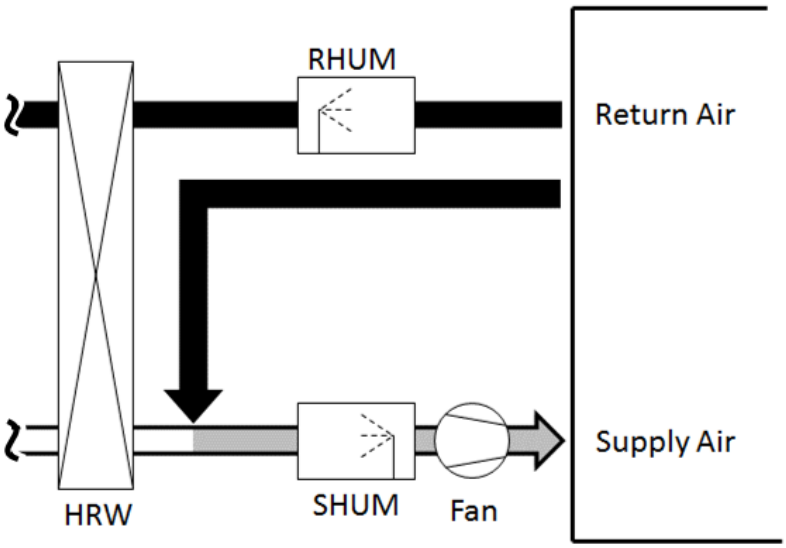

Figure 5.11: Return-air design

The design variant of a return air design recycles a part of the return air from the room and mixes it with the required fresh air supply which is reduced to a minimum depending on the room utilization and occupation. Considering the return air-design especially for operation times of peak ambient latent loads generally allows to reduce the design capacity of the DEC-system.

The climates grouped in cluster S2 (BWh, Cairo and BSh, Maun) also show a substantial DEC-cooling demand with 29% to 37% of the yearly operation time requiring cooling with dehumidification (zone IV). However the analysis further demonstrates that above 90% of this dehumidification demand conglomerates within 5 months of a year.

Thus, in these climates the solar thermal system essentially requires an additional heat sink to also dissipate and use the abundantly available solar heat in times of the year when the DEC-process does not require it. Due to the fact that the low heating demand can be evaluated to be of a theoretical nature and is not practised under these given climatic conditions it is highly recommended to pre-design the overall DEC-system in combination with the provision of hot water (HW) for instance for the purpose in a hotel.

As described, the dehumidification mode (zone IV) is highly relevant to create comfortable indoor conditions in Cairo and Maun. However, it therefore becomes apparent that the DEC-system components desiccant wheel and regeneration air heater are not requested during significant operation times of the year.

Therefore, in contrary to climates in cluster S1, the integration of a return air bypass should especially be considered as illustrated in Figure 5.12. With such a bypass the return air stream is guided past the dehumidifying unit. In operation modes with inactive desiccant wheel a bypass can reduce the pressure loss in the air duct and thus lower the electric power consumption of the fans.

Bejing and Los Angeles, representing the world climates Dwa and Csa were clustered to design strategy S3. Both climates show an existing DEC-cooling demand prevalent in the months June until September combined with a very high heating demand in winter with 40% to 56% of the systems operation time.

Therefore, the overall system is advised to be pre-planned combining solar thermal heating and solar DEC-air-conditioning in order to use the capacity of the solar thermal system. A by-pass is recommended analogue to strategy S4.

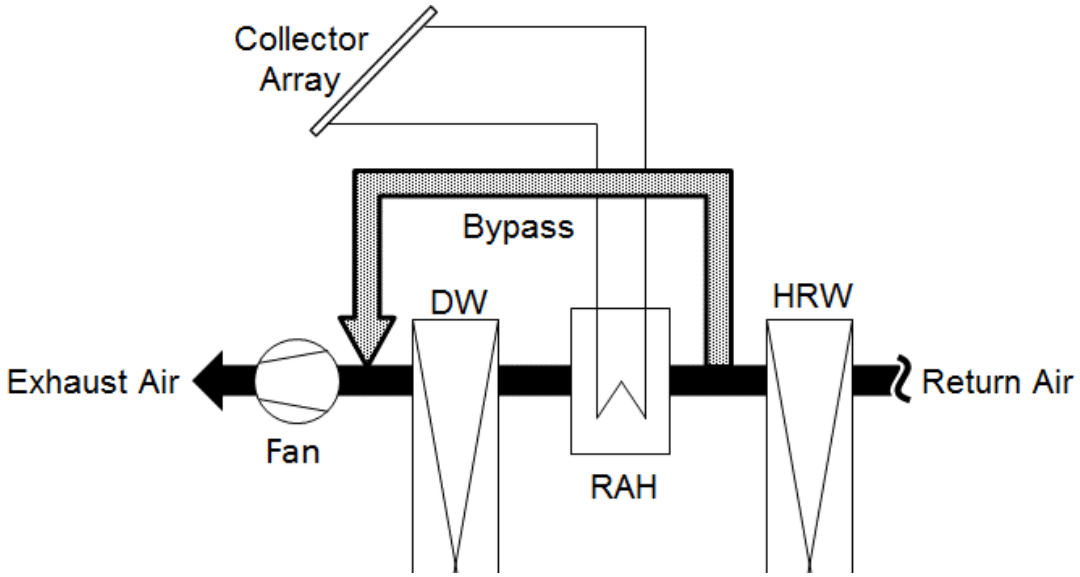

Figure 5.12: Bypass design for dry climates BWh and BSh

The climates of Ingolstadt (Cfb), Vladivostok (Dwb), Johannesburg (Cwb) and Chicago (Dfa) are clustered to design strategy S4. This results for this group show a minor demand for DEC-operation between 8% and 15% combined with the demand for room heating in winter. As the comparably low solar heat demand for dehumidification (337 to 661 hours annually) is spread over four to six months it is considered necessary to follow a multivalent system design integrating both solar heating and solar hot water preparation.

Due to the high winter humidification demand (zones 1a and 1c) it is generally recommended to operate the desiccant wheel (DW) as enthalpy exchanger and to put additional emphasis on the design of the supply air humidifier unit (SHUM). This is also applies for the climate Dwa (Bejing, S3). In general, it is recommended to include a bypass for the reasons already given, however, it must be noted that an extended operation of the DW in winter reduces the potential primary energy saving effect of a bypass.

Specifically, the climate Cwb (Johannesburg) shows a significant demand for sensible cooling (zone II =22%). Therefore, in case a multivalent system design cannot be realised the application of a solar-driven absorbtion or adsorption chiller shall be regarded, realising the relatively minor demand for dehumidification by means of cooling based dehumidification. This conventional operating principle of most common commercial and residential air conditioning systems dehumidifies by chilling the air below its dew-point whereby the humidity condensates.

The climates of Ashgabat (BWk), Santiago (Csb) and Denver (BSk) are characterised by virtually no demand for DEC-cooling (IV ≤ 3%) however with prevalent sensible cooling demand (overall design strategy S5). Accordingly, the application of a solar DEC-system is not recommended for these climates. In fact, the fresh air ventilation system is proposed to be realised in the form of an adiabatic cooling system with focus on heat recovery wheel (HRW) and return air humidifier (RHUM).

The remaining climate, Dfb (Helsinki) clustered to overall design strategy S6 shows a comparably low dehumidification demand as the S5 climates and reveals at the same time an almost non-existent sensible cooling demand. Therefore, it is recommended not to consider active cooling under these given conditions but rather put the focus only on passive cooling concepts.

5.4 Conclusions

While previous approaches examined individual system solutions for the application in different locations, the presented analysis provides fundamental knowledge for a climate-specific pre-design of solar DEC-systems.

Based on the thermal comfort requirements and assuming internal loads according to established standards, the Mollier diagram was subdivided into different zones that necessitate a different air treatment to reach thermal comfort in the room. Thereby, a methodological zoning approach was adjusted and refined.

In order to systematically deduce design-specific outline data for the application of the solar DEC-technology at climatically different sites, a subsequent meteorological analysis for the diverse global climates showed which air treatment functions are desired in a particular climate. Seventeen sites representing an associated world climate classified according to Köppen have been analysed.

Thus, the analysis sheds light on the actually required air treatments in the diverse global climates, on the one hand. This knowledge about the expected activity and operating time of the individual components of a solar DEC-system enables to deduce recommendations for its configuration and the selection of components for different climatic sites.

On the other hand, the analysis additionally provides insights regarding the design of the overall system, especially the need for the inclusion of additional heat sinks at locations where this can contribute to increase the specific annual solar collector yield.

This work has resulted in an understanding of the climate-specific effectiveness of solar DEC-systems. Overall DEC-strategies for the pre-design of solar DEC-systems were derived regarding the overall multivalent system approach as well as regarding exemplary configuration of principally favourable DEC-system configurations. Apart from the discussed designs, the results can be used as a basis to deduce further preferable effective strategies to pre-design DEC-systems at a particular targeted climate.

The approach presented and the information acquired on the effective DEC-system pre-design at a climate are recommended to be taken into consideration prior to the simulation of a solar DEC-system for a particular climatic site. This is intended to ensure that the simulation is respectively carried out with principally relevant and effective DEC-system designs at a site. Thus, this can contribute to boost the international market chances of this climate-friendly technology.

6 Conclusions and Outlook

The overall objective of the work described in this thesis was to carry out an operational monitoring analysis of a solar DEC-system and to analyse the integral system design of multivalent solar DEC-systems.

After an extensive in-situ monitoring with operational analysis, system optimisations were devised for solar DEC-systems with regard to the adequacy and efficiency of components. Moreover, recommendations regarding the integration and control of the solar arrays were derived.

In addition, a detailed simulation model of the overall solar thermal system with multivalent use of solar thermal heat for DEC-cooling, heating and hot water preparation was developed. Based on a fundamental research and a comparative study the strategies for the DEC-control and the supervisory control have been formulated. An advanced integral system design concept for multivalent solar DEC-systems was devised based on the developed simulation model. Owing to the original system layout an optimised supervisory control strategy for multivalent solar DEC-systems was developed and the positive effects on the system performance were demonstrated. As a result of the simulation study, design criteria on system level were derived for the optimised system concept. These criteria are to be adopted in the planning process of future multivalent solar DEC-systems.

Through a further developed, refined methodology it was demonstrated that it is crucial to give the respective climatic conditions priority in the planning of solar DEC-systems. The effectiveness of the solar DEC-technology was evaluated for the worlds` climate zones and appropriate recommendations for the pre-design of solar DEC-systems were devised.

All findings are in line with the research objectives introduced in section 1.3. The overall research work is summarized in the following section; the contributions of this research are elaborated and the impact on future work is evaluated.

6.1.1 Summary of Research Work

Monitoring concept for solar DEC-system. An extended measurement programme was developed to thoroughly analyse the DEC-process and the integration of the solar heat source. Appropriate sensors have been selected based on a detailed measurement error analysis. In order to manage the challenge of an inhomogeneous air distribution when measuring temperature and relative humidity in the duct, special measurement devices have been constructed and integrated. The monitoring analysis was placed in the context of recent monitoring research and its importance was differentiated accordingly.

In-situ system monitoring with operational analysis. It was found that the major reason for the insufficient refrigeration capacity of the DEC-system is grounded in the performance of desiccant wheel and heat recovery wheel. Both components did not reach the efficiency specified by the manufacturer. Additional measurements of the drop in pressure across the heat recovery wheel revealed that very large calcification deposits cause a significant reduction of the heat transfer characteristics. The investigation of the water hardness of the process water showed that the processed water treatment was insufficient to operate DEC-units. The inclusion of a reverse-osmosis system for water treatment, the consideration of an epoxy coated, highly anti corrosive heat recovery wheel and a number of recommendations for the planning of future systems were derived on the basis of these observations. Apart from that it was proven that there was no interdependence between the insufficient refrigeration capacity and the integration of the solar collectors into the DEC-process. However, malfunctions in the solar circuit control were identified and the potentials for an improved operation were described.

Simulation model for the entire multivalent solar DEC-system. Based on a comprehensive research review on existing component models for solar DEC-systems, a simulation model for the multivalent solar DEC-system has been established by means of the simulation environment INSEL 8. The developed model includes the fully modelled DEC-system as well as the sub-systems for the

heat sinks hot water preparation and heating. The respective dynamic room model is based on the previous research work by Pietruschka (2010) and has been implemented in the environment of INSEL 8. The entire system gradually reacts every minute to changing loads and ambient conditions throughout the year. The developed system simulation model allows to output the continuous system performance as well as the defined system responses on a yearly basis: total auxiliary electric energy consumption, primary energy ratio, solar fraction and specific annual collector yield.

Formulation of control strategy for the DEC-process. Due to the fact that the control strategy of the DEC-controller installed in-situ was not documented, a benchmarking was carried out comparing existing scientifically documented control strategies of solar DEC-systems. This comparison revealed that the principal structure of the control mechanisms use a similar cascade sequence, however the strategies are different in terms of the sequence order. Furthermore, all controls use largely different parameters and set values without noting outstanding climatologic or load specific reasons. Including the benchmarking and by means of first-hand information from the manufacturer, an appropriate DEC-control strategy has been formulated and implemented in the model.

Deduction of optimised system layout. The model has been used for a comprehensive investigation of improved system concepts. As a basis for the integral system design study an initial base case evaluation has been carried out. The performance of the initial system with direct sequential sink integration has been compared to an advanced system with solar buffer store. It was found that the overall performance of the multivalent system could be increased significantly with improved values for solar fraction (+21.4%), specific annual collector yield (+24.9%) and primary energy ratio (+18.3%). This results in a reduction of the total auxiliary electric energy consumption by 14.5%.

Development and formulation of optimised supervisory control strategy for multivalent systems. Despite the improved system performance, the analysis of the system with solar buffer store sheds light on the fact that the original sequential control hinders the system in fully utilising available solar heat and

causes unnecessary consumption of auxiliary primary energy. As a result, a novel supervisory control strategy for complex multivalent solar DEC-systems has been developed. A simultaneous supervisory control strategy has been formulated to stabilize the DEC-cooling process while maintaining solar hot water preparation at the same time. It was found that the system concept with simultaneous strategy reached a considerably improved energetic performance resulting in a reduction of the total auxiliary electric energy consumption by 5.2% and an improved room comfort compared to the concept with sequential sink supply strategy.

Sensitivity analysis of optimised system design. The concept with simultaneous control strategy was regarded as favourable and was taken as a basis for a sensitivity analysis to identify optimised system dimensions. A design of experiments study was applied to analyse the effects of the system parameters inclination angle, collector area, solar buffer store volume and hot water store volume on the system performance. In fact, the buffer store volume and size of the collector area were identified to be the critical parameters for the dimensioning of multivalent solar DEC-systems, whereas the design parameters inclination angle and hot water store volume are of inferior significance. A multi response surface analysis was the major approach to identify system optima. Due to generally concurrent optimisation objectives, two system optima were derived. The first optimum favours the minimisation of primary energy consumption, whereas the second optimum focuses on a maximised specific annual collector yield. The first system configuration (A_{col} = 305m^2; V_{SBS} = 32.1 m^3) can reduce the total auxiliary energy consumption by another 7.9% compared to the initial system with simultaneous control and in total by 33.1% compared to the original system at the beginning of the investigation. The second derived optimum (A_{col} = 247m^2; V_{SBS} = 29.9 m^3) can improve the specific collector yield by another 13.2% and in total by 42.9% compared to the original system.

Development of a refined methodological zoning approach. As the application and effectiveness of solar DEC-systems is predominantly dependent on the climatological conditions at a respective site a climate-specific technology

analysis has been conducted. A refined methodological zoning approach has been devised subdividing the Mollier-diagram into appropriate zones that necessitate a certain air treatment with regard to the creation of thermal room comfort.

Global solar DEC-potential analysis. A global climate-specific study on the DEC-technology has been carried out based on a series of climates representing the world climates according to the Köppen classification. The zoning methodology was applied resulting in a systematic understanding of the globally diverse air-conditioning requirements and the corresponding available solar irradiation at a specific climate. Overall DEC-strategies for the pre-design of solar DEC-systems have been devised with a focus on the multivalent system approach and with regard to principally favourable DEC-system configurations.

6.1.2 Research Contributions

The major contributions of this research comprise the following areas:

Recent research studies focused on the analysis of DEC-system components under laboratory conditions. However, a detailed investigation of the solar DEC-process in an industrial environment has not been carried out previously. The recent research neither focused on the integration of the solar collectors into the DEC-process nor the interaction with the hot water preparation in a multivalent system. This research reports the results of an operational system analysis with failure analysis carried out in-situ. An in-depth monitoring creates clear understanding of the performance and operation of a solar DEC-system in a multipurpose environment. The DEC-process and its components (desiccant wheel, heat recovery wheel, humidifiers and water-treatment) have been investigated in detail. The insufficient refrigeration capacity measured in-situ has been predominantly identified in reduced heat transfer characteristics of the HRW due to calcifications because of an inadequate processed water-treatment. In addition, it could be proven that the integration of the solar collectors is not responsible for the lack of refrigeration capacity, however there is potential for

improvement. Beside a series of recommendations for optimisations on system and component level, valuable experiences with the operation of a complex solar DEC-system in an industrial object have been recorded. The monitoring analysis contributed to the “Solar Heating & Cooling Programme” of the International Energy Agency (IEA). The IEA-Task 38 “Solar Air-Conditioning and Refrigeration” was involved in the development of adequate arrangements to improve the market launch of solar-assisted air-conditioning and cooling systems; its main focus is on improved components and system concepts.

Previous simulation studies solely focused on the modelling and investigation of the DEC-plant and its connection with solar collectors whereby the modelling and the investigation of the performance of single components was of priority. Apart from performance analyses the feasibility and potential of the DEC-technology was the main content of the assessments. By contrast, the integration of the solar DEC-technology in a multivalent environment with additional heat sinks in an overall system approach, where solar heat is utilized for DEC-air-conditioning, hot water supply and heating had not been investigated. However, this multivalent integration is regarded to be crucial for the overall effectiveness of the solar technology. Accordingly, a complex multivalent system model has been created and a rigorous DEC-control strategy has been formulated. Alternative system design layouts with solar buffer store have been devised and evaluated. Therefore, a novel simultaneous supervisory control strategy has been introduced and the advancement towards the original design has been demonstrated with regard to the stability of the system behaviour and improved energetic performance.

It has been found that dimensioning standards for the design and planning of multivalent solar DEC-systems are not available and have not been subject to previous research work. However, this calls for an intensive and fault-prone planning phase for every new developed system and is therefore constricting a wide distribution of the technology. This research addressed the systematic development of optimised dimensioning criteria for a multivalent system, based on a sensitivity analysis for the devised favourable system concept. Two optima

have been described by means of the dimensioning parameters collector area and solar buffer store volume. In addition, it was found that the parameters inclination angle and hot water store volume have no significant effect on the system performance in the given range.

The effectiveness of solar DEC-systems is essentially dependant on the respective climatic conditions. Previous research studies examined individual system solutions for DEC-systems and simulated the system for additional locations. However, the interpretation of these results cannot be regarded definite by the fact that the DEC-system design at a certain climate may not be an effective solution for various climates. The analysis presented creates a basis for a climate-specific pre-design of solar DEC-systems.

Based on a derived refined methodology a meteorological analysis is carried out for the global climates classified according to the Köppen classification. The acquired information can serve as a basis to effectively pre-design solar DEC-systems for a particular climate. In conclusion, the study devised appropriate climate-specific recommendations also with regard to the overall multivalent system approach to be considered as principally effective system approaches for future simulation studies.

6.1.3 Outlook

Based on the findings of this research, future research and development work is proposed as follows:

Further Development of the control strategies. The formulated DEC-control strategy and the introduced simultaneous supervisory control strategy are a solid basis for sustained improvement and advancement. Future research could additionally include concepts of a prognosis oriented control taking into consideration alternating loads, such as room occupation or water demand as well as changing ambient conditions. An intelligent short-term oriented prognosis could contribute to design control strategy and make multivalent solar DEC-systems even more energy efficient.

Simulation study for universally valid dimensioning of multivalent systems. The devised planning criteria represent optimised system dimensions for the configuration of the multivalent system. The created multivalent system model can serve as a basis to simulate various load ratios between cooling load, heating load and hot water load, aiming at the deduction of universally valid characteristic dimensioning guidelines.

Simulation of proposed climate-specific pre-design approaches. Apart from the study of universal dimension criteria, future simulation studies are recommended to take into consideration the proposed pre-designs for solar DEC-systems which are devised as principally effective solutions for particular climates. Thereby, the impact of the climatic conditions on the system dimensioning should be investigated.

Experimental study of developed concepts. A detailed experimental investigation of concepts devised in this research is recommended to be carried out under real operating conditions. Therefore, the developed optimised system concept and dimensioning are proposed to be realised in a future hotel with office environment to reproduce the findings in a field work. Thereby, the investigations should also cover the verification of the derived system and component optimisations resulting from the system monitoring of the research work. Apart from that, this realisation is recommended to be accompanied by the analysis of overall investment costs and life-cycle costs of the optimised multivalent solar DEC-system in comparison to a reference system.

Global analysis of the DEC-technology applying probabilistic data of future test reference years. Climate change is discussed to have a considerable impact on the global climates with changing occurrence of air temperature, air humidity and solar irradiation. As test reference years are based on historic observed data, it is recommended to carry out the presented zoning analysis using probabilistic future weather data. Therefore it is advised to build on the approach proposed by Smith and Hanby (2010) giving probabilistic climate projections influencing future weather years for energy modelling.

References

ADAM, M. (2004) *Statistische Versuchsplanung und Auswertung: DoE Design of Experiments* [WWW] Fachhochschule Düsseldorf, Fachbereich Maschinenbau und Verfahrenstechnik. Available from: http://mv.fh-duesseldorf.de/d_pers/Adam_Mario/a_lehre/am_pflicht/0_DoE_Vorlesung_Skript_aktuell.pdf [Accessed 20/01/2013]

ADNOT, J. et al. (2002) Central (commercial) air-conditioning systems in Europe. In: *Proceedings of the 2nd International conference on improving Electricity Efficiency in Commercial Buildings (IEECB),* Nice, France, May 2002.

ASHRAE (2009), *ASHRAE Handbook Fundamentals 2009,* Chapter 9.17 - Thermal Comfort, Atlanta, U.S.A., 2009.

BADER T. et al. (2009) In-situ measurements, simulation and system optimisation of a solar-driven DEC-system in an industrial environment. In: *Proceedings of the 3rd International Conference Solar Air-Conditioning*, Palermo, Italy. Regensburg, Germany: Ostbayerisches Technologie-Transfer-Institut, pp.509-514.

BADER, T. et al. (2010) Feldtest-Messungen und Systemoptimierung an einer solarbetriebenen DEC-Klimatisierungsanlage im industriellen Einsatz. In: *Proceedings of the 20th Symposium Thermische Solarenergie*, Bad Staffelstein, Germany, May 2010, Regensburg, Germany: Ostbayerisches Technologie-Transfer-Institut.

BADER, T. et al. (2010a) Solar-Driven Desiccant and Evaporative Cooling: Technology Overview and Operational Experiences. In: *Proceedings of the 3rd IASTED African Conference on Power and Energy Systems*, Gaborone, Botswana, September 2010.

BADER, T. et al. (2010b). In-Situ Analysis and Operational Optimisation of a Solar-Driven DEC-System. In: *Proceedings of the 2nd International Conference on Solar Heating, Cooling and Buildings Eurosun 2010,* Graz, Austria, September 2010.

BADER, T. et al. (2011) Solar Desiccant air-conditioning in an industrial application: optimisation approaches for solar-thermal integration and air-handling unit. In: *Proceedings of the ISES Solar World Congress 2011*, Kassel, Germany, August 2011, International Solar Energy Society.

BADER, T. et al. (2011a) Component Analysis of a Solar-Driven DEC-System. In: *Proceedings of the 4th International Conference Solar Air-Conditioning,* Larnaca, Cyprus, October 2011. Regensburg, Germany: Ostbayerisches Technologie-Transfer-Institut, pp.329-334.

BADER, T. et al. (2012) Betriebs-erfahrungen mit großen Kollektorfeldern zur solaren Klimatisierung In: *Proceedings of the 22nd Symposium Thermische Solarenergie*, Bad Staffelstein, Germany, Mai 2012. Regensburg: Ostbayerisches Technologie-Transfer-Institut e.V. (OTTI).

BADER, T. et al. (2013) Globale Anwendbarkeit solarer DEC-Systeme zur Klimatisierung: Untersuchung der Relevanz für klimatisch unterschiedliche Standorte. In: *Proceedings of the 23rd Symposium Thermische Solarenergie*, Bad Staffelstein, Germany, April 2013. Regensburg: Ostbayerisches Technologie-Transfer-Institut e.V. (OTTI).

BADER, T. et al. (2013a) Climate specific design and effectiveness of solar DEC-systems: A methodological zoning approach. In: *Proceedings of the 2nd International Conference on Solar Heating and Cooling for Buildings and Industry - SHC 2013*, Freiburg, Germany September 2013. Elsevier ScienceDirect Ltd., Energy Procedia, 48, 2014, pp.778-789.

BADER, T. et al. (2013b) Global Applicability of Solar DEC-Systems: Basic Technology Effectiveness in Climatically Different Regions. In: Proceedings of the 5th International Conference Solar Air-Conditioning, Bad Krozingen, Germany, September 2013. Regensburg, Germany: Ostbayerisches Technologie-Transfer-Institut, pp. 176-181.

BAKMEDEENIYA, L.U. (2010) *Modelling Polygeneration with Desiccant Cooling System for Tropical (and Sub-Tropical) Climates*. Thesis (Msc), Royal Institute of Technology, Department of Energy Technology, Stockholm, Sweden.

BALARAS, C.A. et al. (2007) Solar Air conditioning in Europe - An Overview. *Renewable and Sustainable Energy Reviews*, 11, pp. 299-314.

BANKS, P.J. (1972) Coupled heat and mass transfer in fluid flow through porous media – an analogy with transfer. In: *Proceedings of the 4th International Heat Transfer Conference*, Versailles VIII, 1970, pp. 1-10.

BANKS, P.J. (1985) Prediction of Heat and Mass Regenerator Performance Using Nonlinear Analogy Method: Part 1-Basis. *ASME Journal of Heat Transfer*, 107 (1), pp.222-229.

BARLOW, R. (1981) Analysis of solar desiccant systems and concepts, In: Proceedings of te Active contractors' Review Meeting, Washington DC, USA, September 1981. p. 5, SERI/TP-631-1254 CONF-810912-6.

BASSOLS-RHEINFELDER, J. (1982) Experimental and Numerical Studies on an Open Adsorption System for Solar Space-Cooling. Thesis (Dr.-Ing.) Technische Hochschule, Aachen, Fakultät für Maschinenwesen, Germany.

BAUMGARTH, S. et al. (2003) *Handbuch der Klimatechnik. Band 2: Anwendungen*. 4th ed. Heidelberg: C.F. Müller Verlag.

BECCALI, M. et al. (2003a) Simplified models for the performance evaluation of desiccant wheel dehumidification*. International Journal of Energy Research*. 27, pp. 17-29.

BECCALI, M., BUTERA, F. and ADHIKARI R. (2003b) Solar Assisted Air Conditioning of Buildings. IEA Task 25, Subtask B: Design Tools and Simulation Programmes. ILK Dresden.

BECCALI, M. et al. (2008) Monitoring of a Solar Desiccant Cooling System in Palermo (Italy). First Results and Test Planning. In: Proceedings of the 1st International Conference on Solar Heating, Cooling and Buildings - Eurosun 2008, Lisbon, Portugal, October 2008.

BECCALI, M. and NOCKE, B. (2007) *Solar Heating and Cooling of Buildings: Ecobuildings Guidelines*, Brita in Pubs, EU6 framework programme.

BECCALI, M., FINOCCHIARO, P. and NOCKE, B. (2009a) Solar desiccant cooling system operating in Palermo (Italy): Results and validation of simulation models. In: *Proceedings of the 3rd International Conference Solar Air Conditioning*. Palermo, Italy, September 2009, pp. 368-375.

BECCALI, M., FINOCCHIARO, P. and NOCKE, B. (2009b) Energy and economic assessment of desiccant cooling systems coupled with single glazed air and hybrid PV/thermal solar collectors for applications in hot and humid climate, *Solar Energy*, 83, pp. 1828-1846.

BEGGS, C.B. and HALLIDAY, S. (1999) A theoretical evaluation of solar-powered desiccant cooling in the United Kingdom. *Building Services Engineering Research and Technology,* 20 (3), pp.113-117.

BERND, A. (1997) Entwicklung eines Kennlinienverfahrens für die Berechnung von Sorptionsregeneratoren. Unpublished thesis (Diplom), TU Dresden.

BEST, R. and ORTEGA, N. (1999) Solar refrigeration and cooling. *Renewable Energy*, 16, pp.685-690.

BOLLIN, E. (2009) *Automation regenerativer Wärme- und Kälteversorgung von Gebäuden*. 1st ed. Wiesbaden: Vieweg + Teubner.

BOX, G.E.P. and BEHNKEN, D.W. (1960) Some New Three Level Designs for the Study of Quantitative Variables. *Technometrics*, 2 (4), pp. 455-475.

BRANDSTETTER, F. (2007) *Konzept für eine Solaranlage des „Alpen Adria Hotels“ in Hermagor* [WWW] Arsenal Research. Available from: http://www.ib-

brandstetter.at/fileadmin/user_upload/Planungsaudits/Planungsvorschlag_Alpen_Adria_Hotel.pdf [Accessed 02/03/14].

BRYCHTA, M. and POL, O. (2007) *Reality check in the building Halle J in Ingolstadt: Monitioring and simulation of a solar desiccant and evaporative cooling system*. Arsenal Research, Vienna on 20th February 2007.

BUNDESMINISTERIUM FÜR ARBEIT UND SOZIALORDNUNG (2001) Arbeitsstättenrichtlinie-Richtlinie Raumtemperaturen ASR 6. IIIb 2-34507-17, BArbBI Nr. 6-7.

CAMARGO, J.R. et al. (2005) An Evaporative and Desiccant Cooling System for Air Conditioning in Humid Climates. *Journal of the Brazilian Society of Mechanical Sciences & Engineering*, 27 (3), pp. 243-247.

CASAS, W. and PRÖLSS, G. and SCHMITZ, G. (2005) Modeling of Desiccant Assisted Air Conditioning Systems. In: *Proceedings of the 4th International Modelica Conference, Hamburg, March 2005.* Linköping: Modelica Association pp. 487-496.

CASAS, W. and SCHMITZ, G. (2005) Experiences with a gas driven, desiccant assisted air conditioning system with geothermal energy for an office building. *Energy and Buildings*, 37, pp. 493-501.

CERBE, G. and HOFFMAN, H.-J. (1996) *Einführung die Thermodynamik – Von den Grundlagen zur technischen Anwendung*. Vienna, Austria: Hanser-Verlag, 1996.

CHAROENSUPAYA, D. and WOREK, W. M. (1988a) Effect of Adsorbent Heat and Mass Transfer Resistances on Performance of an Open-Cycle Adiabatic Desiccant Cooling System. *Heat Recovery Systems and CHP*, 1988, 8 (6), pp. 537-548.

CHAROENSUPAYA, D. and WOREK, W. M. (1988b) Parametric study of an open-cycle adiabatic, solid, desiccant cooling system. *Energy*, 13 (9), S. 739-747.

CHIN, W.W. (1998) The partial least square approach to structural equation modelling. In: Marcoulides, G. A. eds. *Modern methods for business research*. Mahwah, New Jersey, USA: Lawrence Erlbaum Associates, pp. 295-358.

CHUNG, J.D., LEE, D.-Y. and YOON, S.M. (2008) Optimization of desiccant wheel speed and area ratio of regeneration to dehumidification as a function of regeneration temperature. *Solar Energy*. 83 pp. 625-635.

CHUNG, J.D. and LEE, D.-Y. (2009) Effect of desiccant isotherm on the performance of desiccant wheel. *International Journal of Refrigeration*, 32, pp. 720-726.

CHUNG, J.D., LEE, D.-Y. and YOON, S.M. (2009) Optimization of desiccant wheel speed and area ratio of regeneration to dehumidification as a function of regeneration temperature. *Solar Energy*, 83, pp. 625-635.

CONCINA, W., SADINENI, S. and BOEHM, R. (2011) Solar Assisted Desiccant Cooling Simulation for Different Climate Zones. In: *Proceedings of the 5th International Conference on Energy Sustainability ASME 2011*, Washington DC, USA, August 7–10, 2011

DAOU, K., WANG, R.Z. and XIA, Z.Z. (2006) Desiccant cooling air conditioning: a review. Renewable and Sustainable Energy Reviews, 10, pp. 55–77.

DAVANAGERE, B.S., SHERIF, S.A. AND GOSWAMI, D.Y. (1999) A feasibility study of a solar desiccant air-conditioning system – Part 1: Psychometrics and analysis of the conditioned zone. *International Journal of Energy Research*, 23, pp.7-21.

DE ANTONELLIS, S., JOPPOLO C.M. and MOLINAROLI, L. (2010) Simulation, performance analysis and optimization of desiccant wheels. *Energy and Buildings*, 42 (9), pp. 1386-1393.

DHAR, P. et al. (1995) Thermodynamic analysis of desiccant – augmented evaporative cooling cycles for Indian conditions. *ASHRAE Transactions*, 101, pp. 735-749.

DEUTSCHES INSTITUT FÜR NORMUNG (1994) DIN 1946-2:1994, *Raumlufttechnik, Gesundheitstechnische Anforderungen* (VDI-Lüftungs-regeln), Part 2. Berlin: Beuth Verlag GmbH.

DEUTSCHES INSTITUT FÜR NORMUNG (2001) DIN EN 12975-1:2001 Thermische Solaranlagen und ihre Bauteile – Kollektoren – Teil 1: Allgemeine Anforderungen. Berlin: Beuth Verlag GmbH.

DEUTSCHES INSTITUT FÜR NORMUNG (2002). DIN 4701-10_2001-02. *Energetische Bewertung heiz- und raumlufttechnischer Anlagen, Teil 10: Heizung, Trinkwassererwärmung, Lüftung*. Berlin: Beuth Verlag GmbH.

DEUTSCHES INSTITUT FÜR NORMUNG (2008) DIN V 18599:2008 - *Energy efficiency of buildings, Parts 1-10*. Berlin: Beuth Verlag GmbH.

DIXON, D. et al. (2006) Application of Design of Experiments (DoE) Techniques to Process Validation in Medical Device Manufacturing. *Journal of Validation Technology*, 12 (2), pp. 92-100.

DOPPELINTEGRAL (2009) INSEL 8 Tutorial [WWW] doppelintegral GmbH. Available from: www.insel.eu/fileadmin/insel.eu/diverseDokumente/inselTutorial/inselTutorial_en.pdf. [Accessed 10/09/10]

DOPPELINTEGRAL (2010) *INSEL 8 Block Reference Manual*. [WWW] doppelintegral GmbH. Available from: www.insel.eu/fileadmin/insel.eu/diverseDokumente/ blockReference/inselBlockReference_en.pdf. [Accessed 10/09/10]

DUFFIE, J.A. and BECKMAN, W.A. (1991) Solar Engineering of Thermal Processes. 2nd ed. New York: John Wiley & Sons.

DUFFIE, J.A. and MITCHELL, J.W. (1980) Systems evaluation study of solar desiccant cooling systems. In: *Proceedings of the annual DOE active solar heating and cooling contractors' review meeting*, Lake Tahoe, USA, March 1980, 3 pp. 14-16.

DUFFIE, J.A. and MITCHELL, J.W. (1982) Component and system evaluation study of solar desiccant cooling. In: *Proceedings of the* annual DOE active solar heating and cooling contractors' review meeting: Proceedings and Proiect Summaries. September 1981. Washington DC, USA, 3 pp. 28-30

DUMONT, E. et.al (2013) Theoretical study of cooling technologies driven by geothermal energy for use in tertiary buildings in Belgium. In: *Proceeedings of the 13th Conference of International Building Performance Simulation Association,* Chambéry, France, August 2013, pp. 1540-1547

DUNKLE, R.C. (1965) A Method of Solar Air Conditioning, Institute Engineers. Australia Mechanical and Chemical Engineering Transmission, 1, pp. 73-78.

DÜRR, H.-P. (2010) *Warum es ums Ganze geht: neues Denken für eine Welt im Umbruch*. 4th ed. Munich: Oekonom Verlag

ECOHEATCOOL (2006) *The European Cold Market – Final Report, Work Package 2*, Brussels, Belgium: Ecoheatcool and Euroheat & Power

EICKER, U. (2001) *Solare Technologien für Gebäude*. 1st ed. Stuttgart: B.G. Teubner Verlag.

EICKER, U. et al. (2002) Komponenten- und Anlagenverhalten solar betriebener sorptionsgestützter Klimaanlagen. *KI – Luft und Kältetechnik*, 27 (11) pp. 541-547.

EICKER, U. (2002) Entwicklungstendenzen solarthermischer Kühlverfahren. In: *Proceedings of the 2nd Symposium Solares Kühlen in der Praxis.* Stuttgart, Germany, pp. 6-16.

EICKER, U. et al. (2006) Betriebserfahrungen und Untersuchungen von DEC-Anlagen: Regelungsoptimierung und Energieanalysen. In: *Proceedings of the 4th Symposium Solares Kühlen in der Praxis,* Stuttgart, Germany, pp. 59-71.

EICKER, U. (2009) *Low Energy Cooling for Sustainable Buildings*. Chichester: John Wiley and Sons.

EICKER, U. (2012) *Solare Technologien für Gebäude*. 2nd ed. Stuttgart: B.G. Teubner Verlag.

EL-SHAARAWI, M. (1994) On the Psychrometric Chart. *ASHRAE Transactions*. 100 (1), paper 3736.

EN 13779 (2007) *Ventilation for non-residential buildings - Performance requirements for ventilation and room conditioning systems.* European Standard, European Committee for Standardisation, Brussels, Belgium.

EN 15243 (2007) *Ventilation for buildings – Calculation of room temperatures and of load and energy for buildings with room conditioning systems.* European Standard, European Committee for Standardisation, Brussels, Belgium. pp. 41-42

EN 15251 (2007) *Indoor environmental input parameters for design and assessment of energy performance of buildings addressing indoor air quality, thermal environment, lighting and acoustics*. European Standard, European Committee for Standardisation, Brussels, Belgium. pp 12-45.

EN 308 (1997) *Heat exchangers – Test procedures for establishing performance of air to air and flue gases heat recovery devices.* European Standard, European Committee for Standardisation, Brussels, Belgium.

ENERGY RESEARCH KNOWLEDGE CENTRE (2013) Energy Research in Europe – A guide to European, national and international energy research programmes and organisations. Luxembourg: Publications Office of the European Union p. 5

ERPENBECK, T. (1999) *Sorptionsgestützte solare Klimatisierung - Experimentelle und theoretische Analyse von Potential und Systemverhalten.* Thesis (PhD), University Karlsruhe.

EUROPEAN COMMISSION. DIRECTORATE GENERAL ENERGY AND TRANSPORT (2004) European Union Energy & Transport in Figures part 2. Brussels: p. 138.

EUROPEAN COMMISSION (2012) *Energy Efficiency Status Report 2012 - Electricity Consumption and Efficiency Trends in the EU-27*. Luxembourg: Publications Office of the European Union, 2012, pp. 117-120

FANGER P.O. (1970) *Thermal Comfort*. Copenhagen, Denmark: Danish Technical Press.

FANINGER, G.(2009) *Bewertung der Wärmeversorgung von Gebäuden – Energetische, Wirtschaftliche und Umweltbezogene Kriterien*. AEE-INTEC-Institut für Nachhaltige Technologien, Klagenfurt, Austria. Available from: www.aee-intec.at/0uploads/dateien644.pdf. Accessed [30/10/13]

FINOCCHIARO, P. (2010) Task 38 - Solar Air Conditioning and Refrigeration - International Energy Agency Solar Heating and Cooling Program, DREAM - Department of Energy and Environmental Research, Universita degli Studi di Palermo.

FITZNER, K. (2008) *Raumklimatechnik Band 2: Raum- und Raumkühltechnik*, 16th ed. Berlin Heidelberg, Germany: Springer Verlag

FONG, K.F. et al. (2010) Advancement of solar desiccant cooling system for building use in subtropical Hong Kong. *Energy and Buildings*, 42 (2010) pp. 2386-2399

FRANZKE, U. (1990) *Ein Beitrag zum Wärme- und Stoffaustausch in rotierenden Speichermaterialien*. Thesis (PhD). TU Chemnitz.

FRANZKE, U. and HEINRICH, G. (1997) *Sorptionsgestützte Klimatisierung.* Heidelberg, Germany: C.F. Müller Verlag.

FRANZKE, U. and STANGL, M. (2000) *Optimierung der Komponenten des DEC-Klimasystems*. Abschlussbericht (Final Report), No. ILK-B-4/00-2796, Institut für Luft-und Kältetechnik (ILK), Dresden, Germany.

FRANZKE, U. and SEIFERT, C. (2005) *Solar Assisted Air Conditioning of Buildings*. Fachbericht (Final Report), No. *ILK-B-31/05-3110 ILK,* Institut für Luft-und Kältetechnik (ILK), Dresden, Germany.

FRANZKE, U. (2008) Offene Verfahren mit festen Sorbentien. In: *Proceedings of DBU Workshop Kälte aus Wärme,* Osnabrück, Germany: Deutsche Bundestiftung Umwelt (DBU), Dezember 2008.

GANSLER, R. A., KLEIN, S. A. and BECKMAN, W. A., 1994. Assessment of the accuracy of generated meteorological data for use in solar energy simulation studies. Solar Energy, Vol. 53, No.3, pp. 279 - 287.

GE, T.S. et al. (2008) A review of the mathematical models for predicting rotary desiccant wheel. *Renewable and Sustainable Energy Reviews*, 12 (6), pp. 1485-1528.

GINESTAT, S., STABAT, P. and MARCHIO, D. (2002) *Control strategies of open cycle desiccant cooling systems minimizing energy consumption*. Centre d'énergétique (Cenerg).

GINESTAT, S., STABAT, P. and MARCHIO, D. (2003) Control design of open-cycle desiccant cooling systems using a graphical environment tool. *Building Services Engineering Research and Technology,* 24 (4), pp. 257-269

GLÜCK, B. (1991) *Zustands und Stoffwerte (Wasser, Dampf, Luft), Verbrennungsrechnung.* Berlin, Germany: Verlag für Bauwesen

GNIEWOSZ, W. (1999) Dynamische Modellierung und Simulation eines Solarkollektors zur Unterstützung der Konstruktion. In: *Proceedings of the 44th International Scientific Colloquium at Technical University Ilmenau*, Germany.

GREIDER, W. (2000) Oil on political waters. *The Nation*, 271 (12), 23rd Oct. 2, pp. 5-6

GUTERMUTH, W. (1980) Untersuchung der gekoppelten Wärme- und Stoffübertragung in Sorptionsregeneratoren. Dissertation, Technische Hochschule Darmstadt.

HAFNER, B., PLETTNER, J. and WEMHÖRNER, C. (1999) CARNOT-Blockset: Conventional And Renewable eNergy systems OpTimization Blockset Version 1.0. User's Guide. Solar-Institut Jülich, University of Applied Sciences Aachen.

HALLER, A. (2004) Analyse einer solar unterstützten DEC-Klimatisierungsanlage in einem Multifunktionsgebäude. Unpublished Thesis. Ingolstadt University of Applied Sciences, Germany.

HALLER, A. et al. (2005) Solar-Assisted DEC-System in a Multipurpose Building. In: *Proceedings of the 1st International Conference on Solar Air-Conditioning*, Bad Staffelstein, Germany, October 2005. Regensburg, Germany: Ostbayerisches Technologie-Transfer-Institut.

HALLER, A. (2007) *The Performance of a Regenerative Heating and Cooling System in a Multipurpose Building.* Thesis (MPhil), De Montfort University Leicester.

HALLIDAY, S., BEGGS, C.B. and SLEIGH P.A. (2002) The use of solar desiccant cooling in the UK : a feasibility study. *Applied Thermal Engineering*, 22, p.1327-1338.

HARRIMAN, L.G. (1990) The dehumidification handbook, Amesbury: Munters Cargocaire.

HATAMI, Z. et al. (2012) Optimization of solar collector surface in solar desiccant wheel cycle. *Energy and Buildings*, 45, pp. 197–201

HEIDARINEJAD. G. and PASDARSHAHRI, H. (2010) The effects of operational conditions of the desiccant wheel on the performance of desiccant cooling cycles. *Energy and Buildings*, 42, pp. 2416–2423.

HENNING, H.-M. (1993) *Regenerierung von Adsorbentien mit solar erzeugter Prozeßwärme*. *Regeneration of adsorbens with solar-produced process heat.* Thesis (PhD), Oldenburg University, VDI Fortschrittsberichte Verfahrenstechnik 350.

HENNING, H.M. et al. (2001) The potential of solar energy use in desiccant cooling cycles. *International Journal of Refrigeration*, 24, pp. 220-229.

HENNING, H.-M. (ed.) (2004a) *Solar-Assisted Air-Conditioning in Buildings - a Handbook for Planners*. Vienna, Austria: Springer-Verlag.

HENNING, H.-M. (2004b) Solare Klimatisierung - Stand der Entwicklung. In: *Proceedings of Conference Solares Kühlen*. Vienna, Austria: Wirtschaftskammer Österreich.

HENNING, H.M. (2005) *Solare Klimatisierung – Stand der Entwicklung*. AEE INTEC – Arbeitsgemeinschaft Erneuerbare Energien, Institut für Nachhaltige Technologien.

HENNING, H.-M. (2007) Solar assisted air conditioning of buildings – an overview. *Applied Thermal Engineering,* 27, 1734–1749.

HENNING, H.-M. (ed.) (2009) *Kühlen und Klimatisieren mit Wärme*. Karlsruhe, Germany: Solarpraxis AG

HENNING, H.-M. (2011) Status and Perspectives of Solar Air-Conditioning and Refrigeration. In: *Proceedings of the 4th International Conference Solar Air-Conditioning*, Larnaca, Cyprus, October 2011. Regensburg, Germany: Ostbayerisches Technologie-Transfer-Institut, pp.18-23.

HENNING, H.-M., MOTTA, M. and MUGNIER, D. (eds.) (2013) *Solar Cooling Handbook – A Guide to Solar Assisted Cooling and Dehumidification Processes*. Vienna, Austria: AMBRA / V.

HILMER, F. et al. (1999) Numerical solution and validation of a dynamic model of solar collectors working with varying fluid flow rat. *Solar Energy*, 65 (5), pp. 305-321.

HINDENBURG, C. (2002) *Solar autarke sorptionsgestützte Klimaanlage mit Solarluftkollektoren-Betriebserfahrungen des ersten Jahres*.[WWW] Fraunhofer Institut für Solare Energiesysteme ISE. Available from http://www.ise.fraunhofer.de/veroeffentlichungen/nach-jahrgaengen/2002/solar-autarke-sorptionsgestutzte-klimaanlage-mit-solarluftkollektoren-betriebserfahrungen-des-ersten-jahres [Accessed 09/03/11]

HIRUNLABH et al. (2007) Feasibility study of desiccant air-conditioning system in Thailand. *Building and Environment*, 42 pp. 572–577.

HOEFKER, G. (2001), *Desiccant Cooling with Solar Energy*, Thesis (PhD), De Montfort University Leicester, United Kingdom.

HWANG, Y. et al. (2008). Review of solar cooling technologies. *HVAC & R Research*, 14, pp. 507-528.

IEA (2012) Technology Roadmap: Solar Heating and Cooling. [WWW] International Energy Agency. Available from http://www.iea.org/publications/freepublications/publication/2012_SolarHeatingCooling_Roadmap_FINAL_WEB.pdf [Accessed 04/05/14]

IEA SHC-Task 26 (2002) *A solar collector model for TRNSYS simulation and system testing*. A Report of IEA SHC – Task 26, Solar combisystems.

IEA SHC-TASK 38 (2011) *Monitoring Procedure for Solar Cooling Systems - A joint technical report of subtask A and B (D-A3a / D-B3b)* [WWW] IEA SHC Task 38, Avalailble from: http://archive.iea-shc.org/publications/downloads/IEA-Task38-Report_A3a-B3b-final.pdf [Accessed 05/12/11]

IESD (2012) *JEPlus – An EnergyPlus simulation manager for parametrics* [WWW] De Montfort University. Available from: http://www.jeplus.org/wiki/doku.php?id=start [Accessed 18/02/14]

ILERI, A. (1997) A Discussion on Performance Parameters for Solar-Aided Absorption Cooling Systems. *Renewable Energy*, 10 (4), pp. 617-624.

ILK (2005) *Software zur Darstellung von Prozessen im Mollier-h,x-Diagramm*. Institut für Luft- und Kältetechnik ILK Dresden

INTERGOVERNMENTAL PANEL ON CLIMATE CHANGE (2007) *Climate Change 2007: Synthesis Report. Contribution of Working Groups I, II and III to the Fourth Assessment Report of the Intergovernmental Panel on Climate Change*. Geneva, Switzerland: IPCC, 2007, 104 pp.

ISO 9806-1 (1994) Solar energy — Test method for solar collectors — Part 1: Thermal performance of glazed liquid heating collectors including pressure drop.

ISO EN 7730 (2005) *Ergonomics of the thermal environment — Analytical determination and interpretation of thermal comfort using calculation of the PMV and PPD indices and local thermal comfort criteria.* International Standard, International Standardisation Organisation, Geneva, Switzerland.

ITW Stuttgart (2003*) Prüfbericht Speicher zur Trinkwassererwärmung und Raumheizung incl. externe Wärmeübertrager*. Prüfbericht Nr.: 03ST091, Institut für Thermodynamik (ITW), Universität Stuttgart 09.10.2003

JAIN, S. et al. (1995). Evaluation of solid-desiccant-based evaporative cooling cycles for typical hot and humid climates. *International Journal of Refrigeration*, 18, pp. 287-296.

JOOS, A., SCHMITZ, G. and CASAS, W. (2008) Enhancement of a Modelica Model of a Desiccant Wheel. In: *Proceedings of the Modelica 2008*, March 2008, pp. 701-707.

JURINAK, J.-J. (1982) *Open cycle solid desiccant cooling*. Thesis (PhD), University of Wisconsin-Madison, USA.

KAELKE et al (2003) *Querschnittsauswertung "Solarunterstützte Klimatisierungsanlagen in Deutschland (QASUK)"*. Forschungsbericht FIA-Projekt Forschungs-Informations-Austausch. Fachinstitut Gebäude-Klima e.V., Bietigheim-Bissingen, Germany.

KIM, D.S. and FERREIRA, C.A.I. (2008) Solar refrigeration options – a state-of-the-art review. *International Journal of Refrigeration*, 31, pp. 3-15.

KLEIN, S.A. and REINDL, D.T. (2005) Solar refrigeration. *ASHRAE Journal,* 47, pp. 526–530.

KLEPPMANN, W. (2011) *Taschenbuch Versuchsplanung – Produkte und Prozesse optimieren*, 7th ed. Munich: Carl Hanser Verlag.

KOEPPEN W. (1923) Die Klimate der Erde. Berlin: Walter de Gruyter.

KELLER, L. (2009) *Leitfaden für Lüftungs- und Klimaanlagen.* Germany: Oldenbourg Industrieverlag GmbH.

KODAMA, A. and GOTO, M. and HIROSE, T. (2002) Solar Desiccant Cooling with Honeycomb Rotor Adsorber. In: *Proceedings of World Renewable Energy Congress VII*, *Cologne, Germany, June 2002.* Elsevier Science Ltd.

KOHLENBACH, P. et al. (2007) Performance Modelling of a Desiccant Cooling System. In: *Proceedings of the 2nd International Conference on Solar Air-Conditioning*. Tarragona, Spain. Regensburg, Germany: Ostbayerisches Technologie-Transfer-Institut, pp. 288-293.

KOHLENBACH, P. and JAKOB, U. (2014) *Solar Cooling: The Earthscan Expert Guide to Solar Cooling Systems*, 1st ed. London and New York: Routledge Chapman & Hall

LA, D. et al. (2010) Technical development of rotary desiccant dehumidification and air conditioning: a review. *Renewable and Sustainable Energy Reviews*, 14, pp.130–147.

LAVAN, Z. et al. (1923) Second Law Analysis of Desiccant Cooling Systems. Journal of Solar Energy Engineering, 104, pp. 229-236.

LOMBØRG, B. (2001) *The Skeptical Environmentalist: Measuring the Real State of the World*. Cambridge, United Kingdom: Cambridge University Press.

MADJID, M. (1996) *Beitrag zur modellbasierten Überwachung und Optimierung des Betriebes heiz- und raumlufttechnischer Anlagen*. Thesis (PhD). Universität Stuttgart.

MANDEGARI A.M. and PAHLAVANZADEH H. (2009) Performance assessment of hybrid desiccant cooling system at various climates. *Energy Efficiency*, 2 (2009), DOI.1007/s12053-009-9059-5

MARTIN, S. (1997) *Neuentwicklung eines Compilers für das Simulationssystem INSEL*. Thesis (Diplom), Universität Oldenburg.

MAVROUDAKI et al. (2002). The potential for solar powered single-stage desiccant cooling in Southern Europe. *Applied Thermal Engineering*, 22, pp. 1129-1140.

MCKNIGHT, T. L. and HESS, D., 2000. Climate Zones and Types. In: Physical Geography: A Landscape Appreciation. Upper Saddle River, NJ: Prentice Hall.

MENDES, J.F. and RODRIGUES, R. and PEREZ, I.V. (2009) Results of DEC Unit Assisted by Solar Energy in Lisbon. In: *Proceedings of the 3rd International Conference on Solar Air-Conditioning*, Palermo, Italy. Regensburg, Germany: Ostbayerisches Technologie-Transfer-Institut, pp. 527-532.

METEONORM 7.0 (2013) Global Meteorological Database. Bern, Switzerland: Meteotest

MITCHELL, J.W.; BECKMAN, W.A. and NELSON, J.S. (1978) Simulations of the performance of open cycle solar-desiccant systems. In: Proceedings of the 3rd workshop on the use of solar energy for the cooling of buildings, San Francisco, USA, February 1978, pp. 108-115

MÖCKEL, R. (2003) *Numerische und experimentelle Untersuchung an einer* sorptionsgestützten Klimaanlage. Thesis (PhD), TU Hamburg-Harburg.

MOLLIER, R. (1923) Ein neues Diagramm für Dampf-Luft-Gemische. In: ZVDI, 67(9), pp. 869-872.

MONTOGOMERY, D.C. (2009) *Design and Analysis of Experiments*. 7th ed. New Delhi: John Wiley & Sons (Asia) Pte Ltd.

MYERS, R.H., MONTGOMERY D.C. and ANDERSON-COOK C.M. (2009) *Response Surface Methodology*. 3rd ed. New Jersey. John Wiley & Sons Inc.

NELSON, J.S. et al. (1978) Simulations of the performance of open cycle desiccant systems using solar energy. *Solar Energy*, 21 (4), pp. 273-278.

NIA, F., VAN PAASSEN, D. and SAIDI, M. (2006) Modeling and simulation of desiccant wheel for air conditioning. *Energy and Buildings*, 38 (10), pp. 1230-1239.

NOCKE, B. et.al. (2008) Monitoring results of DEC system at DREAM - Feedback to the monitoring procedure for solar heating and cooling systems. Dipartimento delle Ricerche Energetiche ed Ambientali. Universitàdi Palermo.

OAK RIDGE NATIONAL LABORATORY (1992) An assessment of desiccant cooling and national dehumidification technology, Tennessee, edited by M. Marietta, for the U.S. Department of Energy Contract No. DE-AC05-840R21400 37831-6285

OLIVA, A., COSTA. M. and PEREZ, C.D. (1991) Numerical simulation of solar collectors: The effect of nonuniform and nonsteady state of the boundary conditions. *Solar Energy*, 47, (5), pp. 259-373.

VAN OORSCHOT, R. (2010) *Desiccant Evaporative Cooling - Optimal strategy for cooling in a Dutch climate*. Final Report, Eindhoven University of Technology, Netherlands, July 2010.

ORTH, D. and MARTENKA, M. (2005) Tagesgänge des Trinkwasserbedarfs - Messergebnisse für Hotels, Krankenhäuser und Wohnheime aus einem Forschungsvorhaben. *TAB Fachzeitschrift für Technische Gebäudeausrüstung*, 1 (2005), pp. 2-5.

OUAZIA et al. (2009) Desiccant-evaporative cooling system for residential buildings. In: *Proceedings of the 12th Canadian Conference on Building Science and Technology,* Montréal, Canada, May, 2009.

PANARAS, G. et al. (2010) Experimental validation of a simplified approach for a desiccant wheel model. *Energy and Buildings*, 42, pp. 1719-1725

PANARAS, G. et al. (2010a) Theoretical and experimental investigation of the performance of a desiccant air-conditioning system. *Renewable Energy*, 35, pp. 1368-1375

PANARAS, G. et al. (2011) Solid desiccant air-conditioning systems: Design parameters. Energy, 36, pp. 2399-2406.

PANARAS, G. et al. (2011a) Proposal of a control strategy for desiccant air-conditioning systems. Energy, 36, pp. 5666-5676.

PAPADOPOULUS, A.M., OXIZIDIS, S. and KYRIAKIS, N. (2003) Perspectives of solar cooling in view of the developments in the air-conditioning sector. *Renewable and Sustainable Energy Reviews,* 7, pp. 419–438.

PARMAR, H. et al. (2011) Desiccant Cooling System for Thermal Comfort: A Review. *International Journal of Engineering Science and Technology (IJEST)*. 3, 5, pp. 4218- 4227.

PEEL, M.C., FINLAYSON, B.L. and MCMAHON, T.A. (2007) Updated world map of the Köppen-Geiger climate classification. *Hydrology and Earth System Sciences,* 11, pp. 1633–1644.

PENNINGNTON, N.A. (1955) Humidity Changer for Air Conditioning. U.S. patent Number 2 700 537. January 1955.

PÉREZ-LOMBARD, L. et al. (2011) A review of HVAC systems requirements in buildings energy regulations. *Energy and Buildings*, 43 (2-3), pp. 255-268.

PESARAN, A.A. and NEYMARK, J. (1995) Potential of solar cooling systems for peak demand reduction. In: *National Renewable Energy Laboratory,* 1995.

PESARAN, A.A., PENNEY, T.R. and CZANDERNA, A.W. (1992) Desiccant Cooling: State-of-the-Art Assessment. Technical report, National Renewable Energy Laboratory. Report NREL/TP-254-4147.

PEUSER. F., REMMERS, K-H. and SCHNAUSS, M. (2001) Langzeiterfahrung Solarthermie. 1st ed. Berlin: Solarpraxis Supernova AG.

PFEIFFER, ST. (1986) *Sorptionsprozesse Klimatechnik*. Unpublished Technical Report. 22/1236, ILK Dresden.

PIETRUSCHKA, D. (2010) *Model Based Control Optimization of Renewable Energy Based HVAC System.* (PhD), Thesis (PhD), De Montfort University.

PIETRUSCHKA, D., EICKER, U. and HANBY, V. (2009) Primary energy optimized operation of solar driven desiccant evaporative cooling systems through innovative control strategies. In: *Proceedings of the 3rd International Conference on Solar Air-Conditioning*, Palermo, Italy, 2009, pp. 63-68.

PODESSER, E. and STIGLBRUNNER, R. (2000) Errichtung und Betrieb einer Desiccant- Klimaanlage zur Technologiedemonstration im Forschungshaus des ÖKOPARK Hartberg, Final Report, No. IEF-B-09/00, ÖKOPLAN, December 2000, Hartberg, Austria.

PREISLER, A. and SELKE; T. (2009) Experience report on two different solar driven air-conditioning systems in Vienna/ Austria based on monitoring data of summer 2008/2009, In: *Proceedings of the 3rd International Conference on Solar*

Air-Conditioning, Palermo, Italy. Regensburg, Germany: Ostbayerisches Technologie-Transfer-Institut, pp. 515-520.

PREISLER, A. and ZUCKER, G. (2013) Development of improved Desiccant Evaporative Cooling control system for full year operation including greenhouse buffer plants. In: *Proceedings of the 5th International Conference on Solar Air-Conditioning*, Bad Krozingen, Germany. Regensburg, Germany: Ostbayerisches Technologie-Transfer-Institut, pp. 305-510.

RACHMAN et al. (2011) Feasibility Study and Performance Analysis of Solar Assisted Desiccant Cooling Technology in Hot and Humid Climate. *American Journal of Environmental Sciences*, 7 (3) pp. 207-211.

RATHEY, A. (2000) *Entwicklung optimierter Regelverfahren für raumlufttechnische Anlagen mit Hilfe des Simulationssystems TRNSYS*. Thesis (PhD), Dresden University of Technology. Dresden, Germany, 2000.

RECKNAGEL H., SPRENGER, E. and SCHRAMEK, E-R. (2007) Taschenbuch für Heizung und Klimatechnik. 73rd ed. Munich: Oldenbourg Industrieverlag.

REITER, C. (2008) *Modellerstellung eines solarthermischen Flachkollektors in Matlab/Simulink – CARNOT Blocksatz*. Unpublished Thesis (Diplom). Ingolstadt University of Applied Sciences.

RUIVO, C.R. et al. (2007) Modelling the Behaviour of Desiccant Wheels. In: *Proceedings of the 2nd International Conference Solar Air-Conditioning*, Tarragona, Spain, October 2007. Regensburg, Germany: Ostbayrisches Technologie-Transfer-Institut, pp. 523-528.

SACE (2003) SACE Solar Cooling Light Computer Tool – Guidelines for Use [WWW] Fraunhofer Institute for Solar Energy Systems ISE. Available from: http://www.solair-project.eu/218.0.html [Accessed 10/11/13].

SAS (2010) Using JMP 9 [WWW] SAS Institute Inc., Cary, NC, USA. Available from: http://support.sas.com/documentation/onlinedoc/jmp/902/Using_JMP.pdf [Accessed 20/02/14].

SCHUMACHER, J. (2011) Fortran Source Code Humidifier Model Block EVCOOL. Doppelintegral. Stuttgart on 23rd March 2011.

SCHUMACHER, J., DUMINIL, E. and EICKER, U.(2012) Automatische Generierung von modularen dynamischen Gebäudemodellen. In: Proceedings of the Fourth German-Austrian IBPSA Conference, BauSIM 2012, Berlin. pp. 8-12.

SCHÜRGER, U. (2003) Teststand für Sorptionsrotoren – Erkenntnisse und Auswertungen. In: *Proceedings of the 13th Symposium Thermische Solar Energie*. Staffelstein, Germany. Regensburg, Germany: Ostbayerisches Technologie-Transfer-Institut, pp. 265-270.

SCHÜRGER, U. (2007). *Investigation into solar powered adsorption cooling systems – Adsorption technology and system analysis*. Thesis (PhD), De Montfort University Leicester, United Kingdom.

SCHWENK CH. (1999) *Sonne für Hotels - Planung von Kollektoranlagen zur Warmwasserbereitung für Beherbergungsbetriebe*, 1st ed. Gleisdorf: Verlag Arbeitsgemeinschaft Erneuerbare Energie AEE.

SHPILRAIN, E.E., POPEL, O.S. and FRID, S.E. (1989) *Mathematical models of solar energy conversion in flat solar collectors and solar ponds*. Institute for High Temperatures USSR, Academy of Sciences Moscow, USSR.

SIMONSON, C.J. and BESANT R.W. (1997) Heat and moisture transfer in desiccant coated rotary energy exchangers: Part I. Numerical model. *International Journal of HVAC Research*, 3, pp. 325-350.

SMITH, S.T. and HANBY, V.I. (2010) Probabilistic climate projections influencing future weather years for energy modelling. In: *Proceedings of the 8th European Conference of Applied Climatology.* Zurich, Switzerland.

SMITH, R.R., HWANG, C.C. and DOUGALL, R.S., (1994) Modeling of solar assisted desiccant air conditioner for a residential building. *Energy*, 19, pp. 679-691.

SOLAHART INDUSTRIES (2004) *Prüfbericht Bt Sonnenkollektor, Prüfbericht-Nr. 04COL339*, Prüflaboratorium TZS Stuttgart, Solahart Industries Pty Ltd.

SOLAIR (2009) Leitfaden – Anforderungen an Auslegung und Konfiguration kleiner und mittlerer Anlagen zur solaren Klimatisierung.

SPARBER, W. et al. (2008) Unified Monitoring Procedure and Performance Assessment for Solar Assisted Heating and Cooling Systems. In: *Proceedings of the Eurosun 2008 – 1st International Conference on Solar Heating, Cooling and Buildings*, Lisbon, Portugal, October 2008.

SIEBERTZ, K., VAN BEBBER, D. and HOCHKIRCHEN, TH. (2010) *Statistische Versuchsplanung - Design of Experiments (DoE)*. London: Springer

THÜR, A. and VUKITS, M. (2009) Solar Heating and Cooling – Town Hall Gleisdorf, In: *Proceedings of the 3rd International Conference on Solar Air-Conditioning*, Palermo, Italy. Regensburg, Germany: Ostbayerisches Technologie-Transfer-Institut, pp. 362-367.

TRINKL, C. et al. (2007) Solar Desiccant Air-Conditioning: Practical Experience Regarding Operation and Performance. In: *Proceedings of the 2nd International Conference Solar Air-Conditioning*, Tarragona, Spain, October 2007. Regensburg, Germany: Ostbayrisches Technologie-Transfer-Institut, pp. 656-661.

TROTTENBURG, U. (2008) *Design of Experiments – Seminar "Robust Design"* [WWW] University of Cologne. Available from: https://www.scai.fraunhofer.de/fileadmin/ArbeitsgruppeTrottenberg/WS0809/seminar/Kapitza.pdf [Accessed 10/09/13].

VDI 2067 (2003) *Economic efficiency of building installation – HVAC systems*. Düsseldorf, Germany: VDI-Verlag GmbH

VDI 2071 (1997) *Heat recovery in heating, ventilation and air conditioning plants*. Berlin, Germany: Beuth Verlag GmbH, 1997.

VDI 2078 (2012) *Calculation of cooling load and room temperatures of rooms and buildings – VDI Cooling Load Code of Practice*. Berlin, Germany: Beuth Verlag GmbH, March 2012.

VDI 2620 (1973) *Fortpflanzung von Fehlergrenzen bei Messungen – Grundlagen*. Düsseldorf, Germany: VDI-Verlag GmbH

VDI 3525 (2007) *Regelung und Steuerung von Raumlufttechnischen Anlagen*. Düsseldorf, Germany: VDI-Verlag GmbH

VDI 3803-3 (2014) *Air-conditioning – System requirements – Central air humidification systems (VDI Ventilation Code of Practice).* Berlin, Germany: Beuth Verlag GmbH, 2014.

VDI 6002 (2014) Solar heating for potable water – Basic principles. Berlin, Germany: Beuth Verlag GmbH, 2014.

VITTE, TH. et al. (2007) Hybrid Control Strategy for Solar Desiccant Cooling System. In: *Proceedings of the 2nd International Conference Solar Air-Conditioning*, Tarragona, Spain, October 2007. Regensburg, Germany: Ostbayrisches Technologie-Transfer-Institut pp. 258-264.

VOSS, K. et al. (2005) Bürogebäude mit Zukunft – Konzepte, Analysen, Erfahrungen. Cologne, Germany: TÜV-Verlag.

VUKITS, M., ALTENBURGER, F. and THÜR, A. (2011) Operation and energy performance as well as simulation results of two solar cooling plants in Gleisdorf. In: *Proceedings of the 4th International Conference Solar Air-Conditioning*, Larnaca, Cyprus, October 2011. Regensburg, Germany: Ostbayrisches Technologie-Transfer-Institut pp. 335-340.

WANG, R.Z. et al. (2009), Solar sorption cooling systems for residential applications: Options and guidelines. *International Journal of Refrigeration.* 30, pp. 1–23.

WEINELT, H. (2013) Wer fragt gewinnt – Warum Platons Dialektik notwendiger den je ist. *Abenteuer Philosophie – Philoscience*, October 2013, 134, pp. 12-15.

WHITE, S. and GOLDSWORTHY, M. (2013) Exploitation in an unfair world: Finding attractive markets for solar cooling. In: *Proceedings of the 5th International Conference on Solar Air-Conditioning*, Bad Krozingen, Germany. Regensburg, Germany: Ostbayerisches Technologie-Transfer-Institut, pp. 19-24.

WIEMKEN E. and PETRY E.A.R (2013) *Solarthermie 2000plus: Wissenschaftliche Programmbegleitung und Begleitforschung "Solarthermische Gebäudeklimatisierung"*, Abschlussbericht, Förderkennzeichen 0329605A [WWW] Fraunhofer Ínstitut für Solare Energiesysteme ISE, Freiburg Germany. Available from: www.solare-kuehlung.info/Projekte/Projekte/ 0329605A_Schlussbericht_oeffentlichST2000plus_05022013.pdf [Accessed 10/06/13].

WIEMKEN, E. et al. (2008) Planungsleitfaden Solare Kühlung.- Solarthermische Anlagen zur Raumkühlung in Einzelgebäuden bzw. Gebäudegruppen. Abschlussbericht Solarthermie 2000plus. Freiburg. Germany

WOLF, D., KUDISH, I. and SEMBIRA, N. (1981) Dynamic simulation and parametric sensitivity studies on a flat-plate solar collector. *Energy*, 6, pp. 333-349.

WOLF ANLAGEN-TECHNIK (2005): Data Sheet DEC-Anlage Typ DEC 101, Product Description Service Center GVZ, Building J.

WROBEL, J, Walter, P.S. and SCHMITZ, G. (2013) Performance of a solar assisted air conditioning system at different locations. *Solar Energy*, 92 (2013), pp. 69-83.

WURTZ et al. (2005) Parametric analysis of a solar desiccant cooling system using the SIMSPARK environment. In: *Proceedings of the 9th International IBPSA Conference,* Montréal, Canada, August, 2005.

ZHANG, X.J., DAI, Y.J. and WANG, R.Z. (2003) A simulation study of heat and mass transfer in a honeycomb rotary desiccant cooling. *Applied Thermal Engineering*, 23, pp. 989-1003.

ZHENG, W. and WOREK, W.M. (1993) Numerical simulation of combined heat and mass transfer processes in a rotary dehumidifier. *Numerical Heat Transfer*, A 23, pp. 211–232.

Appendix A:
Addendum Multivalent System Simulation Model

This section complements descriptions and equations with regard to the multivalent system simulation model presented in chapter 3.

A1. Desiccant Wheel Model (section 3.3.1)

The specific enthalpy of the supply air h_{sup} is calculated with the empirical Eqs. (A.1) to (A.3) as established by Glück (1991).

$$h_{sup} = h_{sup,dry} + x_{sup} * h_{w,V} = \left(c_{p,G} + x_{sup} * c_{p,V}\right) * T_{sup} + x_{sup} * h_V(T) \quad \text{(A.1)}$$

$$h_V(T) = h_{S,air}(T) + h_{E,air}(T) \quad \text{(A.2)}$$

$$h_{S,air}(T) = a + b * T + c * T^2 + d * T^3 \quad \text{(A.3)}$$

$$a = 2.501482 * 10^6 \ \frac{J}{kg} \qquad b = 1.789736 * 10^3 \ \frac{J}{°Ckg}$$
$$c = 8.957546 * 10^{-1} \ \frac{J}{°C^2kg} \quad d = -1.300254 * 10^{-2} \ \frac{J}{°C^3kg}$$

$$h_{E,air}(T) = A + B * T + C * T^2 + D * T^3 \quad \text{(A.4)}$$

$$A = 9.38 * 10^2 \ \frac{J}{kg} \quad B = 4.204902 * 10^3 \ \frac{J}{°Ckg}$$
$$C = -5.942827 * 10^{-1} \ \frac{J}{°C^2kg} \quad D = 4.310326 * 10^{-3} \ \frac{J}{°C^3kg}$$

where,

h_{sup}	specific enthalpy supply air [J kg^{-1}]
$h_{sup,dry}$	specific enthalpy of dry supply air [J kg^{-1}]
$h_{w,V}$	specific enthalpy of water vapor [J kg^{-1}]
$h_V(T)$	specific enthalpy of evaporation heat [J kg^{-1}]
$h_{S,air}(T)$:	specific enthalpy of saturated air [J kg^{-1}]
$h_{E,air}(T)$:	specific enthalpy of air in boiling state [J kg^{-1}]
x_{sup}:	absolute supply air humidity [kg kg^{-1}]
T_{sup}:	supply air temperature [°C]
$c_{p,G}$, $c_{p,V}$:	specific heat capacities of dry air and water [J kg^{-1}K^{-1}]

The supply air temperature and absolute humidity downstream the desiccant is analytically calculated with Eq. (A1) using an iterative method (regula falsi). This iterative calculation is continued until the value of the relative supply air humidity is equal to the relative humidity of regeneration air, whereas the supply air enthalpy is kept constant.

A2. Solar Thermal Collector Model (section 3.5.1)

The applied solar thermal collector model simulates a solar thermal flat plate collector array with the basic collector equation given by ISO 9806-1 (1994, Eq. A5). The model is based on Doppelintegral (2010) and does not include the thermal collector capacity.

$$\eta_{col} = \eta_0 - U_{eff,1} * \frac{T'_m - T'_{amb}}{G} - U_{eff,2} * \frac{(T'_m - T'_{amb})^2}{G} \qquad (A.5)$$

where,

η_{col}	Collector efficiency [-]
η_0	Optical efficiency [-]
T'_m	Average temperature collector fluid [°C]
T'_{amb}	Ambient temperature [°C]
G	Irradiation in collector plane [W m^{-2}]
$U_{eff,1}$	Linear heat loss coefficient [W m^{-2}K^{-1}]
$U_{eff,2}$	Quadratic heat loss coefficient [W m^{-2}K^{-2}]

Thereby, the average temperature of the collector fluid T'_m is determined to a good approximation with the arithmetic mean of the collector return temperature T'_{in} and flow temperature T'_{out}.

$$T'_m = \frac{T'_{in} + T'_{out}}{2} \qquad (A.6)$$

The available power of the collector $\dot{Q}_{use}$ results from Eq. (A.7).

$$\dot{Q}_{use} = \eta_{col} * G * A = \dot{m}_{WG} * c_{WG(T)} * (T'_{out} - T'_{in}) \qquad (A.7)$$

where,

A:	Absorber area [m²]
$\dot{m}_{WG}$:	Mass flow rate collector fluid [kg s^{-1}]

$c_{WG(T)}$: Specific heat capacity of collector fluid [J (kg^{-1}K^{-1})]

In case $U_{eff,2} = 0$ the flow temperature results in

$$T'_{out} = \frac{\eta_0 * G + \frac{T'_{in} * \dot{m}_{WG} * c_{WG(T)}}{A} - \frac{U_{eff,1} * T'_{in}}{2} + U_{eff,1} * T'_{amb}}{\frac{\dot{m}_{WG} * c_{WG(T)}}{A} + \frac{U_{eff,1}}{2}} \quad (A.8)$$

Thereby, T'_{out} can maximally attain the value of the stagnation temperature $T'_{\max}$.

$$T'_{\max} = \frac{\eta_0 * G - \frac{U_{eff,1} * T'_{in}}{2} + U_{eff,1} * T'_{amb}}{U_{eff,1}} \quad (A.9)$$

Taking into account optical losses due to radiation ($U_{eff,2} \neq 0$), the flow temperature T'_{out} is the positive solution of the quadratic Eq. (A.10).

$$T'_{out,1/2} = -\frac{a}{2} \pm \sqrt{\left(\frac{a}{2}\right)^2 - b} \quad (A.10)$$

where,

$$a = \frac{2 * U_{eff,1}}{U_{eff,2}} + \frac{2 * \dot{m}_{WG} * c_{WG(T)}}{A * U_{eff,2}} + 2 * T'_{in} - 4 * T'_{amb}$$

$$b = \left(\frac{2 * U_{eff,1}}{U_{eff,2}} - \frac{4 * \dot{m}_{WG} * c_{WG(T)}}{A * U_{eff,2}} + T'_{in} - 4 * T'_{amb}\right) * T'_{in} - 4 * \left(\frac{\eta_0 * G}{U_{eff,2}} + \frac{U_{eff,1} * T'_{amb}}{U_{eff,2}} + {T'_{amb}}^2\right)$$

In addition to the input variables return temperature T'_{in}, collector mass flow $\dot{m}_{WG}$, global radiation on the inclined collector plane G and the ambient temperature T'_{amb}, the parameters absorber area A, specific heat capacity of the collector fluid $c_{WG(T)}$ as well as the efficiency values η_0, $U_{eff,1}$, $U_{eff,2}$ and the

number of serial and parallel connected collectors are considered by the model calculating T'_{out}.

In addition to the collector inlet temperature, the model provides the outputs $\dot{Q}_{use}$, η_{col} and the overall heat loss coefficient U_{loss}.according to Eq. (A.11)

$$U_{loss} = U_{eff,1} + U_{eff,2} * (T'_m - T'_{amb}) \quad \text{(A.11)}$$

A3. Stratified Storage Model (section 3.5.3)

The applied stratified storage model by Eicker (2001) is principally based on Eq. (A.12) calculating the simple energy balance in homogenously mixed tanks.

$$mc\frac{dT_s}{dt} = \dot{Q}_{col} - \dot{Q}_{load} - UA(T_s - T_{amb}) \tag{A.12}$$

where,

m	Mass storage content [kg]
c	Specific heat capacity fluid [J kg^{-1}K^{-1}]
T_s	Storage temperature [K]
$\dot{Q}_{col}$	Charged heat quantity by solar collector [J s^{-1}]
$\dot{Q}_{load}$	Discharged thermal load [J s^{-1}]
U	Heat loss coefficient [W m^{-2}K^{-1}]
A	Storage surface [m^2]
T_{amb}	Ambient temperature [°C]

With defined modes for the operation of the collector circuit θ_{col} (0,1) and for the storage discharge in the load circuit θ_{load} (0,1) the energy balance ensues as a function of the collector arrays flow temperature $T_{col,fl}$, the return temperature of the load $T_{load,ret}$ and the storage temperature T_s.

In a fully homogeneously mixed storage T_s can be regarded as withdrawal temperature for both circuits. The solution of the differential equation (Eq. A.13) determining T_s at time step $(n+1)$ results from forward differentiation of the values of the previous time step n.

$$T_{s,n+1} = T_{s,n} + \frac{\Delta t}{(mc_p)_s}\left[\theta_{col}(\dot{m}c)_{col}\left(T_{col,fl,n} - T_{s,n}\right) - \theta_l(\dot{m}c)_{load}\left(T_s - T_{l,ret}\right) - UA\left(T_{s,n} - T_{amb,n}\right)\right] \tag{A.13}$$

Attaining a realistic simulation of the solar system operation the storage model is divided into different layers. According to Eicker (2012), an energy balance is

conducted for each layer, whereas each layer reproduces the complete state of a storage unit without stratification.

Convection and conduction of a layer i with its neighboring layers $i-1$ and $i+1$ are included in the model calculation with the respective exchange of the heat quantity $\dot{Q}_f$. For this purpose the heat exchange $\dot{Q}_f$ is reproduced in a simplified way with the effective vertical heat conductivity λ_{eff} (Eq. A.14).

$$\dot{Q}_f = \dot{Q}_{f,i-1\rightarrow i} - \dot{Q}_{f,i\rightarrow i+1} = A_s \frac{\lambda_{eff}}{z}(T_{s,i+1} - 2T_{s,i} + T_{s,i+1}) \quad \text{(A.14)}$$

where,

λ_{eff}	Effective vertical heat conductivity [W m^{-1}K^{-1}]
z	Layer height z [m]
A_s	Cross-sectional area storage [m^2]

In addition to heat conduction and free convection heat quantities $\dot{Q}_e$ are exchanged between the layers by enforced convection. Eq. (A.15) applies for layers without external connections.

$$\dot{Q}_e = (\dot{m}c)_i\,(T_{i-1} - T_{i+1}) \quad \text{(A.15)}$$

Taking into account external heat flows for layers with connection the total balance of a storage layer is obtained by Eq. (A.16).

$$mc\frac{dT_{s,i}}{dt} = \dot{Q}_{col,i} - \dot{Q}_{load,i} - UA_i\left(T_{s,i} - T_{amb}\right) + \dot{Q}_{f,i-1,i+1} + \dot{Q}_{e,i-1,i+1} \quad \text{(A.16)}$$

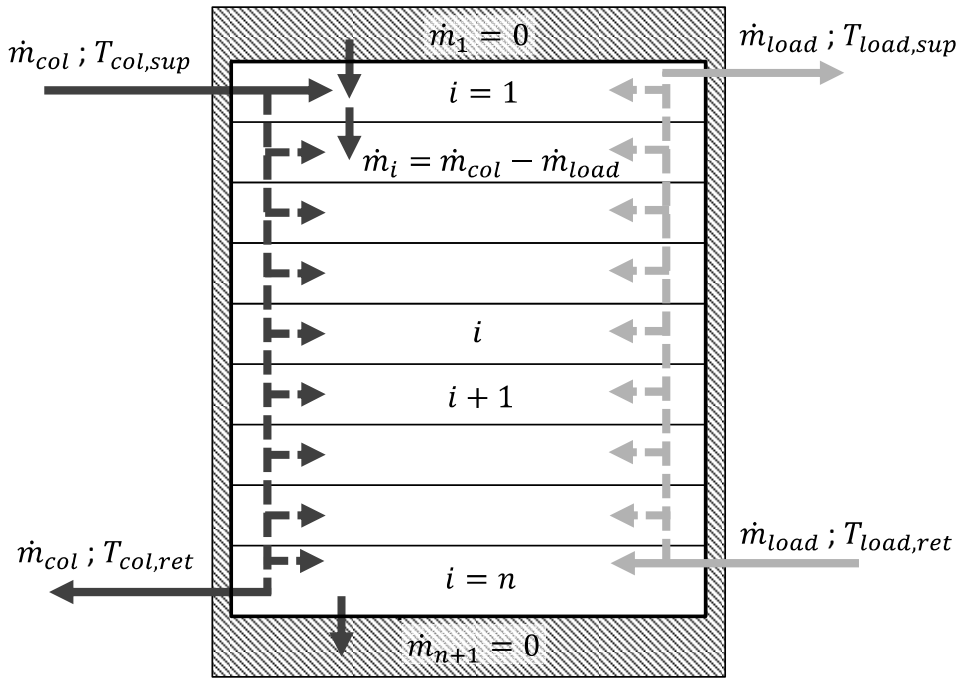

Figure A.1: Stratified storage model with n layers (cf. Doppelintegral 2010)

As illustrated in Figure A.1, the model considers two storage connections for the collector circuit with mass flow $\dot{m}_{col}$ and two connections for the load circuit with mass flow $\dot{m}_{load}$ in opposite flow direction. The storage flow into the load circuit ($\dot{m}_{load}, \dot{T}_{load,sup}$) exits in the upper storage layers, the return in the collector circuit ($\dot{m}_{col}, \dot{T}_{col,ret}$) is connected at the storage bottom.

The effective mass flow between the layers $\dot{m}_i$ is calculated as the difference of the two mass flows $\dot{m}_{col}$ and $\dot{m}_{load}$. With $\delta_i^+ = 1$ indicating a heat input from layer $i-1$ into layer i with mass flow m_i and and $\delta_i^- = 1$ indicating a negative effective mass flow from layer $i+1$ into layer i (cooling of the layer due to load surplus) the energy balance in temperature node i results in Eq. (A.17, Eicker 2012).

$$(m_i c)_s \frac{dT_{s,i}}{dt} = \delta_i^{col}(\dot{m}c)_{col}\left(T_{col,ret} - T_{s,i}\right) - \delta_i^{l}(\dot{m}c)_{load}\left(T_{s,i} - T_{load,ret}\right) \quad \text{(A.11)}$$
$$-UA_i\left(T_{s,i} - T_{amb}\right) + \delta_i^{+}\dot{m}_i c\left(T_{s,i-1} - T_{s,i}\right)$$
$$+\delta_i^{-}\dot{m}_{i+1} c\left(T_{s,i} - T_{s,i+1}\right) - A_s \frac{\lambda_{eff}}{z}\left(T_{s,i} - T_{s,i-1}\right)$$

where,

A_i = Outer storage surface of a particular node [m^2]

δ_i^{col} = $\begin{matrix} 1 & \text{for} & i = 1 \\ 0 & \text{for} & i \neq 1 \end{matrix}$ Collector supply in top layer

δ_i^{load} = $\begin{matrix} 1 & \text{for} & i = N \\ 0 & \text{for} & i \neq N \end{matrix}$ Load return in bottom layer

δ_i^{+} = $\begin{matrix} 1 & \text{for} & \dot{m}_i > 0 \\ 0 & \text{for} & \dot{m}_i \leq 0 \end{matrix}$ Heat input from layer $i-1$ into layer i

δ_i^{-} = $\begin{matrix} 1 & \text{for} & \dot{m}_i < 0 \\ 0 & \text{for} & \dot{m}_i \geq 0 \end{matrix}$ Heat input from layer $i+1$ into layer i

A4. Thermal and Latent Room Model and Load (section 3.7)

The static humidity model according to Pietruschka (2010) calculates the average absolute room air humidity x_{room} from the latent internal loads as well as the humidity input due to ventilation and infiltration (Eq. A.18).

Hence, according to VDI 2067 (2003) sheet 11 a release of water vapor $\dot{m}_V$ amounting to 50 g h^{-1} per person is considered for the latent human heat input into the room assuming light physical activity (activity grade I to II) according to DIN 1946-2. Thereby, the model considers no capacitive storage of moisture in the spatial structure such as in furniture.

$$x_{room} = x_{ret} = \frac{x_{sup} \cdot \dot{V}_{sup} \cdot \rho_{air} + \dot{m}_V \cdot n_{pers}}{\dot{V}_{sup} \cdot \rho_{air}} \quad \text{(A.18)}$$

where,

x_{room}	absolute humidity room air [g kg^{-1}]
x_{ret}	absolute humidity return air [g kg^{-1}]
$\dot{V}_{sup}$	volume flow supply air [m^3 h^{-1}]
ρ_{air}	density of air [kg m^3]
n_{pers}	room occupancy [-]

Based on the absolute room air humidity the relative humidity is determined with state equation according to Glück (1991).

$$\varphi_{room} = \varphi_{ret} = \frac{x_{room}}{x_{room} + 0.622} \cdot \frac{p}{p_{sat}(T_{room})} \quad \text{(A.19)}$$

$$p_{sat}(T) = 611\ Pa \cdot exp \begin{Bmatrix} a + b \cdot T_{room} + c \cdot T_{room} \\ + d \cdot {T_{room}}^3 + e \cdot {T_{room}}^4 \end{Bmatrix} \quad \text{(A.20)}$$

$$a = -1.91275 * 10^{-4};\ b = 7.258 * 10^{-2}\ \frac{1}{°C};\ c = -2.939 * 10^{-4}\ \frac{1}{°C^2};$$

$$d = 9.841 * 10^{-7}\ \frac{1}{°C^3};\ e = -1.920 * 10^{-9}\ \frac{1}{°C^4}$$

where,

p_{sat} saturation vapour pessure of humid air [Pa]
p nominal pressure [Pa]
φ_{room} relative humidity room air [%]
φ_{ret} relative humidity return air [%]
(scope of application 0.01 °C ≤ T_{room} < 100 °C)

Appendix B:
Flowchart Developed DEC-Control Strategy

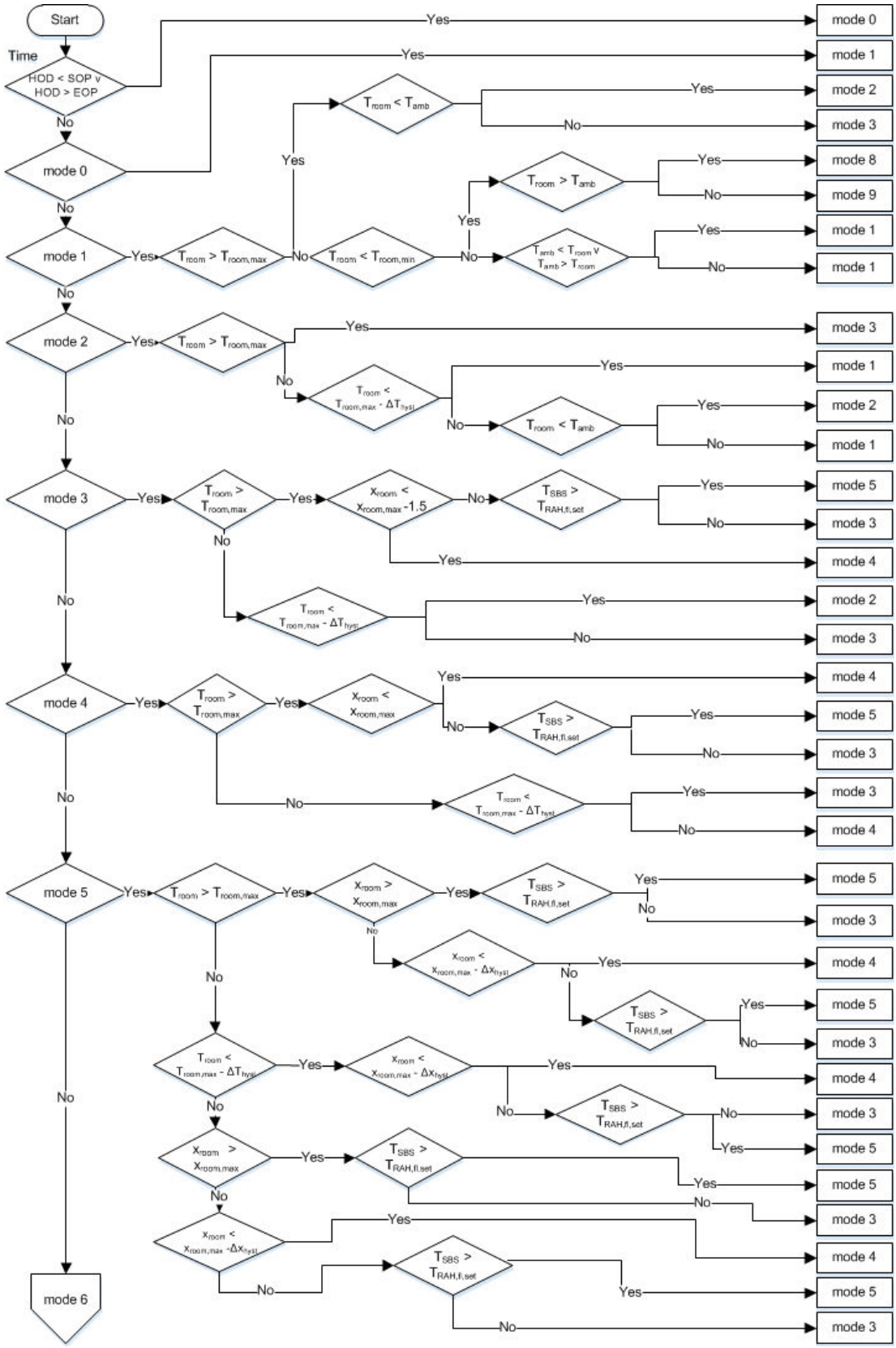

Figure B.1: Flowchart Developed DEC-Control Strategy (part 1)

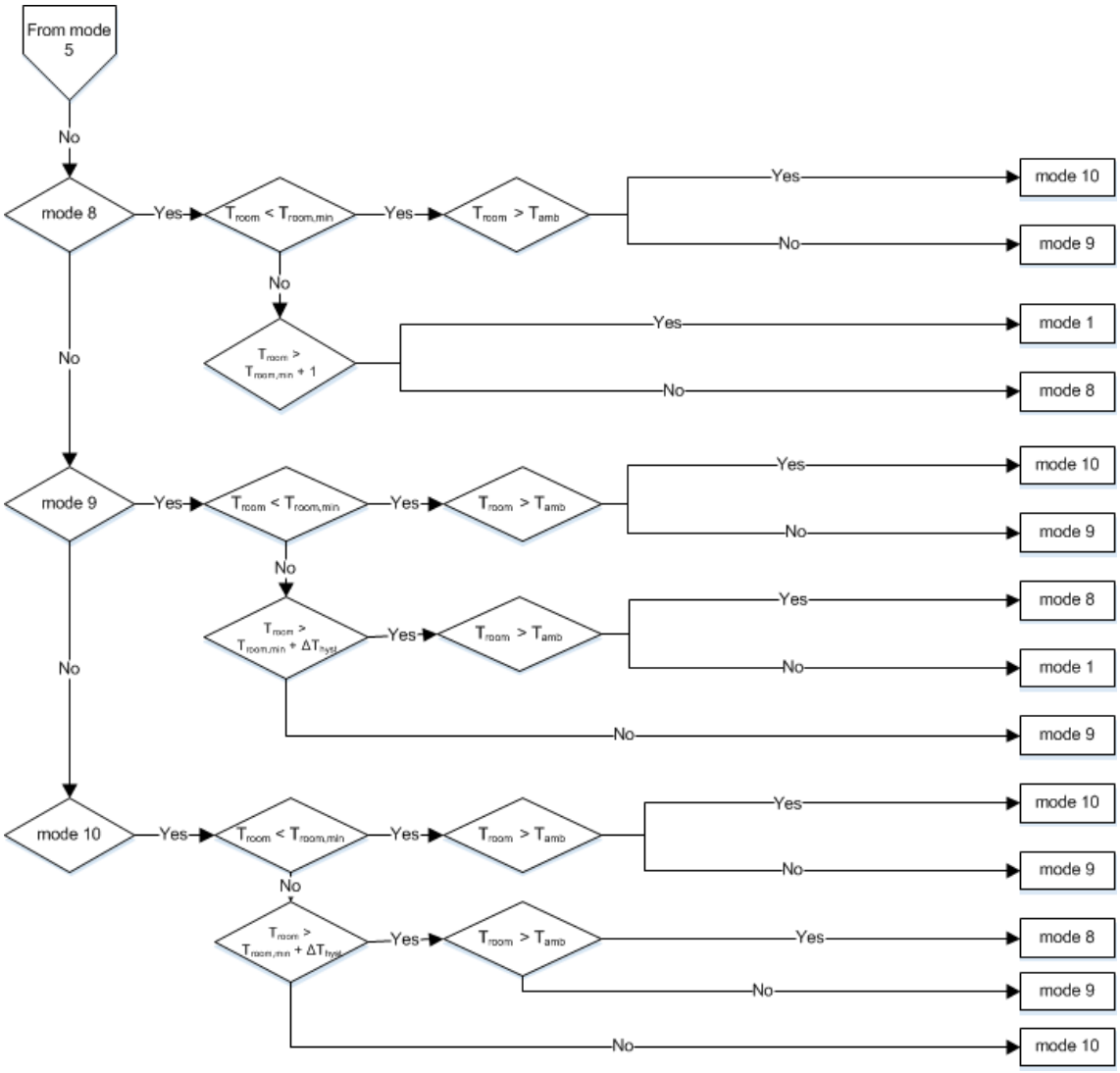

Figure B.2: Flowchart Developed DEC-Control Strategy (part 2)

Appendix C:
Overview Multivalent System Model in INSEL 8

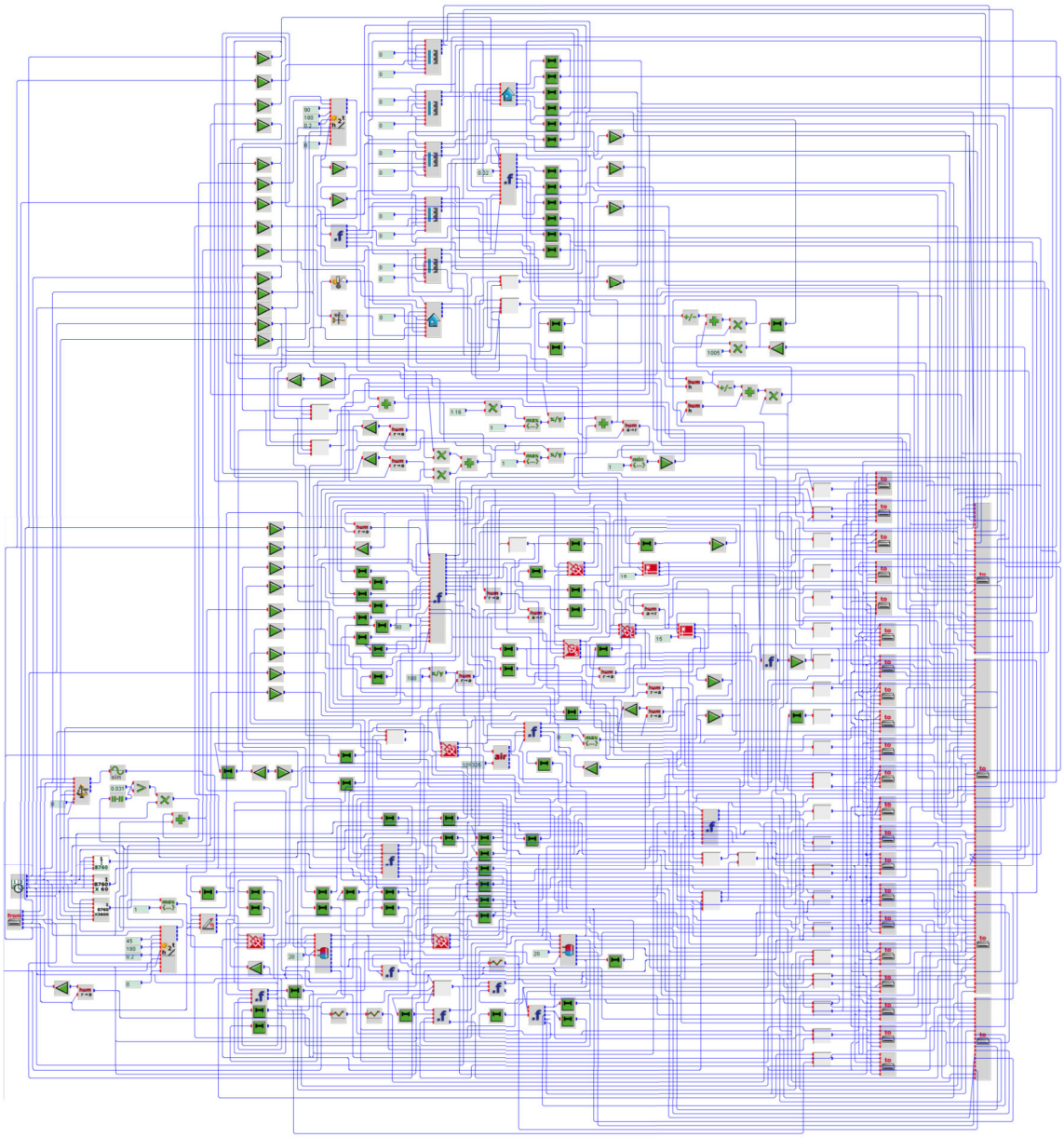

Figure C.1: Screenshot overall multivalent system model in INSEL 8

Appendix D:
Legend to Köppen Classification Climate Abbreviations

The Köppen classification recognises five major climate types based on the annual and monthly averages of temperature and precipitation, being linked with the particular air humidity level (Köppen 1923). Each type of climate is designated by a capital letter, as presented in Table D.1.

Table D.1: Köppen code first letter (Peel et al. 2007)

Code	Type	Description
A	Tropical climate	Monthly average temperature over 18°C; no winter season; strong annual precipitations (higher than evaporation)
B	Dry climate	Annual evaporation higher than precipitations; no permanent rivers
C	Temperate climate	Three coldest months average temperatures between -3°C and 18°C; hottest month average temperature over 10°C; summer and winter seasons well defined
D	Continental climate	Coldest month average temperature below 3°C; hottest month average temperature over 10°C; summer and winter seasons well defined
E	Polar climate	Average temperatures below 10°C in all twelve months of the year

Further subgroups are designated by a second letter distinguishing specific seasonal characteristics of temperature and precipitation (Table D.2)

Table D.2: Köppen code first letter (Peel et al. 2007)

Code	Applies to	Description
S	B	Semi-arid climate
W	B	Arid climate
f	A, C, D	Wet climate; precipitations occur every month of the year; no dry season
w	A, C, D	Dry season in winter
s	C	Dry season in summer
m	A	Monsoon climate; annual precipitations over 1500 mm; driest month precipitations below 60 mm
T	E	Hottest month average temperature between 0°C and 10°C
F	E	Hottest month average temperature below 0°C

A third letter allows refining a climate type with regard to occurring temperature variations (Table D.3).

Table D.3: Köppen code third letter (Peel et al. 2007)

Code	Applies to	Type	Description
a	C, D	Hot summer	Hottest month average temperature over 22°C
b	C, D	Moderate summer	Hottest month average temperature below 22°C; 4 hottest months average temperatures over 10°C
c	C, D	Short and cold summer	Hottest month average temperature below 22°C; monthly average temperatures over 10°C for less than 4 months; coldest month average temperature over -38°C
d	D	Very cold winter	Average temperature of the coldest month below 38°C
h	B	Dry and heat	Annual average temperature over 18°C
k	B	Dry and cold	Annual average temperature below 18°C

Appendix E:
Global Meteorological Technology Analysis – Results Overview

Singapore (Singapore, tropical rainforest climate Af)

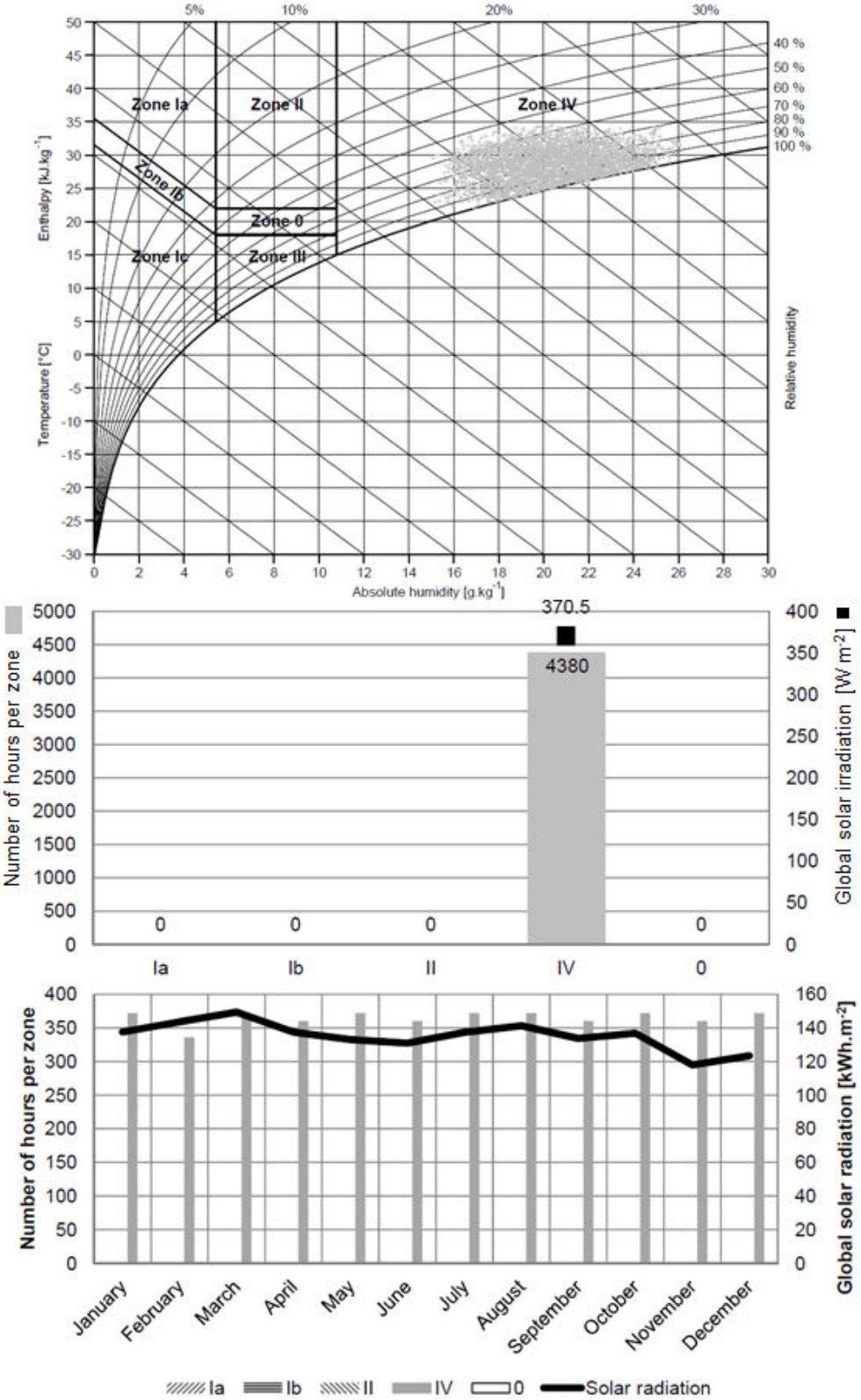

Figure E.1: Zoned meteorological ambient air conditions and expected global solar irradiation in climate Af (Singapore, Singapore)

Miami (USA, tropical monsoon climate Am)

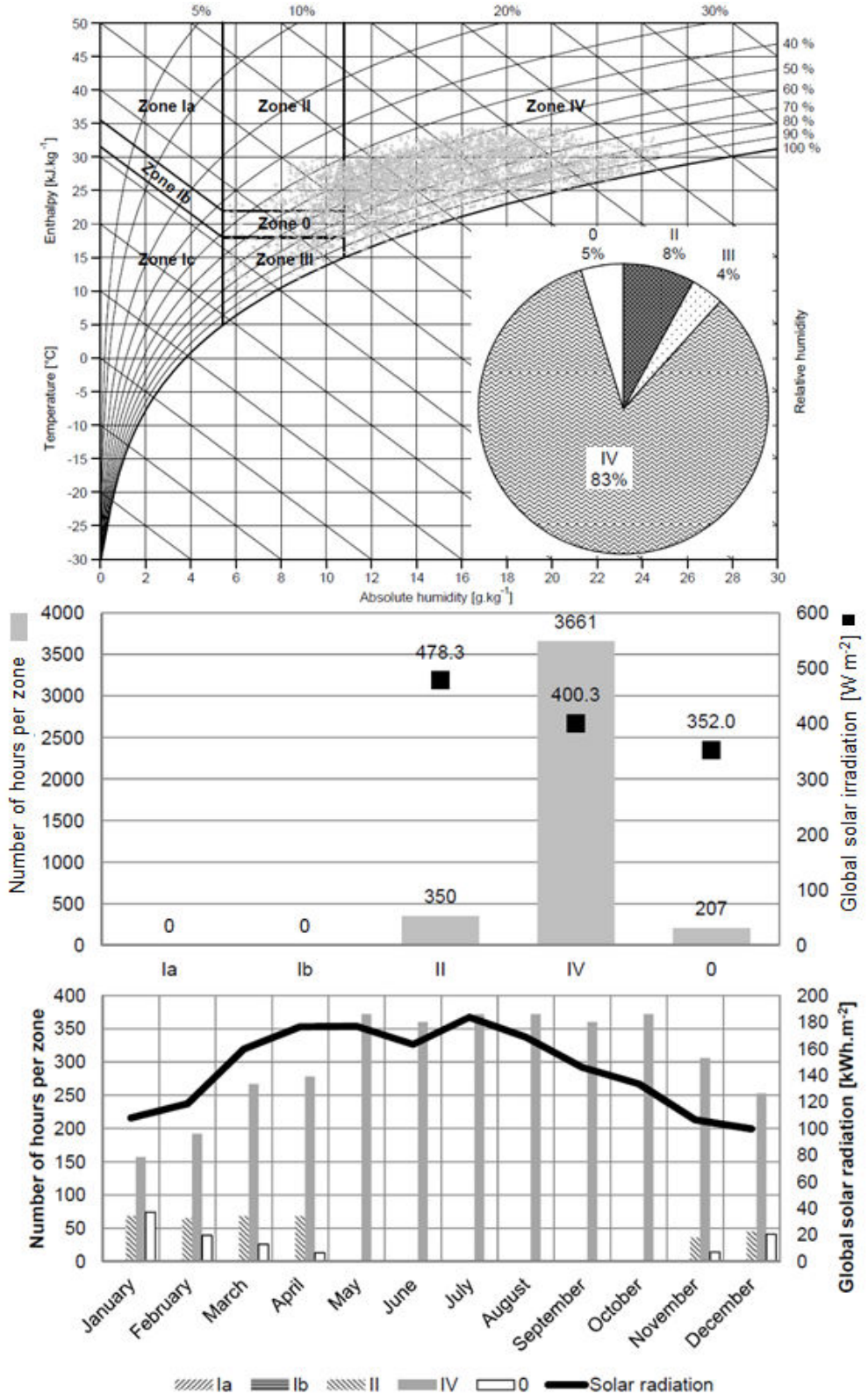

Figure E.2: Zoned meteorological ambient air conditions and expected global solar irradiation in climate Am (Miami, USA)

Mumbai (India, tropical savannah climate Aw)

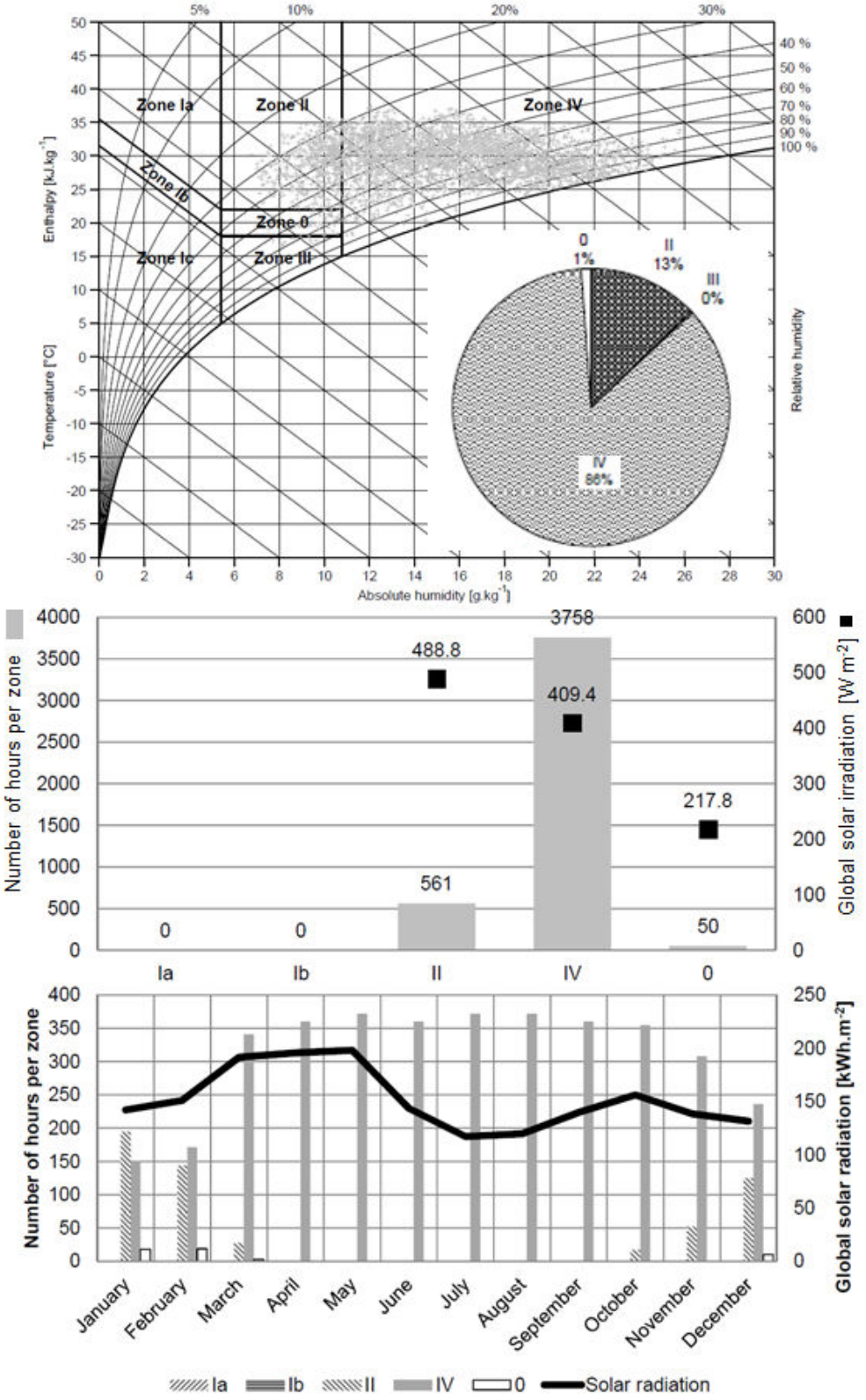

Figure E.3: Zoned meteorological ambient air conditions and expected global solar irradiation in climate Aw (Mumbai, India)

Maun (Botswana, hot semi-arid climate BSh)

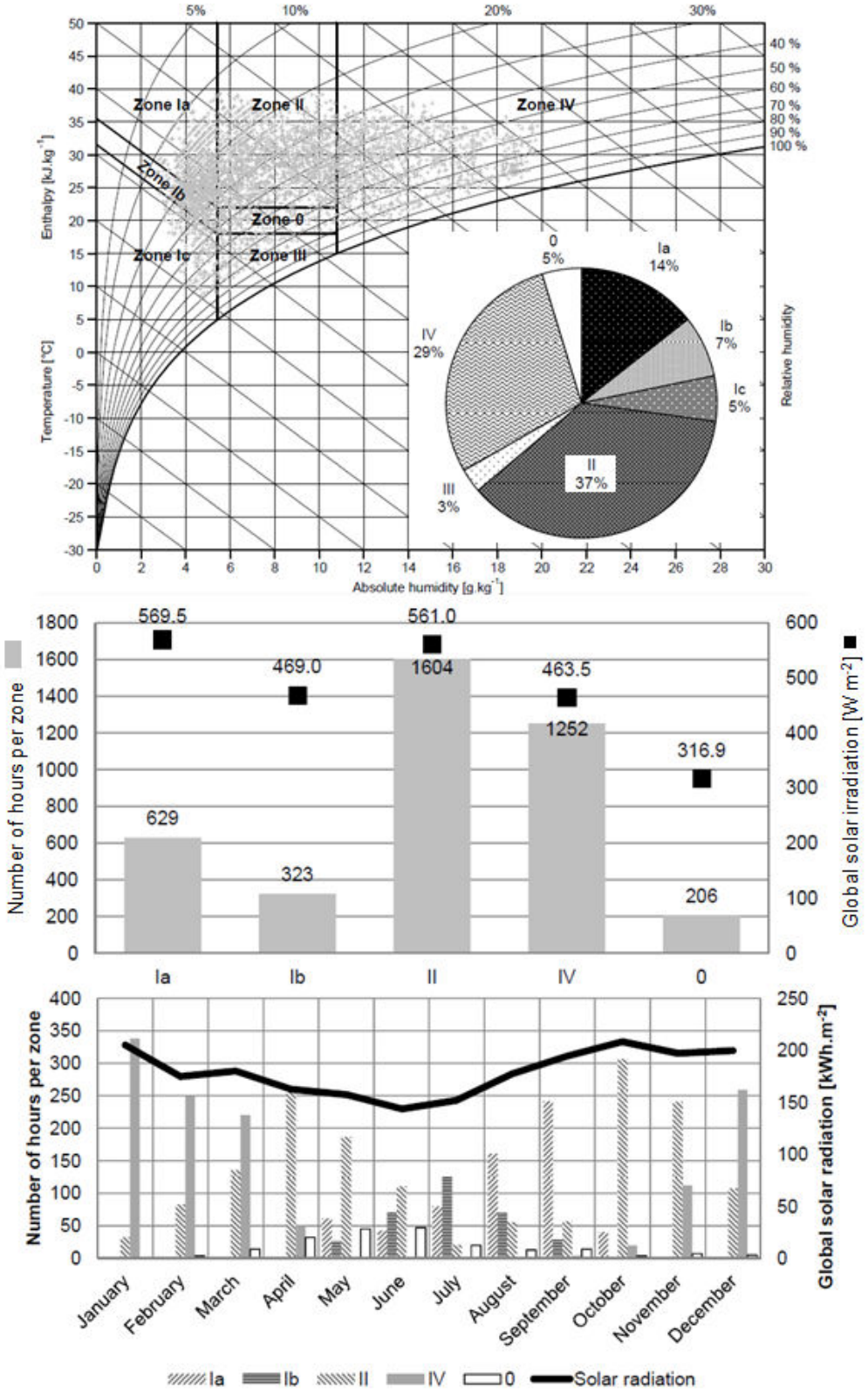

Figure E.4: Zoned meteorological ambient air conditions and expected global solar irradiation in climate BSh (Maun, Botswana)

Denver (USA, cold semi-arid climate BSk)

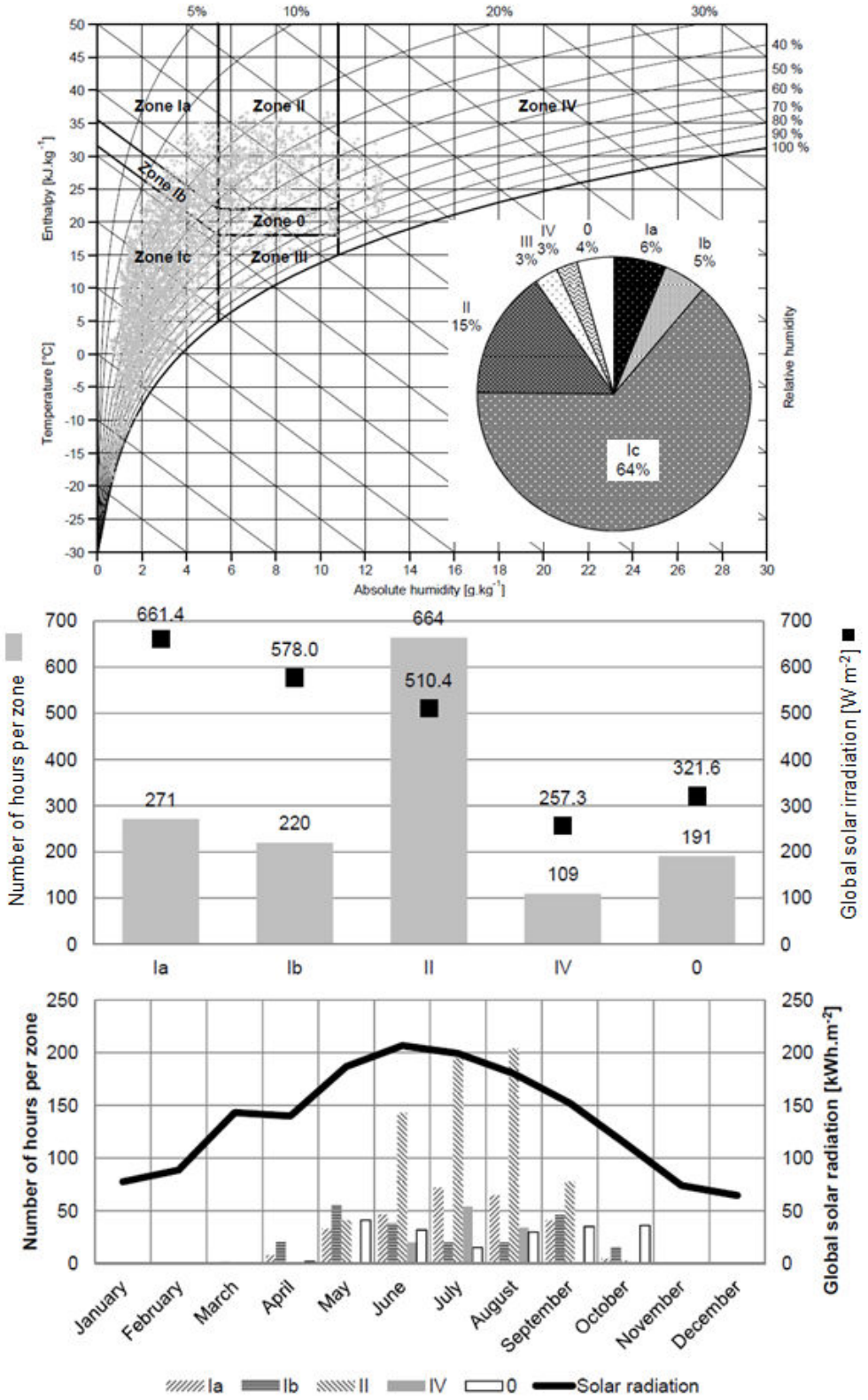

Figure E.5: Zoned meteorological ambient air conditions and expected global solar irradiation in climate BSk (Denver, USA)

Cairo (Egypt, hot arid climate BWh)

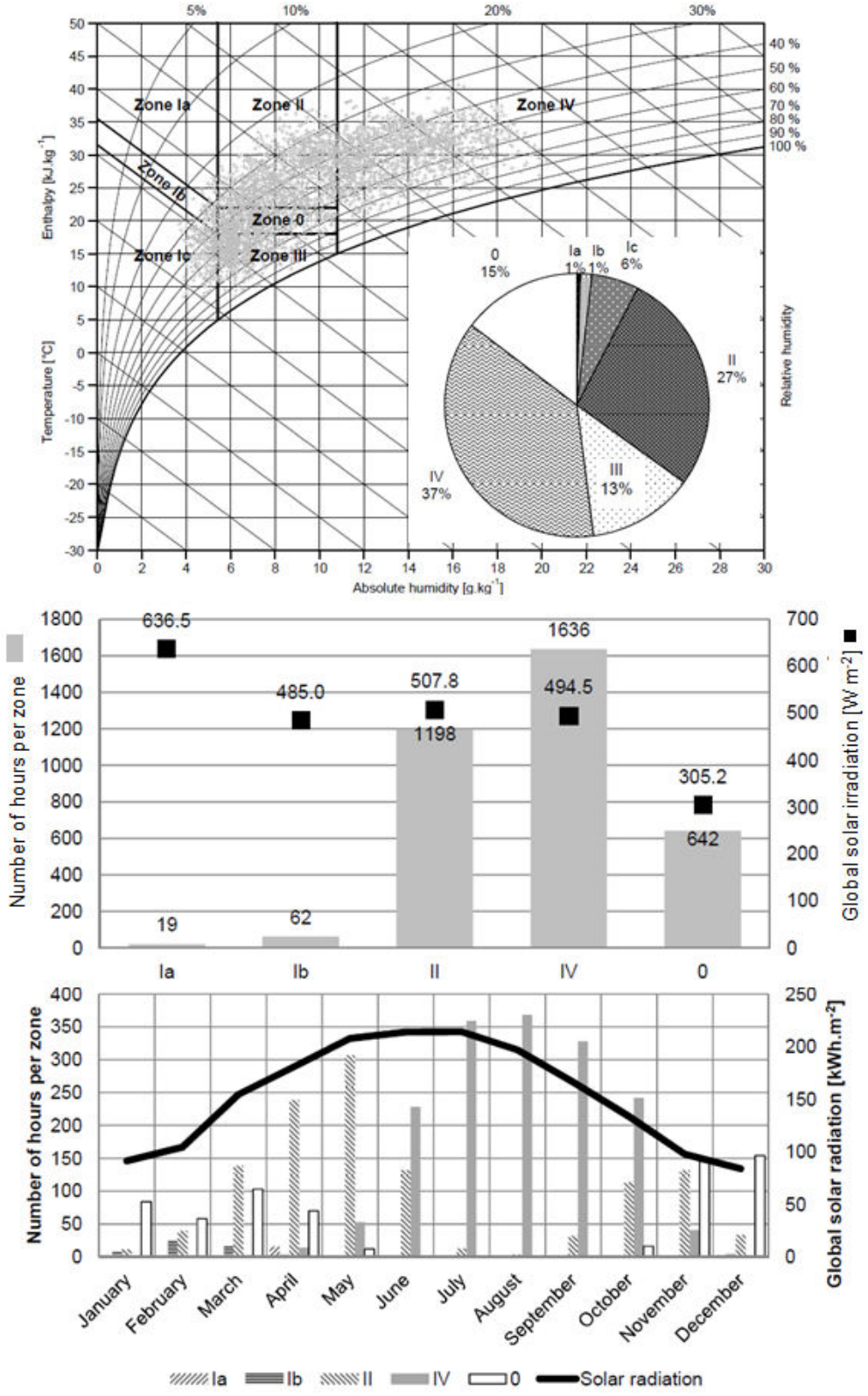

Figure E.6: Zoned meteorological ambient air conditions and expected global solar irradiation in climate BWh (Cairo, Egypt)

Ashgabat (Turkmenistan, cold arid climate BWk)

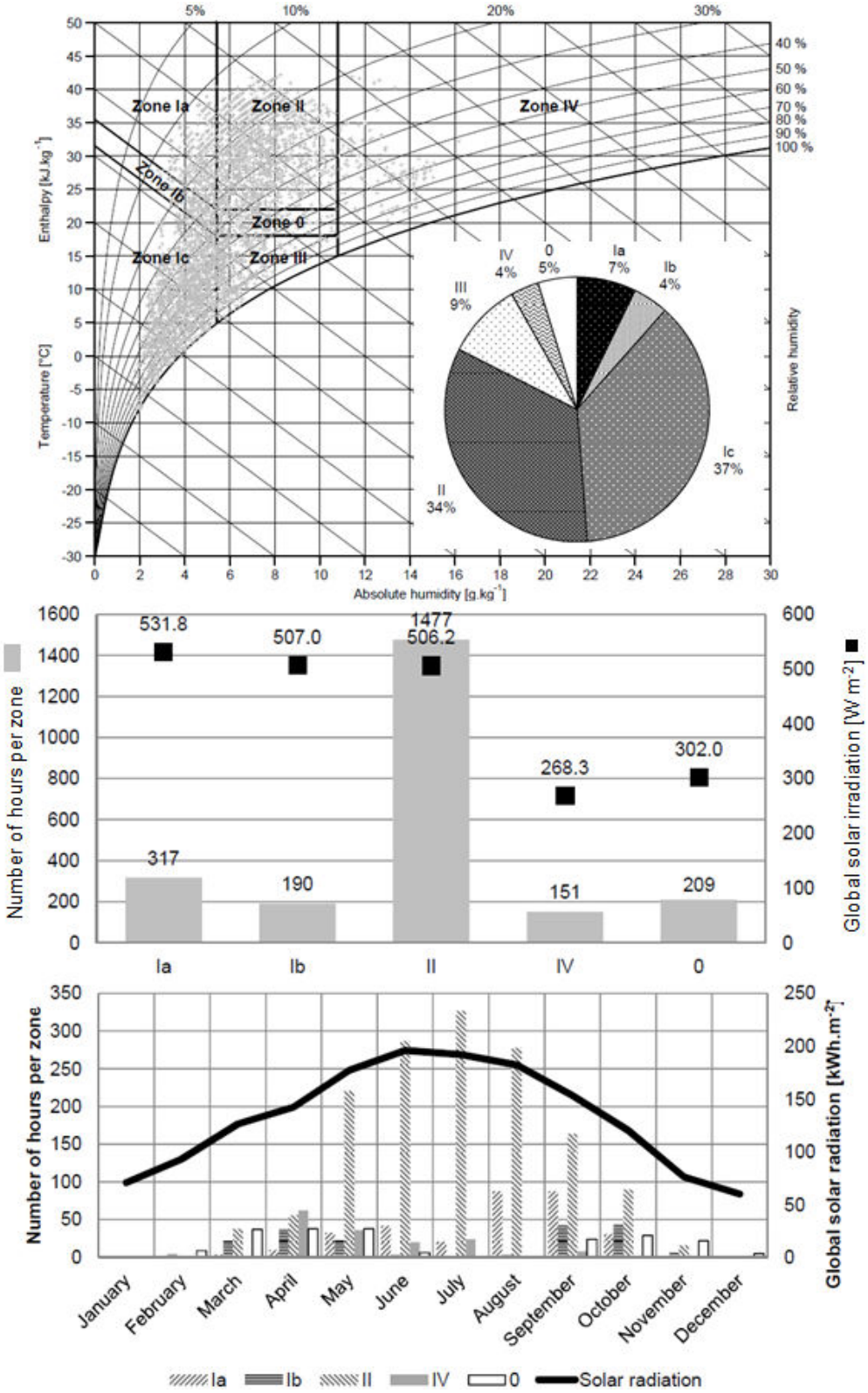

Figure E.7: Zoned meteorological ambient air conditions and expected global solar irradiation in climate BWk (Ashgabat, Turkmenistan)

Houston (USA, humid subtropical climate Cfa)

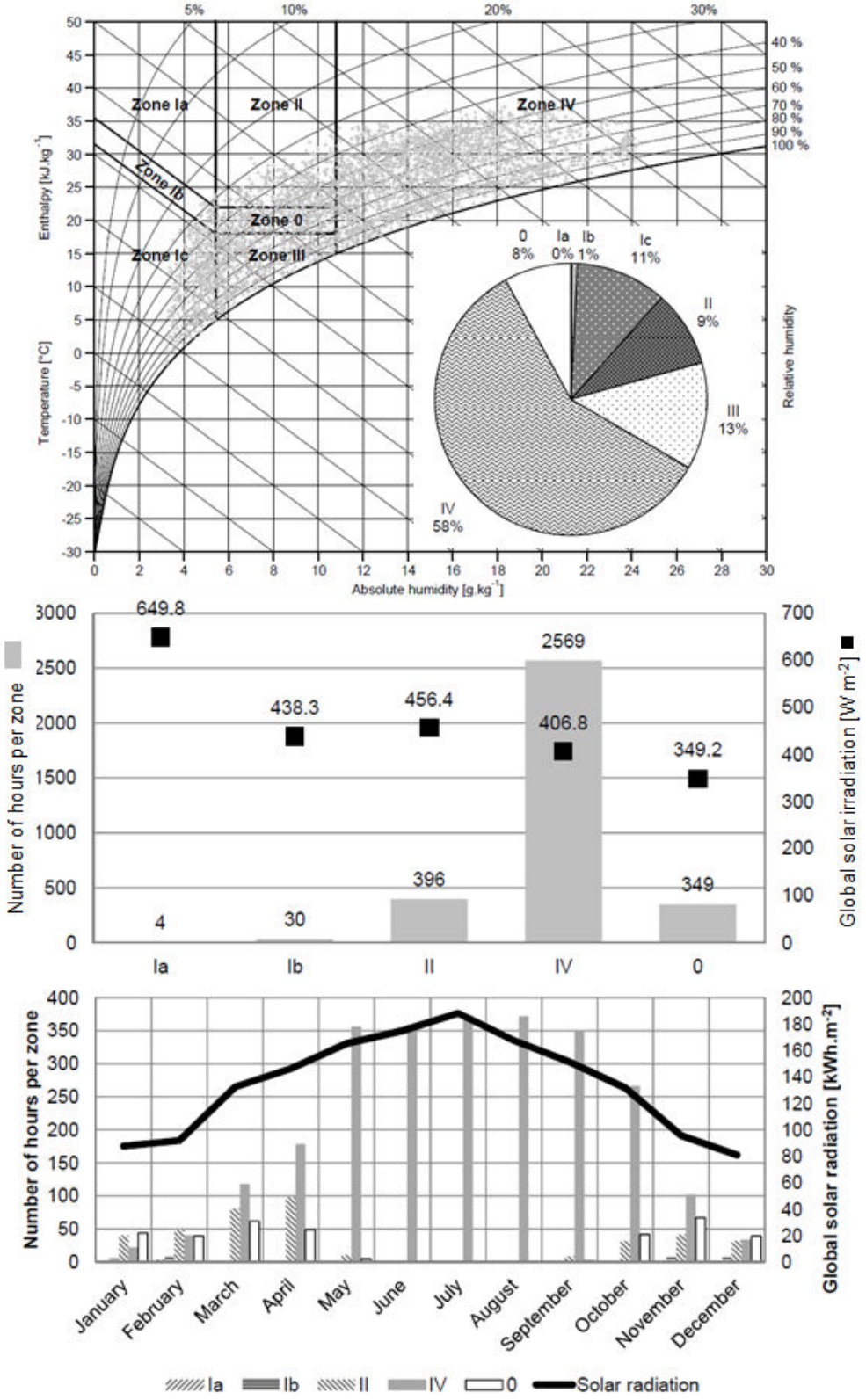

Figure E.8: Zoned meteorological ambient air conditions and expected global solar irradiation in climate Cfa (Houston, USA)

Ingolstadt (Germany, oceanic climate Cfb)

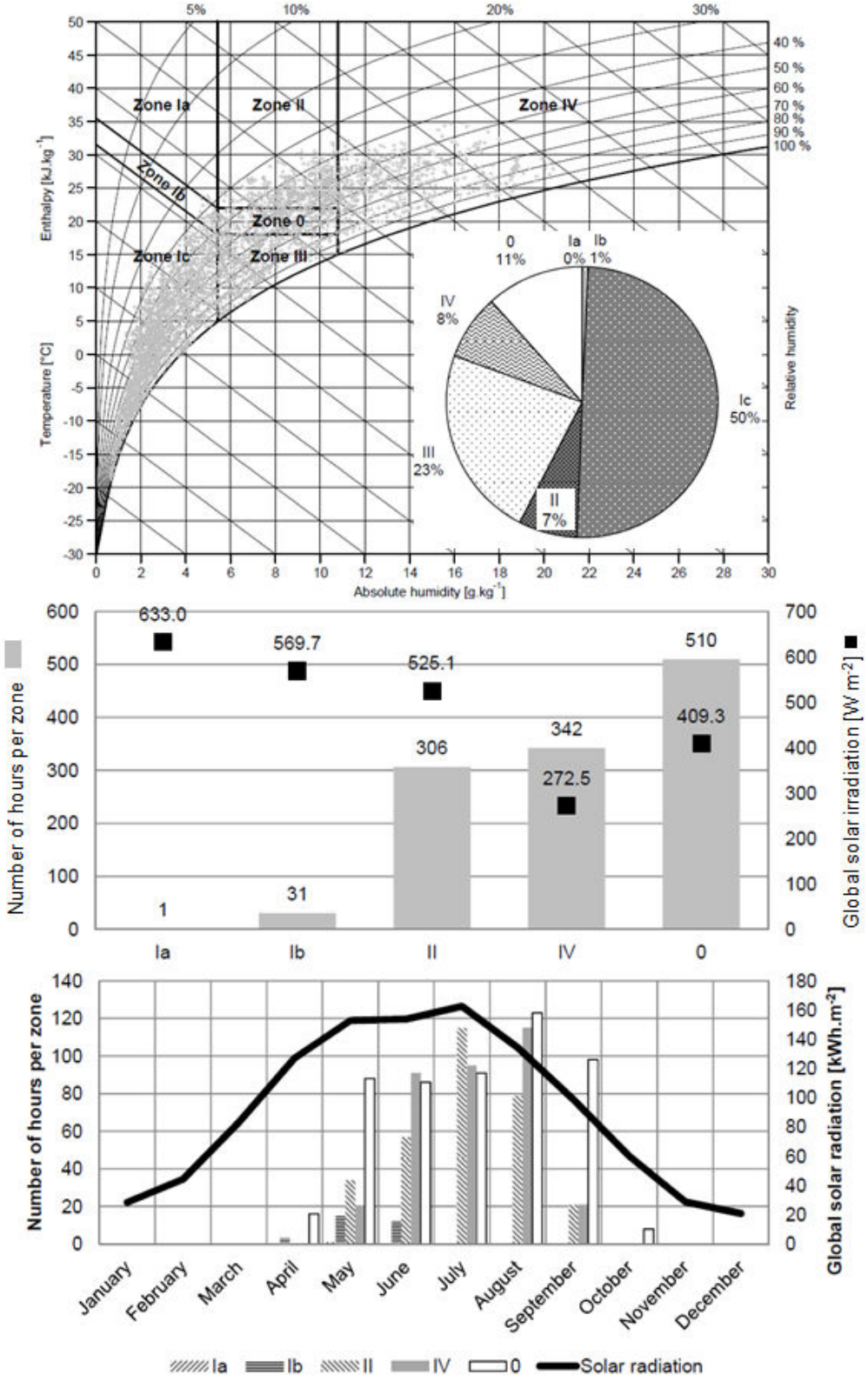

Figure E.9: Zoned meteorological ambient air conditions and expected global solar irradiation in climate Cfb (Ingolstadt, Germany)

Los Angeles (USA, hot-summer Mediterranean climate Csa)

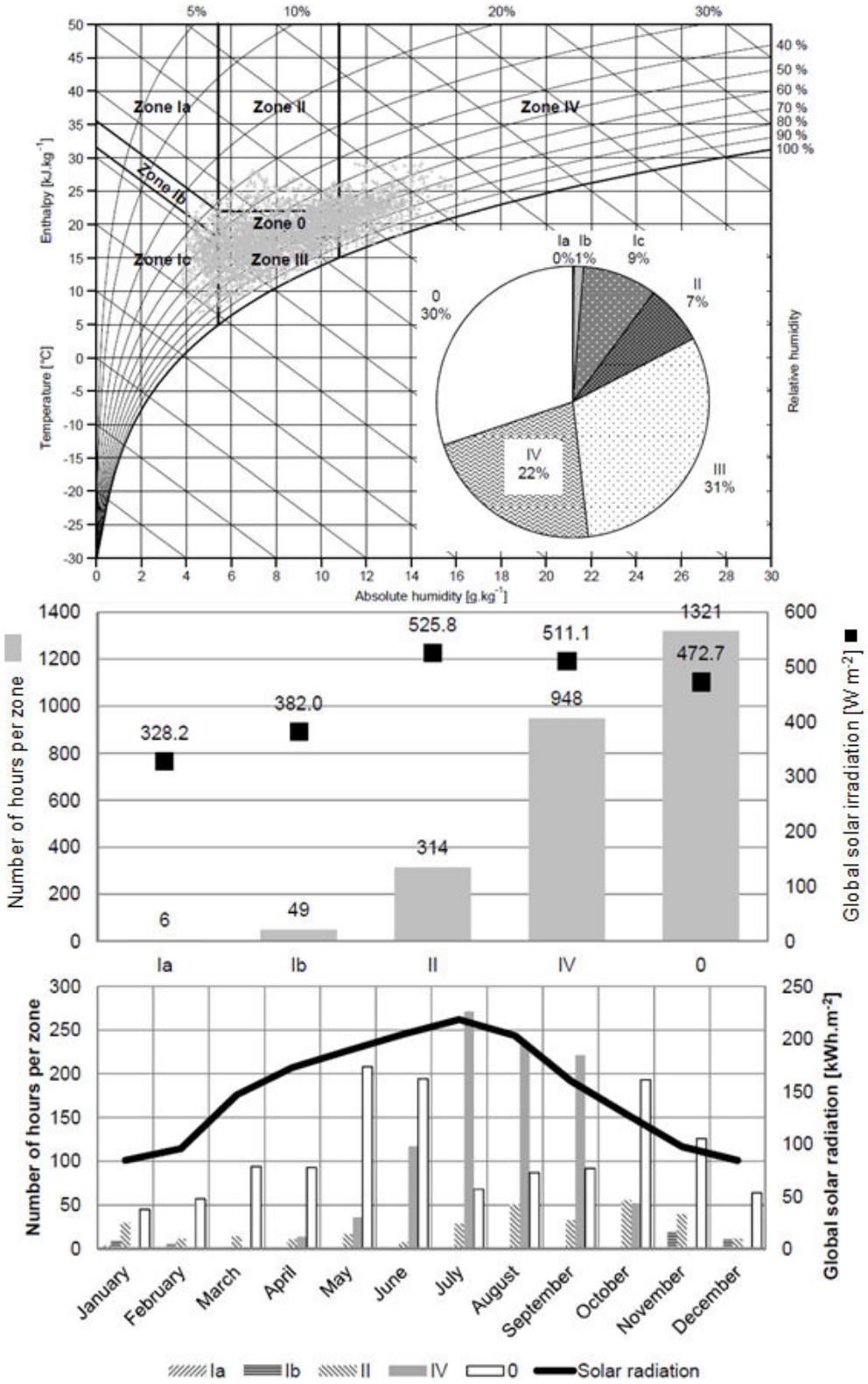

Figure E.10: Zoned meteorological ambient air conditions and expected global solar irradiation in climate Csa (Los Angeles, USA)

Santiago (Chile, warm-summer Mediterranean climate Csb)

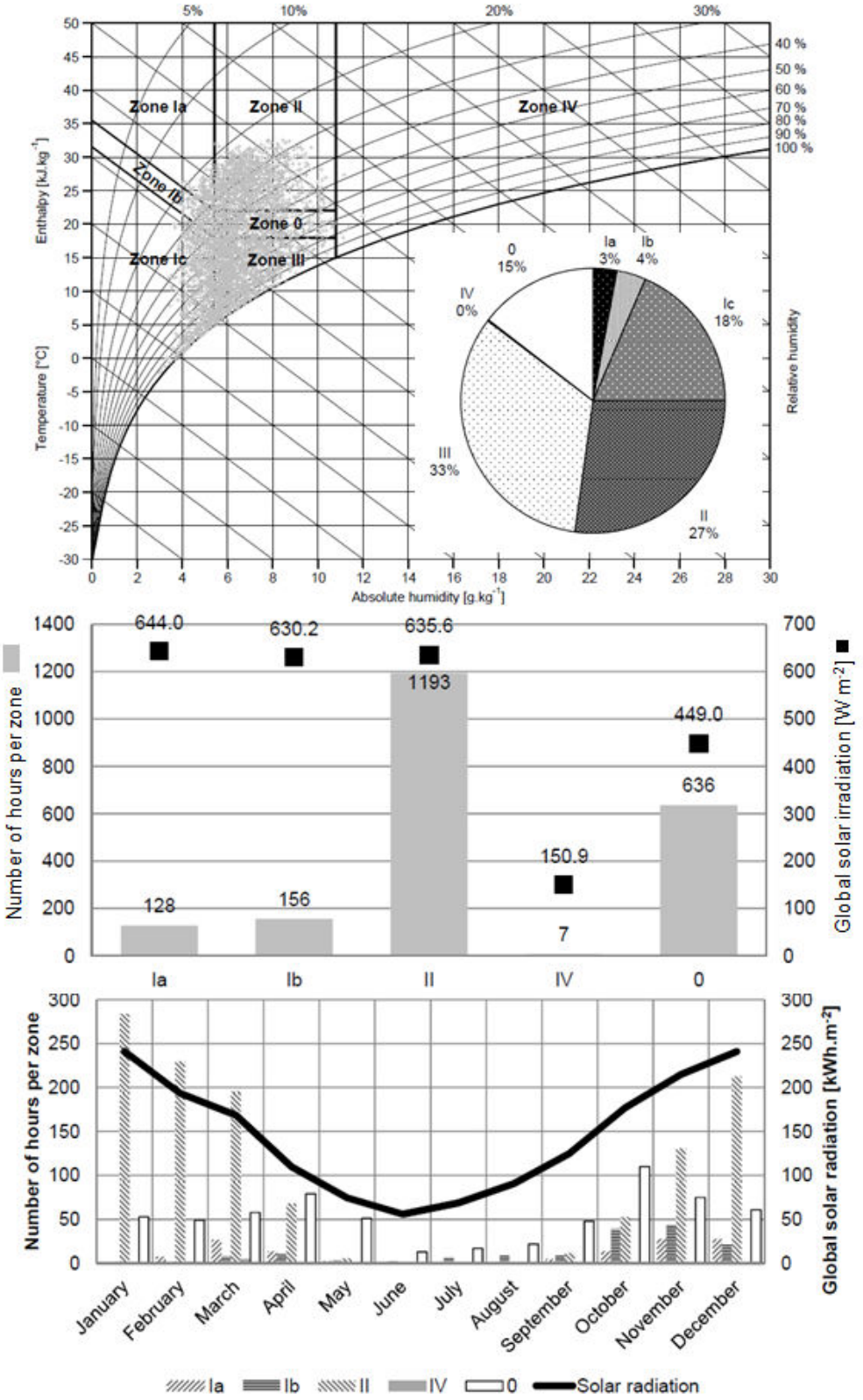

Figure E.11: Zoned meteorological ambient air conditions and expected global solar irradiation in climate Csb, (Santiago, Chile)

Hong Kong (China, humid subtropical climate Cwa)

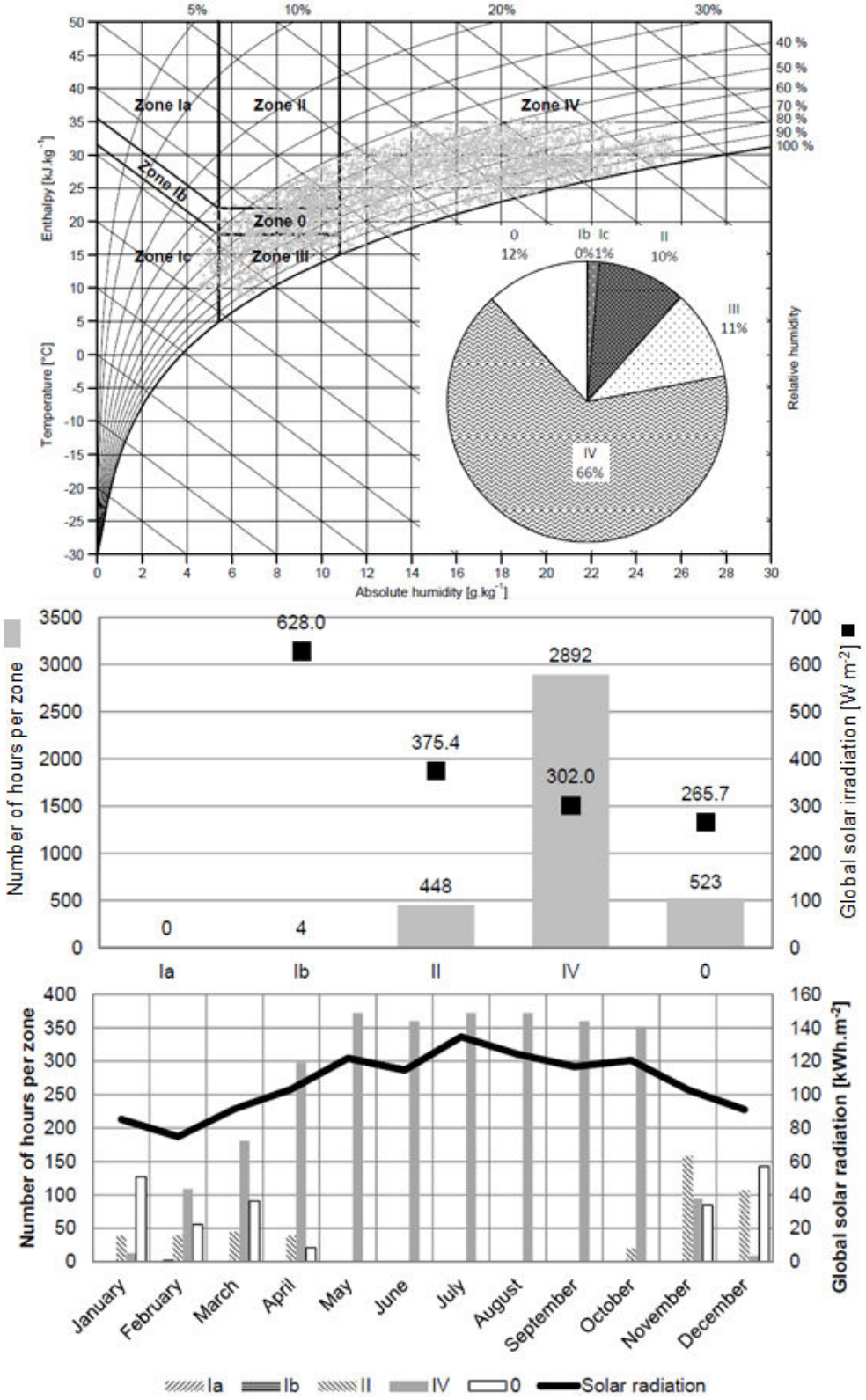

Figure E.12: Zoned meteorological ambient air conditions and expected global solar irradiation in climate Cwa (Hong Kong, China)

Johannesburg (South Africa, subtropical highland climate Cwb)

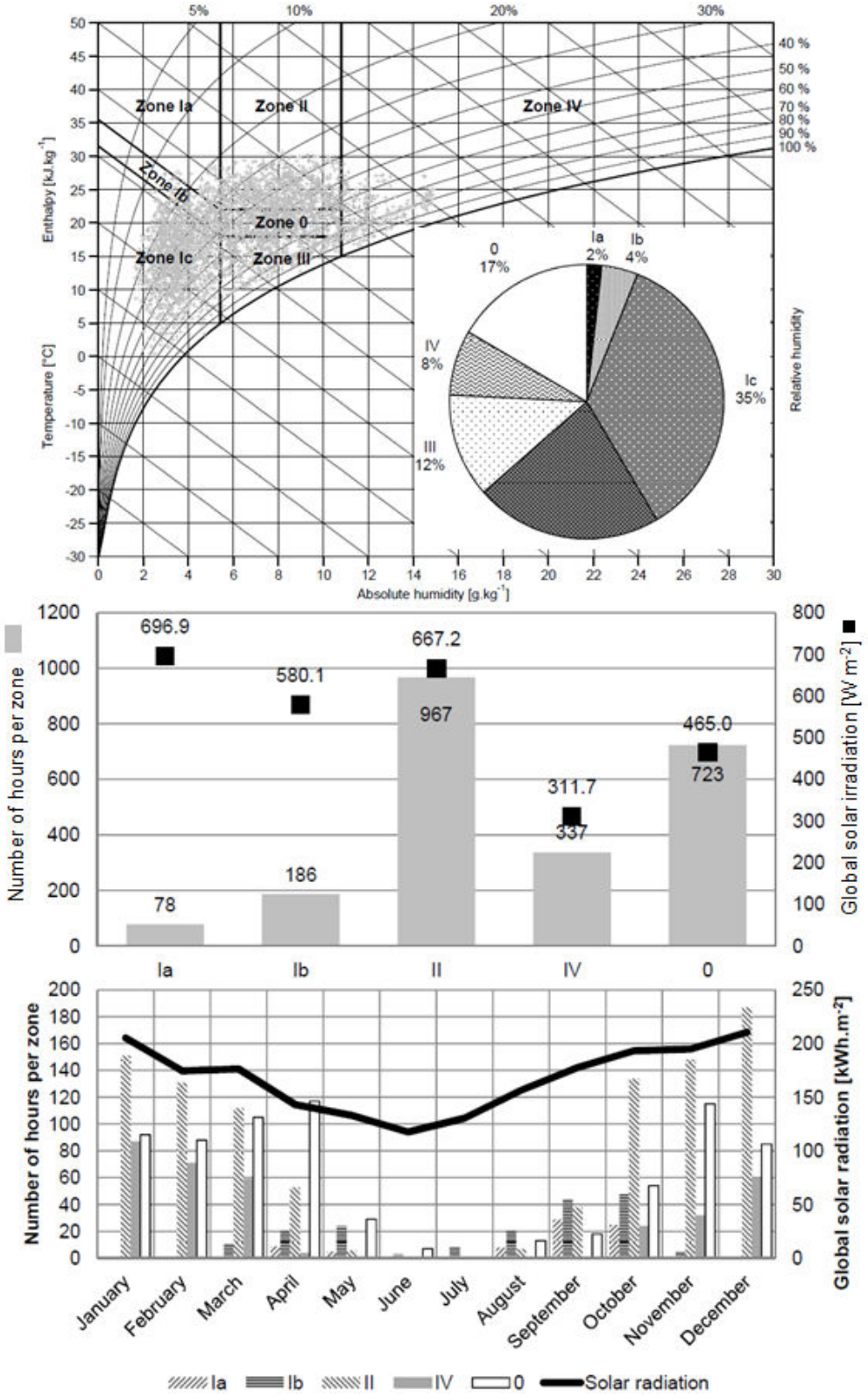

Figure E.13: Zoned meteorological ambient air conditions and expected global solar irradiation in climate Cwb (Johannesburg, South Africa)

Chicago (USA, humid continental climate Dfa)

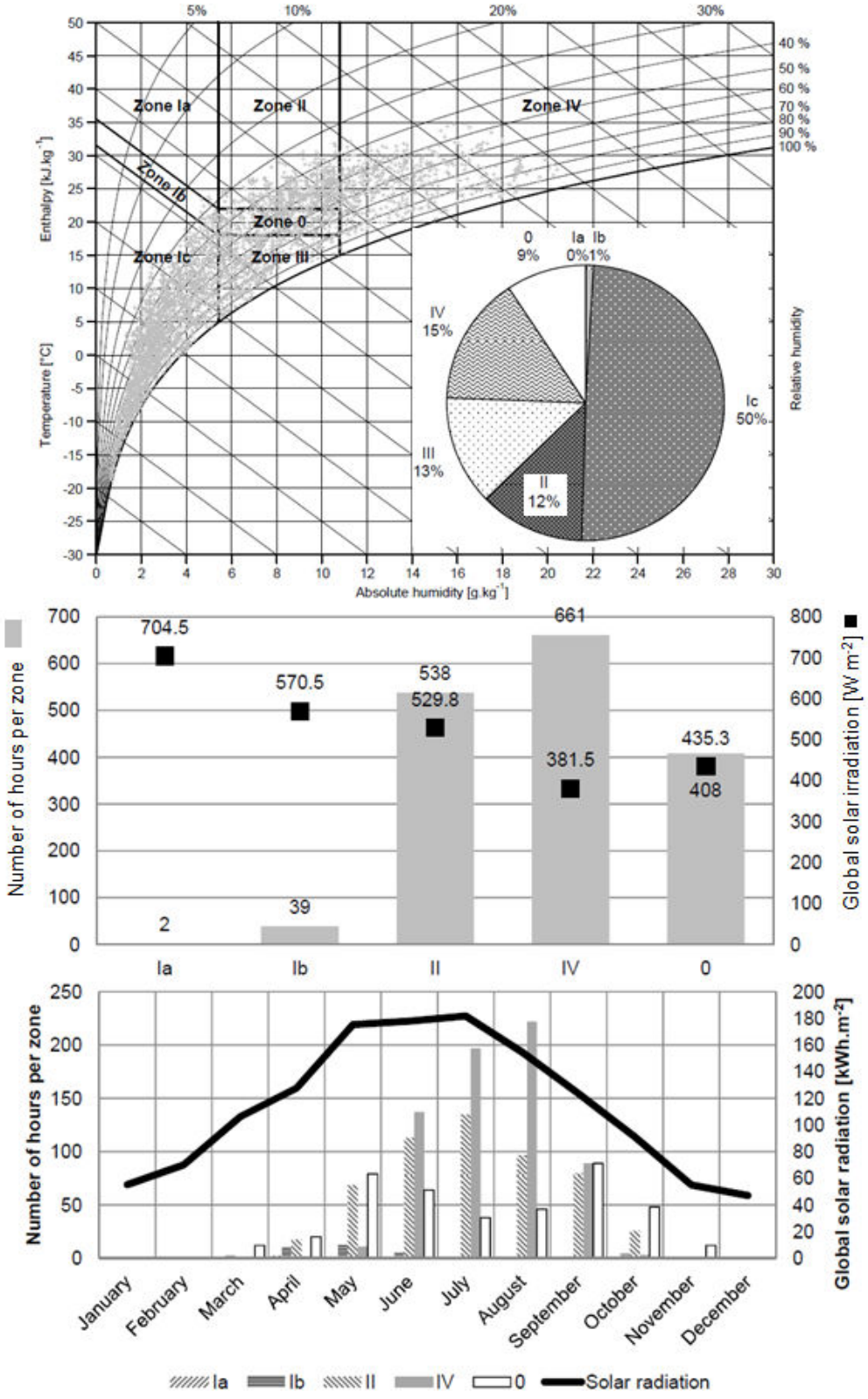

Figure E.14: Zoned meteorological ambient air conditions and expected global solar irradiation in climate Dfa (Chicago, USA)

Helsinki (Finland, humid continental climate Dfb)

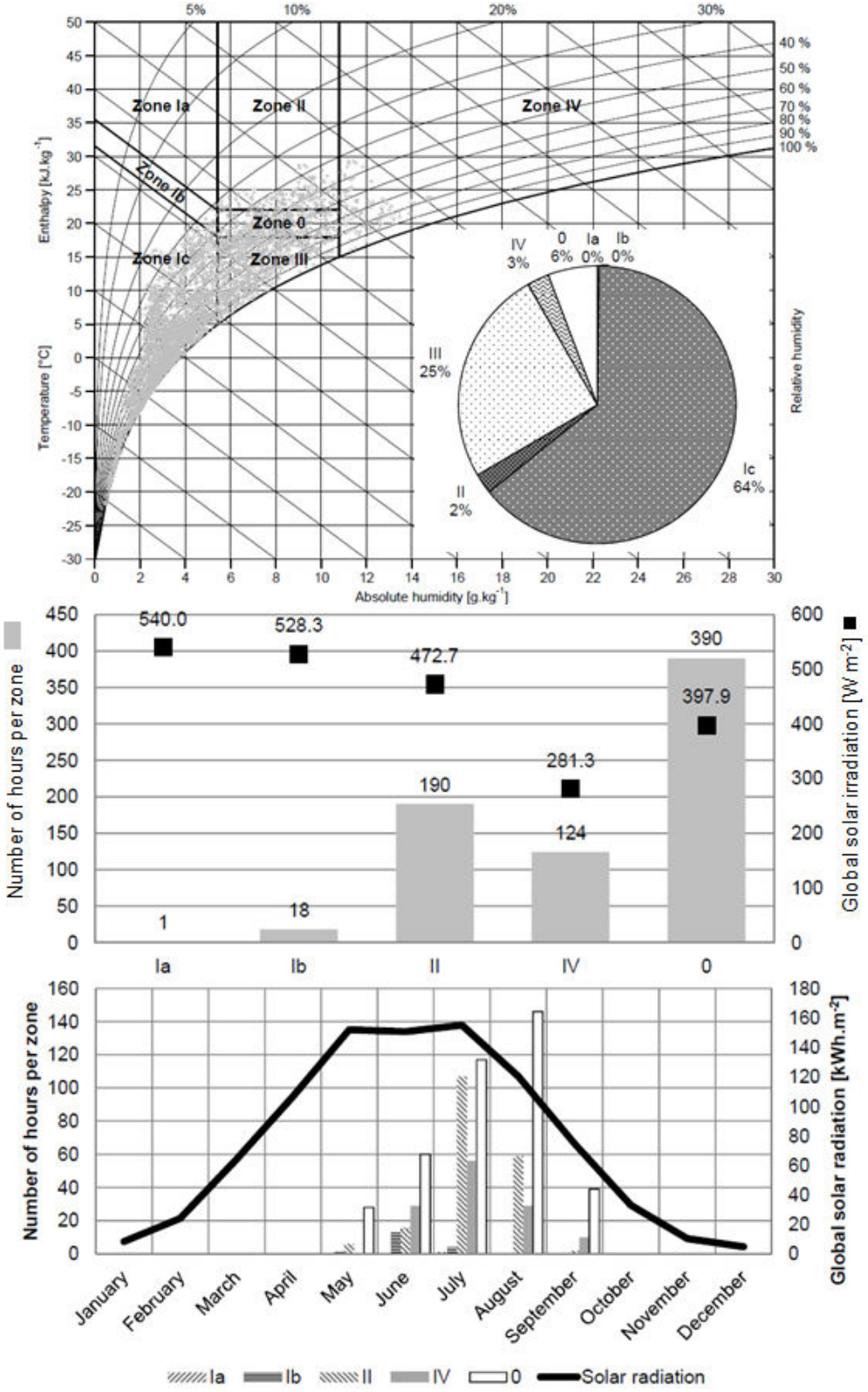

Figure E.15: Zoned meteorological ambient air conditions and expected global solar irradiation in climate Dfb (Helsinki, Finland)

Beijing (China, humid continental climate Dwa)

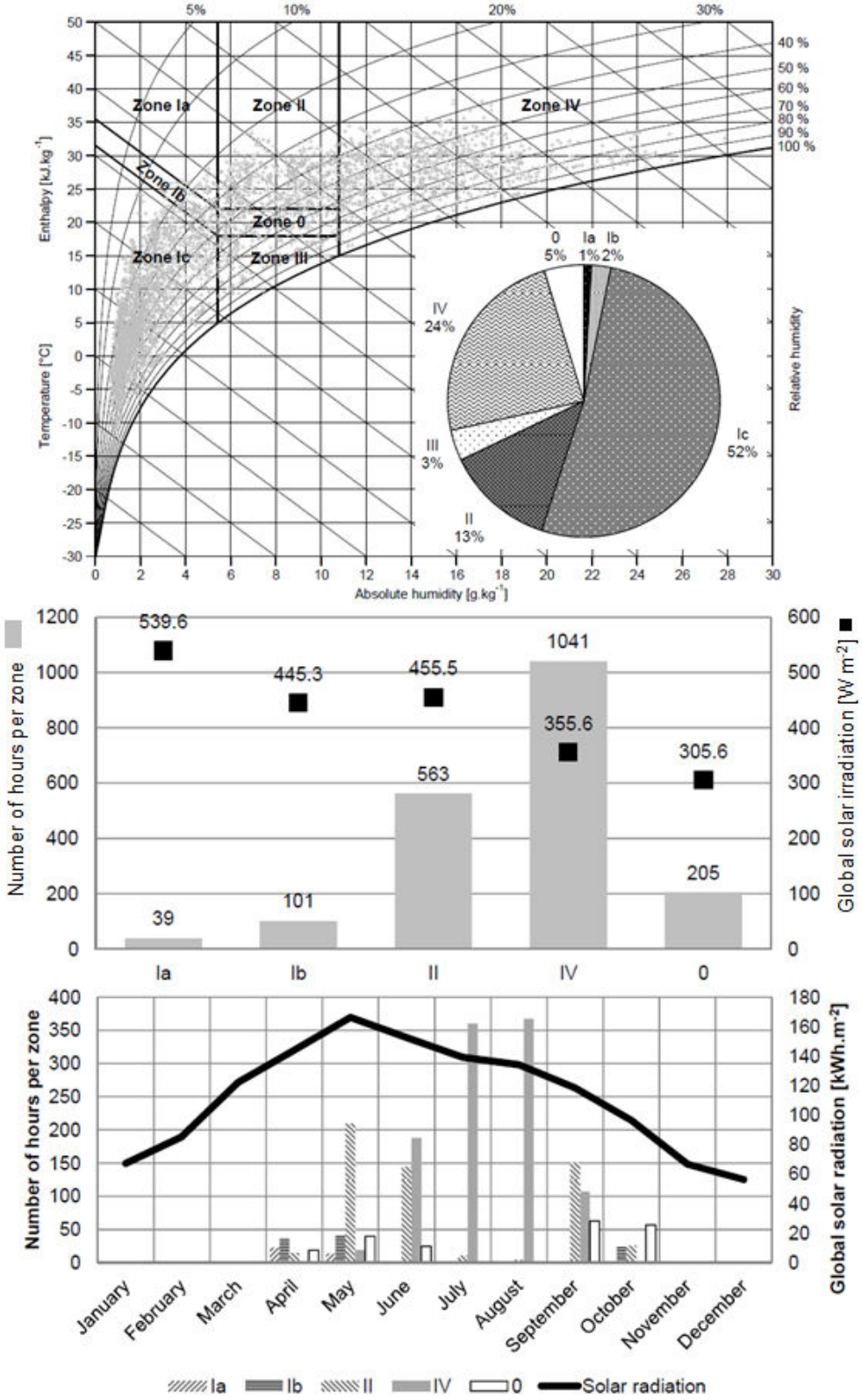

Figure E.16: Zoned meteorological ambient air conditions and expected global solar irradiation in climate Dwa (Beijng, China)

Vladivostok (Russia, humid continental climate Dwb)

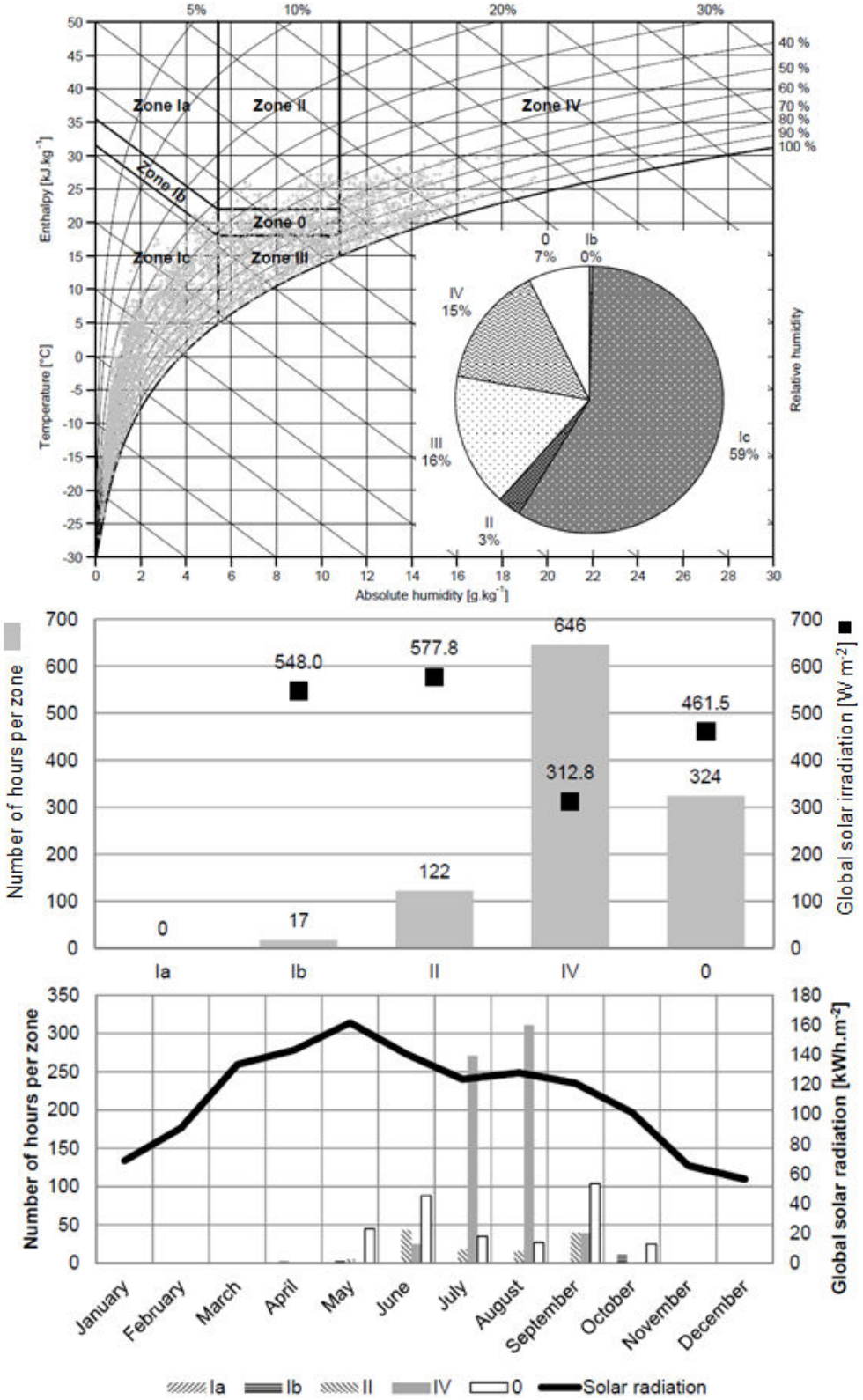

Figure E.17: Zoned meteorological ambient air conditions and expected global solar irradiation in climate Dwb (Vladivostok, Russia)

Appendix F:
Own Publications

BADER, T. et al. (2009) In-Situ Measurements, Simulation and System Optimisation of a Solar-Driven DEC-System in an Industrial Environment. In: *Proceedings of the 3rd International Conference Solar Air-Conditioning,* Palermo, Italy, October 2009. Regensburg, Germany: Ostbayerisches Technologie-Transfer-Institut, pp.509-514.

BADER, T. et al. (2010) Feldtest-Messungen und Systemoptimierung an einer solarbetriebenen DEC-Klimatisierungsanlage im industriellen Einsatz. In: *Proceedings of the 20th Symposium Thermische Solarenergie*, Bad Staffelstein, Germany, May 2010, Regensburg, Germany: Ostbayerisches Technologie-Transfer-Institut.

BADER, T. et al. (2010a) Solar-Driven Desiccant and Evaporative Cooling: Technology Overview and Operational Experiences. In: *Proceedings of the 3rd IASTED African Conference on Power and Energy Systems*, Gaborone, Botswana, September 2010.

BADER, T. et al. (2010b). In-Situ Analysis and Operational Optimisation of a Solar-Driven DEC-System. In: *Proceedings of the 2nd International Conference on Solar Heating, Cooling and Buildings Eurosun 2010,* Graz, Austria, September 2010.

BADER, T. et al. (2011) Solar Desiccant air-conditioning in an industrial application: optimisation approaches for solar-thermal integration and air-handling unit. In: *Proceedings of the ISES Solar World Congress 2011*, Kassel, Germany, August 2011, International Solar Energy Society.

BADER, T. et al. (2011a) Component Analysis of a Solar-Driven DEC-System. In: *Proceedings of the 4th International Conference Solar Air-Conditioning,* Larnaca, Cyprus, October 2011. Regensburg, Germany: Ostbayerisches Technologie-Transfer-Institut, pp.329-334.

BADER, T. et al. (2012) Betriebs-erfahrungen mit großen Kollektorfeldern zur solaren Klimatisierung In: *Proceedings of the 22nd Symposium Thermische Solarenergie*, Bad Staffelstein, Germany, Mai 2012. Regensburg: Ostbayerisches Technologie-Transfer-Institut e.V. (OTTI).

BADER, T. et al. (2013) Globale Anwendbarkeit solarer DEC-Systeme zur Klimatisierung: Untersuchung der Relevanz für klimatisch unterschiedliche Standorte. In: *Proceedings of the 23rd Symposium Thermische Solarenergie*, Bad Staffelstein, Germany, April 2013. Regensburg: Ostbayerisches Technologie-Transfer-Institut e.V. (OTTI).

BADER, T. et al. (2013a) Climate specific design and effectiveness of solar DEC-systems: A methodological zoning approach. In: *Proceedings of the 2nd International Conference on Solar Heating and Cooling for Buildings and Industry - SHC 2013*, Freiburg, Germany September 2013. Elsevier ScienceDirect Ltd., Energy Procedia, 48, 2014, pp.778-789.

BADER, T. et al. (2013b) Global Applicability of Solar DEC-Systems: Basic Technology Effectiveness in Climatically Different Regions. In: *Proceedings of the 5th International Conference Solar Air-Conditioning,* Bad Krozingen, Germany, September 2013. Regensburg, Germany: Ostbayerisches Technologie-Transfer-Institut, pp. 176-181.